

Solid phase microextraction: a versatile technique for lipid analysis

by

Hernando Fabian Alonso Rosales Solano

A thesis

presented to the University of Waterloo

in fulfillment of the

thesis requirement for the degree of

Doctor of Philosophy

in

Chemistry

Waterloo, Ontario, Canada, 2023

© Hernando Fabian Alonso Rosales Solano 2023

## Examining committee members

The following served on the Examining Committee for this thesis. The decision of the Examining committee is by majority vote.

External Examiner	Prof. Michael Lämmerhofer Institute of Pharmaceutical Sciences Eberhard-Karls-University Tuebingen
Supervisor	Prof. Janusz Pawliszyn University Professor and Canada Research Chair, Department of Chemistry University of Waterloo
Internal Member	Prof. Scott Hopkins Associate Professor, Department of Chemistry University of Waterloo
Internal Member	Dr. David S. Bell Research Fellow Restek Corporation
Internal-External Member	Prof. Ken Stark University Professor and Canada Research Chair Faculty of Kinesiology and Health Sciences University of Waterloo

## **Author's Declaration**

This thesis consists of material all of which I authored or co-authored: see Statement of Contributions included in the thesis. This is a true copy of the thesis, including any required final revisions, as accepted by my examiners.

I understand that my thesis may be made electronically available to the public.

## Statement of Contributions

Chapter 2 contains a small excerpt from a technical note titled “Standard Water Generating Vials for Lipophilic Compounds” (*Analytical Chemistry*, **2022**) which was recently accepted for publication. The manuscript was co-authored with Demet Dincel and Shakiba Zeinali and co-authored/supervised by Janusz Pawliszyn. All instances of experimental planning and execution, data analysis and interpretation for phospholipids were made by the author of the thesis; original draft writing was done with Demet Dincel as an equal contributor. All experimental work related to endocannabinoids was done by Demet Dincel and Shakiba Zeinali. Janusz Pawliszyn supervised the study.

Chapter 2 also includes a small excerpt from the article titled “Investigation of binding of fatty acids to serum albumin to determine free concentrations: Experimental and *in-silico* approaches” (*Analytica Chimica Acta*, **2022**, 1192: 339370.) which was co-authored with Mohammad Huq and Janusz Pawliszyn. In all cases, sample/probe preparation, experimental execution was done by the author of this thesis. Experimental design and manuscript writing was equally done with Mohammad Huq. Everything related to the calculations made on COMSOL calculations was performed by Mohammad Huq. Janusz Pawliszyn supervised the study.

Chapter 4 has been published as a short technical note titled “Profiling of Unsaturated Lipids by Raman Spectroscopy Directly on Solid-Phase Microextraction Probes” (*Analytical Chemistry*, **2022**, *94*, 2, 606–611) co-authored with Victor Galievsky, Khaled Murtada, Pavle Radovanovic, and Janusz Pawliszyn. Probe preparation, experimental planning and execution, and manuscript writing was done by the author of this thesis. Experimental execution and data analysis was done equally with Victor Galievsky and Khaled Murtada. Victor Galievsky performed all Raman measurements and Raman data acquisition and curation. Janusz Pawliszyn and Pavle Radovanovic supervised the collaboration.

## **Abstract**

Extensive multidisciplinary research and improvements to instrumentation and workflows are continuously enabling new insights into the role of lipids in health and disease. As with other metabolites, the accurate analysis of lipids in biological samples requires robust and efficient analytical methodologies that enable reliable quantitation. Since its introduction in the 1990s, solid phase microextraction (SPME) has proven well-suited for numerous applications in various scientific fields (environmental chemistry, forensics, clinical, and others) thanks to its many advantages and compatibility with different instruments. Despite being present on the bioanalytical landscape for a decade, SPME research aimed at lipids remains unusual and often qualitative. This thesis documents the development of three approaches for the analysis of lipids based on SPME coupled with different instrumental platforms, namely: liquid chromatography-mass spectrometry (LC-MS) (Chapter 2); mass spectrometry (MS) (Chapter 3), and Raman spectroscopy (Chapter 4).

Chapter 2 details the development of an LC-MS platform, the analysis of sampling parameters crucial to SPME, the steps taken to determine the total concentration of glycerophospholipids in human plasma and strategies for the analysis of the free concentration of model lipids. The reversed-phase liquid chromatography (RPLC) method was applied to analyze exogenous lipids in human blood plasma. It was validated with respect to instrumental linearity and dynamic linear range, inter- and intra-day accuracy and precision, and limits of quantitation. The SPME method was optimized by

investigating several crucial parameters, including coating chemistry, extraction time, and desorption conditions. This proposed SPME-RPLC-MS/MS platform was utilized to construct matrix-matched calibration curves for the total concentration in four plasma lots, including NIST™ SRM® 1950 human blood plasma. Moreover, SPME probes were used to quantitate endogenous lipid compounds present in the NIST™ SRM® 1950 plasma using a standard addition approach, which resulted in good agreement with previous studies on this sample. Furthermore, the lipidome of NIST™ SRM® 1950 was qualitatively assessed via an untargeted approach using high-resolution mass spectrometry. The lipidome obtained using SPME, an unconventional technique, is in good agreement with previous studies. This chapter also proposes a simple approach for the calibration of free concentration of lipid metabolites using SPME devices and external calibration curves free of binding matrix components. To this end, this section evaluated a ‘standard generating vial’ to produce and maintain a stable free concentration in aqueous media. The standard generating vial employs a lipid laden PDMS film coated onto a carbon mesh acting as an analyte reservoir. These vials were evaluated regarding their equilibration time, short-term stability, and linearity attained at various spiking concentrations. Finally, this chapter briefly explores the binding between human serum albumin and two long-chain fatty acids using experimental and *in silico* approaches. This study took advantage of SPME’s extraction mechanism from the pool of unbound analytes; thus, the free concentration of fatty acids was measured with SPME fibres and used to construct Scatchard plots to estimate the binding affinities with human serum albumin. The mass uptake of fatty acids by the SPME probes under different *kinetic* conditions (static extraction, agitated

extraction, and agitated extraction with a binding matrix component) was validated by mathematical modelling using the COMSOL Multiphysics® software package.

In Chapter 3, solid-phase microextraction is directly coupled to mass spectrometry (SPME–MS) for the analysis of glycerophospholipids in plasma while bypassing chromatographic separation. Coated blade spray (CBS), the initial SPME–MS technology surveyed, is a sword-like device that provides the sampling/pre-concentration capabilities of SPME devices while also serving as an ion source requiring minimal additional instrumentation. While lipid detection was easily achieved through the proper selection of modifiers, CBS's geometry and *ambient* nature posed a challenge regarding lipids' fast and reproducible desorption. As an alternative, the flow-isolated desorption chamber of an open microfluidic interface (MOI)—the second SPME–MS technology assessed—was employed to study the desorption of lipids with *virtually* no evaporation. Substantial ionization/absolute matrix effects were detected for SPME–MS technologies, mirroring the phenomena observed in other MS-based lipid analyses.

Chapter 4 presents a simple, proof-of-concept approach for the on-fibre detection of unsaturated lipids based on the direct coupling of SPME probes and Raman spectroscopy. The SPME protocol was optimized by investigating various parameters influencing extraction efficiency, including the coating chemistry, extraction time, extraction temperature, and washing solvent. Our findings show that the developed SPME–Raman method is suitable for detecting lipids enriched on the coating. A clear dependence is observed between the number of double bonds and the ratio of the Raman bands at



1655/1445  $\text{cm}^{-1}$ . Although additional studies are needed to establish how these double bonds contribute to the observed Raman bands, the proposed platform has great potential for fast profiling applications.

## **Acknowledgements**

I would like to express my sincere gratitude to my advisor Janusz Pawliszyn for his invaluable guidance and support throughout my dissertation journey. Without his unwavering encouragement, insightful feedback, and endless patience, this work would not have been possible.

I am also grateful to the examining committee, Scott Hopkins, David Bell, Ken Stark, and Michael Lämmerhofer, for accepting the invitation to read and evaluate my thesis and the precious feedback provided.

I also want to the University of Waterloo for providing the resources and funding needed to conduct this research, with special thanks to the Administrative Graduate Coordinator, Catherine van Esch, for her assistance in my numerous queries.

Finally, I would like to express my deepest appreciation to my family and friends for their unwavering love, encouragement, and support throughout this (very) challenging journey.

Thank you all for your contributions to this work and for helping me to achieve this significant milestone in my academic career.

## Table of Contents

Examining committee members	ii
Author's Declaration	iii
Statement of Contributions	iv
Abstract	vi
Acknowledgements	x
List of Figures	xiii
List of Tables	xix
List of abbreviations	xx
Chapter 1 Introduction	1
1.1 Lipids	1
1.2 Instrumental platforms for lipid analysis	7
1.3 Extraction methods for lipids	10
1.4 Solid phase microextraction: a brief summary	13
1.5 Research objectives	17
Chapter 2 Towards the determination of total and free lipid concentrations	20
2.1 Towards lipid total concentration with solid phase microextraction devices	22
2.1.1 Introduction	22
2.1.2 Experimental	24
2.1.3 Results and discussion	31
2.2 Towards lipid free concentration: testing a standard generating water system	66
2.2.1 Introduction	66
2.2.2 Experimental	69
2.2.3 Results and Discussion	74
2.3 Towards determination of free concentration of lipids: Binding of fatty acids to serum albumin: experimental and <i>in silico</i> approach	85
2.3.1 Introduction	85
2.3.2 Experimental	89
2.3.3 Results and discussion	92
2.4 Summary and conclusions	98
Chapter 3 Coupling SPME to direct to MS approaches	101

3.1	Introduction	101
3.2	Experimental	107
3.2.1	Standards, materials, and probes	107
3.2.2	Mass spectrometers	107
3.2.3	CBS as the SPME–MS approach	109
3.2.4	MOI interface as SPME–MS approach	110
3.3	Results and Discussion	113
3.3.1	Coated Blade Spray	113
3.3.2	Microfluidic Open Interface	119
3.4	Conclusions	127
Chapter 4	Profiling of unsaturated lipids by Raman spectroscopy directly on SPME probes	130
4.1	Introduction	130
4.2	Experimental	133
4.2.1	Materials, supplies, and chemicals	133
4.2.2	Raman measurements	134
4.2.3	Sample preparation and SPME procedure.	135
4.3	Results and discussion:	136
4.3.1	Evaluation of SPME coating chemistry.	136
4.3.2	SPME optimization procedure.	138
4.3.3	Spectra analysis of lipids.	142
4.4	Chapter conclusions	145
	Conclusions and future directions	148
	Conclusions	148
	Future Perspectives	150
	Letters of copyright permission	153
	References	155

## List of Figures

Figure 1.1 Structural variety within glycerophospholipids class, with phosphatidylcholines and phosphatidylethanolamines being the common lipids found in cell membranes. Figure adapted from Han <sup>1</sup> and the LIPID MAPS consortium website. <sup>2</sup> .....	5
Figure 1.2 A brief (and very much reduced) qualitative example of a lipidome showcasing the diversity of lipid subclasses found across mammal tissues. CE, cholesteryl esters; TG, triglycerides; SM: sphingomyelins; DG, diacylglycerides; PC, phosphatidylcholines; FA, fatty acyls; PI, phosphatidylinositol; PA, phosphatidic acids; S1P; sphingosine 1-phosphate; LPA, lysophosphatidic acid; Acyl CoA, acyl Coenzyme A. Figure adapted from Tumanov & Kamphorst. <sup>16</sup> .....	6
Figure 1.3. Typical workflow for the analysis of lipids from biological samples. Adapted from Yang and Han. <sup>27,28</sup> .....	8
Figure 1.4 SPME sample preparation and analyte absorption over time. (A) Sample preparation scheme for SPME. VF, fiber coating volume; KFS, fiber/sample distribution coefficient; VS, sample volume; CO, initial concentration of analyte in the sample. (B) The typical profile of analyte uptake in SPME devices. t <sub>50</sub> , time required for extraction of half maximum analyte; t <sub>95</sub> , time required for extraction of 95% maximum analyte. <sup>68</sup> .....	14
Figure 1.5 Schematic depiction of analyte extraction from a sample with a binding component. Analyte extraction depends on its coating–sample distribution constant, KFS, and its binding constant with the matrix binding components, K <sub>a</sub> . The binding constant is a relationship between the forward, k <sub>F</sub> , and backward, k <sub>r</sub> , binding reaction constants. Figure adapted from Alam and Pawliszyn. <sup>79</sup> .....	16
Figure 2.1. (A) Comparison between three different coating chemistries for extraction of lipids from PBS (pH 7.4, 100 ng/mL). (B) Desorption solvent comparison between two solvent mixtures of different organic content ratio. Mixture 1 was composed of methanol and isopropanol in equal volumes	

(MeOH/IPA, 1:1, v/v), while mixture 2 was composed of methanol, isopropanol and water (MeOH/IPA/H<sub>2</sub>O, 45/45/10, v/v/v)..... 36

Figure 2.2. (A) Carryover evaluation for the SPME probes used by carrying out a second (60 min, 1000 rpm) desorption step with both solvents evaluated in Figure 2.1B. The carryover is represented as the area ratio between the second and first desorption steps. (B) Desorption time profile constructed for selected lipid standards using desorption mixture 2, done under agitation at 1000 rpm. .... 37

Figure 2.3. Comparison of three spiking approaches of exogenous, odd-chain lipids standards in human plasma. .... 40

Figure 2.4. Extraction time profiles from plasma samples using C18-coated fibers for selected lipid analytes. (A) LPC 17:0; (B) LPE 17:1; (C) PC 15:0\_15:0; (D) PE 17:0\_17:0; (E) PS 17:0\_17:0; (F) TG (19:0)<sub>3</sub>.... 41

Figure 2.5. Plasma modification with acetonitrile to artificially increase the free concentration of lipids, thus increasing the total amount recovered by SPME fibers. .... 45

Figure 2.6. Absolute matrix effects evaluated for extraction of exogenous lipids from human plasma. (A) Absolute matrix effects were obtained for extraction with SPME fibers upon plasma modification with acetonitrile. (B) Absolute matrix effects were determined for neat and modified plasma (at the lowest level, 25 µL ACN) using two SPME probe geometries: fiber and coated blade. .... 47

Figure 2.7. Matrix matched calibration curves for exogenous lipid, LPC 17:0. (A) Extraction from SRM® 1950 plasma using SPME fibers; (B) Extraction from other plasma lots using SPME fibers; (C) Extraction from ACN-modified SRM® 1950 plasma using SPME blades; (D) Extraction from ACN-modified plasma lots using SPME blades; (E) Lower range for the matrix-matched calibration curves from all plasma lots using blades; (F) Upper range of calibration curves for all plasma lots using blades..... 49

Figure 2.8. Matrix matched calibration constructed for exogenous, very hydrophobic lipids in various plasma samples. (A) Extraction of PC 15:0\_15:0 from neat plasma using SPME fibers, (B) Extraction of PC 15:0\_15:0 from modified plasma using SPME blades, (C) Extraction of PE 17:0\_17:0 from modified plasma using SPME blades, (D) Extraction of TG (19:0)<sub>3</sub> from modified plasma using blades..... 50

Figure 2.9. Standard addition curves prepared in SRM® 1950 plasma sample for the endogenous lipid, lyso-palmitoylphosphatidylcholine, LPC 16:0. (A) Extraction using SPME fibers from neat plasma. (B). Extraction using SPME blades from modified plasma. .... 54

Figure 2.10. Standard addition curves for two endogenous glycerophospholipids prepared in plasma SRM® 1950 using fibers (from neat plasma) and SPME blades (from modified plasma). (A) Extraction of PC 16:0\_16:0 from neat plasma. (B) Extraction of PE 16:0\_18:1 from neat plasma. (C) Extraction of PC16:0\_16:0 from modified plasma. (D) Extraction of PE 16:0\_18:1 from modified plasma ..... 55

Figure 2.11 Extraction time profiles and calibration curves in PBS constructed using miniaturized C18-coated probes for model lipids. (A) ETP for LPC 16:0 by itself (void triangles) and when mixed with LPC 17:0 (filled triangles). (B) ETP for LPC 17:0 by itself (empty diamonds) and when mixed with LPC 16:0 (filled diamonds). (C) Matrix-free calibration curves for LPC 16:0 alone and as part of a mixture. (D) Matrix-free calibration curve for LPC 17:0 alone and as part of a mixture. .... 75

Figure 2.12. Equilibration of the aqueous concentration prepared for LPC and DPPC over five days from their preparation. Total concentrations for the standard-generating vials for LPC and DPPC are 2.5 µg/vial and 125 ng/vial, respectively. .... 78

Figure 2.13. Calibration curves prepared for LPC 16:0 by spiking the PDMS thin films for vials with aqueous media..... 80

Figure 2.14. Estimated free aqueous concentration for DPPC at various amounts spiked onto the PDMS thin film. At the lowest spiked level (125 ng/vial)..... 80

Figure 2.15. Aqueous concentration for model phospholipids *during* a 60 min extraction with a C18-coated SPME minitip..... 81

Figure 2.16 Sequential SPME extractions to assess the repeatability of extractions from the SGVs prepared for LPC 16:0 (at 2.0 µg/vial total conc.) and DPPC (125 ng/vial total conc.), using two aqueous media. The inter-sampling interval was fixed to 5 min for extractions 1-7, and to overnight (15 hours) between the seven<sup>th</sup> and eight<sup>th</sup> extractions. .... 82

Figure 2.17. Structures for <b>(A)</b> linoleic acid and <b>(B)</b> $\alpha$ -linoleic acid, indicating the $\omega$ -6 and $\omega$ -3 carbons where the double bonds start from the non-carboxylic end. ....	86
Figure 2.18. Scheme for binding between a bi-valent protein receptor, <b>P</b> , and two fatty acid ligands, <b>F</b> , in a stoichiometric fashion. ....	87
Figure 2.19. Experimental and in silico extraction time profiles for $\alpha$ -LA under different extraction modes. <b>(A)</b> Static extraction from a PSB-agar gel, <b>(B)</b> Agitated extraction under convection (500 rpm) in PBS; <b>(C)</b> Extraction in the presence of serum albumin at an equimolar ratio (20 $\mu$ M). ....	94
Figure 2.20. Binding isotherm curves constructed for $\alpha$ -LA and LA in the presence of serum albumin as the binding receptor. ....	96
Figure 3.1. Schematic designs of some direct-to-MS techniques coupled to SPME devices: <b>(A)</b> Desorption electrospray ionization, DESI; <b>(B)</b> Direct analysis in real-time, DART; <b>(C)</b> Coated blade spray, CBS; <b>(D)</b> Microfluidic open interface. ....	104
Figure 3.2. Schematics for the MOI interface for SPME–MS. The MOI interface is comprised of <b>(A)</b> the desorption chamber; <b>(B)</b> a tubing ‘tee’ electrically grounded; <b>(C)</b> a syringe which supplies the desorption solvent; and <b>(D)</b> the tubing diverting the solvent inflow towards the instrument’s ESI source. Adapted from Dr. Nazdrajić’s dissertation. <sup>305</sup> ....	106
Figure 3.3. Coated blade spray interfaces for the MS instruments <b>(A)</b> TSQ Vantage and <b>(B)</b> TSQ Quantiva. The black arrow points at the position of the SPME CBS device within each interface. <b>(C)</b> Scheme of desorption/ionization process occurring directly on the blade and the x,y,z alignment of the probe in front of the MS inlet. <b>(D)</b> Example of the resulting transient signal for two model compounds, LPC 17:0 and LPE 17:1. ....	109
Figure 3.4. Evaluation of the high voltage required for effective ionization in TSQ Vantage. The areas are acquired for 20 s at each voltage value and then normalized to the maximum area. Mixture of lipids injected as a methanolic mixture (50 ng/mL) and continuous flow of 20 $\mu$ L/min. <b>(A)</b> LPC 17:0 and LPE 17:1; <b>(B)</b> PC 15:0_15:0 and PE 17:0_17:0; <b>(C)</b> PG 17:0_17:0 and PS 17:0_17:0; <b>(D)</b> TG (19:0) <sub>3</sub> .....	114



Figure 3.5. (A) Solvent comparison for desorption of selected lipids from CBS blades using TSQ Vantage and its open interface. (B) When a solvent is applied to the blade, the total ion chromatogram/transient signal for PC 15:0\_15:0 ( $m/z$  706.5 > 184.1) is obtained for up to 20 min..... 115

Figure 3.6. Comparison between solvent mixtures regarding desorption performance (18  $\mu$ L solvent, 30 s desorption time,  $n = 5$ ). The highlighted section portrays the obtained area counts for desorption from the *open-air* CBS interface (Vantage TSQ)..... 118

Figure 3.7. Desorption time profiles for studied lipids in the MOI interface with four solvents. Extractions were performed on PBS *dispersions* (100 ng/mL, 60 min) using C18 fibers (10 mm length  $\times$  13  $\mu$ m thickness,  $n=5$ ). Lipid analytes: (A) LPC 17:0, (B) LPE 17:1, (C) LPS 17:1, (D) PC 15:0\_15:0, (E) PE 17:0\_17:0, (F) TG (19:0)<sub>3</sub>. ..... 122

Figure 3.8. Instrumental calibration curves manually prepared in the MOI desorption chamber. Desorption solvent: MeOH/IPA/H<sub>2</sub>O (7/2/1, v/v/v) with 0.1% acetic acid and 10 mM ammonium acetate. Lipid analytes: (A) LPC 17:0, (B) LPE 17:1, (C) LPS 17:1, (D) PC 15:0\_15:0, (E) PE 17:0\_17:0, (F) TG (19:0)<sub>3</sub>. ..... 123

Figure 3.9. Matrix-free calibration curves prepared for lipids in PBS (pH 7.4, 30 min extraction at 1000 rpm). Static desorption was conducted for 30 s using MeOH/IPA/H<sub>2</sub>O (7/2/1, v/v/v) containing 0.1% acetic acid and 10 mM ammonium acetate. Lipid analytes: (A) LPC 17:0, (B) LPE 17:1, (C) LPS 17:1, (D) PC 15:0\_15:0, (E) PE 17:0\_17:0, (F) TG (19:0)<sub>3</sub>. Loss of linearity is likely caused by self-assembly of lipids in PBS. .... 124

Figure 3.10. Sequential desorption steps from the same SPME probe for lipid standards extracted from PBS (pH 7.4, 100 ng/mL). Desorption time was 30 s for each step using MeOH/IPA/H<sub>2</sub>O (7/2/1, v/v/v) containing 0.1% acetic acid and 10 mM ammonium acetate. Lipid analytes: (A) LPC 17:0, (B) LPE 17:1, (C) LPS 17:1, (D) PC 15:0\_15:0, (E) PE 17:0\_17:0, (F) TG (19:0)<sub>3</sub>..... 125

Figure 4.1. Raman spectra of blank SPME fiber probes bearing different coating chemistries and liquid solutions of fatty acids with an increasing number of double bonds. The Raman spectra of probes normalized at line 2242  $\text{cm}^{-1}$  and the spectra of FAs normalized at the line of 1445  $\text{cm}^{-1}$ ..... 138

Figure 4.2 SPME extraction method development using cod liver oil and 1655  $\text{cm}^{-1}$  Raman shift as the response variable (due to unsaturated lipids, C=C stretching). **A:** Comparison of washing solvent composition. **B:** Extraction time profile; and **C:** Effect of temperature on the extraction of unsaturated lipids. All extractions were performed from 1.0 mL of oil under vortex agitation at 1500 rpm. .... 140

Figure 4.3 On-fiber Raman spectra of fatty acids with increasing double bonds. The spectra normalized at the PAN line of 2242  $\text{cm}^{-1}$ . Extractions performed using C18 coated probes from aqueous *solutions* of fatty acids (0.5 mM, PBS at 25 °C). .... 141

Figure 4.4. On-fiber Raman spectra of pure eicosapentaenoic (TG 20:5\_20:5\_20:5, TG EPA) and docosahexaenoic (TG 22:6\_22:6\_22:6, TG- DHA) triglycerides, locally acquired fish oil, fish oil enriched/doped with 50 mM of each PUFA triglyceride ..... 141

Figure 4.5. Degree of unsaturation obtained from PUFAs solutions with increasing double bonds (0.5 mM in PBS, at 25 °C). The degree of unsaturation is determined as the ratio of Raman band areas at 1655 and 1445  $\text{cm}^{-1}$ , obtained by integrating the spectral ranges of 1601–1700  $\text{cm}^{-1}$  and 1425–1475  $\text{cm}^{-1}$ , respectively. .... 143

Figure 4.6. **(A)** Spectra of coconut oil enriched with 50 mM of two unsaturated fatty acids: oleic acid (FA 18:1) and linoleic acid (FA 18:3). **(B)** Spectra of vegetable cooking oils measured on fiber. **(C)** Spectra of dietary supplements enriched with PUFA triglycerides. .... 145

## List of Tables

Table 1.1 Examples of six categories as proposed by LIPID MAPS consortium. <sup>6,7</sup> .....	3
Table 1.2. Overview the various platforms available for lipid analysis.....	12
Table 2.1. LC-MS/MS parameters employed for targeted quantitation of lipid standards. ....	29
Table 2.2. HPLC-HRMS parameters used in Waters Q-ToF for untargeted analysis. ....	29
Table 2.3. Standards employed in this study with their hydrophobicity expressed as LogP <sup>2</sup> , the monitored MS/MS transitions, and collision energy (ColIE) in V.....	32
Table 2.4 Figures of merit for validation of LC-MS/MS method on TSQ Vantage.....	33
Table 2.5. Lipid metabolites identified in extracts from the NIST SRM® 1950 plasma. ....	62
Table 2.6. Main features of some methods to measure free concentrations. Adapted from Seyfinejad et al. <sup>179</sup> .....	68
Table 2.7. LC-MS/MS conditions for the analysis of model compounds.....	71
Table 2.8. LC-MS/MS conditions used for the analysis of fatty acids. <sup>91</sup> Table 3.1. Source parameters for each SPME-MS approach used.....	108
Table 3.2. MS/MS transitions for the model compounds used for the SPME-MS approaches. ....	108
Table 3.3. Aspiration flow for each solvent and the average peak width using the ESI source for the Vantage and the conditions listed in Table 3.1. ....	120
Table 4.1 Major peaks of different SPME fiber coatings and their assignment. ....	136
Table 4.2 Assignment for Raman band for the fatty acids used as analytes, using the small library presented in Figure 4.1. <sup>64</sup> .....	142

## List of abbreviations

<b>AC</b>	Affinity chromatography
<b>ACN</b>	Acetonitrile
<b>AME</b>	Absolute matrix effects
<b>APCI</b>	Atmospheric pressure chemical ionization
<b>APPI</b>	Atmospheric pressure photoionization
<b>BET</b>	Brunauer –Emmett–Teller
<b>BHT</b>	Butylated hydroxytoluene
<b>CBS</b>	Coated blade spray
<b>CE</b>	Cholesteryl ester
<b>CapE</b>	Capillary electrophoresis
<b>CHCl<sub>3</sub></b>	Chloroform
<b>CLO</b>	Cod liver oil
<b>CMC</b>	Critical micelle concentration
<b>ColIE</b>	Collision Energy
<b>DESI</b>	Desorption electrospray ionization
<b>DG</b>	Diacylglycerides
<b>DHA</b>	Docosahexaenoic acid
<b>DMF</b>	<i>N, N</i> -dimethylformamide
<b>DPPC</b>	Di-palmitoyl phosphatidylcholine
<b>ECD</b>	Electron capture detector
<b>ED</b>	Equilibrium dialysis
<b>EPA</b>	Eicosapentaenoic acid
<b>ESI</b>	Electrospray ionization
<b>ETP</b>	Extraction time profile
<b>FA</b>	Fatty acid
<b>FC</b>	Fold change
<b>FID</b>	Flame ionization detector
<b>HILIC</b>	Hydrophilic interaction liquid chromatography
<b>HV</b>	High voltage

<b>HLB</b>	Hydrophilic-lipophilic balance
<b>HRMS</b>	High resolution mass spectrometry
<b>HSA</b>	Human serum albumin
<b>IMS</b>	Ion mobility spectrometry
<b>IPA</b>	Isopropanol alcohol
<b>IS</b>	Internal standard
<b>LA</b>	Linoleic acid
<b>LC</b>	Liquid chromatography
<b>LLE</b>	Liquid-liquid extraction
<b>LOD</b>	Limit of detection
<b>LogP</b>	Logarithmic octanol–water partition coefficient
<b>LOQ</b>	Limit of quantitation
<b>LP</b>	Lipoprotein
<b>LPC</b>	Lyso-phosphatidylcholine
<b>LPE</b>	Lyso-phosphatidylethanolamine
<b>LPS</b>	Lyso-phosphatidylserine
<b>MALDI</b>	Matrix-assisted laser desorption/ionization
<b>MeOH</b>	Methanol
<b>MG</b>	Monoglycerides
<b>MOI</b>	Microfluidic open interface
<b>MRM</b>	Multiple reaction monitoring
<b>MS</b>	Mass spectrometry, mass spectrometer
<b>nd-SPME</b>	Non-depletive solid phase microextraction
<b>NIST</b>	National Institute of Standards and Technology
<b>NMR</b>	Nuclear magnetic resonance
<b>NPLC</b>	Normal phase liquid chromatography
<b>PA</b>	Phosphatidic acid
<b>PAN</b>	Polyacrylonitrile
<b>PC</b>	Phosphatidylcholine
<b>PDMS</b>	Polydimethylsiloxane
<b>PE</b>	Phosphatidylethanolamine
<b>PEEK</b>	Polyetheretherketone

<b>PG</b>	Phosphatidylglycerol
<b>PI</b>	Phosphatidylinositol
<b>PL</b>	Glycerophospholipid, phospholipid
<b>PP</b>	Protein precipitation
<b>PS</b>	Phosphatidylserine
<b>PUFA</b>	Polyunsaturated fatty acids
<b>QC</b>	Quality control
<b>QqQ</b>	Triple quadrupole
<b>RPLC</b>	Reverse-phase liquid chromatography
<b>RSD</b>	Relative standard deviation
<b>SFC</b>	Supercritical fluid chromatography
<b>SGV</b>	Standard generating vial
<b>SI</b>	Supplementary information
<b>SM</b>	Sphingomyelin
<b>SPE</b>	Solid phase extraction
<b>SPR</b>	Surface plasmon resonance
<b>SPME</b>	Solid phase microextraction
<b>SRM</b>	Standard reference material
<b>TC</b>	Titration calorimetry
<b>TG</b>	Triglycerides
<b>TLC</b>	Thin layer chromatography
<b>TOF</b>	Time of flight
<b>UC</b>	Ultracentrifugation
<b>UF</b>	Ultrafiltration
<b>UPLC</b>	Ultra performance liquid chromatography
<b><math>\alpha</math>-LA</b>	$\alpha$ -Linolenic acid

*hic sunt dracones*

## Chapter 1 Introduction

### 1.1 Lipids

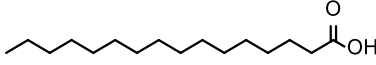
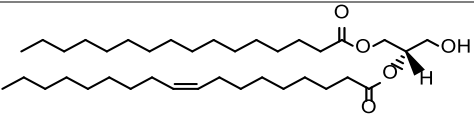
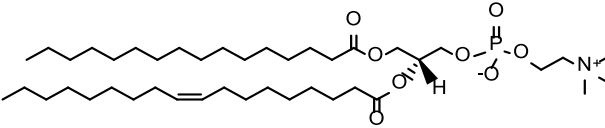
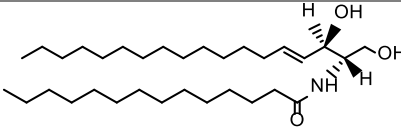
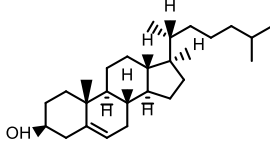
Lipids have been somewhat historically overlooked from a biochemical perspective due to their high structural diversity and poor understanding of their biological functions. After all, defining lipids solely on their high solubility in non-polar compounds, as usually found in most high-school textbooks, are oversimplifications. The most accurate definition for lipids, encompassing the high diversity of molecular lipid structures, was recently coined by the chemists who formed the consortium of lipid metabolites and pathways strategy (LIPID MAPS)<sup>1</sup>. Lipids are small molecules, either hydrophobic or amphipathic (containing both hydrophobic and hydrophilic parts), which originated entirely or, in part, by carbanion-based condensation of thioesters (e.g., fatty acids) and/or by carbocation-based condensation of isoprene units (e.g., prenols, sterols)<sup>1,2</sup>. This classification groups together individual molecular lipid species, viz. those with unique molecular structures, with those sharing chemical structural moieties. The LIPID MAPS consortium classifies lipids into eight categories, namely fatty acyls, glycerolipids, glycerophospholipids, sphingolipids, sterol lipids, prenol lipids, saccharolipids, and polyketides.<sup>2</sup> Some examples of lipids belonging to these categories are shown in Table 1.1. In addition, lipids can be classified into classes within a lipid category. For example, lipid molecular species with a common glycerol backbone linked to an identical polar head group (e.g., choline, serine, or ethanolamine) belong to the same lipid class (e.g., phosphatidylcholines, phosphatidylserines, or phosphatidylethanolamines, respectively). Fatty acyls (FA) are the most known lipid category, which are synthesized by successive elongation steps of an



acetyl-CoA primer with malonyl-CoA groups. Glycerol is present in two categories: glycerolipids (GL) and glycerophospholipids (PL), which include a phosphate group esterified to one of the hydroxyl groups from glycerol. Sterol lipids and prenol lipids are synthesized through a shared pathway; however, their eventual structures differ considerably. Sphingolipids contain intriguing long chain *sphingoid* bases in their core structures. Saccharolipids, as a category, accounts for lipids with fatty acyl groups linked directly to a sugar backbone. Polyketides, the final category, is comprised by a diverse group of metabolites commonly found in plant and microbial sources.<sup>3</sup>

Ever since the discovery of a biologically active phospholipid, the platelet-activating factor, unique biological roles of lipids have been recognized, other than their functions as sources of energy or as building blocks for membranes. It is now acknowledged the influence lipids have on cellular trafficking and activity of membrane proteins and signals.<sup>4</sup> For instance, it is very well known how long-chain fatty acids act as an energy source in the heart and skeletal muscle via a  $\beta$ -oxidative pathway, the sequential removal of two-carbon units from the acyl chains.<sup>5</sup> Hepatic  $\beta$ -oxidation provides ketone bodies to the circulatory system, which are another significant fuel for fasting periods, sustained exercise, or stress. Fatty acids also can be either converted to triglycerides or membrane phospholipids, depending on the tissue and its metabolic demand.

Table 1.1 Examples of six categories as proposed by LIPID MAPS consortium.<sup>6,7</sup>

Categories	Structure examples	Examples of subclasses
Fatty acyls, FA	 Hexadecanoic acid	Fatty acids, Eicosanoids
Glycerolipids	 1-Hexadecanoyl-2-(9Z-octadecenoyl)-sn-glycerol	Monoradylglycerols Diradylglycerols Triglycerides, TG
Glycero-phospholipids, PL	 1-Hexadecanoyl-2-(9Z-octadecenoyl)-sn-glycero-3-phosphocholine	Glycerophosphatidylcholines, PC Glycerophosphatidylethanolamines, PE Glycerophosphatidylserines, PS Glycerophosphatidylglycerols, PG Glycerophosphatidylinositols, PI
Sphingolipids	 N-(tetradecanoyl)-sphing-4-enine	Sphingoid bases Ceramides
Sterol lipids	 Cholesterol	Cholesterol and derivatives Steroids Bile acids and derivatives

Lipids are also well known for their role in cellular membranes, providing a hydrophobic barrier that protects cells from outside medium and helps to separate cellular compartments within the cell. Polar lipids, those with amphipathic properties, easily self-associate in water-rich environments to reduce the total area of hydrophobic ends exposed to the water, resulting in overall energy-stable conformations such as micelles and, more

important to cells, bilayers. Properties of these polar lipids (such as the head group size, the acyl chain length and the degree of unsaturation) have apparent effects on membrane curvature, viscosity, and thickness. For instance, Figure 1.1 portrays the structure of the polar heads for a few glycerophospholipid classes and the possible existing bonds between phosphorylated glycerol and the fatty acyl moieties. Furthermore, there are specialized subdomains within cellular membranes, termed *lipid rafts*, where various signalling proteins are shown to anchor and partition.<sup>8</sup> The fatty acyls of the phospholipids present in lipid rafts tend to be more highly saturated than those in the surrounding membrane. In addition, these lipid rafts have a higher content of sterols (mainly cholesterol in mammals) and sphingolipids and a lower amount of phosphocholines (PC), which results in liquid-ordered domains, membrane rigidity;<sup>9</sup> and the signature property of lipid rafts: insolubility in non-ionic detergents.<sup>10,11</sup>

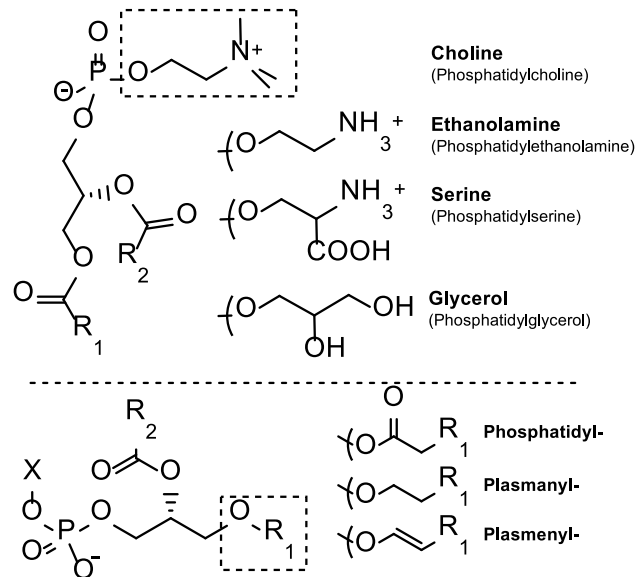


Figure 1.1 Structural variety within glycerophospholipids class, with phosphatidylcholines and phosphatidylethanolamines being the common lipids found in cell membranes. Figure adapted from Han<sup>1</sup> and the LIPID MAPS consortium website.<sup>2</sup>

Lipids are also recognized as key inter- and intracellular signalling molecules for different processes. Polyunsaturated fatty acids serve as *de novo* sources for precursors for molecular messengers; for instance, derivatives of arachidonic acid, such as prostaglandins and lipoxins, are heavily involved in inflammatory responses.<sup>12,13</sup> Sphingolipids are a prominent group of signalling bioactive lipids involved in numerous processes, in addition to being a very diverse lipid category on their own. Sphingosine and related sphingoid bases have roles in endocytosis, cell cycle and apoptosis by exerting effects on protein kinases, regulating responses related to inflammation, cell migration, and apoptosis.<sup>12</sup> Other regulatory molecules for a myriad of processes in mammalian nervous system, such as sleep, mood, appetite, and memory, are the endocannabinoids, a group of endogenous lipid-based neurotransmitters.<sup>14,15</sup>

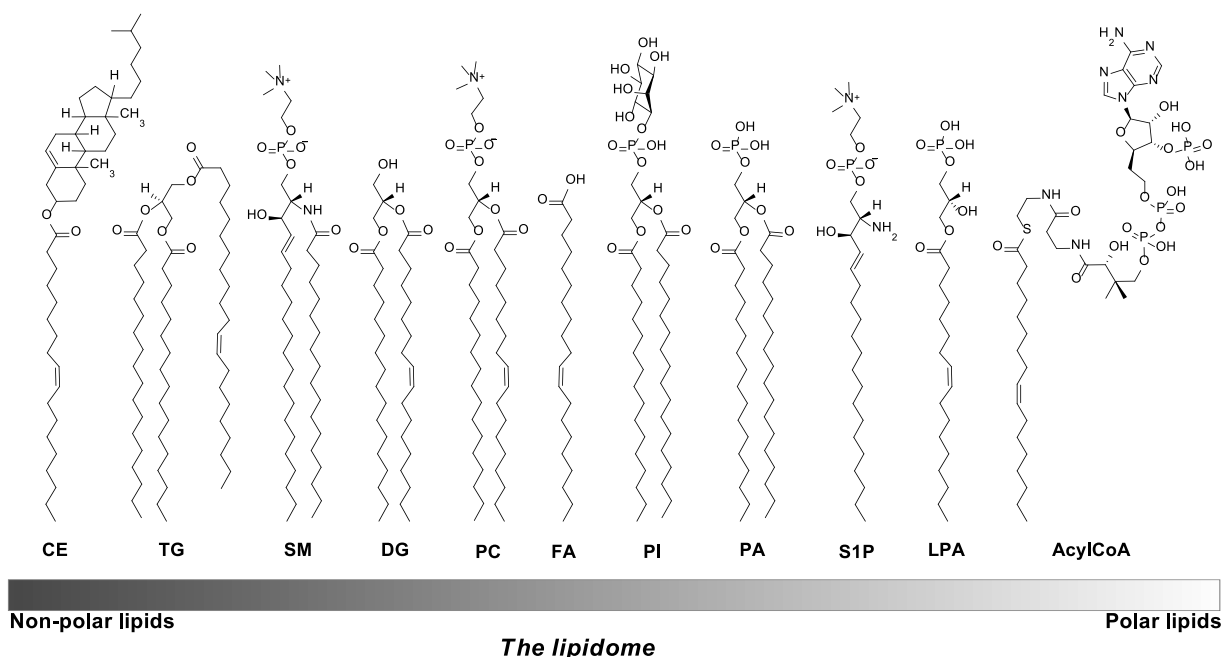


Figure 1.2 A brief (and very much reduced) qualitative example of a lipidome showcasing the diversity of lipid subclasses found across mammal tissues. CE, cholesteryl esters; TG, triglycerides; SM: sphingomyelins; DG, diacylglycerides; PC, phosphatidylcholines; FA, fatty acyls; PI, phosphatidylinositol; PA, phosphatidic acids; S1P; sphingosine 1-phosphate; LPA, lysophosphatidic acid; Acyl CoA, acyl Coenzyme A. Figure adapted from Tumanov & Kamphorst.<sup>16</sup>

The concentration of specific lipid compounds could differentiate healthy from disease states in several serious diseases. Extensive and upcoming evidence in biomedical research has shown the disruption of pathways of lipid metabolism in human diseases; for example, diabetes,<sup>17</sup> asthma,<sup>18</sup> atherosclerosis,<sup>19</sup> Alzheimer’s disease,<sup>20</sup> and many types of cancer. Therefore, lipid analysis has become necessary for both academic and clinical communities as an essential tool for disease research and has become a research field itself: Lipidomics. Lipidomics is a branch of the metabolomics field that has gained popularity with recent advances in analytical method development. Lipidomics is defined as “the full characterization of lipid molecular species and their biological roles concerning the

expression of proteins involved in lipid metabolism and function, including gene regulation.”<sup>21</sup> In other words, lipidomics is about mapping the entire spectrum of lipids in a biological system, including the relation to other molecules of biological interest, to gain an understanding of biochemical mechanisms of lipid metabolism and lipid-associated diseases and to discover lipid biomarkers for disease diagnosis, prognostic monitoring, and as targets for therapeutic monitoring.<sup>22–24</sup> For example, Figure 1.2 portrays eleven lipid species (not counting possible isomers) covering a wide range of polarities, with only two distinct acyl chains, derived from stearic and oleic acids.

## **1.2 Instrumental platforms for lipid analysis**

Due to the vast diversity of lipids, lipidomic studies are very challenging analytical analyses and often require different approaches for comprehensive characterization. Mass Spectrometry (MS), nuclear magnetic resonance (NMR), and other spectroscopic approaches are examples of analytical disciplines used for lipidomic (and lipidomic adjacent) studies. Nonetheless, spectroscopic technologies present some drawbacks that limit their application, such as complicated spectra that demand the expert ability to obtain information, the inability to discriminate information of individual molecules in a complex mixture, and relatively low sensitivity compared to MS.<sup>25</sup> At the same time, NMR spectroscopy has been used for the analysis of lipid extracts; nevertheless, its sensitivity in the high micro-molar to the milli-molar range is limited, and the signals are constricted to a small chemical-shift range.<sup>26</sup> On the other hand, spectroscopic technologies help study dynamic biological processes and are great tools for visualization analysis, similar to mass spectrometric imaging.

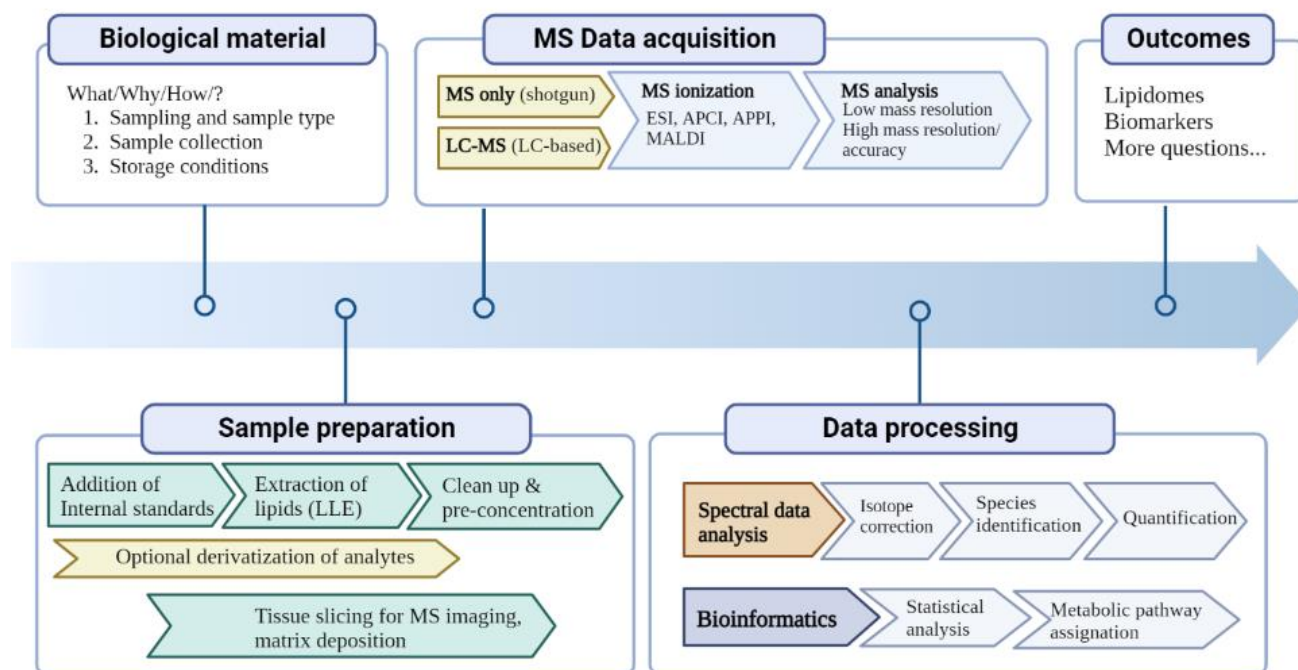


Figure 1.3. Typical workflow for the analysis of lipids from biological samples. Adapted from Yang and Han.<sup>27,28</sup>

A large part of the progress in lipidomics is linked to the development of mass spectrometry (MS) techniques; for instance, Figure 1.3 portrays a general MS-based workflow for the lipidomics analysis of biological samples. The direct infusion MS approach usually referred to as shotgun lipidomics, does not require any previous separation, offering an alternative technology with a less time-consuming nature. In shotgun lipidomics, whole lipid extracts are directly and continuously introduced into the mass spectrometer, with the possibility of analyzing a wide range of molecules with varying physicochemical properties (e.g., polarity, solubility, molecular weight, proton affinity) with concentrations over several orders of magnitude. Because of this, shotgun lipidomics became rather popular in studies requiring high throughput due to many samples, such as in clinical studies or large cohorts.<sup>24,29</sup>

Since ion suppression and ion enhancement are a matter of concern in shotgun lipidomics, the occurrence of matrix effects should be eliminated or minimized during optimization and validation. Internal standards (IS) are directly added to the raw extracts for quantitation effects and to assess matrix effects and efficiency. It is traditional for quantitative methods to use separation technologies such as gas chromatography (GC), liquid chromatography (LC), supercritical fluid chromatography (SFC) and/or capillary electrophoresis, as they are essential tools for the comprehensive analysis of complex samples. When these separation technologies are coupled to MS, the resulting hyphenated techniques can provide large amounts of information. Coupling LC to MS will avoid limitations due to direct infusion of the sample, e.g., ion-suppression effects due to molecules competing for ionization and detection of isomers and isobars. The separation of lipids in LC-MS-based analyses occurs (in a broad sense) either by lipid species or by lipid class, with reverse-phase liquid chromatography (RPLC) used for the former and normal-phase LC (NPLC) or hydrophilic liquid chromatography (HILIC) for the latter. The separation of lipids in RPLC is based on hydrophobicity; carbon chain length and degree of unsaturation play the most prominent roles. Species with longer acyl chains are eluted later than shorter chain lipids, and saturated structures are eluted later than their polyunsaturated analogues. On the other hand, NPLC and HILIC differentiate lipid classes based on their hydrophilic functionalities: their polar head-group classes. Then, parallel use of HILIC and RPLC chromatographic approaches is an alternative to achieve good comprehensive coverage. However, RPLC is used mainly due to lipids' substantially increased separation efficiency as the "intrinsic hydrophilic content of the lipidome is poor



compared to the hydrophobic content present.”<sup>30</sup> In addition, RPLC columns have more widespread use in laboratories for analytes other than lipids.

### **1.3 Extraction methods for lipids**

During sample preparation for lipidomics analysis, lipid extraction and removal of interfering molecules from complex matrices are paramount. Lipidome profile preservation throughout the sample handling processes must be strongly emphasized, as lipids are prone to degradation (i.e., oxidation, peroxidation, and hydrolysis). Nevertheless, degradation can be minimized physically and chemically. For instance, samples should be snap-frozen immediately after collection and stored at very low temperatures ( $-80\text{ }^{\circ}\text{C}$ ) to inhibit enzymatic activity and be thawed slowly. Addition of antioxidants, e.g., butylated hydroxytoluene, at low concentrations (ranging from 0.01 – 0.1% w/v, or 0.1 – 10 mM)<sup>31,32</sup> to the extraction solvents, or bubbling an inert gas (e.g., nitrogen) through the lipid extracts prior to storage, are strategies used to reduce degradation due to reactive oxygen species.<sup>31</sup>

In lipidomics analysis, there is a global need to harmonize sample preparation procedures from sample collection to data processing.<sup>33</sup> Liquid-liquid extraction (LLE) methods take advantage of the relatively high solubility of lipids in non-polar solvents for their extraction from biological samples, such as blood, tissue, or cell cultures. Different solvents used as extraction phases have been introduced for lipidomic analysis to increase lipid recovery, prevent analyte degradation, focus on the extraction of a specific lipid category, and minimize the use of toxic organic solvents. For instance, Matyash et al. introduced a mixture of methanol and tert-butyl methyl ether as a less-toxic alternative to

chlorine-containing organic solvents for the LLE step.<sup>34</sup> Though, there are still some disadvantages for LLE for lipid analysis, namely the formation of emulsions, the need to reconstitute extracts into another solvent, and matrix effects for untargeted analysis.<sup>35,36</sup>

On the other hand, there are other extraction methods used in the typical lipidomic analysis, other than LLE and solid phase extraction (SPE), which have been performed with high efficiency and comprehensive coverage, e.g., ultrasound-assisted extraction of fatty alcohols from olive leaves,<sup>37</sup> pressurized fluid extraction (ethanol, in this case) of lipids from microalgae,<sup>38</sup> and dispersive liquid-liquid microextraction of fatty acids in water samples.<sup>39</sup> Solid-phase micro-extraction has too been used for targeted lipid analysis, namely of fatty acids in beer,<sup>40</sup> low-volatility hydrocarbons in model solutions using polymeric ionic liquids,<sup>41</sup> fatty acid profiling on human buccal mucosal cells,<sup>42</sup> and quantification of polyunsaturated fatty acids in biological fluids.<sup>43</sup>

Table 1.2. Overview the various platforms available for lipid analysis.

Analytical platform	Key features	Advantages	Limitations	Refs.
GC-based	GC-FID, GC-ECD, GC-MS GC-MS/MS	Great resolution and well-understood. Quantitative	Limited to volatile analytes. Derivatization may be required. Loss of biological <i>information</i>	44
LC-based	RPLC HILIC	May be able to separate isomers/isobars Soft ionization of analytes. Quantitative	Low throughput. Sufficient knowledge required <i>a priori</i>	45–47
TLC		Easy to use. Popular for preparative chromatography	Time-consuming	48
SFC		Efficient separation of lipid classes Almost solvent-free	Pressurized fluids Low availability of instruments.	49
Silver chromatography	Coordination complex between silver and $\pi$ electrons	Separation based on unsaturations (number of double bonds, cis/trans configurations, etc.)	Bleeding columns. “Purple fingers” on users	50–52
Shotgun	Tandem MS High Res. MS multidimensional	Straight-forward; simple and fast; semi-qualitative; quantitative	Ion suppression, unable to differentiate isomers and isobars	53–58
MS imaging	MALDI, DESI	Various resolutions are available. Minimal preparations	Prone to experience ion suppression	53,54,59,60
Ion mobility	IMS FAIMS	High-resolution. May separate isomer/isobars without chromatographic separation.	Recent technology, with limited instrument availability.	61,62
NMR spectroscopy	NMR	Non-destructive. Relatively easy data collection	Deuterated solvents are required. Requires high-purity extracts. Multiple signals per compound/s	63
Raman spectroscopy	Raman	Non-destructive. Minimal sample prep. Structural information.	Low sensitivity. Multiple signals per compound.	64,65

FID, flame ion detector; ECD, electron capture detector; TLC, thin layer chromatography; SFC, supercritical fluid chromatography; MALDI, matrix-assisted laser/desorption ionization; DESI, desorption electrospray ionization; IMS, ion mobility spectrometry; FAIMS; Field asymmetric Ion Mobility Spectrometry.

#### 1.4 Solid phase microextraction: a brief summary

Solid phase microextraction (SPME) was introduced in the early 1990s to overcome some limitations of conventional sample preparation techniques, such as LLE and SPE. SPME is a non-exhaustive extraction method which encompasses sampling, sample preparation and analyte enrichment/pre-concentration in one single step, thus reducing the number of analytical steps and, consequently, analytical error.<sup>66</sup>

For analyte extraction, an SPME device, consisting of a small amount of extracting phase immobilized on a solid support (Figure 1.4), is exposed to a sample volume for a defined period. Analytes diffuse from the sample matrix to the extracting phase, where analytes are either absorbed within the extracting polymer or adsorbed in its surface. Figure 1.4, shows the profile of analyte absorption onto the SPME coating over time. Determination of the amount of extracted analyte under appropriate comparable conditions leads to quantification. Calibration methods suitable for SPME, each one with its advantages and disadvantages, rely on principles of mass transfer of analytes. Additionally, to traditional calibration methods, i.e., external standard, internal standard, and standard addition, SPME calibration approaches also include equilibrium extraction, exhaustive extraction, and diffusion-based calibration.<sup>67,68</sup>

On the other hand, there are other extraction methods used in lipidomic analysis, other than LLE and SPE, which have been performed with high efficiency and wide coverage, e.g., ultrasound-assisted extraction of fatty alcohols from olive leaves,<sup>37</sup> pressurized fluid extraction (ethanol, in this case) of lipids from microalgae,<sup>38</sup> and dispersive liquid-liquid

microextraction of fatty acids in water samples.<sup>39</sup> Solid-phase micro-extraction has too been used for targeted lipid analysis, namely of fatty acids in beer,<sup>40</sup> low-volatility hydrocarbons in model solutions using polymeric ionic liquids,<sup>41</sup> fatty acid profiling on human buccal mucosal cells,<sup>42</sup> and quantification of polyunsaturated fatty acids in biological fluids.<sup>43</sup>

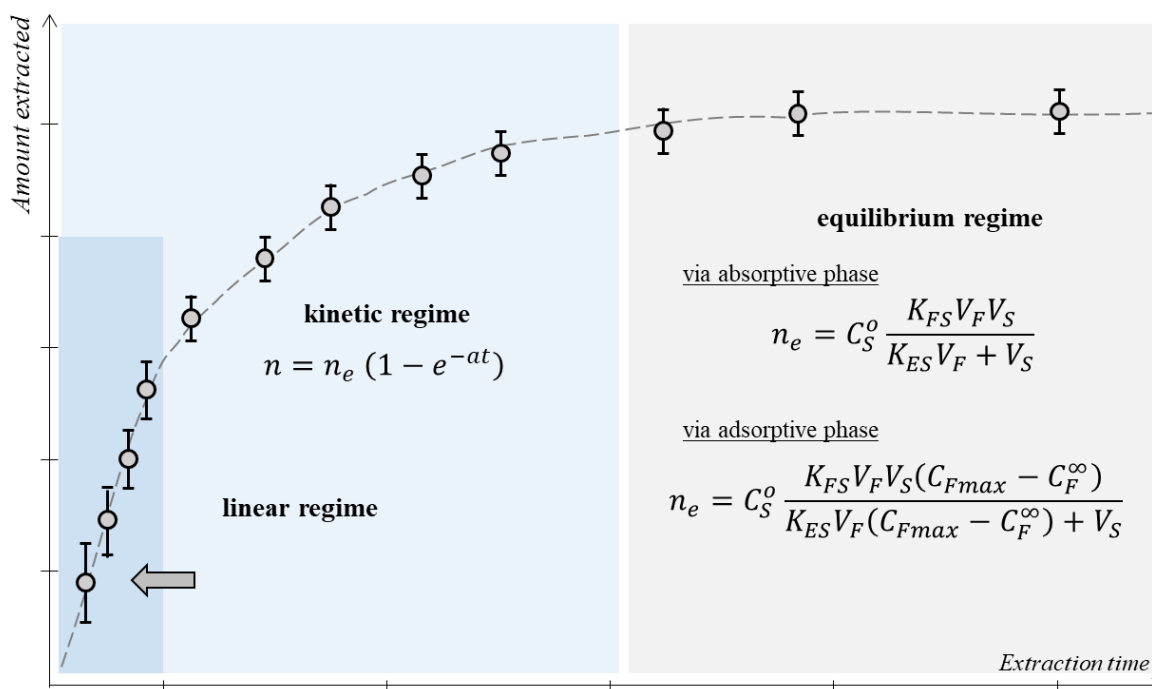


Figure 1.4 SPME sample preparation and analyte absorption over time. (A) Sample preparation scheme for SPME.  $V_F$ , fiber coating volume;  $K_{FS}$ , fiber/sample distribution coefficient;  $V_S$ , sample volume;  $C_O$ , initial concentration of analyte in the sample. (B) The typical profile of analyte uptake in SPME devices.  $t_{50}$ , time required for extraction of half maximum analyte;  $t_{95}$ , time required for extraction of 95% maximum analyte.<sup>68</sup>

Practical equilibrium times are assumed to be achieved when 95% of the equilibrium amount is extracted from the sample because actual equilibrium times would be infinitely long. One advantage of using sampling times near such times,  $t_{95}$ , is the low relative error on the amount of analyte extracted compared to sampling on the steep slope in the kinetic

regime. Analysis performed prior to  $t_{95}$  require precisely timed extractions to minimize the relative error in the amount of analyte extracted. Nevertheless, extractions performed in the kinetic regime are faster and more real-life convenient.

$$C_O V_S = C_S^\infty V_S + C_F^\infty V_F \quad \text{Eq. 1}$$

$$K_{FS} = \frac{C_F^\infty}{C_S^\infty} \quad \text{Eq. 2}$$

$$n = C_F^\infty V_F = C_O \frac{K_{FS} V_S V_F}{K_{FS} V_F + V_S} \quad \text{Eq. 3}$$

$$n = n_e (1 - e^{-at}) \quad \text{Eq. 4}$$

Equation 4 is a non-linear equation describing the kinetics of analyte absorption and the relationship between analyte extracted,  $n$ , as a function of extraction time, the initial concentration of the analyte in the sample,  $C_O$ . The extraction rate is constant,  $a_e$ , refers to how fast equilibrium is attained and depends on volumes of extracting phase, sample volume, mass transfer and partition coefficients, and the surface area of the extracting phase.<sup>69,70</sup> This mathematical description of kinetic uptake can, therefore, be used for quantification, as introduced by Chen & Pawliszyn.<sup>71,72</sup> Equilibration time depends on the distribution constant, so the higher the affinity the analyte has for the coating, the longer the time to reach equilibrium.<sup>73</sup>

A significant improvement in the application of SPME in biological samples is the introduction of polyacrylonitrile (PAN) based coatings, acting as a binding agent to immobilize coating particles. PAN-based coatings did not absorb proteins onto their

surface, proving biocompatible and preventing SPME fiber fouling.<sup>74</sup> Overcoated SPME is another recent improvement in matrix-compatible coatings: the coating is embedded by a biocompatible protection layer, which prevents matrix attachment. These matrix-compatible coatings developments have shown a balanced coverage of analytes extracted from complex matrixes, selectivity for small molecules, robustness to direct exposure to complex, untreated matrixes, and suitability for in vivo sampling.<sup>75–78</sup>

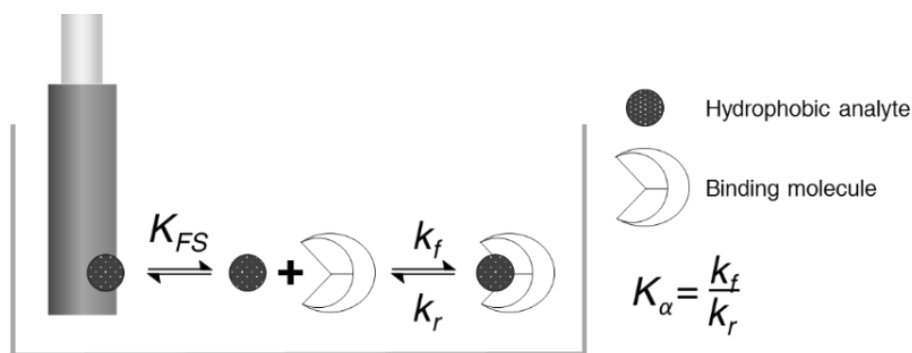


Figure 1.5 Schematic depiction of analyte extraction from a sample with a binding component. Analyte extraction depends on its coating–sample distribution constant,  $K_{FS}$ , and its binding constant with the matrix binding components,  $K_\alpha$ . The binding constant is a relationship between the forward,  $k_f$ , and backward,  $k_r$ , binding reaction constants.

Figure adapted from Alam and Pawliszyn.<sup>79</sup>

One key feature offered by SPME is its extraction from the pool of freely dissolved analytes.<sup>67</sup> However, the kinetics of bound components in complex matrixes must be considered, as free–form extraction depends on the desorption kinetics from matrix components; a general depiction is shown in Figure 1.5. Hydrophobic compounds are typically heavily bound to the matrix, so their free concentration is low (e.g., fatty acids are bound by plasma albumin), yet total recoveries are relatively high because of their high affinity for the extracting phase. On the other hand, polar compounds are at a high free concentration in the sample due to light matrix-binding. Therefore, a proportionally higher

amount is extracted despite a lower affinity for the coating.<sup>70,79</sup> These combined effects result in a balanced coverage of extracted analytes from a complex matrix.<sup>79</sup>

## **1.5 Research objectives**

SPME has been applied for the analysis of lipid compounds, either as the primary analytes or as an analyte subgroup, in a variety of samples of biological or clinical interest, including cell cultures,<sup>80</sup> human breast milk,<sup>81</sup> beetle homogenates,<sup>82</sup> rat brain,<sup>83-86</sup> fish muscle tissue,<sup>87-89</sup> a variety of cancer-related samples in/from human (such as ovarian,<sup>90</sup> lungs,<sup>91,92</sup> urinary/bladder,<sup>93</sup> breast carcinoma,<sup>93</sup> gastric-related cancer,<sup>94</sup> gliomas<sup>95</sup>). These semi-quantitative studies are examples of SPME's latest niche application: -omics and clinical studies. AP. Birjandi et al.'s work on quantifying polyunsaturated fatty acids in plasma samples sparked research toward other quantitative applications of SPME for analyzing lipids in biological samples.<sup>43</sup> The research group has a broad objective of developing methods for (potential) SPME users. Previous studies suggest that SPME is a promising technique for quantitating polar lipids, but challenges exist when quantitating hydrophobic lipids. As such, the extraction and quantitation of polar lipids are more beneficial. The dissertation aims to prove SPME's quantitative capabilities for lipid extraction, aligning with SPME's drive for quantitative analysis of biological samples.

This dissertation seeks to further this line of inquiry by studying extraction with SPME devices, specifically concerning lipid analysis. To this end, three SPME-based methods are used to assess their quantitative capabilities: SPME coupled to liquid-chromatography-mass spectrometry (SPME-LC-MS), SPME directly coupled to mass spectrometry



(SPME–MS); and SPME coupled to Raman spectroscopy. Each of the chapters in this thesis, which respectively detail the SPME-based methods, supports the overall research objective: to appraise SPME as a viable method for sampling and quantitation of lipids in biological matrices.

Chapter 2 details the approaches toward determining the total and free concentration of various lipids using SPME devices and LC-MS/MS as the analytical platform. First, an SPME method was optimized for total concentration by studying coating chemistry, extraction time, desorption solvent type and time. The selected method enabled the construction of good matrix-matched calibration curves using four lots of human plasma. Chapter 2 also details the free concentration determinations' approaches to estimate the binding affinity between human serum albumin and a polyunsaturated fatty acid. This approach involved the experimental determination of key parameters for SPME calibration, such as the partition coefficient and the active surface area for the SPME device with a solid sorbent. Then, mathematical modelling was used to validate the mass uptake profiles obtained experimentally under three distinct cases: static extraction, agitated extraction, and extraction with a binding matrix.

Chapter 3 presents a method entailing the direct coupling of SPME and mass spectrometry. Here, two approaches for sample introduction to the mass spectrometer were considered: coated blade spray (CBS) and microfluidic open interface (MOI). Chapter 3 intended to develop a viable method for quantifying glycerophospholipids in a shotgun

fashion. Both sample introduction approaches evaluated desorption solvent type and time, probe carryover, and absolute matrix effects.

Chapter 4 documents the coupling of matrix compatible SPME fibers and Raman spectroscopy as a non-destructive approach. This proof-of-concept study examined the on-fibre detection of unsaturated fatty acids, with the Raman shifts being assigned to motifs in the chemical structures of standards of polyunsaturated fatty acids (PUFAs) and triglycerides with PUFA acyl residues. The method evaluated coating chemistry, extraction time, extraction temperature, and the cleaning solvent aiming at intense Raman signals. The developed method was then applied to detect PUFAs with increasing numbers of double bonds in their structures.

## **Chapter 2 Towards the determination of total and free lipid concentrations**

### **Preamble**

This chapter contains an excerpt from a manuscript accepted for publication as a technical note to *Analytical Chemistry*. The manuscript is titled: “Standard generating water vial system for hydrophobic compounds” and was coauthored with Demet Dincel and Shakiba Zeinali and co-authored/supervised by Janusz Pawliszyn. The author of this thesis participated in all stages of the preparation of this manuscript (regarding phospholipid analysis): namely experimental planning and execution, data processing and curation, data analysis, manufacturing of devices, manuscript writing and submission.

This chapter also contains a short excerpt from a manuscript entitled, “Investigation of binding of fatty acids to serum albumin to determine free concentrations: Experimental and *in-silico* approaches,” which was co-authored with Mohammad Huq and supervised by Janusz Pawliszyn (*Analytica Chimica Acta*, **2022**, 1192: 339370.). Apart from the COMSOL calculations, which were performed by Mohammed Huq, the author of this thesis participated in all stages of the manuscript-preparation process: namely experimental planning and execution, data processing and curation, data analysis, manufacturing of extraction devices, manuscript writing, submission and replies to reviewers.

This chapter is divided into three sub-chapters, each of which covers distinct applications of solid phase microextraction (SPME) devices for the analysis of lipids using liquid chromatography coupled to mass spectrometry (LC-MS) as the instrumental

platform. The sub-chapters highlight the versatility of the SPME technology to address the challenge of quantitating the total concentration of lipids in plasma (as shown in subchapter 2.1) and the challenges for the quantitation of free concentration (as shown in subchapters 2.2 and 2.3). Subchapter 2.1 features the study of experimental parameters that are relevant during the method development stage. Subchapter 2.2 addresses the challenge of determining the free concentration of hydrophobic compounds, using a few model bioactive lipids as analytes. This short subchapter entails the simple steps towards miniaturization of the extraction device in a non-depletive fashion, in addition to the initial evaluation of the standard generating vials as a viable strategy to generate external calibration curves. Finally, subchapter 2.3 addresses the study of the multi-phase equilibria between a fatty acid, a binding component, and the extraction device. In conclusion, these sub-chapters follow the overarching theme of lipid analysis using solid phase microextraction devices (and its fundamentals) and using LC-MS as the analytical platform.

## **2.1 Towards lipid total concentration with solid phase microextraction devices**

### **2.1.1 Introduction**

Lipids are indispensable biomolecules involved in numerous physiological functions, such as energy storage, insulation, signalling, and cell membrane structure. Several clinical disorders, such as obesity and insulin resistance,<sup>17</sup> diabetes mellitus,<sup>17</sup> and Alzheimer's disease,<sup>96</sup> have been associated with alterations in lipid metabolism. The study of the total concentration of lipids in plasma gives crucial data about a person's metabolic health and is commonly employed in the clinical diagnosis of lipid-related disorders such as hyperlipidemia, cardiovascular disease, and obesity.<sup>17</sup>

Lipoproteins (LPs) are highly dynamic, soluble protein-lipid complexes that transport lipids in vertebrates' circulation (and even in insects).<sup>97</sup> LPs are synthesized in the liver, modified from precursor LPs, or assembled at cell membranes from existing cell lipids. LPs undergo enzymatic reactions of their lipid components, spontaneous and assisted lipid transfers, and soluble apolipoprotein transfer. LPs are commonly categorized based on their hydrated density (in descending order) into chylomicrons; very low-density lipoproteins (VLDL), low-density lipoproteins (LDL), and high-density lipoproteins (HDL). Their diameters correlate inversely with their density. Each type of lipoprotein has a unique composition of lipids, proteins, and enzymes, which allows it to perform specific functions in lipid transport and metabolism. The composition and relative levels of different lipoproteins in plasma can provide important information about lipid metabolism and

health status. Lipoproteins are key markers of cardiovascular health and dyslipidemia, and their levels can be tested in a regular blood test as part of a lipid profile.<sup>98</sup>

However, not only are lipids exceedingly complex in composition and structure, but their concentration is also highly dynamic. The plasma lipidome is estimated to consist of over 500 distinct lipid molecular species with varying concentrations.<sup>99</sup> The headgroup and the kind of connection between the headgroup and acyl chains determine the classes and subclasses of lipids. The acyl chains vary in length (i.e., number of carbon atoms), unsaturation degree, and potential branching. These variations in lipid headgroup and acyl chain contribute to the vast number of distinct lipid molecular species, making it nearly impossible to fully characterize the whole lipidome by a single approach.

Solid phase microextraction (SPME) is a relatively new and innovative technique that has gained recognition in the analytical field due to its simplicity, speed, and low sample consumption.<sup>100</sup> Despite its growing popularity, the importance of proper lipid extraction and analysis techniques cannot be overstated, as variations in sample preparation can significantly impact the accuracy and reproducibility of lipid analysis results. The presented research, albeit *short*, investigates some parameters to be considered during a method development geared towards determination of the total concentration of lipids in plasma using SPME devices. The findings of this study may contribute to developing reliable and robust SPME-based lipid analysis protocols for use in clinical and research settings.

## 2.1.2 Experimental

### Materials, supplies, and standards

LC–MS grade methanol (MeOH), isopropanol (IPA), acetonitrile (ACN), and water (H<sub>2</sub>O) were purchased from Fisher Scientific (Hampton, NJ, USA). LC–MS-grade formic acid, acetic acid, ammonium acetate (NH<sub>4</sub>Ac) were acquired from Sigma Aldrich (Oakville, ON, Canada). LC–grade acetone, mixture of hexanes, chloroform (CHCl<sub>3</sub>), polyacrylonitrile (PAN), *N, N*-dimethylformamide (DMF), and butylated hydroxytoluene (BHT) were acquired from Millipore-Sigma (Oakville, ON, Canada).

Pooled human plasma (non-filtered, stabilized with K<sub>2</sub>EDTA) was obtained from BioIVT (NY, USA) and kept frozen at –80 °C until needed. Appropriate plasma aliquots were thawed over ice prior to each experiment, never allowing more than one freeze-thaw cycle. Lipid standards were purchased from Avanti Lipids (Birmingham, IL, USA). Individual primary stock standard solutions of individual lipids were prepared using chloroform and stored at –80 °C for up to 4 months, after which they were discarded and prepared anew. Working standard solutions were prepared weekly by sequential dilution using MeOH and stored at –80 °C. Instrumental calibration curves and quality control (QC) samples were prepared in the 0.1– 500 ng/mL range and at 25 ng/mL, respectively.

Silica particles functionalized with octadecyl (C18, 40 µm and 5 µm particle size) and custom-made SPME C18-coated fibers (40 µm coating thickness) were a kind gift from Supelco (Oakville, ON, Canada). Commercial hydrophobic lipophilic balance particles

(Oasis HLB) were a kind gift from Waters Corporation. In-house HLB particles used were synthesized (not by the author) following the protocol published elsewhere.<sup>101</sup>

#### Suspension of particles preparation and fabrication of SPME probes

In-house preparation of SPME probes utilized either stainless-steel probes from Shimifrez Inc. (Concord, ON, Canada) or nitinol wire (SE508 alloy, 200  $\mu\text{m}$  diameter) from Confluent Medical (Fremont, CA, USA) as the solid support. To manufacture the SPME probes, polymeric particles were deposited onto a solid support following a coating dipping procedure developed in our laboratory and reported previously.<sup>102</sup> All probes underwent an etching process to increase the mechanical stability of the thin coating layer. For instance, stainless-steel probes (Shimifrez, ON, Canada) were chemically etched by submersing the probes in concentrated hydrochloric acid while being agitated at 90 rpm (60 min total); then, two washing steps with water and one with methanol were made (15 min each, 90 rpm); then dried in an oven at 120 °C for an hour. Contrary to the stainless-steel probes, nitinol wires (SE508 alloy, 200  $\mu\text{m}$  diameter) were mechanically etched using 320-Grit sandpaper, quickly rinsed with methanol under agitation (30 min, 1000 rpm), and allowed to air-dry.

The coating for the SPME probes employed a suspension of sorbent particles – also referred to as a coating *slurry*. Briefly, the polyacrylonitrile (PAN) matrix-compatible binder was prepared by dissolving 2.5 g of PAN in 36.5 mL of *N, N*-dimethylformamide (DMF) – aided by heating to approximately 90 °C while stirring every 15 min, until complete dissolution. This binder was mixed with particles to obtain a 10% (w/w)



suspension (a coating *slurry*), vortexed at 2000 rpm for 10 min and left stirring overnight at 800 rpm with a magnetic bar.

Each probe was coated initially using the binder solution (only PAN/DMF, *sans* particles) to create a thin (<0.5  $\mu\text{m}$  thickness) coating, referred to as *undercoating*, intended to minimize direct interactions of the matrix with the solid support.<sup>103</sup> Then, the coating was achieved via repeated dipping of the probe into the particle-containing slurry until the desired coating thickness was obtained. Desired thicknesses were achieved by varying the withdrawal speed and the number of layers. After each layer, the probe was allowed to air-dry in a fume hood, then cured in an oven for 60 s at 125 °C.<sup>104</sup> The coating thickness for the probes was measured using a digital micrometre (Uline, ON, Canada). The probes were cleaned (30 min, 100 rpm) with a solvent mixture (MeOH/ACN/IPA/H<sub>2</sub>O, 3/3/3/1, v/v) to remove impurities from handling and debris from fabrication, then kept immersed in fresh solution until needed.

#### General procedure for extractions

A typical sample preparation using the SPME probes involves five steps: probe cleaning; preconditioning the coating for extraction; extraction from the sample; a quick rinse step; and solvent desorption. First, an additional cleaning step using the same solvent mixture (MeOH/ACN/IPA/H<sub>2</sub>O, 3/3/3/1, v/v) with agitation at 1000 rpm for 30 min. For preconditioning, the probes were exposed for 30 min to MeOH/H<sub>2</sub>O (1/1, v/v) under agitation at 1000 rpm to activate the reverse-phase sorbent pores in the extracting phase prior to exposure to an aqueous sample. Then, the extraction occurred under vortex

agitation at 1000 rpm for a pre-determined period, ensuring all the coating was fully submerged in the sample. Then, a quick rinse step (3–5 s) in acetone/water (9/1, v/v) to dislodge loosely attached analytes/matrix components from the probes. Occasionally, lint-free tissue was used to clean the probes with visible attachments further. Finally, the probes were desorbed in the solvent under agitation at 1000 rpm for 60 min. Unless specified differently for a particular experiment or section, the desorption solvent was composed of IPA/MeOH/H<sub>2</sub>O (45/45/10, v/v). The desorption solvent also contained 1 mM of butylated hydroxytoluene as an antioxidant, added as a precautionary measure to minimize any possible lipid peroxidation.<sup>105</sup>

#### Liquid chromatography and (Targeted) Mass Spectrometry

The chromatographic separation conditions used are described in Table 2.1, using the method by Monnin et al. as reference.<sup>106</sup> Table 2.1 summarizes chromatographic conditions used for separation. Targeted experiments were carried out on a TSQ Vantage™ triple-quadrupole mass spectrometer (Thermo Scientific, CA, USA) equipped with a heated ESI ionization source. Optimum collision energy and S-lenses conditions were determined for each compound via direct infusion of standards. Data processing was done using Trace Finder 4.1 from Thermo Scientific. The amount of lipids extracted in nanograms was determined based on instrumental calibration curves of target analytes spiked in neat desorption solvent in the 0.1–500 ng/mL range.

Absolute relative matrix effects were evaluated according to the method proposed by Matuszewski et al.<sup>107</sup> Concisely, if one depicts the peak areas obtained in neat solution

standards as *A*, and the corresponding peak areas for standards in *blank* plasma extracts spiked *after* extraction as *B*, then absolute matrix effects (AME) for analytes are estimated with the equation below (provided both *A* and *B* are spiked at the same concentration level). Hence, between 80 – 120 % AME values are regarded as minimal/no absolute matrix effects from the method; AME values higher than 120% are an indication of positive matrix effects causing ion enhancement by concomitant extraction of matrix components; and AME values under 80% represent negative matrix effects resulting from ion suppression from coextracted matrix components.

$$AME = (B/A) \times 100 \quad \text{Eq. 5}$$

#### Qualitative glance for SRM® 1950 plasma using Liquid chromatography and high-resolution mass spectrometry

For the qualitative analysis of the standard reference material SRM® 1950, an untargeted approach with high-resolution mass spectrometry (HRMS) coupled with ultra liquid chromatography (UPLC). The chromatographic separation was carried out by Waters Acquity M-class UPLC system M-class system coupled to a Q-tof mass analyser Waters Xevo Q-Tof G2-S (Waters Corporation, Manchester, UK) with the conditions summarized in

Table 2.2 for positive and negative ionization modes. Data acquisition was conducted using full scan mode in the *m/z* range 100–1000 and using MassLynx software (version 4.1). The *raw* data files were converted into the mzXML using the MSconvert toolkit (ProteoWizard 3.0).<sup>108</sup> The IPO<sup>109</sup> package was applied for optimization of peak picking and retention time correction, followed by online-based XCMS<sup>110</sup> package for peak extraction, filling, grouping, and alignment via the R script developed in-house.<sup>87,111</sup> The resulting list of *features* underwent filtering to discard peaks with significant variance and

artifacts from blank samples: Peaks exhibiting relative standard deviation in their intensity across all samples above 30%, as well as signal-to-noise under 5 (relative to blank desorption solvent samples and blank SPME probes samples) we discarded, as per the acceptance criteria. The xMSAnnotator Integrative Scoring Algorithm was used to annotate features based on retention time clusters, adduct formation, isotope patterns, and abundance, and pathway analysis.<sup>112</sup> Then, these features were manually curated against databases such as LIPID MAPS<sup>6,7,113</sup> and METLIN<sup>113</sup> to provide (*realistic*) identities.

Table 2.1. LC-MS/MS parameters employed for targeted quantitation of lipid standards.

<b>Mass spectrometry conditions – Thermo TSQ Vantage™</b>	
Spray voltage	3.0 kV in positive mode
Vaporizer temperature	300 °C
Transfer capillary temp.	350 °C
Sheath gas, arb	30 arb
Auxiliary gas, arb	40 arb
Sweep gas, arb	10 arb
Dwell time	10 ms/ transition
<b>Liquid Chromatographic conditions – Thermo Vanquish Flex UHPLC</b>	
Column	Waters Acquity CSH® C18 1.7 µm, 2.1×75 mm
Mobile phase A	H <sub>2</sub> O/MeOH (6/4)
Mobile phase B	MeOH/IPA (2/8)
Additives in + mode	1 mM acetic acid, 10 mM ammonium acetate
Additives in – mode	0.05 % (v/v) acetic acid
Flow rate	350 µL/min
Column temperature	55 °C
Samples temperature	5 °C
Injection volume	10 µL
Gradient [min, %B]	0.0 min, 20%; 1.0 min, 20%; 4.0 min, 80%; 6.0 min, 95%; 8.8 min, 95%; 8.9 min, 20%; 10 min, 20%

Table 2.2. HPLC-HRMS parameters used in Waters Q-Tof for untargeted analysis.

<b>Xevo G2-S</b>	Spray voltage	1.2 kV
------------------	---------------	--------

<b>Q-ToF MS</b>	Cone voltage	40 V
	Source offset	80 V
	Capillary temperature	250 °C
	Source block temperature	100 °C
	Acquisition mode	MS Sensitivity
	Scan time	250 ms
	Mass range	100 – 1000 <i>m/z</i>
	Lock Mass acquisition	LeuEnk ( <i>m/z</i> 556.2371 [M+H] <sup>+</sup> , <i>m/z</i> 556.2371 [M-H] <sup>-</sup> ); scan time 50 ms, interval 30 s, 10 scans to average
	Mass Calibration	0.5 mM sodium formate; MS mode between 110–1000 <i>m/z</i>
<b>Waters UPLC M-class</b>	Column	Waters Acquity CSH® C18 1.7 μm, 2.1×75 mm
	Mobile phase A	H <sub>2</sub> O/MeOH (6/4, v/v)
	Mobile phase B	MeOH/IPA (2/8, v/v)
	Additives in + mode	1 mM acetic acid, 10 mM ammonium acetate
	Additives in – mode	0.1 % (v/v) acetic acid
	Flow rate	300 μL/min
	Column temperature	55 °C
	Temperature autosampler	5 °C
	Injection volume	10 μL
	Gradient [%B]	0.0 min, 20%; 2.0 min, 20%; 2.5 min, 50%; 14.0 min, 90% 17.0 min, 95%; 17.1 min, 20%; 21.0 min, 20%

### 2.1.3 Results and discussion

#### Liquid chromatography and mass spectrometry

The target analytes were selected for method development based on their availability, aiming at ultimately covering multiple lipid classes of those likely to be found in plasma. Though, a certain focus was taken on glycerophospholipids (PL): the most abundant on a weight basis,<sup>99</sup> and they drew the author's scientific curiosity. Overall in this dissertation, the studied compounds represented few of the major categories, such as fatty acids (including saturated and poly-unsaturated), glycerolipids, and various glycerophospholipids subclasses, and offered a wide range of polarities, as inferred from their LogP values in the 6–20 range.<sup>2</sup> Synthetic lipid standards were selected as these odd-chained lipids (also referred to as *exogenous* lipids) portray fragmentation patterns that reflect naturally occurring lipids (i.e., *endogenous* lipids),<sup>24,59</sup> while being rarely found in most biological samples. Shorthand lipid notation is used throughout the dissertation to refer to studied compounds.<sup>114</sup> A complete list of lipid standards used is included in Table 2.3. Choosing reverse phase column chromatography (RPLC) was preferred over other chromatographic separation, as the used of RPLC substantially increases the separation efficiency of lipids compared to normal phase or HILIC, as the intrinsic hydrophilic content of the lipidome is poor.<sup>30,31,115</sup> The chromatographic method is based on a previous method intended for untargeted studies of lipids extracted from proxy brain tissue.<sup>106,116</sup> By modifying the flow and solvent gradient, enough separation was obtained for the major lipid categories in a single 10-minute run. The method's validation parameters are presented in Table 2.4.

Table 2.3. Standards employed in this study with their hydrophobicity expressed as LogP<sup>2</sup>, the monitored MS/MS transitions, and collision energy (CollE) in V.

Lipid standard	LogP	m/z Precursor	m/z Frag. 1 [CE]	m/z Frag. 2 [CollE]	S lens (V)
LPC 17:0	6.40	510.4	184.1 [16]	104.1 [23]	15
LPC 16:0	6.01	496.4	184.1 [16]	104.1 [23]	15
LPE 17:1	6.23	465.3	324.1 [19]	–	17
LPS 17:1	5.68	510.4	324.1 [19]	–	17
PC 15:0_15:0	11.26	706.5	184.1 [25]	464.3 [32]	19
PC 16:0_16:0 (DPPC)	12.04	734.5	184.1 [25]	492.3 [32]	20
PE 17:0_17:0	12.87	720.6	579.6 [15]	253.2 [25]	17
PE 16:0_18:1	12.65	718.5	577.5 [15]	265.3 [27]	17
PS 17:0_17:0	12.33	764.5	579.5 [25]	494.2 [34]	16
PG 17:0_17:0	12.55	768.6	579.5 [24]	327.3 [27]	16
TG 19:0_19:0_19:0	20.80	950.9	635.6 [24]	–	19
$\alpha$ -LA (FA 18:3- $\omega$ 6) §	5.66	277.3	277.3 [5]	229.1 [24]	12
LA (FA 18:2- $\omega$ 3) §	5.88	279.3	279.3 [5]	231.1 [24]	12
FA 13:0 §	4.38	213.2	213.2 [5]	169 [24]	12

§ Negative ion mode.

The MS/MS spectra for FA also included dehydration products  $[M - H - H_2O]^-$  with CV set at 15 V.

Table 2.4 Figures of merit for validation of LC-MS/MS method on TSQ Vantage.

Standard	LOD (ng/mL)	LOQ (ng/mL)	Dynamic range	Precision, %	
				Inter-day	Intraday
LPC 17:0	0.1	0.5	0.5 – 500	2	7
LPC 16:0	0.1	0.5	0.5 – 500	2	3
LPE 17:1	1.0	5.0	5 – 500	3	5
LPS 17:1	1.0	5.0	5 – 500	2	6
PC 15:0/15:0	0.05	0.5	0.5 – 750	2	3
PC 17:0/17:0	0.05	0.5	0.5 – 700	3	4
PC 19:0/19:0	0.05	0.5	0.5 – 750	2	4
PC 16:0/16:0	0.05	0.5	0.5 – 750	2	3
PE 17:0/17:0	0.5	1.0	1 – 750	3	6
PE 16:0/18:1	1.0	5.0	5 – 500	4	7
PS 17:0/17:0	0.5	1.0	1 – 750	3	7
PG 17:0/17:0	0.5	1.0	1 – 750	3	7
TG (19:0) <sub>3</sub>	1.0	5.0	5 – 500	6	10

By tuning in the presence of the chosen mobile phases, in a 1:1 ratio by volume, the source settings for efficient ionization and subsequent fragmentation were obtained, as presented in Table 2.3. Ionization of PLs occurred primarily by formation of protonated adducts with typical fragmentation patterns based on their polar heads (e.g., neutral head loss for PE, PS and PG; phosphocholine ion formation for PC), and less intense fragments based on their fatty acyl moieties. In contrast, very hydrophobic lipids such as triglycerides and cholesteryl esters exclusively formed ammonium adducts. The ionization of fatty acids readily occurred via deprotonated adducts, yet they exclusively produced dehydrated and decarboxylated fragments. Analysis of unesterified fatty acids in samples of biological interest is typically carried out using derivatization strategies to increase their selectivity and sensitivity.<sup>117–119</sup> Fatty acids were not further regarded as analytes for this subsection for two main reasons: (i) dehydration and decarboxylation fragments are typically disregarded in MS for their lack of specificity, which would have posed a problem for real



(complex) plasma samples without additional sample preparation steps; (ii) Birjandi et al. had already proposed a SPME-based study on the quantitation of (polyunsaturated) fatty acids from plasma samples using a LC-MS/MS platform using unfragmented deprotonated molecular ions.<sup>43</sup> Instead, these fatty acids are used as model compounds for the study presented in sub-chapter 2.3.

As lipids are known to lack water solubility; therefore, in instances where a sample is prepared in PBS, self-aggregation of lipids due to *over-spiking* is expected. The PBS samples are a mere simplification of the matrix complexity to study lipids, with the same pH and ionic strength as normal physiological conditions.<sup>120</sup> Moreover, lipids are known to self-assemble into diverse configurations (e.g., bilayers, micelles, vesicles, liposomes, etc.) with varying degrees of order and molecular organization.<sup>121</sup> For this thesis, these aggregates are referred to using the umbrella term ‘micelles’; their exact physicochemical nature was not investigated, as that was way outside the scope of the research; and assumed to not participate during SPME mass transfer, as SPME’s extraction is believed to occur via free concentration.<sup>66,68</sup>

### **Coating selection, desorption conditions and carryover**

Coating selection is the classic initial part of SPME method development, as the SPME performance highly depends on the affinity between analytes and the extraction phase. Said affinity is represented by the SPME coating/sample matrix distribution constant,  $K_{eS}$ , at equilibrium. Additionally, when selecting a coating for a complex matrix such as plasma, the affinity/selectivity of the coating towards possible matrix interferences should also be

considered.<sup>120,122</sup> Considering this, C18 seems like the obvious choice for a coating that exhibits a high affinity towards hydrophobic compounds, as previously reported.<sup>116,120,123</sup> In addition, other studies conducted in the research group have indicated that hydrophilic-lipophilic balanced (HLB) particles are efficient for extracting hydrophobic compounds.<sup>70</sup> Hence, HLB particles were also considered using two particular sources: Waters particles from a kind gift and in-house synthesized particles. Extraction took place for 90 min using SPME fibres (10 mm long, 40  $\mu\text{m}$  thickness), from 1 mL of sample with exogenous lipids at 100 ng/mL. Figure 2.1A shows the amounts of lipids extracted by each tested coating type. For this set of analytes, HLB particles (regardless of origin/source) showed the highest performance towards *polar* lipids, such as lyso-glycerophospholipids, with lower recoveries towards more hydrophobic lipids, such as PLs and TGs. Nevertheless, C18 showed a better coverage toward the more hydrophobic lipids in addition to slightly better reproducibility, thus it was selected moving forward.

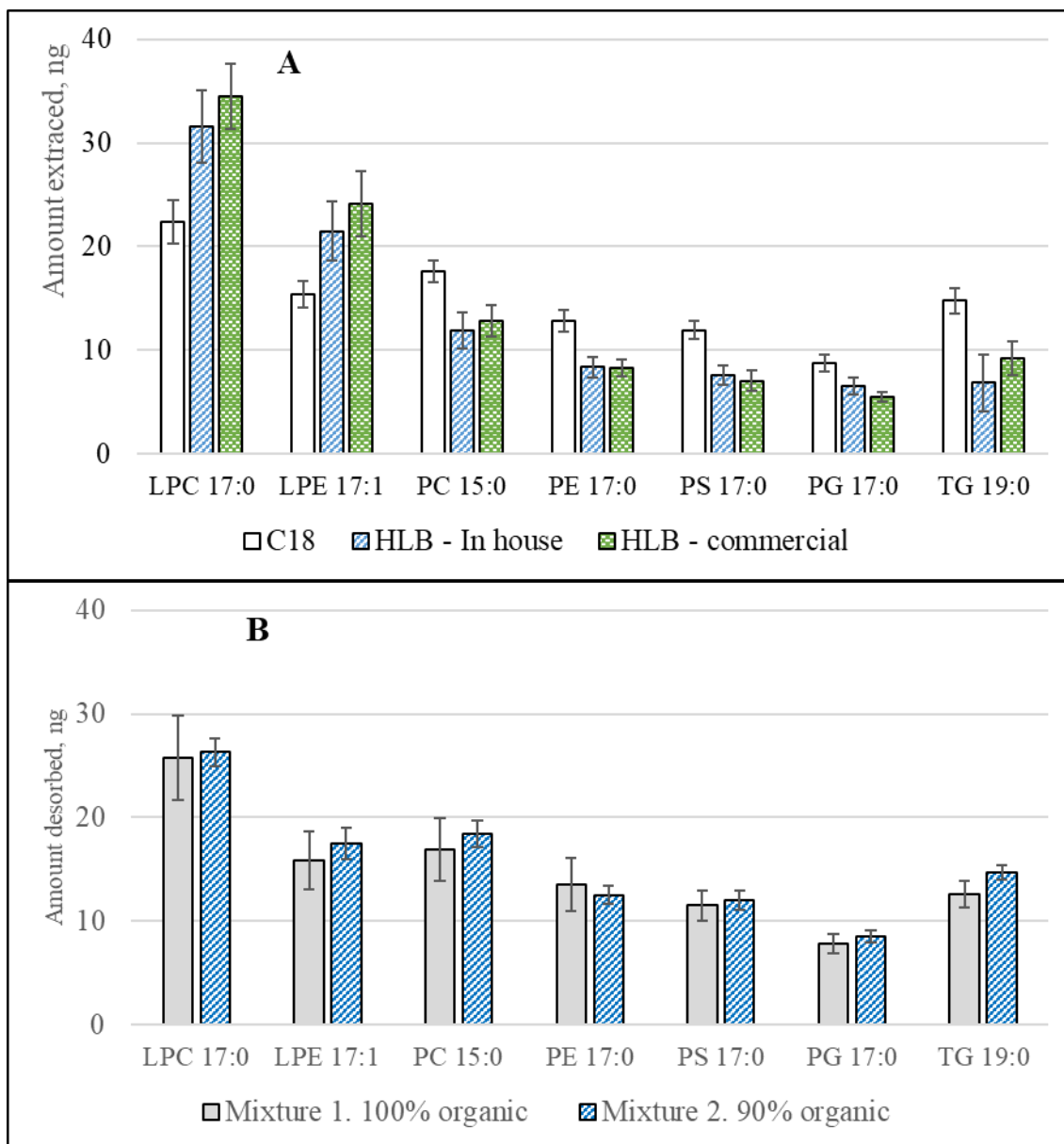


Figure 2.1. (A) Comparison between three different coating chemistries for extraction of lipids from PBS (pH 7.4, 100 ng/mL). (B) Desorption solvent comparison between two solvent mixtures of different organic content ratio. Mixture 1 was composed of methanol and isopropanol in equal volumes (MeOH/IPA, 1:1, v/v), while mixture 2 was composed of methanol, isopropanol and water (MeOH/IPA/H<sub>2</sub>O, 45/45/10, v/v/v).

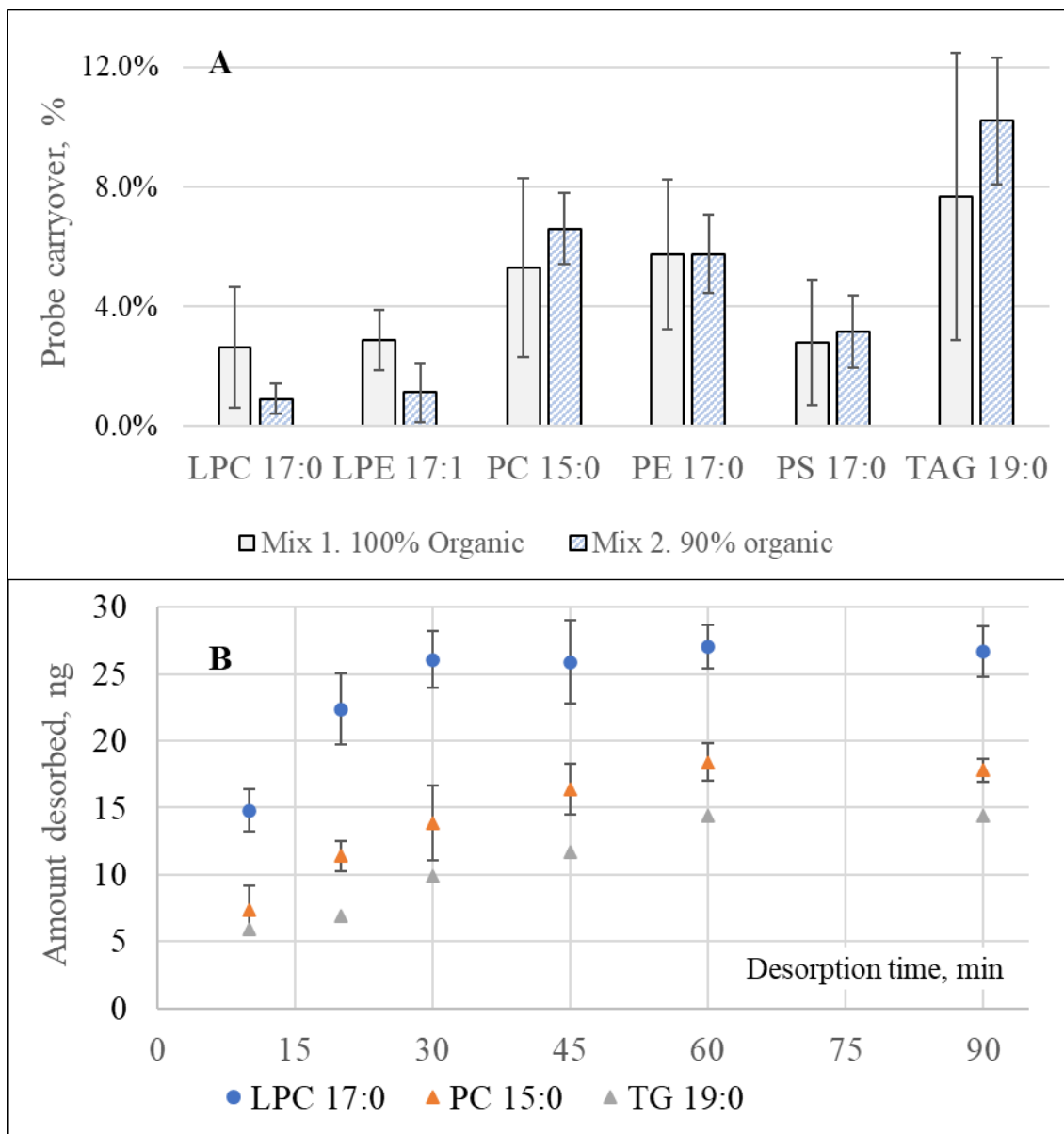


Figure 2.2. (A) Carryover evaluation for the SPME probes used by carrying out a second (60 min, 1000 rpm) desorption step with both solvents evaluated in Figure 2.1B. The carryover is represented as the area ratio between the second and first desorption steps. (B) Desorption time profile constructed for selected lipid standards using desorption mixture 2, done under agitation at 1000 rpm.

Then, two solution mixtures were compared in terms of the desorption performance of extracted lipids from C18-coated probes, as seen in Figure 2.1B. Ideally, a desorption solution should offer minimal carryover and be compatible with the LC conditions to

ensure good chromatographic separation and peak shapes. The carryover was assessed by performing a second desorption step from the probes, defined as the ratio of the amount desorbed in the second desorption step over the initial desorbed amount. The carryover for each solvent tested is plotted in Figure 2.2A. Mixture 2, containing isopropanol/methanol/water (45/45/10, v/v), was determined as the better-performing desorption solution regarding its reproducibility and carryover. While Mixture 1 showed similar desorption performance to Mixture 2, it also showed higher variability and significant carryover toward the relatively polar lysophospholipids. Following the selection of the desorption solvent, finding an optimum desorption time was the next step for the selected desorption solvent. Times in the 10 – 60 min range were studied, and results are shown in Figure 2.2B. Considering the high ratio of organic solvent, 90% by volume, fast equilibration between the extracted analytes in the SPME coating and the desorption medium was expected. However, the *rate* of desorption seems to increase greatly for lipids of higher hydrophobicity, alluding to their higher affinity towards the coating chemistry used.

### **Spiking approach and extraction time**

While it is recommended for SPME method development to use ~1% volume of organic solvent for biological samples, the specifics on how to spike are analyte dependent. Furthermore, it is agreed that calibration approaches with SPME may be sensible to the kind of solvent used for spiking – methanol being the preferred choice for spiking of aqueous samples based on its *similarity* to water.<sup>120,124</sup> However, lipid standards are

occasionally dissolved in chloroform, a much *stronger* organic solvent than methanol, which could disrupt/modify the sample even with spiking volumes below 1%.

To this end, as described below, three ways of mixing a small amount of a lipid standards mixture (10  $\mu\text{L}$ , 500  $\mu\text{g}/\text{mL}$  in  $\text{CHCl}_3$ ) and a plasma aliquot (2.0 mL) were compared, and the results are shown in Figure 2.3. All spiked plasma samples were incubated overnight at 4  $^\circ\text{C}$ , then shaken gently (500 rpm, 30 min) the following day to temperate before performing any SPME extractions using C18 fibres (15 mm long, 40  $\mu\text{m}$  thickness,  $n = 5$ ):

**I. Standard + plasma:** a small volume (10  $\mu\text{L}$ ) of the standard was added directly into 2 mL of plasma. Turbidity is seen immediately around the pipette tip, suggesting localized protein precipitation.

**II. Plasma + Standard:** 10  $\mu\text{L}$  of the standard is added to the bottom of a glass vial, and rapidly 2 mL of plasma is added on top.

**III. Drying + Plasma:** A small volume (10  $\mu\text{L}$ ) is added to a vial's bottom, then the solvent is evaporated with a gentle nitrogen stream, followed by the addition of 2 mL of plasma.

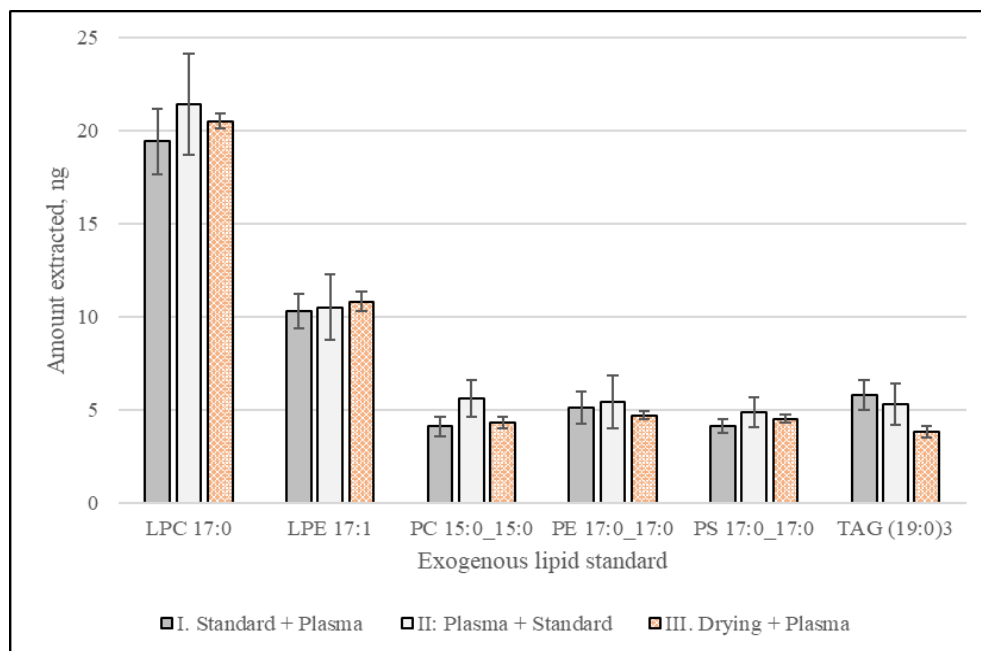


Figure 2.3. Comparison of three spiking approaches of exogenous, odd-chain lipids standards in human plasma.

These three spiking approaches resulted in similar analyte recoveries from the plasma matrix, though approach III has the lowest standard deviation. The low deviation was attributed to the lack of *strong*-organic solvent, thus minimizing local protein precipitation, and maintaining sample integrity. While any spiking approach could seemingly be used, approach III was used onward as per its low deviation. In addition, approach III would allow spiking volumes over 1%, provided the organic solvent is duly evaporated. Undeniably, this comparison was carried out with SPME probes which would extract from the unbound pool of analytes; thus, as executed, this experiment fails to verify the binding of exogenous lipids to the matrix. Yet, compelling evidence exists to assume adequate binding by exchange of soluble monomers and from collisions,<sup>125,126</sup> such as observed between micellar bodies<sup>127</sup> and among lipoproteins.<sup>128</sup>

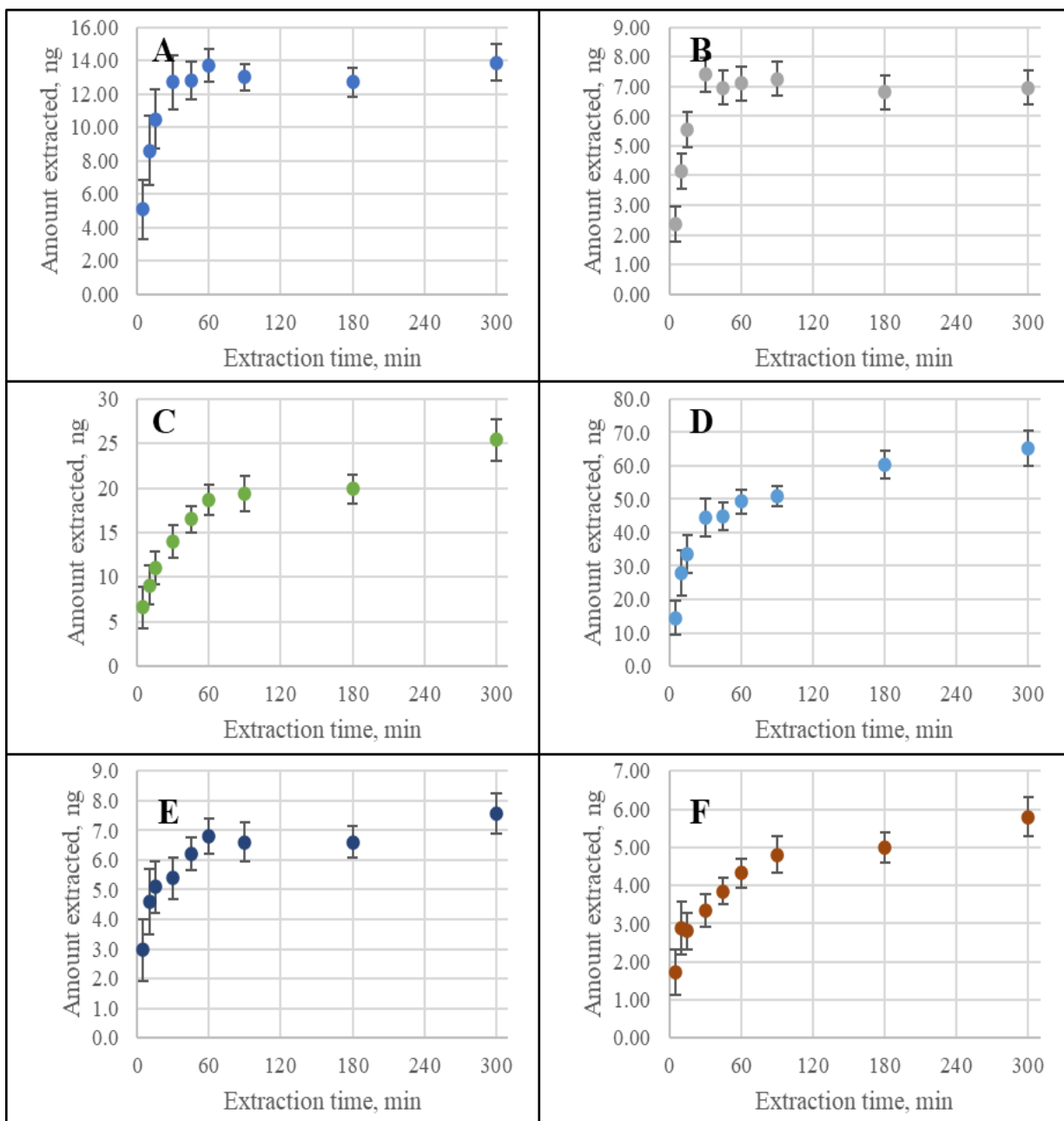


Figure 2.4. Extraction time profiles from plasma samples using C18-coated fibers for selected lipid analytes. (A) LPC 17:0; (B) LPE 17:1; (C) PC 15:0\_15:0; (D) PE 17:0\_17:0; (E) PS 17:0\_17:0; (F) TG (19:0)<sub>3</sub>.

Keeping on with the coating chemistry, desorption condition and spiking approach selected, the SPME coating was selected, and the desorption conditions were carefully



optimized, other extraction parameters such as time and various agitation rates were studied using extraction time profiles (ETP). Extended extraction times allow improved sensitivity, and reduced variability, in addition to allowing the equilibrium-based quantitation approach. Extraction was performed on plasma samples, using a long-time frame to expect equilibrium to be achieved for all lipid species. The extraction time profiles were constructed using agitation at 1000 rpm, as convection conditions are known to significantly increase the mass transfer between the matrix and coating by effectively reducing the thickness of the boundary layer. Figure 2.4 shows the ETPs obtained for exogenous lipids in plasma. The more polar lysophospholipids required relatively short times (around 30 min) for equilibration, whereas more hydrophobic lipids took over an hour to equilibrate. Surprisingly, particularly for hydrophobic lipids (e.g., PL and TG), a second plateau was observed at very long extraction times (> 90 min). AP. Birjandi et al. had assigned this phenomenon to temperature-driven changes to the lipoprotein composition resulting from long periods of agitation.<sup>123</sup> Similarly, Reyes-Garcés et al. had observed this behaviour for hydrophobic drugs and assigned it to the “complexity of the system”.<sup>124</sup> From my perspective, continuous analyte uptake by the sorption phase implies that true equilibrium was not reached for hydrophobic lipids, due to their incredibly low solubility in aqueous media,<sup>129,130</sup> and their (vastly) high affinities,<sup>68</sup> towards the various lipid-carrier proteins in plasma. It is very likely that very hydrophobic lipids (such as triglycerides and cholesteryl esters, which are carried in the core of lipoproteins) present very slow desorption rates from these lipid-binding particles.<sup>131</sup> Furthermore,

apolipoproteins B-100 and ApoA-II are determinants of cholesterol and triglyceride efflux, thus these could mediate their desorption into free-concentration.<sup>132</sup>

### **Matrix modification, matrix effects and matrix-matched calibration**

In this study, a matrix-matched calibration was considered as an SPME quantitation strategy to estimate the total concentration of the odd-chain analytes. With matrix-matched calibration, the total concentration is calculated by spiking known quantities of analyte to a *blank* matrix that can mimic the studied sample. It is *essential* in SPME that the simulation of the sample matrix is adequately done since any changes in the sample (such as pH, ionic strength, or organic matter) may affect the degree of binding of analytes to matrix components. While a plasma sample free of lipids is unattainable, using a standard reference material presents a high-priced alternative. The SRM 1950®, a “normal” human plasma, was chosen as a viable choice to *standardize* the proposed SPME method.<sup>133</sup> SRM 1950® has been used comprehensively for various interlaboratory comparisons aiming at harmonizing measurements, methodologies, and nomenclature; creating consensus on expected physiological values; and recognizing areas needing improvement.<sup>33,99,134–136</sup> In addition to SRM 1950®, other plasma lots were considered to assess the relative matrix effects for the proposed SPME methodology.

However, preliminary experiments (results not shown) alerted of possible challenges to a simple matrix-matched calibration approach: first, the expected high (excessive) degree of binding between the matrix and the analytes places an additional constrain on the attainable limits of detection and quantitation for SPME,<sup>124,137–139</sup> which is further

exacerbated by the limitation in sample volume available for costly samples (such as SRM 1950®) or clinically relevant samples (e.g., plasma samples from infants or elders). Second, the vast differences in concentration for distinct lipid classes make it difficult (if not impossible) to select single calibration levels to target various lipid classes simultaneously. While a “one-fits-all” tactic could work well,<sup>123</sup> it would not be an appropriate representation of “normal/physiological” lipid levels in a plasma sample. Third, there are challenges associated with spiking lipid analytes to the plasma matrix, as described before. For example, methanol is preferred from its high solubility in water/aqueous media, yet most lipid standards are prepared in stronger solvents (such as chloroform) that rapidly cause localized changes in plasma during spiking (seen as a cloudy formation). Moreover, self-aggregation of lipids during spiking from localized hot spots may not mimic the matrix accordingly.

Hence, two considerations were taken to estimate the total concentration via a matrix-matched calibration in plasma. First, another SPME probe geometry was considered: the *legacy* fiber geometry and a coated blade, as an example of a thin-film device which offers a larger surface area for enhanced sensitivity and faster analyte uptake.<sup>69,101,124</sup> Second, plasma ought to be modified with an organic solvent, a normal practice during method development, with the intention of increasing the free analyte concentration.<sup>140–143</sup> This approach boosts the free concentration of the analytes, which promotes their extraction onto the SPME device. Nevertheless, the addition of solvent to a matrix causes additional challenges to the analyte extraction. If there is too much organic solvent, the analyte

partition may be driven onto the solvent-rich medium rather than the extractive particles due to a substantial drop in the partition coefficient,  $K_{FS}$ , therefore reducing the amount extracted. Likewise, a low amount of solvent leads to a limited release of analytes and, as a result, low limits of quantitation. This approach is not viable for studies interested in the determination of binding parameters.

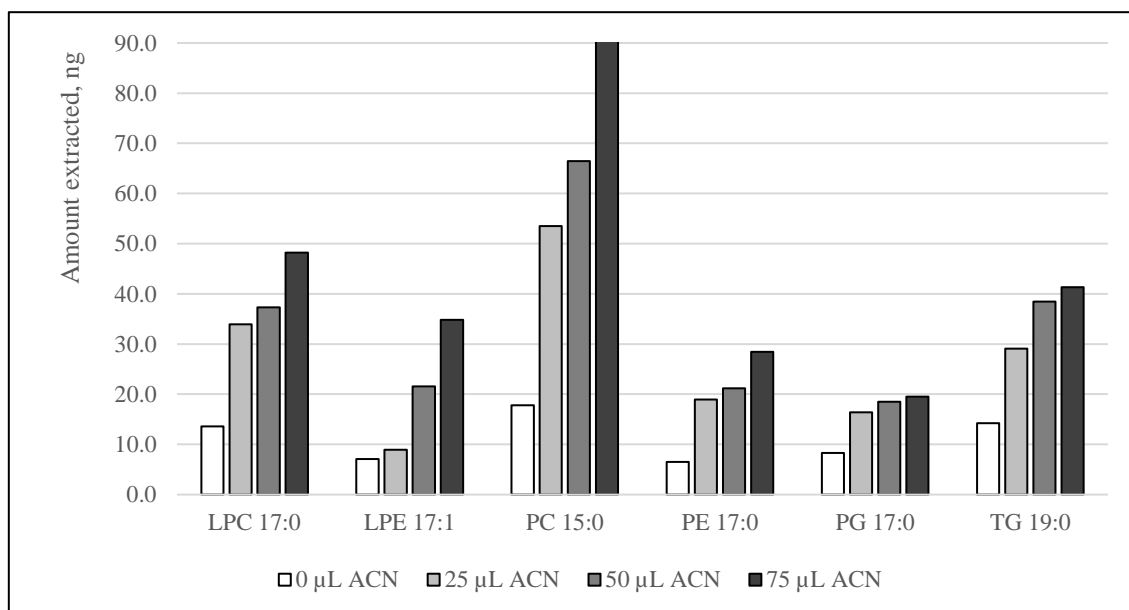


Figure 2.5. Plasma modification with acetonitrile to artificially increase the free concentration of lipids, thus increasing the total amount recovered by SPME fibers.

The results depicted in Figure 2.5 portrays the *enhanced* extraction of analytes with increasing ACN content (100  $\mu$ L of plasma, 0–75  $\mu$ L ACN, completing to 200  $\mu$ L with PBS). However, Figure 2.6A showcases the absolute matrix effects stemming from the addition of 25  $\mu$ L acetonitrile for extractions with fibers and blades. It is worth noting that SPME probes have minimal AMEs on extractions done from neat plasma (regardless of the geometry). While more lipids are extracted upon modification, significant AMEs are a by-product of said modification – a dilemmatic situation to increase the recovered amounts

by SPME probes in a timely, practical manner. The findings in Figure 2.6B portray the AMEs obtained for extractions using blades at different ACN ratios. The lowest ratio of ACN used/tested also resulted in the lowest induction of AMEs, though not for all tested analytes. The observed AMEs indicated primarily ion suppression for lipid analytes from minor lipid classes in plasma such as LPE, LPS, PG, and PS. Conversely, positive matrix effects, indicating ion enhancement, were mainly observed on PCs, one of the most abundant lipid classes in plasma and other tissues. PCs are widely known to cause matrix and ionization effects in various MS-based analysis.<sup>107,144,145</sup> In fact, additional steps for clean-up extracts to remove these zwitterionic species are part of workflows intended for quantitation of minor lipid species.<sup>145</sup> Triglycerides were not significantly affected compared to glycerophospholipids, possibly from low overall solubility in ACN or other confounding factor from matrix modification.

Thus, matrix-matched calibration curves on plasma entailed two sequential extractions using different geometries: An initial extraction employing fibers (C18 coated, length 10 mm, thickness 40  $\mu\text{m}$ ) done on neat plasma (100  $\mu\text{L}$ , 60 min extraction at room temperature); followed by plasma matrix modification (adding 25  $\mu\text{L}$  ACN and 75  $\mu\text{L}$  PBS) and gentle agitation for 10 min; and finally, a second extraction employing thin-coated blades (C18 coated, 10 mm long, 15  $\mu\text{m}$ ) done on modified plasma. In all cases for the matrix-matched calibration, four independent probe replicates were used for extraction.

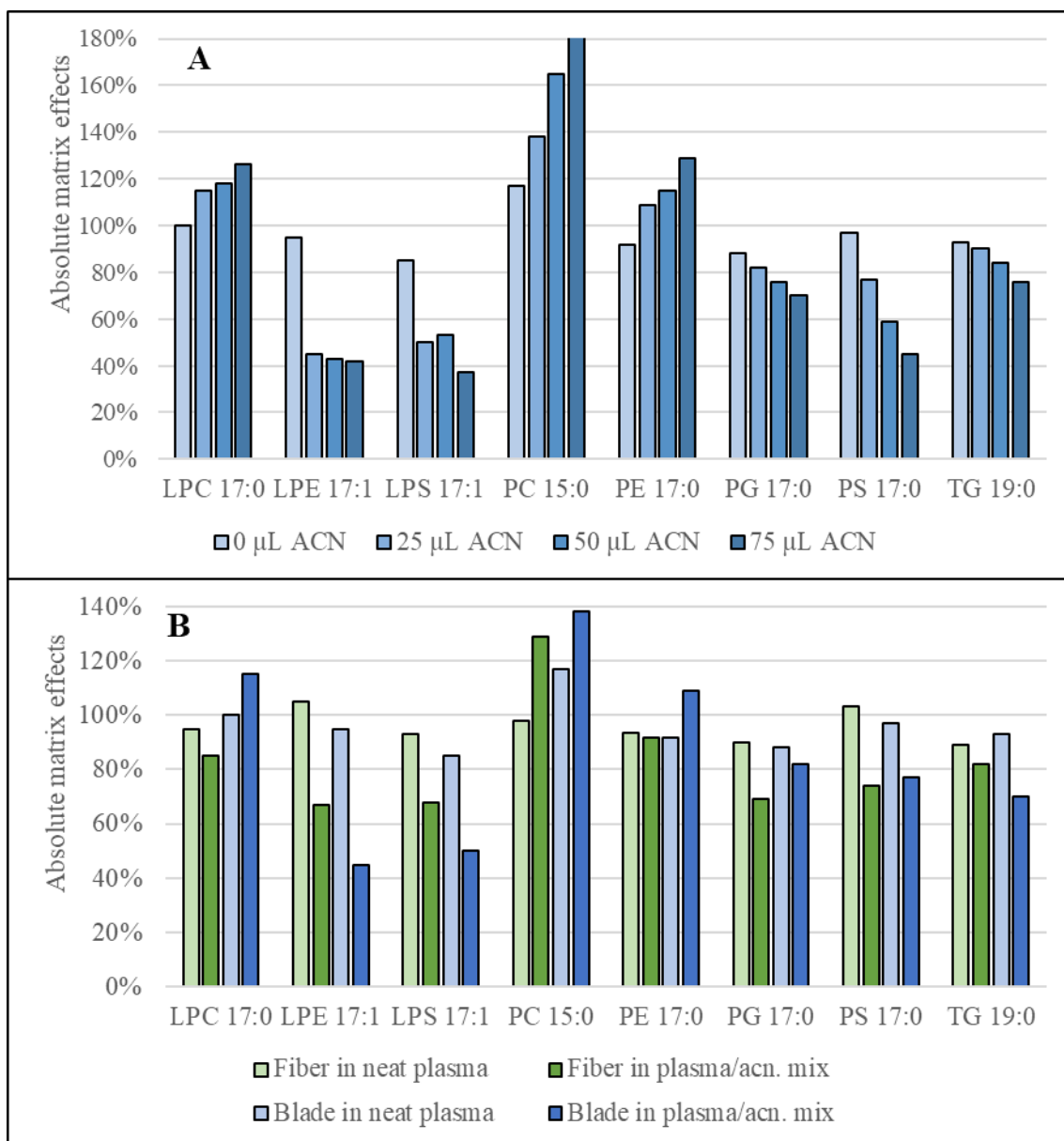


Figure 2.6. Absolute matrix effects evaluated for extraction of exogenous lipids from human plasma. (A) Absolute matrix effects were obtained for extraction with SPME fibers upon plasma modification with acetonitrile. (B) Absolute matrix effects were determined for neat and modified plasma (at the lowest level, 25  $\mu\text{L}$  ACN) using two SPME probe geometries: fiber and coated blade.

The best results were obtained for LPC 17:0 in terms of relative matrix effects obtained given that the slopes four different plasma lots exhibited relative standard deviation (RSD) values below 20% for extraction from neat plasma. Moreover, the calibration curves

obtained show linearity within the studied concentration range, 0.1–10 ppm, for the different plasma lots employed as seen in Figure 2.7. Good results may be considered for the slopes constructed on modified plasma with RSD of 11% and 4% for the lower and upper ranges, respectively. However, there is a loss of linearity for this approach taken the linearity is dubious for calibration curves prepared from modified matrix. In conclusion, matrix modification coupled to extraction with blades seemed a viable option to increase the amount extracted from lipids, yet at the cost of AMEs, a tough compromise. The results by comparing this small sample set of plasma lots suggests the presence of relative matrix effects. Relatively small recoveries might be highly influenced by the high affinity hydrophobics have towards lipoproteins and possible micelle-like matrix components present in plasma, effecting large competition to the extracting phase, as observed by the small amounts recovered from neat plasma. While this venue, extraction from neat plasma, may be explored further for applications, immense efforts are required to understand from the dynamics of mass transfer taking place between distinct lipid *compartments* (i.e., bound pools of lipid analytes) and the coating phase. Additionally, plasma composition is too variable between individuals (influenced by factors such as gender, age, race, etc.) and even within the same individual (i.e., varying levels of lipoproteins with diet and circadian rhythm). Thus, the best (and perhaps the easiest) path to improve the obtained findings is having a plasma homogenization step, to minimize inter-sample variability and increase the free concentration of lipids. Similar approaches had been used for highly bound analytes, such as immunosuppressants in whole blood.<sup>140,146</sup>

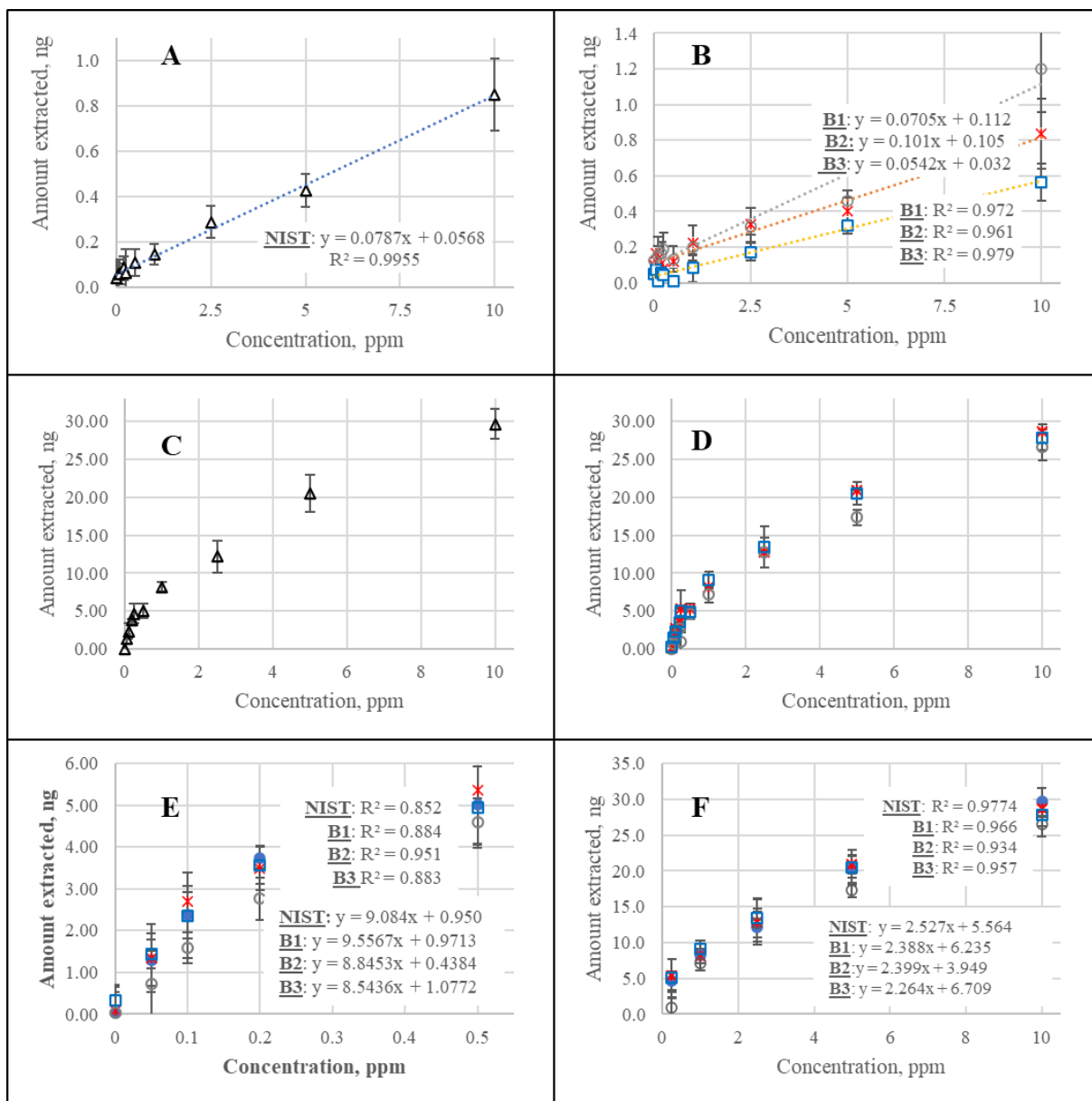


Figure 2.7. Matrix matched calibration curves for exogenous lipid, LPC 17:0. (A) Extraction from SRM® 1950 plasma using SPME fibers; (B) Extraction from other plasma lots using SPME fibers; (C) Extraction from ACN-modified SRM® 1950 plasma using SPME blades; (D) Extraction from ACN-modified plasma lots using SPME blades; (E) Lower range for the matrix-matched calibration curves from all plasma lots using blades; (F) Upper range of calibration curves for all plasma lots using blades.



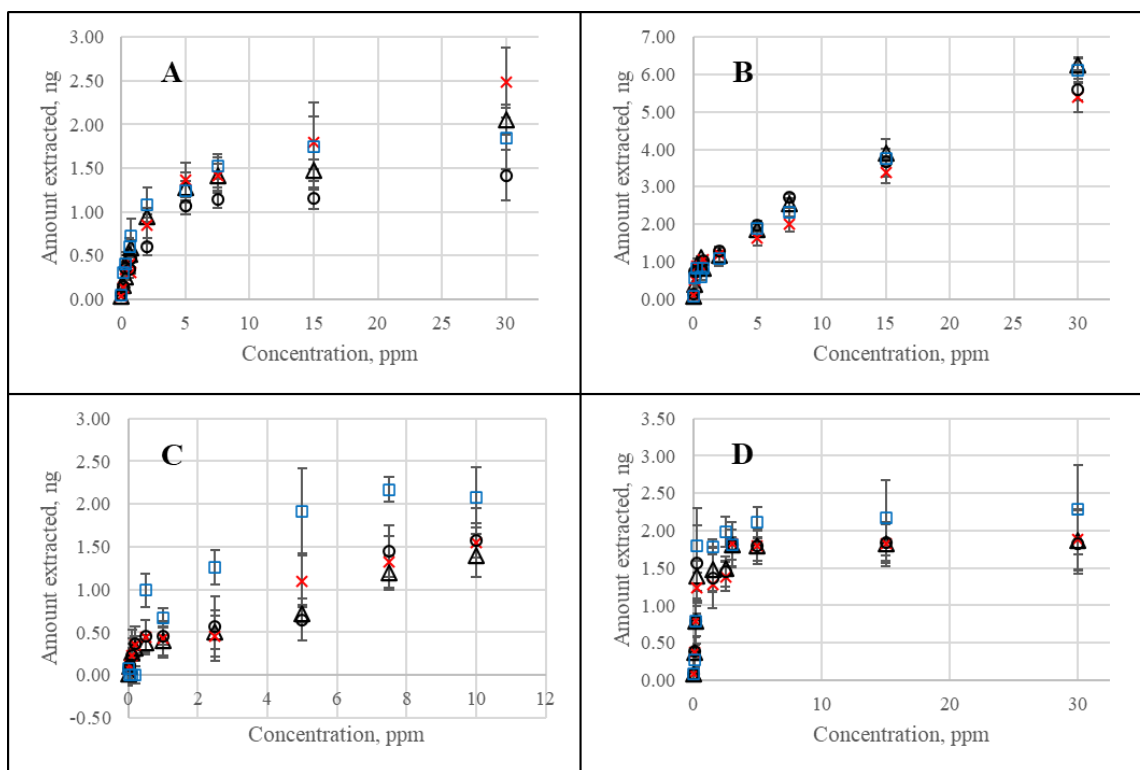


Figure 2.8. Matrix matched calibration constructed for exogenous, very hydrophobic lipids in various plasma samples. (A) Extraction of PC 15:0\_15:0 from neat plasma using SPME fibers, (B) Extraction of PC 15:0\_15:0 from modified plasma using SPME blades, (C) Extraction of PE 17:0\_17:0 from modified plasma using SPME blades, (D) Extraction of TG (19:0)<sub>3</sub> from modified plasma using blades.

Nevertheless, extraction of very hydrophobic compounds from plasma using SPME is feasible but significantly more complex. For instance, the matrix–matched calibration curves obtained for PC 15:0\_15:0 from various sources of plasma, presented in Figure 2.8, suggest the presence of relative matrix effects, as suggested by the different amounts extracted in the upper range of exogenous lipid spiked. However, these relative matrix effects can be minimized by introducing a matrix-modification step, as shown in Figure 2.8B. Though, including a matrix-modification step may cause losses of

linearity for other lipids present in the sample, as resulting for exogenous PE 17:0\_17:0 and TG (19:0)<sub>3</sub> as shown in Figure 2.8C and Figure 2.8D, respectively.

Parameters as polarity and the affinity of an analyte for the matrix binding components (e.g., the distinct lipoprotein classes) and the extraction phases should be considered. Regarding the polarity, it is especially important to emphasize that highly polar compounds typically display shorter equilibration times from their low affinities to the SPME coatings. Within the current set of analytes, polar lipids such as lyso-phospholipids (and presumably fatty acids and other single-chained lipids) are behaving as *polar* analytes would, with higher affinities instead. Efficient convection conditions, such as faster agitation conditions, enable for a decrease in the thickness of the boundary layer, which accelerates the mass transfer process occurring from the sample matrix.

$$t_{eq} \cong t_{95\%} = \frac{\delta KL}{D_S \Gamma^{max}} \quad \text{Eq. 6}$$

Equation 6 shows equilibration time for SPME as a function of the distribution constant ( $K$ ), the thickness of the SPME coating ( $L$ ) and the boundary layer ( $\delta$ ), the diffusion of the analyte through the sample ( $D_S$ ), and the coating capacity ( $\Gamma^{max}$ ).<sup>137,147</sup> Within this frame of reference, when extractions are performed close to equilibrium (as intended in this thesis), the amount of analyte collected is mostly determined by the analyte's distribution constant. In contrast, diffusion of analytes plays a bigger role if extraction process is interrupted far from equilibrium. Membrane lipids such as phospholipids are known to exhibit fast lateral diffusion in layers (monolayers, bilayers, membranes).<sup>148</sup> However,

studies directed at understanding the dynamics of compounds at the oil–water interface are exceptionally rare.<sup>149</sup> Negishi et. al found that diffusion of phospholipids at a water/oil interface seems to be determined by the oil viscosity.<sup>150</sup> While protein-attachment and co-extraction of interferences by SPME devices is relatively uncommon for other small molecules; one could even consider some lipids as interferences to themselves – particularly phospholipids. Clearly any adoption of a matrix-modification step would need careful consideration to ensure analyte stability without negatively impacting additional extraction parameters derived from the modified chemical environment. The affinity to the sorbent coating may be severely impacted in the modified matrix’s chemical makeup, resulting in this strategy has been exploited to increase sorption selectivity. Other examples of matrix modifications which could be used for increased selectivity in lipid analysis could include changes in pH (e.g., fatty acids, acid trace phospholipids, sphingolipids); changes to the ionic strength (i.e., phosphoserines for tissues); volume (e.g., dilution of undesired concomitant polar co-extractants); or even a sample derivatization step. These approaches could potentially lead to a broader applicability of SPME for lipids/lipidomics studies before the urge for harmonization excludes SPME even further.

Standard addition curves were also prepared for the SRM® 1950 plasma sample for a few available endogenous lipids to further explore the quantitative capabilities of SPME. The total concentration for these endogenous lipids is estimated using the calibration curves parameters (i.e., slope and intercept), and are compared to those reported by Quehenberger et al. for NIST™ SRM® 1950 plasma.<sup>151</sup> The best results among these

endogenous lipids were attained for LPC 16:0, the most *polar* lipid: Figure 2.9 portrays the standard addition curves for the extractions with SPME fibers from neat plasma and SPME blades from modified plasma. The concentration of LPC 16:0 was estimated as 13.31 ( $\pm 1.15$ )  $\mu\text{g/mL}$  and 10.67 ( $\pm 1.07$ )  $\mu\text{g/mL}$  for the fiber and blade approaches, respectively, which are in good agreement with 14.8 ( $\pm 2.3$ )  $\mu\text{g/mL}$  as reported by Quehenberger et al. Similarly, the standard addition curves for the endogenous phospholipids PC 16:0\_16:0 and PE 16:0\_18:1 using the SRM® 1950 plasma is shown in Figure 2.10. While these compounds are extracted from neat plasma using SPME fibers, the lack of linearity shows a clear drawback by this sample preparation approach, as discussed previously. Estimation of the total concentration was only feasible from the matrix modified curves, for instance a concentration of 9.05 ( $\pm 0.95$ )  $\mu\text{g/mL}$  was obtained for PC 16:0\_16:0 compared to the reported value of 8.39 ( $\pm 0.43$ )  $\mu\text{g/mL}$ . On the other hand, for PE 16:0\_18:1, the concentration estimated in the sample using the curve from SPME blades results in 15.73 ( $\pm 1.59$ )  $\mu\text{g/mL}$ , which drastically overestimates the reported value of 4.27 ( $\pm 0.13$ )  $\mu\text{g/mL}$ . It would be improper to directly compare these results with those reported by Quehenberger et al., as the experimental conditions used differ vastly in both studies; yet the author's findings are reasonably consistent for *polar* phospholipids.

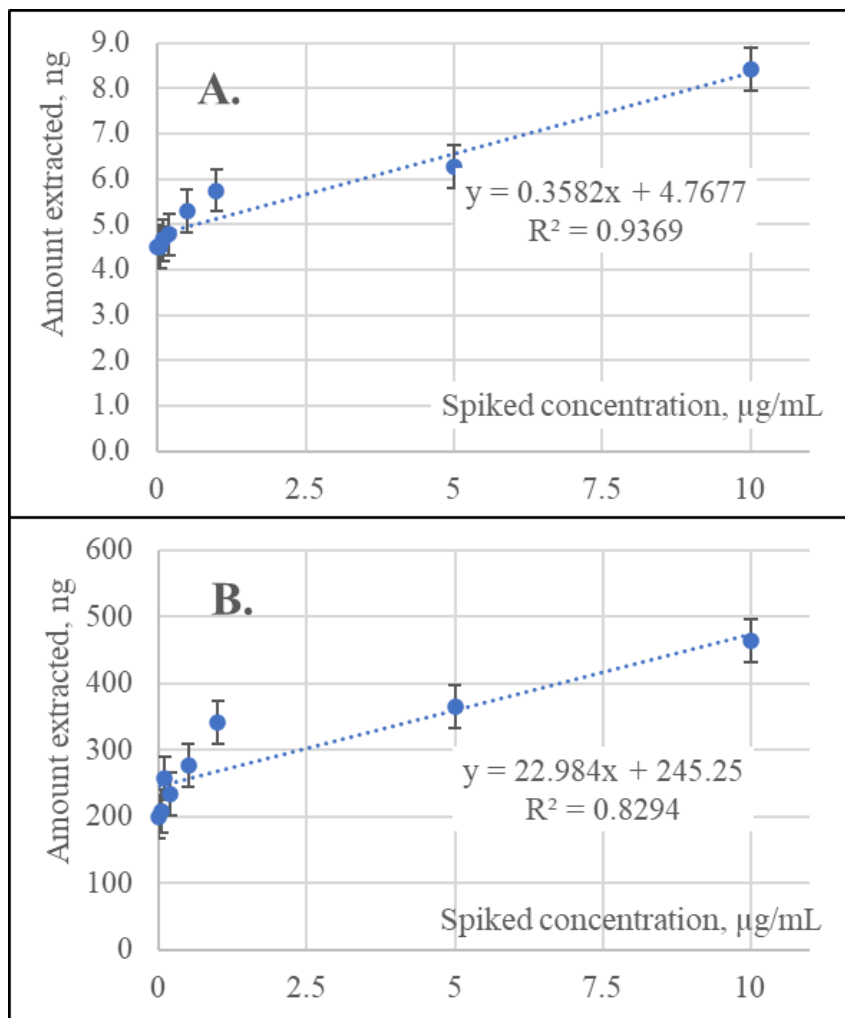


Figure 2.9. Standard addition curves prepared in SRM® 1950 plasma sample for the endogenous lipid, lyso-palmitoylphosphatidylcholine, LPC 16:0. (A) Extraction using SPME fibers from neat plasma. (B). Extraction using SPME blades from modified plasma.

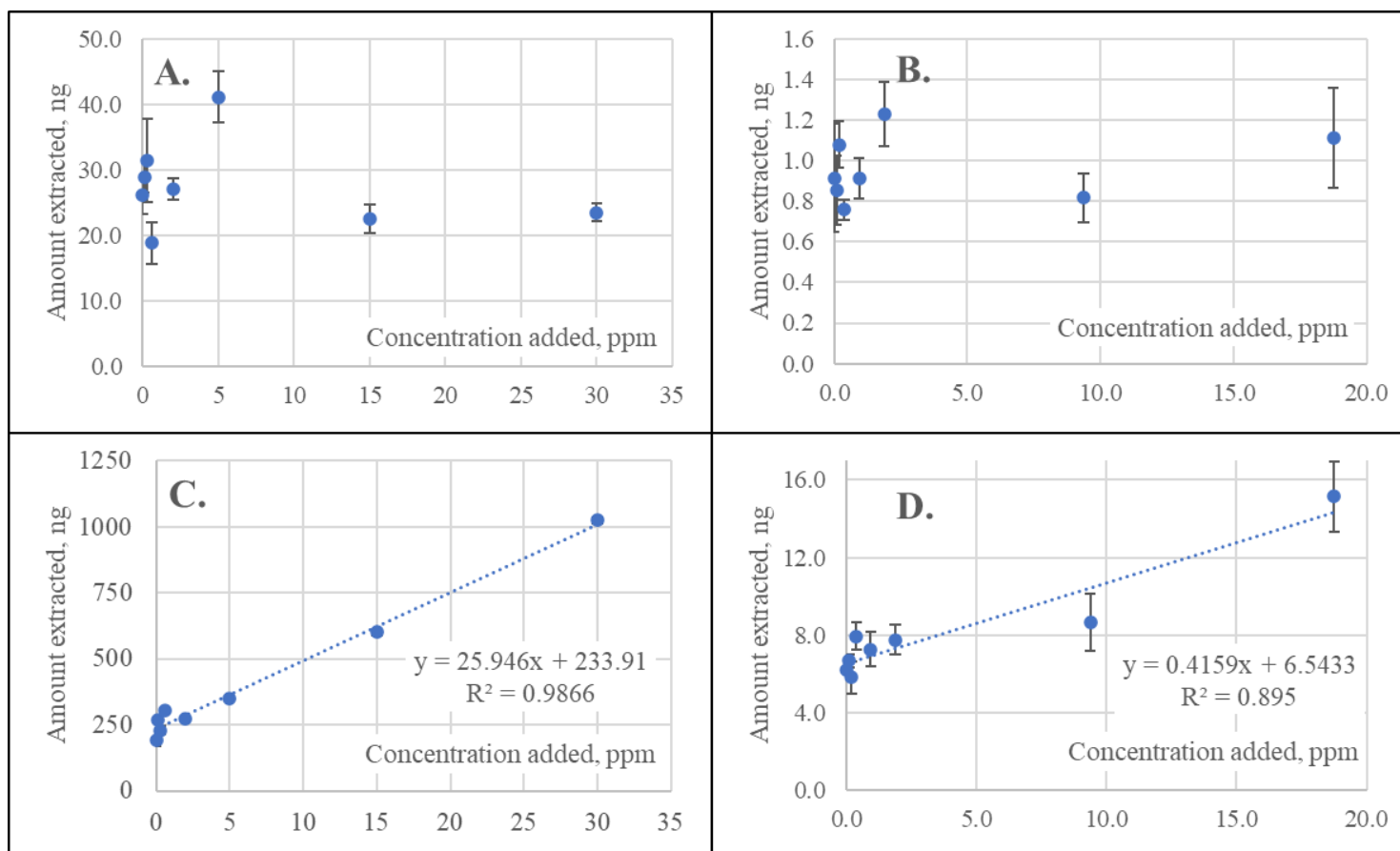


Figure 2.10. Standard addition curves for two endogenous glycerophospholipids prepared in plasma SRM® 1950 using fibers (from neat plasma) and SPME blades (from modified plasma). (A) Extraction of PC 16:0\_16:0 from neat plasma. (B) Extraction of PE 16:0\_18:1 from neat plasma. (C) Extraction of PC 16:0\_16:0 from modified plasma. (D) Extraction of PE 16:0\_18:1 from modified plasma

In summary, SPME has provided extraction in a *quantitative* fashion for lipids, as displayed using matrix-matched calibration and standard-addition curves for selected exogenous and endogenous lipids, respectively. While the extraction of very hydrophobic lipids is hindered by their exceedingly low free concentration and high affinity towards the plasma matrix (e.g., such as lipoproteins for lipid transport), quantitation of their free concentration is still feasible using SPME devices. Moreover, the extraction of these very hydrophobic lipids is clearly feasible by SPME probes, as demonstrated by the results obtained, which may be also appropriate for qualitative studies focused on profiling of the lipidome. Similarly, the quantitation of total concentration of very hydrophobic may still be addressed by modifying the matrix with an organic solvent, thus overcoming the interplay between high matrix affinity and low free concentration (though caution must be taken as this approach may lead to excessive concomitant extraction of endogenous compounds which may result in significant matrix effects for the analytes). Nevertheless, the SPME devices used were capable of extracting lipids of diverse characteristics, thus highlighting the balanced coverage capabilities of the technique. Given the superior results obtained for polar lipids, such as lyso-phosphatidylcholines, and the marked differences observed among the lipids under study, the author recommends future studies on SPME for lipid analysis to narrow their focus into distinct lipid sub-classes.

SPME's quantitative capabilities were demonstrated for the exogenous lipids studied with good results using the matrix-matched calibration approach. They may nevertheless be improved on additional research. SPME's quantitative capabilities were also

demonstrated for a few endogenous lipid metabolites in SRM® 1950 plasma using the standard addition calibration technique, with a high agreement with data from other selected studies. That said, quantification of more endogenous substances may be possible if such standards are available, utilizing my dissertation results as a starting point. Quantitation of endogenous compounds in a complex sample using SPME is not a trivial matter. The developing a SPME calibration methods requires a solid understanding of the parameters driving the mass transfer of multiple analytes in multiphase systems, such as the distribution coefficient of the analyte,  $K_{es}$ , between the SPME coating and the sample. Knowing the distribution coefficient is also essential in other calibration approaches that could be used for SPME quantitation of lipid metabolites, such as the kinetic calibration (with extraction occurring before equilibrium).<sup>152</sup> A simple strategy to estimate the distribution coefficient for lipid compounds is briefly outlined in the following section, sub-chapter 2.2.

#### A survey into the NIST SRM® 1950 plasma by SPME via untargeted HRMS

The estimation of the total concentration of multiple endogenous lipids naturally present in a plasma sample (such as SRM® 1950 plasma), is a feat that currently escapes the capabilities of the author. Which is an everyday reality in the lipidomics field, owing to the absence of harmonization within this (rapidly growing) field of study. Thus far, untargeted solutions in this field are unable of exact quantification instead relying on relative quantitation or just qualitative data. Given that the amount of analyte extracted by SPME is proportional to the initial concentration in the sample and to the affinity of each



analyte for the sorbent coating, this correlation must take into consideration the affinity of each individual lipid species for the sorbent coating - a rather complex task resulting from SPME's inherent extraction mechanism.

Untargeted lipidomics is a powerful approach for studying the chemical makeup that occurs in various biological samples. However, the untargeted analysis is quite challenging due to the complexity and diversity of lipids (and other metabolites) present. Achieving accurate quantitation and identification of metabolites is challenging, as extensively reported.<sup>28,153–156</sup> Various methodologies (i.e., extraction protocols, sample preparation steps, derivatization strategies, clean up steps), instruments (i.e., orthogonal chromatographic columns, ionization sources and modes, in-source separation, etc.), and data processing strategies (i.e., multivariate statistical analysis) have been proposed to address these challenges and to increase the coverage, with trade-offs between analysis time and data complexity.

Untargeted lipidomics strategies, such as the one applied here, enable qualitative profiling of the “macro-lipidome” (the major lipid components present in a sample) and identify the lipids from the *features* resulting from data processing. It is appropriate to introduce the term “*feature*”, which arises at the pre-identification stage of data processing as a two-dimensional data point that contains chromatographic and mass spectral response. However, the presence of multiple adducts and ions with different charges or isotopes means that a particular peak may correspond to several metabolites. As a result, the number

of detected features is often greater than the number of actual detected metabolites – a concept that is crucial for understating the capabilities of untargeted -omics research.

Opposite to untargeted lipidomics, targeted lipidomics approaches comprise pre-specifying the analytes to be evaluated and may include the use of specific solvents, standards, and analytical (chromatographic and mass spectrometric) settings. This strategy (which was considerably outside the scope of this dissertation) is widely used to evaluate low-abundance lipids that comprise the “micro-lipidome”, which consists of bioactive lipid molecules involved in acute metabolism and signaling. The micro lipidome includes diacylglycerols, phosphatidylinositols, ceramides, and oxylipins.<sup>157</sup> Aside from the low abundance of the micro-lipidome, stability is an issue that must be carefully studied. However, SPME has a significant advantage over typical sample preparation techniques for in vivo applications and this advantage should be investigated further.

Table 2.5 displays the lipids putatively identified from the SRM® 1950 plasma sample extracts. Only the sum compositional information for the lipids is provided, which indicated the lipid class and the overall number of carbons and double bonds of the fatty acyl components of complex lipids. The extracted lipid metabolites were confidently identified using the parent ion mass alone without tandem MS. The identified lipid metabolites mostly belong to the most abundant classes that exist in plasma, such as glycerophospholipids and glycerolipids. From these lipid classes, phosphatidylcholines (PC), phosphatidylethanolamines (PE) and triglycerides (TG) are the among the most

abundant extracted lipids with 26, 15 and 32 species identified, respectively. Conversely, the number of species identified for other glycerophospholipid subclasses is quite lower in comparison; for instance, only six species were identified for phosphatidylserine (PS), five for phosphatidylglycerols (PG), three for phosphatidylinositol (PI), and two for phosphatidic acids (PA). Similarly, for glycerolipids, only six species were identified for monoglycerides (MG) and eight for diacylglycerides (DG). Regarding the sterol class, seven cholesteryl esters (CE) were putatively identified. Undeniably, characterization of the lipidome requires multiple instrumental approaches that address the differences in extraction, separation, and ionization of this diverse group of biomolecules.<sup>33</sup> These extracted lipid metabolites belong to multiple sub-classes of lipids with diverse physicochemical parameters (e.g., wide scale of *hydrophobicity*), thus verifying the balanced-coverage capabilities of SPME extraction. In addition, these lipid metabolites have been previously identified in the SRM® 1950 plasma by other studies.<sup>33,151,158</sup> The author is pleased with the outcomes from their easy but possibly basic method. Direct comparisons with other studies should also consider differences in the targeted experimental parameters (i.e., exhaustive sample preparation techniques, chromatographic separations, ionization conditions, and acquisition modes) that can influence the diversity of micro-lipidome compounds detected. For instance, Quehenberger used seven different workflows to characterize the NIST™ SRM® 1950 plasma lipidome, with some analytical interest (read as bias) towards eicosanoids.<sup>99</sup> Besides, in the interlaboratory exercise by Bowden et al., variable outcomes in the lipidome profile for SRM® 1950 plasma were obtained and significant variation in the lipid amounts identified and reported across the

participating laboratories.<sup>159</sup> As the harmonization debate is ongoing and presented research opportunities, the author feels hopeful in the proposed unconventional, versatile, yet powerful sample preparation for the lipid extraction stage. The ongoing discussion surrounding harmonization of lipid quantification strategies may benefit from the versatility and advantages provided by the SPME technique, representing a promising first step towards its integration into the expanding field of lipidomics.

Table 2.5. Lipid metabolites identified in extracts from the NIST SRM® 1950 plasma.

Compound	Molecular formula	Rt, min	<i>m/z</i>	Adduct	Mass defect, ppm	<i>m/z</i> theoretical
FA 14:0	C <sub>14</sub> H <sub>28</sub> O <sub>2</sub>	7.0	227.2015	[M-H] <sup>-</sup>	0	227.2017
FA 16:0	C <sub>16</sub> H <sub>32</sub> O <sub>2</sub>	6.2	255.2327	[M-H] <sup>-</sup>	0	255.2330
FA 18:0	C <sub>18</sub> H <sub>36</sub> O <sub>2</sub>	8.9	283.2641	[M-H] <sup>-</sup>	0	283.2643
FA 18:1	C <sub>18</sub> H <sub>34</sub> O <sub>2</sub>	8.2	281.2484	[M-H] <sup>-</sup>	0	281.2486
FA 18:2	C <sub>18</sub> H <sub>32</sub> O <sub>2</sub>	7.3	279.2328	[M-H] <sup>-</sup>	0	279.2330
FA 18:3	C <sub>18</sub> H <sub>30</sub> O <sub>3</sub>	6.4, 6.9	277.2171	[M-H] <sup>-</sup>	0	277.2173
FA 20:0	C <sub>20</sub> H <sub>40</sub> O <sub>2</sub>	7.9	311.2953	[M-H] <sup>-</sup>	1	311.2956
FA 20:3	C <sub>20</sub> H <sub>34</sub> O <sub>2</sub>	7.0	305.24864	[M-H] <sup>-</sup>	0	305.2486
FA 20:4	C <sub>20</sub> H <sub>32</sub> O <sub>2</sub>	6.4	303.2280	[M-H] <sup>-</sup>	0	303.2330
FA 20:5	C <sub>20</sub> H <sub>30</sub> O <sub>2</sub>	7.8	301.21731	[M-H] <sup>-</sup>	0	301.2173
FA 22:5	C <sub>22</sub> H <sub>34</sub> O <sub>2</sub>	7.0	329.2484	[M-H] <sup>-</sup>	0	329.2486
FA 22:6	C <sub>22</sub> H <sub>32</sub> O <sub>2</sub>	6.8	327.2327	[M-H] <sup>-</sup>	0	327.2330
MG 16:0	C <sub>19</sub> H <sub>38</sub> O <sub>4</sub>	10.8	348.3109	[M+NH <sub>4</sub> ] <sup>+</sup>	0	348.3108
MG 18:0	C <sub>21</sub> H <sub>42</sub> O <sub>4</sub>	12.1	376.3423	[M+NH <sub>4</sub> ] <sup>+</sup>	0	376.3421
MG 18:1	C <sub>21</sub> H <sub>40</sub> O <sub>4</sub>	11.1	374.3266	[M+NH <sub>4</sub> ] <sup>+</sup>	0	374.3265
MG 18:2	C <sub>21</sub> H <sub>38</sub> O <sub>4</sub>	10.2	372.311	[M+NH <sub>4</sub> ] <sup>+</sup>	0	372.3108
MG 20:4	C <sub>23</sub> H <sub>38</sub> O <sub>4</sub>	10.2	396.3108	[M+NH <sub>4</sub> ] <sup>+</sup>	0	396.3108
MG 22:5	C <sub>25</sub> H <sub>40</sub> O <sub>4</sub>	9.9	422.3267	[M+NH <sub>4</sub> ] <sup>+</sup>	0	422.3265
LPE 16:0	C <sub>21</sub> H <sub>44</sub> NO <sub>7</sub> P	9.4	454.2929	[M+H] <sup>+</sup>	0	476.2772
LPE 18:0	C <sub>23</sub> H <sub>48</sub> NO <sub>7</sub> P	10.9	482.3243	[M+H] <sup>+</sup>	0	482.3241
LPE 18:1	C <sub>23</sub> H <sub>46</sub> NO <sub>7</sub> P	9.8	480.3086	[M+H] <sup>+</sup>	0	480.3084
LPE 18:2	C <sub>23</sub> H <sub>44</sub> NO <sub>7</sub> P	8.9	478.2929	[M+H] <sup>+</sup>	0	478.2928
LPE 20:3	C <sub>25</sub> H <sub>46</sub> NO <sub>7</sub> P	9.5	504.3085	[M+H] <sup>+</sup>	0	504.3085
LPE 20:4	C <sub>25</sub> H <sub>44</sub> NO <sub>7</sub> P	9.0	524.2750	[M+Na] <sup>+</sup>	0	524.2748
LPE 22:5	C <sub>27</sub> H <sub>46</sub> NO <sub>7</sub> P	9.4	528.3075	[M+H] <sup>+</sup>	0	528.3085
LPE 22:6	C <sub>27</sub> H <sub>44</sub> NO <sub>7</sub> P	9.0	526.2927	[M+H] <sup>+</sup>	0	526.2928
LPC 14:0	C <sub>22</sub> H <sub>46</sub> NO <sub>7</sub> P	7.5	468.3086	[M+H] <sup>+</sup>	0	468.3085
LPC 16:0	C <sub>24</sub> H <sub>50</sub> NO <sub>7</sub> P	8.5	482.3243	[M+H] <sup>+</sup>	0	496.3398
LPC 16:1	C <sub>24</sub> H <sub>48</sub> NO <sub>7</sub> P	7.7	494.3242	[M+H] <sup>+</sup>	0	494.3241
LPC 18:0	C <sub>26</sub> H <sub>54</sub> NO <sub>7</sub> P	10.4	524.3710	[M+H] <sup>+</sup>	0	524.3711
LPC 18:1	C <sub>26</sub> H <sub>52</sub> NO <sub>7</sub> P	9.7	522.3555	[M+H] <sup>+</sup>	0	522.3554
LPC 18:2	C <sub>26</sub> H <sub>50</sub> NO <sub>7</sub> P	8.8	520.3398	[M+H] <sup>+</sup>	0	520.3398
LPC 18:3	C <sub>26</sub> H <sub>48</sub> NO <sub>7</sub> P	7.9	518.3242	[M+H] <sup>+</sup>	0	518.3241
LPC 20:3	C <sub>28</sub> H <sub>52</sub> NO <sub>7</sub> P	9.4	546.3552	[M+H] <sup>+</sup>	0	546.3554
LPC 20:4	C <sub>28</sub> H <sub>50</sub> NO <sub>7</sub> P	8.5	544.3397	[M+H] <sup>+</sup>	0	544.3398

LPC 20:5	C <sub>28</sub> H <sub>48</sub> NO <sub>7</sub> P	7.9	542.3243	[M+H] <sup>+</sup>	0	542.3241
LPC 22:5	C <sub>30</sub> H <sub>52</sub> NO <sub>7</sub> P	9.3	570.3549	[M+H] <sup>+</sup>	0	570.3554
LPC 22:6	C <sub>30</sub> H <sub>50</sub> NO <sub>7</sub> P	8.5	568.3399	[M+H] <sup>+</sup>	0	568.3398
DG 34:0	C <sub>37</sub> H <sub>72</sub> O <sub>5</sub>	17.5	614.5718	[M+NH <sub>4</sub> ] <sup>+</sup>	1	614.5718
DG 34:1	C <sub>37</sub> H <sub>70</sub> O <sub>5</sub>	17.0	612.5562	[M+NH <sub>4</sub> ] <sup>+</sup>	1	612.5561
DG 36:0	C <sub>39</sub> H <sub>76</sub> O <sub>5</sub>	18.2	642.6032	[M+NH <sub>4</sub> ] <sup>+</sup>	1	642.6031
DG 36:1	C <sub>39</sub> H <sub>74</sub> O <sub>5</sub>	17.7	640.5875	[M+NH <sub>4</sub> ] <sup>+</sup>	0	640.5874
DG 36:2	C <sub>39</sub> H <sub>72</sub> O <sub>5</sub>	17.2	638.5718	[M+NH <sub>4</sub> ] <sup>+</sup>	0	638.5718
DG 40:5	C <sub>43</sub> H <sub>74</sub> O <sub>5</sub>	20.2	688.5874	[M+NH <sub>4</sub> ] <sup>+</sup>	0	688.5874
DG 42:5	C <sub>45</sub> H <sub>78</sub> O <sub>5</sub>	20.9	716.6189	[M+NH <sub>4</sub> ] <sup>+</sup>	0	716.6187
DG 42:6	C <sub>45</sub> H <sub>76</sub> O <sub>5</sub>	20.4	714.6032	[M+NH <sub>4</sub> ] <sup>+</sup>	0	714.6031
PE 34:1	C <sub>39</sub> H <sub>76</sub> NO <sub>8</sub> P	15.9	718.5381	[M+H] <sup>+</sup>	0	718.5381
PE 34:2	C <sub>39</sub> H <sub>74</sub> NO <sub>8</sub> P	15.5	716.5222	[M+H] <sup>+</sup>	0	716.5225
PE 36:1	C <sub>41</sub> H <sub>80</sub> NO <sub>8</sub> P	16.5	746.5696	[M+H] <sup>+</sup>	0	746.5694
PE 36:2	C <sub>41</sub> H <sub>78</sub> NO <sub>8</sub> P	16.1	744.5536	[M+H] <sup>+</sup>	0	744.5538
PE 36:3	C <sub>41</sub> H <sub>76</sub> NO <sub>8</sub> P	15.6	742.5380	[M+H] <sup>+</sup>	0	742.5381
PE 36:4	C <sub>41</sub> H <sub>74</sub> NO <sub>8</sub> P	15.5	740.5224	[M+H] <sup>+</sup>	0	740.5225
PE 38:1	C <sub>43</sub> H <sub>84</sub> NO <sub>8</sub> P	16.1	774.6005	[M+H] <sup>+</sup>	0	774.6007
PE 38:2	C <sub>43</sub> H <sub>82</sub> NO <sub>8</sub> P	15.7	772.5850	[M+H] <sup>+</sup>	0	772.5851
PE 38:3	C <sub>43</sub> H <sub>80</sub> NO <sub>8</sub> P	15.2	770.5694	[M+H] <sup>+</sup>	0	770.5694
PE 38:4	C <sub>43</sub> H <sub>78</sub> NO <sub>8</sub> P	15.0	768.5541	[M+H] <sup>+</sup>	0	768.5538
PE 38:6	C <sub>43</sub> H <sub>74</sub> NO <sub>8</sub> P	15.4	764.5226	[M+H] <sup>+</sup>	0	764.5225
PE 40:3	C <sub>45</sub> H <sub>84</sub> NO <sub>8</sub> P	15.8	798.5400	[M+H] <sup>+</sup>	0	798.6007
PE 40:4	C <sub>45</sub> H <sub>82</sub> NO <sub>8</sub> P	15.6	796.5853	[M+H] <sup>+</sup>	0	796.5851
PE 40:6	C <sub>45</sub> H <sub>78</sub> NO <sub>8</sub> P	16.1	792.5541	[M+H] <sup>+</sup>	0	792.5538
PE 42:4	C <sub>47</sub> H <sub>86</sub> NO <sub>8</sub> P	16.3	824.6172	[M+H] <sup>+</sup>	0	824.6164
PC 30:0	C <sub>38</sub> H <sub>76</sub> NO <sub>8</sub> P	14.9	706.5382	[M+H] <sup>+</sup>	0	706.5381
PC 30:1	C <sub>38</sub> H <sub>74</sub> NO <sub>8</sub> P	14.3	704.5225	[M+H] <sup>+</sup>	0	704.5225
PC 32:0	C <sub>40</sub> H <sub>80</sub> NO <sub>8</sub> P	15.6	734.5694	[M+H] <sup>+</sup>	0	734.5694
PC 32:1	C <sub>40</sub> H <sub>78</sub> NO <sub>8</sub> P	15.1	732.5537	[M+H] <sup>+</sup>	0	732.5538
PC 32:2	C <sub>40</sub> H <sub>76</sub> NO <sub>8</sub> P	14.6	730.5380	[M+H] <sup>+</sup>	0	730.5381
PC 34:0	C <sub>42</sub> H <sub>84</sub> NO <sub>8</sub> P	16.2	762.6010	[M+H] <sup>+</sup>	0	762.6007
PC 34:1	C <sub>42</sub> H <sub>82</sub> NO <sub>8</sub> P	15.8	760.5848	[M+H] <sup>+</sup>	0	760.5851
PC 34:2	C <sub>42</sub> H <sub>80</sub> NO <sub>8</sub> P	15.3	758.569	[M+H] <sup>+</sup>	0	758.5694
PC 34:3	C <sub>42</sub> H <sub>78</sub> NO <sub>8</sub> P	14.8	756.5537	[M+H] <sup>+</sup>	0	756.5538
PC 34:4	C <sub>42</sub> H <sub>76</sub> NO <sub>8</sub> P	14.6	754.5382	[M+H] <sup>+</sup>	0	754.5381
PC 36:1	C <sub>44</sub> H <sub>86</sub> NO <sub>8</sub> P	16.4	788.6161	[M+H] <sup>+</sup>	0	788.6164
PC 36:2	C <sub>44</sub> H <sub>84</sub> NO <sub>8</sub> P	16.0	786.6002	[M+H] <sup>+</sup>	0	786.6007

PC 36:3	C <sub>44</sub> H <sub>82</sub> NO <sub>8</sub> P	15.5	784.5846	[M+H] <sup>+</sup>	0	784.5851
PC 36:4	C <sub>44</sub> H <sub>80</sub> NO <sub>8</sub> P	15.4	782.5691	[M+H] <sup>+</sup>	0	782.5694
PC 36:5	C <sub>44</sub> H <sub>78</sub> NO <sub>8</sub> P	14.8	780.5542	[M+H] <sup>+</sup>	0	780.5538
PC 38:0	C <sub>46</sub> H <sub>92</sub> NO <sub>8</sub> P	17.0	818.2251	[M+H] <sup>+</sup>	1	818.6633
PC 38:2	C <sub>46</sub> H <sub>88</sub> NO <sub>8</sub> P	16.5	814.6320	[M+H] <sup>+</sup>	1	814.632
PC 38:3	C <sub>46</sub> H <sub>86</sub> NO <sub>8</sub> P	16.2	812.6163	[M+H] <sup>+</sup>	1	812.6164
PC 38:4	C <sub>46</sub> H <sub>84</sub> NO <sub>8</sub> P	16.0	810.6007	[M+H] <sup>+</sup>	1	810.6007
PC 38:5	C <sub>46</sub> H <sub>82</sub> NO <sub>8</sub> P	15.7	808.5852	[M+H] <sup>+</sup>	1	808.5851
PC 38:6	C <sub>46</sub> H <sub>80</sub> NO <sub>8</sub> P	15.3	806.5693	[M+H] <sup>+</sup>	1	806.5694
PC 40:4	C <sub>48</sub> H <sub>88</sub> NO <sub>8</sub> P	16.5	838.6323	[M+H] <sup>+</sup>	1	838.6320
PC 40:5	C <sub>48</sub> H <sub>86</sub> NO <sub>8</sub> P	16.1	836.6165	[M+H] <sup>+</sup>	1	836.6164
PC 40:6	C <sub>48</sub> H <sub>84</sub> NO <sub>8</sub> P	16.0	834.6007	[M+H] <sup>+</sup>	1	834.6007
PC 40:7	C <sub>48</sub> H <sub>82</sub> NO <sub>8</sub> P	16.0	832.5827	[M+H] <sup>+</sup>	1	832.5851
PC 40:8	C <sub>48</sub> H <sub>80</sub> NO <sub>8</sub> P	15.1	830.5703	[M+H] <sup>+</sup>	1	830.5694
PS 34:0	C <sub>40</sub> H <sub>78</sub> NO <sub>10</sub> P	12.8	762.5277	[M-H] <sup>-</sup>	2	762.5291
PS 36:0	C <sub>42</sub> H <sub>82</sub> NO <sub>10</sub> P	14.1	790.5573	[M-H] <sup>-</sup>	4	790.5604
PS 36:1	C <sub>42</sub> H <sub>80</sub> NO <sub>10</sub> P	13.8	788.5414	[M-H] <sup>-</sup>	4	788.5447
PS 38:4	C <sub>44</sub> H <sub>78</sub> NO <sub>10</sub> P	14.7	810.5238	[M-H] <sup>-</sup>	5	810.5291
PS 38:5	C <sub>44</sub> H <sub>76</sub> NO <sub>10</sub> P	14.2	808.5096	[M-H] <sup>-</sup>	5	808.5134
PS 40:6	C <sub>46</sub> H <sub>78</sub> NO <sub>10</sub> P	15.2	834.526	[M-H] <sup>-</sup>	4	834.5291
PG 34:0	C <sub>40</sub> H <sub>79</sub> O <sub>10</sub> P	15.0	768.5801	[M+NH <sub>4</sub> ] <sup>+</sup>	6	768.5749
PG 34:1	C <sub>40</sub> H <sub>77</sub> O <sub>10</sub> P	15.1	766.5535	[M+NH <sub>4</sub> ] <sup>+</sup>	7	766.5593
PG 36:1	C <sub>42</sub> H <sub>81</sub> O <sub>10</sub> P	15.9	794.5958	[M+NH <sub>4</sub> ] <sup>+</sup>	6	794.5906
PG 38:5	C <sub>44</sub> H <sub>77</sub> O <sub>10</sub> P	16.6	814.552	[M+NH <sub>4</sub> ] <sup>+</sup>	7	814.5593
PG 38:6	C <sub>44</sub> H <sub>75</sub> O <sub>10</sub> P	16.1	812.5417	[M+NH <sub>4</sub> ] <sup>+</sup>	2	812.5436
PA 36:2	C <sub>39</sub> H <sub>73</sub> O <sub>8</sub> P	11.0	699.4917	[M-H] <sup>-</sup>	7	699.4970
PA 36:4	C <sub>39</sub> H <sub>69</sub> O <sub>8</sub> P	10.2	695.462	[M-H] <sup>-</sup>	5	695.4657
PI 34:2	C <sub>43</sub> H <sub>79</sub> O <sub>13</sub> P	9.7	833.5128	[M-H] <sup>-</sup>	7	833.5186
PI 36:2	C <sub>45</sub> H <sub>83</sub> O <sub>13</sub> P	10.3	861.5424	[M-H] <sup>-</sup>	5	861.5499
PI 38:4	C <sub>47</sub> H <sub>83</sub> O <sub>13</sub> P	10.7	885.5410	[M-H] <sup>-</sup>	9	885.5499
CE 18:1	C <sub>45</sub> H <sub>78</sub> O <sub>2</sub>	22.7	668.6342	[M+NH <sub>4</sub> ] <sup>+</sup>	1	668.6340
CE 18:2	C <sub>45</sub> H <sub>76</sub> O <sub>2</sub>	22.2	666.6181	[M+NH <sub>4</sub> ] <sup>+</sup>	1	666.6183
CE 18:3	C <sub>45</sub> H <sub>74</sub> O <sub>2</sub>	21.7	664.6027	[M+NH <sub>4</sub> ] <sup>+</sup>	1	664.6027
CE 20:3	C <sub>47</sub> H <sub>78</sub> O <sub>2</sub>	22.4	692.6341	[M+NH <sub>4</sub> ] <sup>+</sup>	1	692.6340
CE 20:4	C <sub>47</sub> H <sub>76</sub> O <sub>2</sub>	22.0	690.6183	[M+NH <sub>4</sub> ] <sup>+</sup>	1	690.6183
CE 20:5	C <sub>47</sub> H <sub>74</sub> O <sub>2</sub>	21.5	688.6027	[M+NH <sub>4</sub> ] <sup>+</sup>	1	688.6027
CE 22:6	C <sub>49</sub> H <sub>76</sub> O <sub>2</sub>	21.9	714.6183	[M+NH <sub>4</sub> ] <sup>+</sup>	1	714.6183
TG 48:0	C <sub>51</sub> H <sub>98</sub> O <sub>6</sub>	22.5	824.7703	[M+NH <sub>4</sub> ] <sup>+</sup>	1	824.7702

TG 48:1	C <sub>51</sub> H <sub>96</sub> O <sub>6</sub>	22.0	822.7545	[M+NH <sub>4</sub> ] <sup>+</sup>	1	822.7545
TG 48:2	C <sub>51</sub> H <sub>94</sub> O <sub>6</sub>	21.4	820.7390	[M+NH <sub>4</sub> ] <sup>+</sup>	1	820.7389
TG 48:3	C <sub>51</sub> H <sub>92</sub> O <sub>7</sub>	20.8	818.7234	[M+NH <sub>4</sub> ] <sup>+</sup>	1	818.7232
TG 50:1	C <sub>53</sub> H <sub>100</sub> O <sub>6</sub>	22.6	850.7852	[M+NH <sub>4</sub> ] <sup>+</sup>	1	850.7858
TG 50:2	C <sub>53</sub> H <sub>98</sub> O <sub>6</sub>	22.1	848.7700	[M+NH <sub>4</sub> ] <sup>+</sup>	1	848.7702
TG 50:3	C <sub>53</sub> H <sub>96</sub> O <sub>6</sub>	21.6	846.7543	[M+NH <sub>4</sub> ] <sup>+</sup>	1	846.7545
TG 50:4	C <sub>53</sub> H <sub>94</sub> O <sub>6</sub>	21.1	844.7391	[M+NH <sub>4</sub> ] <sup>+</sup>	1	844.7390
TG 50:5	C <sub>53</sub> H <sub>92</sub> O <sub>6</sub>	20.5	842.7236	[M+NH <sub>4</sub> ] <sup>+</sup>	1	842.7237
TG 52:0	C <sub>55</sub> H <sub>106</sub> O <sub>6</sub>	23.4	880.8329	[M+NH <sub>4</sub> ] <sup>+</sup>	1	880.8328
TG 52:1	C <sub>55</sub> H <sub>104</sub> O <sub>6</sub>	23.1	878.8169	[M+NH <sub>4</sub> ] <sup>+</sup>	1	878.8171
TG 52:2	C <sub>55</sub> H <sub>102</sub> O <sub>6</sub>	22.7	876.8007	[M+NH <sub>4</sub> ] <sup>+</sup>	1	876.8015
TG 52:3	C <sub>55</sub> H <sub>100</sub> O <sub>6</sub>	22.3	874.785	[M+NH <sub>4</sub> ] <sup>+</sup>	1	876.8015
TG 52:4	C <sub>55</sub> H <sub>98</sub> O <sub>6</sub>	21.8	872.7698	[M+NH <sub>4</sub> ] <sup>+</sup>	1	872.7702
TG 52:5	C <sub>55</sub> H <sub>96</sub> O <sub>6</sub>	21.5	870.7546	[M+NH <sub>4</sub> ] <sup>+</sup>	1	870.7545
TG 52:6	C <sub>55</sub> H <sub>94</sub> O <sub>6</sub>	20.9	868.7391	[M+NH <sub>4</sub> ] <sup>+</sup>	1	868.7389
TG 54:0	C <sub>57</sub> H <sub>110</sub> O <sub>6</sub>	22.5	908.8641	[M+NH <sub>4</sub> ] <sup>+</sup>	1	908.8641
TG 54:1	C <sub>57</sub> H <sub>108</sub> O <sub>6</sub>	22.0	906.8484	[M+NH <sub>4</sub> ] <sup>+</sup>	1	906.8484
TG 54:2	C <sub>57</sub> H <sub>106</sub> O <sub>6</sub>	23.2	904.8328	[M+NH <sub>4</sub> ] <sup>+</sup>	1	904.8328
TG 54:3	C <sub>57</sub> H <sub>104</sub> O <sub>6</sub>	22.8	902.8164	[M+NH <sub>4</sub> ] <sup>+</sup>	1	902.8171
TG 54:4	C <sub>57</sub> H <sub>102</sub> O <sub>6</sub>	22.4	900.8008	[M+NH <sub>4</sub> ] <sup>+</sup>	1	900.8015
TG 54:5	C <sub>57</sub> H <sub>100</sub> O <sub>6</sub>	22.0	898.7857	[M+NH <sub>4</sub> ] <sup>+</sup>	1	898.7858
TG 54:6	C <sub>57</sub> H <sub>98</sub> O <sub>6</sub>	21.8	896.7701	[M+NH <sub>4</sub> ] <sup>+</sup>	1	896.7702
TG 54:7	C <sub>57</sub> H <sub>96</sub> O <sub>6</sub>	21.4	894.7546	[M+NH <sub>4</sub> ] <sup>+</sup>	1	894.7545
TG 54:8	C <sub>57</sub> H <sub>94</sub> O <sub>6</sub>	20.6	892.7389	[M+NH <sub>4</sub> ] <sup>+</sup>	1	892.7389
TG 56:0	C <sub>59</sub> H <sub>114</sub> O <sub>6</sub>	23.0	936.8958	[M+NH <sub>4</sub> ] <sup>+</sup>	1	936.8954
TG 56:1	C <sub>59</sub> H <sub>112</sub> O <sub>6</sub>	22.6	934.8799	[M+NH <sub>4</sub> ] <sup>+</sup>	1	934.8797
TG 56:2	C <sub>59</sub> H <sub>110</sub> O <sub>6</sub>	22.1	932.8639	[M+NH <sub>4</sub> ] <sup>+</sup>	1	932.864
TG 56:3	C <sub>59</sub> H <sub>108</sub> O <sub>6</sub>	23.2	930.8485	[M+NH <sub>4</sub> ] <sup>+</sup>	1	930.8484
TG 56:4	C <sub>59</sub> H <sub>106</sub> O <sub>6</sub>	22.9	928.8328	[M+NH <sub>4</sub> ] <sup>+</sup>	1	928.8328
TG 56:5	C <sub>59</sub> H <sub>104</sub> O <sub>6</sub>	22.8	926.8171	[M+NH <sub>4</sub> ] <sup>+</sup>	1	926.8171
TG 56:6	C <sub>59</sub> H <sub>102</sub> O <sub>6</sub>	22.4	924.8014	[M+NH <sub>4</sub> ] <sup>+</sup>	1	924.8015

FA: fatty acid; MG: monoglyceride; DG: diacylglyceride; TG: triglyceride; CE: cholesteryl ester; LPE: lyso-phosphatidylethanolamine; LPC: lyso-phosphatidylcholine, PE: phosphatidylethanolamine; PC: phosphatidylcholine; PS: phosphatidylserine; PG: phosphatidylglycerol; PA: phosphatidic acid; PI: phosphatidylinositol; FC: fold change.



## **2.2 Towards lipid free concentration: testing a standard generating water system**

### **2.2.1 Introduction**

Measuring the concentration of a compound (i.e., drugs, pollutants, metabolites) in biological samples is of paramount importance in multiple research areas. For instance, the amount of drug in a biological sample can be reported as its total concentration, ignoring the drug's interactions with the sample, or as free concentration, which reflects the proportion of molecules that can diffuse through membranes and exert biological activity.<sup>160,161</sup> While total concentration determination has been the traditional approach, measurements of free concentrations are becoming increasingly crucial as emerging evidence suggests a stronger correlation between free concentration and pharmacological and toxicological effects.<sup>161</sup> However, the bioavailability of a compound may be impacted by its partition to matrix components such as dissolved organic matter,<sup>162</sup> proteins,<sup>163–167</sup> or other cellular structures.<sup>168</sup> Thus, measuring the free concentration of a drug is essential not only for bioavailability studies but also for determining its binding affinity or partition coefficient.

Multiple methods have been developed in the past decades to measure analyte protein binding affinities by determining an analyte's free concentration, most of which involve separating the analyte into free and bound portions, followed by the direct analyses of the unbound analyte. A summary of some drug–protein binding methods is presented in Table 2.6, showcasing the main features of each one. The most prevalent separation-based methods are dialysis, ultrafiltration, ultracentrifugation, and affinity chromatography.<sup>169,170</sup>

Nevertheless, all these methods are often time-consuming, the analytes may be irreversibly removed from the sample by the devices utilized, and they could produce inaccurate results if the binding equilibrium changes during the separation process.<sup>171</sup> In contrast, some methods used to determine the free drug concentration in a sample without separating the drug from the binding protein include surface plasmon resonance, calorimetry, and spectroscopy.<sup>172–175</sup> While these methods do not significantly disrupt the existing binding equilibrium, they are rarely used to analyze complex samples. Ultimately, the method of choice should consider the sample type (i.e., isolated proteins vs. raw biological samples), the desired sensitivity, and the preferred throughput.

SPME offers yet another alternative for free concentration determination, as the amount extracted is proportional to the unbound analyte's concentration in the sample. Non-depletive SPME (nd-SPME) introduced a specific application of SPME to measure free concentrations relying on *negligible* depletion of the unbound analyte pool, thus conserving the existing equilibrium in the sample.<sup>138,176</sup> This negligible extraction approach inherently adds pressure on detection systems due to the minimal amount of analyte isolated, particularly for low-volume samples in pharmacology and toxicology. Likewise, nd-SPME relies on meticulous method development as this approach's outcomes are prone to variations in temperature, extraction time, and impurities. Nevertheless, this approach has been adapted to several applications since its introduction, as noted by a few reviews on this niche field.<sup>176–178</sup>

Table 2.6. Main features of some methods to measure free concentrations. Adapted from Seyfinejad et al.<sup>179</sup>

Method	Throughput	Analysis time	Selectivity / Sensitivity	Advantages	Disadvantages	Refs
ED	Low	12 – 48 hrs	No / $\mu\text{mol L}^{-1}$	<u>Gold standard</u> Extensively used Temperature controlled	Time-consuming Prone to analyte binding to the dialysis membrane Likely dilution of analytes in perfusate, thus requires a sensitive detector	171,180,181
UF	Low	< 1 hour	No / $\mu\text{mol L}^{-1}$ to $\text{mmol L}^{-1}$	Extensively used Easy, fast, and inexpensive.	Potential analyte binding to filter Likely equilibrium shift and protein leakage	169,171,182
UC	Low	4 – 16 hrs	No / $\text{mmol L}^{-1}$	Extensively used Minimal binding to the device	Time-consuming Expensive centrifuge	169,171,182
AC	Moderate	< 1 hour	Yes / $\mu\text{mol L}^{-1}$	Able to measure total and free conc. Able to assess multiple ligands at once High precision, selectivity, and reproducibility	Limited by protein immobilization Protein conformation may change Possible equilibrium shift	183–185
SPR	Moderate	1 – 2 hrs	Yes / $\mu\text{mol L}^{-1}$	Simple	Only feasible for fluorescent (tagged) compounds. Limited to high-binding analytes	172,175,185,186
TC	Low	3 hrs	No / $\text{mmol L}^{-1}$	Thermodynamic info provided	Requires a large amount of sample Requires highly pure reagents	173,187,188
CapE	Moderate to high	1 – 2 hrs	No / $\text{mmol L}^{-1}$	Rapid and simple Low sample requirement	Low sensitivity Possible capillary wall adsorption	189,190
SPME	Moderate to high	1 – 2 hrs	No / $\mu\text{mol L}^{-1}$	No (or minimal) sample prep	Needs correct model for quantitation Model parameters are determined separately	69,138,176,177,191–193

ED, equilibrium dialysis; UF, ultrafiltration; UC, ultracentrifugation; AC, affinity chromatography; SPR, surface plasmon resonance; TC, titration calorimetry; CapE, capillary electrophoresis; SPME, solid phase microextraction

The correct application of nd-SPME requires negligible depletion of the free fraction – an idealistic expectation, as depletion will never be 0%. Therefore, the maximum allowed depletion and its effect on the experiment's outcome should dictate the choice of an appropriate limit (e.g., depletion limits are typically in the 1– 10% range).<sup>177,194,195</sup> Furthermore, the correct method for calibrating nd-SPME measurements for free concentration is through an external calibration curve using samples with known analyte concentrations. These samples must not contain any binding matrix to ensure that all the analyte is in a freely dissolved state, thus ensuring the calibration curve relates the free concentration exposed to the SPME fiber and the measured signal response.

Taking into accounts the requirements to calibrate an analyte's free concentration using SPME devices, it is hypothesized that a miniaturized SPME probe can be used to achieve this in a non-depletive fashion estimate, and that the standard generating vial may be a viable method for the construction of external calibration curves.

### **2.2.2 Experimental**

#### Materials, supplies, and standards

The SYLGARD 184 silicone elastomer mix was acquired from Dow Corning (Midland, MI). The carbon fibre mesh weave (Panex 30) was provided by Zoltec Co. (Bridgetown, MO). An Elcometer 4340 motorized automatic film applicator and coating bar (adjustable gap of 0–250  $\mu\text{m}$ ) were acquired from Elcometer Ltd. (Rochester Hills, MI, USA). These materials were employed to manufacture the standard generating vial.

Lyso-palmitoyl phosphatidylcholine (LPC 16:0), lyso-heptadecanoyl phosphatidylcholine (LPC 17:0), and di-palmitoyl phosphatidylcholine (DPPC, PC 16:0/16:0) were purchased from Avanti Lipids/Sigma Aldrich (Oakville, ON, Canada). These glycerophospholipids were used as model compounds and will be referred to as phospholipids in this subchapter.

The miniaturized SPME probes (mini-tips) were prepared using nitinol wire as the solid support, which was mechanically etched, coated with a C18/PAN slurry (5  $\mu\text{m}$  particle size), and cleaned according to the methods described in Section 0. The general workflow for the extractions using the SPME probes was the same as that described in Section 0, except for using a mixture of H<sub>2</sub>O/MeOH/IPA (10:20:60, v/v/v) during analyte desorption (50  $\mu\text{L}$ , 30 min, 1000 rpm).

All other solvents and materials used in this work are the same as those described in Section 0.

#### LC-MS/MS instrumentation conditions

A short isocratic method was employed for the chromatographic separation of the model compounds using the same column type described in Section 0. This isocratic method enabled baseline separation of all three compounds within 2 min. Targeted experiments were carried out on a TSQ Vantage™ triple-quadrupole mass spectrometer (Thermo Scientific, CA, USA) equipped with a heated ESI (H-ESI) ionization source. Table 2.7 contains additional information on the LC-MS/MS conditions used. These

instrumental conditions enabled all compounds' LOQ of 0.05 ng/mL and a linear dynamic range within 0.05–250 ng/mL.

Table 2.7. LC-MS/MS conditions for the analysis of model compounds.

<b>Liquid Chromatographic conditions – Thermo Vanquish Flex UHPLC</b>			
Column	Waters Acquity CHS® C18		
Column dimensions	2.1× 75 mm, 1.7 μm		
Mobile phase	H <sub>2</sub> O/MeOH/IPA (10/20/60)		
Additives used	0.1 % (v/v) acetic acid		
Flow rate	350 μL/min		
Column temperature	55 °C		
Samples temperature	5 °C		
Injection volume	10 μL		
<b>Mass spectrometry conditions – Thermo TSQ Vantage™</b>			
Spray voltage	2.5 kV, positive mode		
Vaporizer temperature	300 °C		
Transfer capillary temp.	350 °C		
Sheath gas, arb	30 arb		
Auxiliary gas, arb	40 arb		
Sweep gas, arb	10 arb		
Dwell time	10 ms/ transition		
<b>MS/MS transitions for phospholipids under study</b>			
Standard	LPC 16:0	LPC 17:0	DPPC
Parent mass, <i>m/z</i>	496.3	510.3	734.5
Fragment mass, <i>m/z</i>	184.1	184.1	184.1
Collision energy / S–lens [V]	19 V/ 10 V	19 V/ 10 V	22 V / 12 V

### Preparation of standard-generating vials

The PDMS-coated meshes employed for the standard generating vial (SGV) were prepared based on a procedure developed in previous work.<sup>196–198</sup> Briefly, a PDMS slurry was prepared by mixing Sylgard 186 PDMS base (4.54 g) and hexane (5.8 mL) in a plastic syringe and mixing for 3 min with a stainless-steel spatula; then Sylgard 186 cross-linking agent (0.46 g) was added, and the slurry was further mixed for one more minute. The

resulting PDMS slurry was then spread over a 25 cm (length) by 30 cm (width) carbon-mesh sheet by the Elcometer film applicator; and heated in a nitrogen atmosphere (using a nitrogen-purged vacuum oven, 15 mm Hg pressure) at 90 °C for one hour. To coat the other side, fewer quantities are required for the PDMS slurry: 3.81 g of Sylgard 186 PDMS base, 4.9 mL of hexane, and 0.39 g of Sylgard 186 cross-linking agent. The resulting PDMS-coated carbon mesh was cut into 4 cm × 7 cm pieces, cleaned (30 min, 500 rpm in a glass jar) using MeOH/IPA/ACN/H<sub>2</sub>O (3/3/3/1, v/v). Then, the 4 cm × 7 cm pieces were spiked with the model lipids on one side – the side coated first with higher PDMS content – following a grid pattern: 10 µL of lipid solution was applied to each 1 cm × 1 cm cell of the side that would become the inner leaflet. The lipid-laden PDMS mesh was rolled carefully, placed inside a 20 mL silanized amber vial, and filled with 20 mL of aqueous media (either LC-MS-grade water or PBS, pH 7.4). Each vial was provided with a small Teflon magnetic stirrer, sonicated briefly (20 s) to dislodge air bubbles from the carbon mesh, and left to equilibrate at 18 °C under agitation at 1000 rpm.

#### Equilibration and short-term reusability

To assess the SGV's equilibration time among its different components (e.g., aqueous sample, PDMS film/coating, outer leaflet of the PDMS-coated sheet, glass walls), three independent vials were prepared for each lipid, and their aqueous lipid concentration monitored over multiple/five days using the LLE method described in Section 0. The SGV vials were spiked with 2.5 µg to result in a 125 ng/mL *total* concentration for LPC 16:0, whereas 125 ng was used for a 6.25 ng/mL concentration of DPPC. Then, the SPME

minitips were used to assess the system's recovery rate. The SPME minitips were introduced through a syringe tip piercing the SGV's septum and exposed for at least 60 min under magnetic agitation. The septum had an opening to allow for the simultaneous extraction of aliquots while the SPME extraction took place. The RR considered this way permitted to study the SGV reusability when using SPME minitips. To examine the SGV's short-term reusability, multiple sequential extractions were performed on recently prepared and equilibrated, independent vials ( $n = 3$  per lipid, using 100 ng/mL and 6.25 ng/mL for LPC and DPPC, respectively). Seven sequential extractions were done from each vial using SPME minitips (keeping a 5 min *recovery/gap* time between extractions), followed by daily extractions performed over four days.

A short LLE extraction step was applied to aqueous aliquots taken from SWSs, to avoid the introduction of non-volatile phosphate salts from PBS samples.<sup>34</sup> Briefly, 100  $\mu$ L of MeOH/MTBE (30/70) were added to a 50  $\mu$ L aqueous aliquot, agitated for 30 min at 1000 rpm, and centrifuged at 10000 rpm for 10 min. The upper phase was collected, and the lower phase was subject to a second LLE extraction. Both upper phases were pooled together, vacuum evaporated for 10 min at 30 °C, and reconstituted using the desorption solvent mentioned above (50  $\mu$ L). The volume of the aliquot was replenished immediately after with a fresh aqueous sample.



### 2.2.3 Results and Discussion

#### Negligible extraction of lipids using miniaturized probes

SPME is recognized as a *green* sample preparation technique thanks to its minimized solvent usage, single-step sampling and preconcentration into the coating, and extraction via free concentration. The accurate determination of the free concentration of analytes is interesting from a toxicological and pharmacological point of view, as these freely dissolved forms of organic compounds are generally considered to be the only form that could cross membranes via passive diffusion and exert bioactivity. Other techniques used for free concentration determination include passive samplers, solvent microextraction, and microdialysis, among others.<sup>85,199–203</sup> However, lipids used in this niche field are generally used as an additional binding matrix (i.e., as any self-assembled structure),<sup>204,205</sup> with very few exceptions on studying bioactive lipids (i.e., progesterone, estradiol, oxylipins).<sup>85,200</sup>

To this end, the coating dimensions in fiber probes were optimized for non-depletive extractions at equilibrium using LPC 16:0 in PBS, with a cut-off value set at 5%. This extent of negligible depletion using C18-coated fibers was achieved at a length of 2.0 ( $\pm 0.1$ ) mm and a thickness of 6.5 ( $\pm 0.7$ )  $\mu\text{m}$ . These dimensions were tested as well for LPC 17:0, resulting in negligible depletion as well (60 ppb, 1.5 mL, 90 min extraction time), with excellent reproducibility (RSD <10%, n=5). Smaller dimensions attained lower depletion extent at the cost of decreased reproducibility (RSD >20%), stemming from coating loss during agitated extraction.

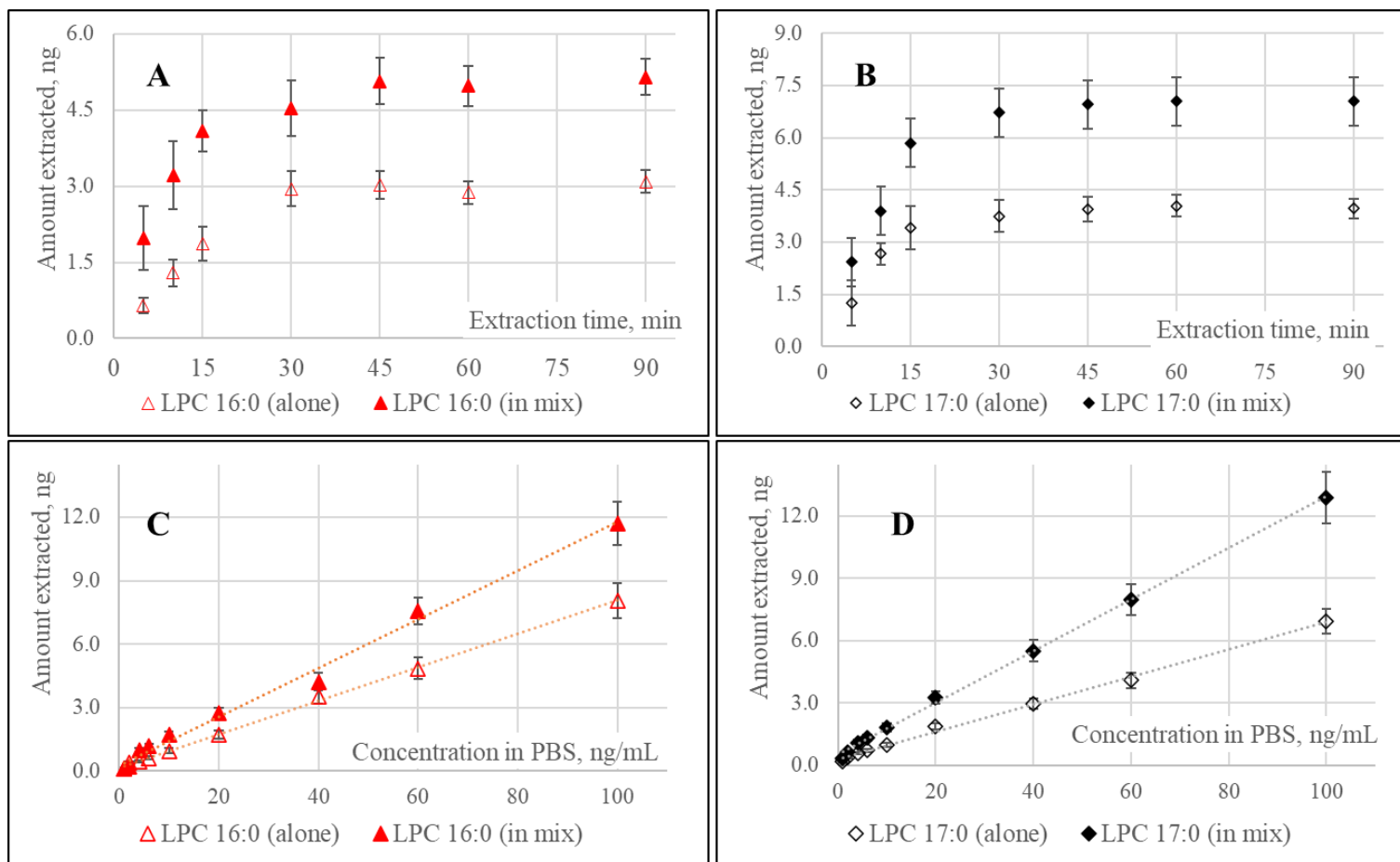


Figure 2.11 Extraction time profiles and calibration curves in PBS constructed using miniaturized C18-coated probes for model lipids. (A) ETP for LPC 16:0 by itself (void triangles) and when mixed with LPC 17:0 (filled triangles). (B) ETP for LPC 17:0 by itself (empty diamonds) and when mixed with LPC 16:0 (filled diamonds). (C) Matrix-free calibration curves for LPC 16:0 alone and as part of a mixture. (D) Matrix-free calibration curve for LPC 17:0 alone and as part of a mixture.

The extraction time profile was carried out for both model compounds, LPC 16:0 and LPC 17:0, and are shown in Figure 2.11A and Figure 2.11B, respectively. These extraction time profiles were conducted for each individual lipid and for a mixture of both compounds, the latter for practical purposes. Intriguingly, the amount extracted at equilibrium is higher when both compounds are mixed than when each individual lipid is considered. This behaviour was also observed for mixtures of polyunsaturated fatty acids during preliminary experiments. Moreover, the calibration curves (Figure 2.11C and Figure 2.11D) for the compound mixture exhibited higher sensitivity, as indicated by their steeper slopes, compared to the individual compounds. Positively, there is an excellent linear relationship between the amount extracted and the nominal amount present, regardless of the lipid being present by itself or in a mixture. The synergism was attributed by the author to the surfactant properties of these amphiphilic lipids, as observed in multiphase systems with surfactant blends that modify various solution parameters (e.g., surface tension, conductivity, foamability).<sup>206–208</sup>

$$f_C = K_{FS}V_S \quad \text{Eq. 7}$$

The coating capacity, expressed as the fiber constant ( $f_C$ ), was estimated using equation 7 for LPC 16:0 and LPC 17:0 as  $51.7 \mu\text{L} (\pm 15.5 \mu\text{L})$  and  $69.6 \mu\text{L} (\pm 20.9 \mu\text{L})$ , respectively. The sorbent volume,  $V_S$ , computed from the coating dimensions as  $8.4 \times 10^{-3} \mu\text{L} (\pm 3.0 \times 10^{-3} \mu\text{L})$ . The partition coefficients,  $K_{FS}$ , for LPC 16:0 and LPC 17:0 was estimated from the experimental parameters as  $6.15 \times 10^3 (\pm 1.23 \times 10^3)$  and  $8.15 \times 10^3 (\pm 1.66 \times 10^3)$ , respectively. Nevertheless, it must be noted that analytes are

adsorbed on the active surface of solid coatings (such as C18 used here) rather than being partitioned. Considering this limitation, it is highly advisable to determine the adsorption equilibrium constant – experimentally more challenging – for each lipid instead. Relatedly, it is important to consider the effect of multiphase systems on the adsorption process to avoid any wild extrapolation in more complex biological samples.

### **Standard generating vials**

Sorbent coating dimensions were figured out for non-depletive extraction of the model polar lipids (as described in the previous section); however, the external calibration curves prepared could only be used once before significant depletion would occur. Therefore, a system that can allow multiple, sequential extractions without experiencing significant depletion *and* can maintain a stable free concentration at the same time is highly desirable for the calibration of the free concentration. The standard generating vials (developed and evaluated for GC-amenable volatile compounds)<sup>101,196</sup> were thus adapted and evaluated for aqueous media with a couple of lipids as the model compounds. The vials were prepared as described in section 0, and their reusability evaluated as described in section 0.

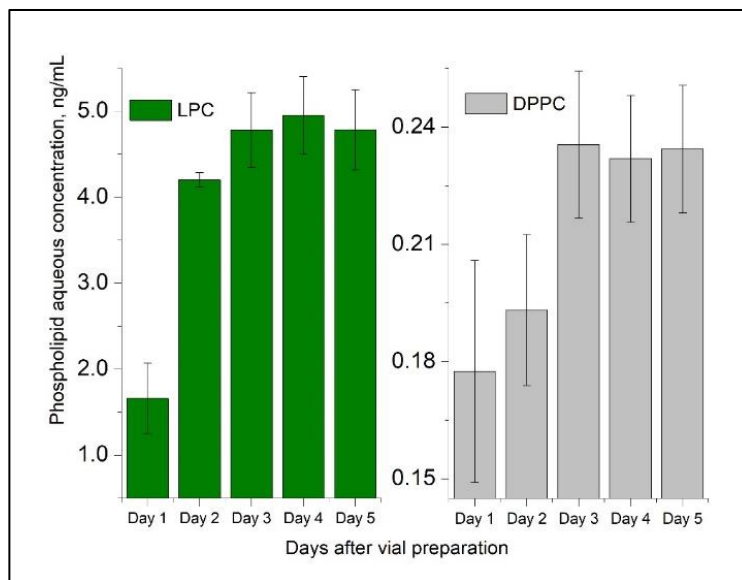


Figure 2.12. Equilibration of the aqueous concentration prepared for LPC and DPPC over five days from their preparation. Total concentrations for the standard-generating vials for LPC and DPPC are 2.5  $\mu\text{g}/\text{vial}$  and 125  $\text{ng}/\text{vial}$ , respectively.

The standard generating vial prepared for the phospholipids showed stabilization by the third day after preparation, as depicted in Figure 2.12. Each bar represents the average of three aliquots taken and analyzed from three independent vials. The highest variation was observed for the aliquots taken on the first day since equilibrium had not been reached. It is important to note that phosphatidylcholines, as other zwitterionic surfactants, are known to form monolayers on water-air interfaces, which would result in concentration *hot spots* within the vial. Thus, a sonication step was implemented to minimize possible *hot spots*, with 15–20 seconds being enough to remove visible bubbles. Sonication for longer times was avoided to prevent cavitation damage on the PDMS film and to minimize any potential phospholipid self-aggregation. Similarly, the PDMS thin film is believed to act as a reservoir matrix for the phospholipids and any desorption from this thin film occurs as freely dissolved lipids.

A linear relationship was not observed between the total amount spiked to the vial and the final aqueous concentration for phospholipids over the studied concentration range (Figure 2.13). Despite that, linear behaviour between the amount spiked onto the PDMS thin film and the is attained for LPC 16:0 within a short spiking range (i.e., 0.2–2.5  $\mu\text{g}$ ) before the free concentration starts plateauing around 8 ng/mL and 5 ng/mL for water and PBS, respectively. Conversely, the aqueous concentration for DPPC plateaus around 0.3 ng/mL as portrayed in Figure 2.14. This plateauing in the free concentration suggests the aggregation of monomeric molecules of DPPC in the aqueous portion at its critical micelle concentration (CMC,  $4.5 \times 10^{-10} \text{ M}$ )<sup>24</sup>. CMCs for phospholipids with biological relevance fall in the  $10^{-10}$ – $10^{-8} \text{ M}$  range, with a clear dependence on the length and saturation of their hydrophobic tails; thus, virtually all phospholipids are above their respective CMCs at physiological concentrations. While, a dynamic equilibrium certainly exists between the freely dissolved monomers and the micellar structures, the free concentration of these very hydrophobic phospholipids is infinitesimally small, which must be considered for extrapolating results to complex biological samples.

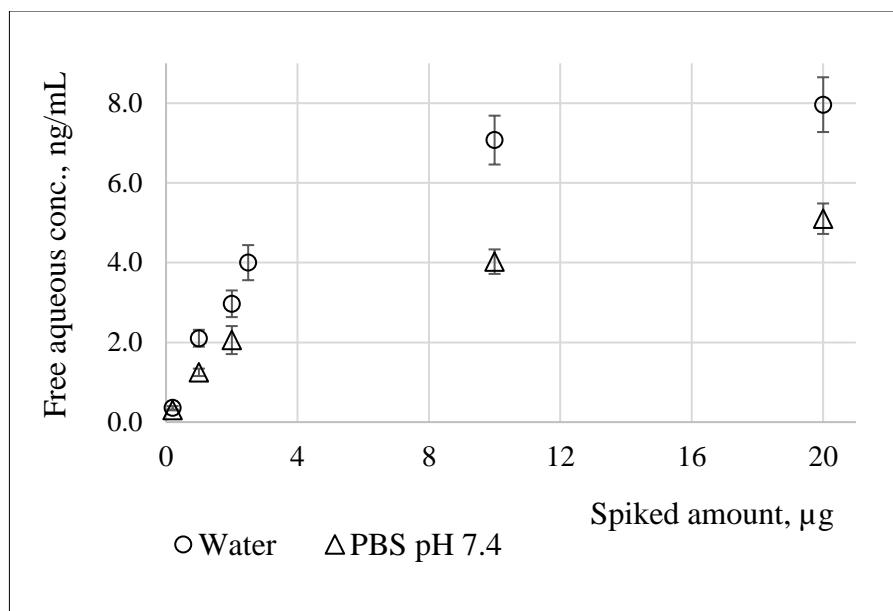


Figure 2.13. Calibration curves prepared for LPC 16:0 by spiking the PDMS thin films for vials with aqueous media.

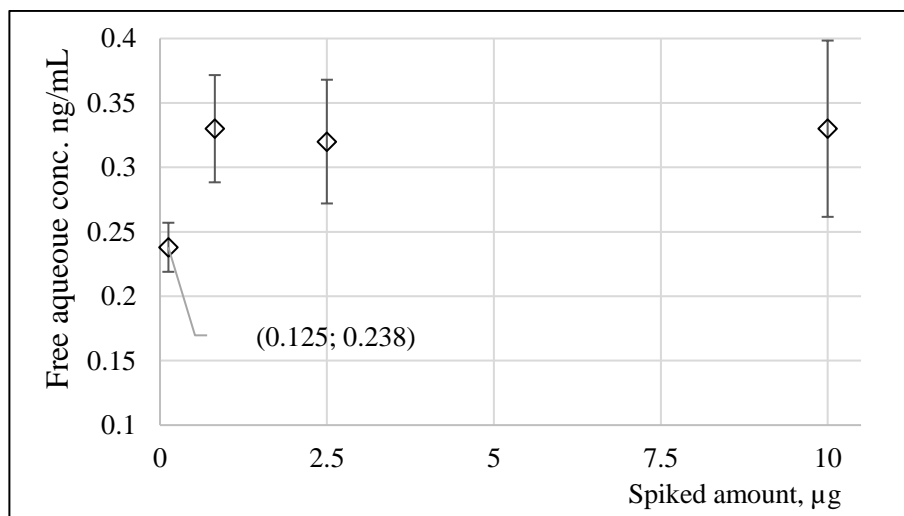


Figure 2.14. Estimated free aqueous concentration for DPPC at various amounts spiked onto the PDMS thin film. At the lowest spiked level (125 ng/vial).

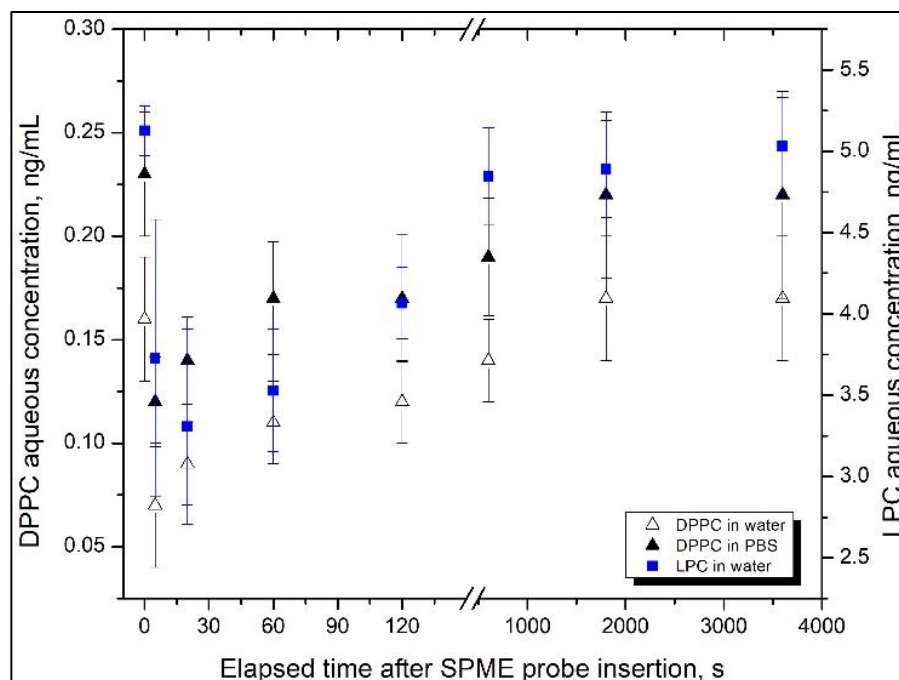


Figure 2.15. Aqueous concentration for model phospholipids *during* a 60 min extraction with a C18-coated SPME minitip.

The *pace* at which the PDMS reservoir replenished the free concentration during extraction with a SPME minitip was assessed for the studied phospholipids is portrayed in Figure 2.15. The concentration decreased rapidly within the first minute of extraction, which is consistent with the fast uptake by the SPME fiber extraction phase. However, the time required for the system to replenish the *initial* concentration varied significantly for each tested phospholipid: about ten minutes for LPC 16:0 and over 60 minutes for DPPC. The markedly slower recovery rate for DPPC is attributed to its meager solubility in addition to a kinetically hindered desorption from the PDMS membrane, as lipid/lipid interactions in membranes heavily influence the desorption of hydrophobic compounds.<sup>25</sup> Regardless of the initial *rate*, both systems appeared to replenish the initial concentration



after 60 min of extraction, which was exploited to assess the repeatability of the systems for either SPME extractions or direct measurement of the aqueous concentration (Figure 2.16).

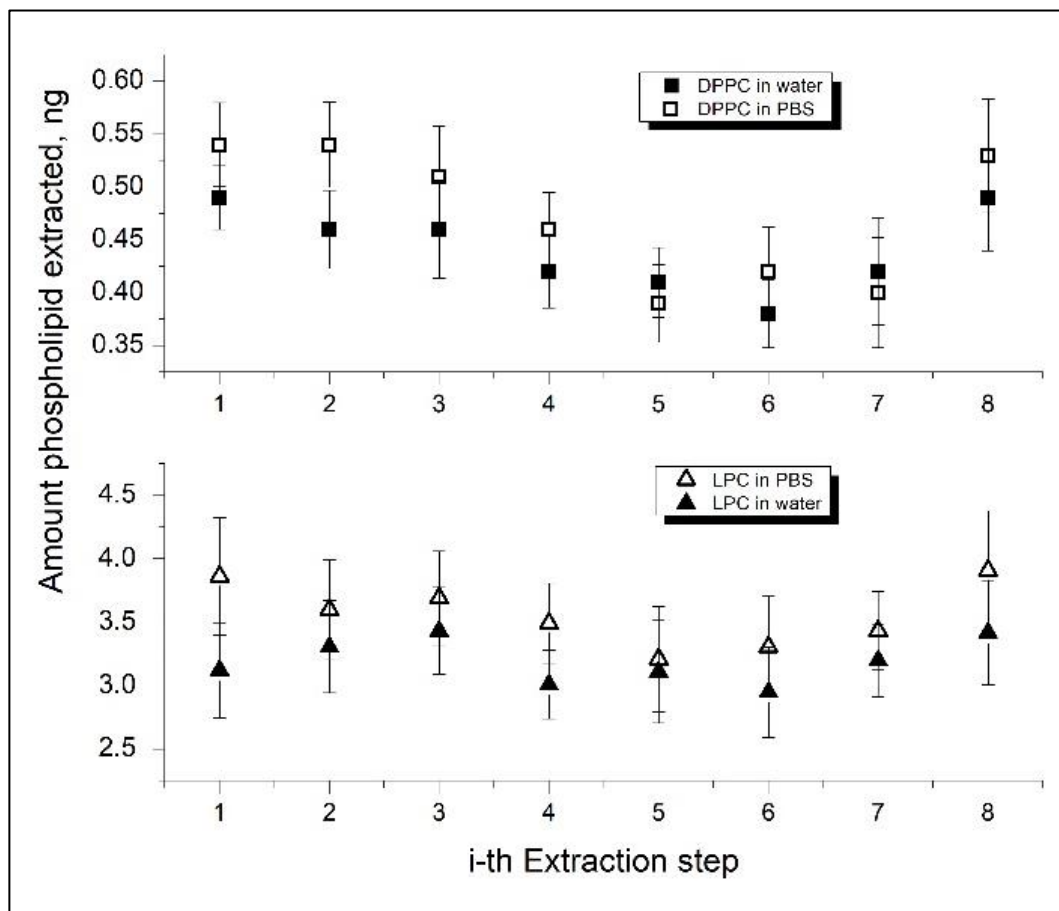


Figure 2.16 Sequential SPME extractions to assess the repeatability of extractions from the SGVs prepared for LPC 16:0 (at 2.0  $\mu\text{g}/\text{vial}$  total conc.) and DPPC (125 ng/vial total conc.), using two aqueous media. The inter-sampling interval was fixed to 5 min for extractions 1-7, and to overnight (15 hours) between the seven<sup>th</sup> and eight<sup>th</sup> extractions.

The short-term repeatability of these SGV was evaluated by performing multiple sequential extractions using the SPME minitips. A total of eight extractions were performed: seven extractions taking place for one day, and an eight-extraction taking place

the following day (following over 15 hours of system recovery). In all cases, the effects of SPME extraction were negligible, accounting for only ~5% depletion of the free concentration. For example, SPME extraction accounted for only ~1.3% of the drop in phospholipids compared to the total amount spiked to the vial. If the same amounts are extracted, up to 40 extractions could be performed before significant depletion of the lipid laden PDMS film is depleted (its reservoir concentration would be reduced by 10%). For the other lipid, DPPC lacks good intra-day repeatability and presents significant depletion by the miniaturized probe after the fifth SPME consecutive extraction (within the same day). This result is attributable to DPPC's very high affinity towards the hydrophobic coating and its low water solubility, which results in a prolonged desorption rate from the PDMS membrane and, consequently, long re-equilibration times. However, by adjusting the time between successive extractions (as observed by the eight-extraction step following overnight recovery), one could *in principle* extract repeatable amounts of DPPC for up to 12 days prior to significant depletion of the total spiked amount. The markedly slower re-equilibration rate for DPPC is likely due to kinetically hindered desorption from the PDMS membrane, as lipid/lipid interactions in membranes heavily influence the desorption of hydrophobic compounds.

Obtaining external calibration curves for hydrophobic compounds poses challenges such as rapid self-association of freely dissolved monomers, partition into various surfaces (e.g., water–air interfaces, glass and plastic walls), and insufficient stability related to their poor solubility and the lack of a binding matrix. However, these challenges were addressed

through the development of the standard generating vial. This approach utilized a PDMS film in direct contact with the water, which provided a partitioning matrix for the lipids, and served as a reservoir for the bulk of the lipids, thus stabilizing the concentration over time. By overcoming these obstacles, the standard generating vial offers a promising strategy for accurately determining the free concentration of hydrophobic compounds in a variety of applications.

In conclusion, the approach of miniaturizing the probes was shown to be a successful strategy in obtaining non-depletive extraction at equilibrium for model lipids. These miniaturized devices were then used in combination with the standard generating vial, which was found to be a viable and efficient method to construct external calibration curves to determine free concentration. While this combination is a promising avenue for future studies to determine the free concentration of other bioactive lipids, it is important to consider the synergistic effect of extracting more than one lipid in a sample and the biological control existing for some bioactive lipids. Despite these challenges, the study adequately evaluated the viability of the standard generating vial for constructing external calibration curves in an easy and fast manner. Ultimately, these findings provide a hopeful outlook for future research in this field, as the miniaturization of probes and use of the standard generating vial offer a promising and efficient means of determining free concentration in a variety of bioactive lipid samples.

## 2.3 Towards determination of free concentration of lipids: Binding of fatty acids to serum albumin: experimental and *in silico* approach

### 2.3.1 Introduction

Regardless of being seemingly *simple*, fatty acids play major physiological roles in all cells: as an energy source via  $\beta$ -oxidation, taking place in skeletal muscles as well as in *E. coli*,<sup>209,210</sup> as “building blocks” for more complex lipids such as phospholipids, thereby influencing cell membrane’s fluidity and flexibility; and as the substrate for multiple signalling molecules.<sup>4,211–216</sup> The enzymatic machinery for *de novo* fatty acid (FA) biosynthesis is highly conserved across kingdoms of life. However, some organisms need essential polyunsaturated fatty acids (PUFAs) that either cannot be synthesized sufficiently for their metabolic demands or cannot be synthesized at all. As a result, it is acknowledged that all PUFAs in food webs derive from plants (and other primary producers) and that animals can only modify PUFAs through bioconversion and elongation as they move through the food web.<sup>217</sup>

Extensive research has been conducted on the effects of dietary FAs on human health. For instance, highly elevated levels of saturated fatty acids are linked to health-related risks in insulin resistance diabetes, myocardial infarction, and arthritis. On the other hand, PUFAs (particularly  $\omega$ -3 and  $\omega$ -6 PUFAs) are essential in reducing health risks, particularly for newborns’ visual and nervous systems,<sup>218–220</sup> as well as functioning as precursors for a plethora of signalling lipids related to inflammation.<sup>211,221,222</sup> These PUFAs contain at least 18 carbons and multiple non-conjugated double bonds. Like other FAs, PUFAs have common and shorthand names that designate the number of carbon atoms, double bonds,

and position of the first double bond (counting from the non-carboxyl end of the FA chain). For example, the shorthand notations for linoleic acid (LA) and  $\alpha$ -linolenic acid ( $\alpha$ -LA) are FA 18:2  $\omega$ -6 and FA 18:3  $\omega$ -3, respectively (as depicted in Figure 2.17). These two are the major precursors in animals for producing longer  $\omega$ -3 and  $\omega$ -6 PUFAs.<sup>217</sup>

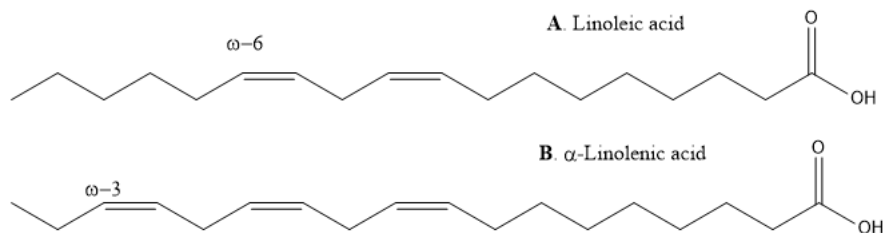


Figure 2.17. Structures for (A) linoleic acid and (B)  $\alpha$ -linolenic acid, indicating the  $\omega$ -6 and  $\omega$ -3 carbons where the double bonds start from the non-carboxylic end.

Human serum albumin (HSA), the most abundant protein in human blood, handles the transport of fatty acids, among other compounds (and functions). HSA counts with numerous binding sites for FAs in its structure, and if the FA-to-HSA molar ratio increases, so will the number of FAs that bind to HSA. At least seven FA binding sites have been found for palmitic acid (FA 16:0) using high-resolution X-ray crystallography, all heterogeneously distributed across the three HSA domains.<sup>223</sup> Whereas, at least nine FA binding sites (with varying affinity strength) for the HSA–palmitate complex using 2D nuclear magnetic resonance.<sup>224</sup> Although numerous FA binding sites have been identified and classified, we are unaware of any research that has attempted to determine the binding affinity of FAs to a particular binding site. Undeniably, site-specific binding affinities alter due to allosteric interactions between two sites; therefore, these binding affinities are theoretically changing and not fixed.<sup>225,226</sup> The degree of binding (i.e., number of FAs, FA

identity, binding site affinity) between HSA and FAs has been shown to influence the protein's structural integrity and affinity toward other compounds.<sup>227–229</sup> Consequently, studying these FA–HSA interactions can aid in understanding HSA's behaviour in pharmacokinetic/pharmacodynamic studies, drug development and its regulatory role in other physiological processes (e.g., pH buffering, osmotic pressure regulation). To understand FA-HSA binding better, Goodman et al. experimentally measured the apparent binding constants of FAs anions to three HSA binding sites using the Scatchard equation.<sup>230</sup>

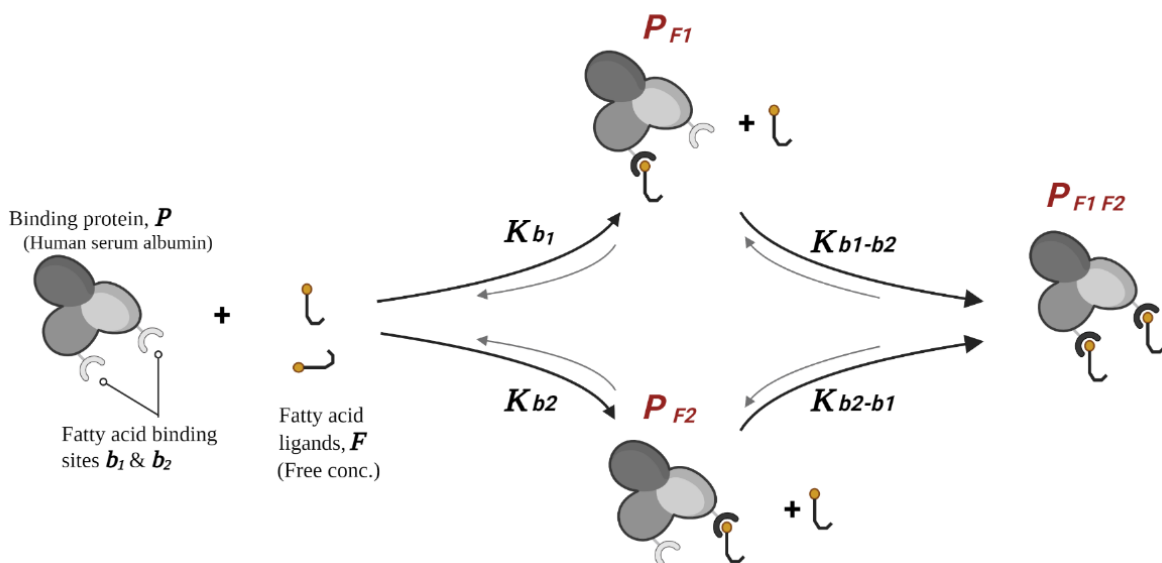


Figure 2.18. Scheme for binding between a bi-valent protein receptor,  $P$ , and two fatty acid ligands,  $F$ , in a stoichiometric fashion.

Figure 2.18 portrays the site-oriented and stoichiometric equilibria for a bi-valent protein receptor with two binding sites,  $b_1$  and  $b_2$ . On a site-oriented approach, four equilibria are established together with the FA ligand with four site-specific binding

constants (namely,  $K_{b1}$ ,  $K_{b2}$ ,  $K_{b1b2}$ , and  $K_{b2b1}$ ). In contrast, the stoichiometric binding constants ignore the intermediates  $P_{F1}$  and  $P_{F5}$ ; rather, both  $K_{b1}$  and  $K_{b2}$  are merged into the first equilibrium constant,  $K_1$ . Likewise,  $K_{b1b2}$  and  $K_{b2b1}$  are joined into the second equilibrium constant,  $K_2$ . Notably, with increasing number of binding sites (and inter-site cooperativity, not described here), the site-oriented approach becomes increasingly more difficult. In such instances, the stoichiometric binding approach is more practical.

$$B = \sum_{i=1}^b \frac{k_i \cdot F_{free}}{1 + k_i \cdot F_{free}} \quad \text{Eq. 8}$$

$$B = \frac{F_{Bound}}{P_{Total}} = \frac{F_{Total} - F_{free}}{P_{Total}} \quad \text{Eq. 9}$$

For instance, for a receptor with a given set of binding sites ( $b$ ), stoichiometric binding constants ( $k_i$ ), the degree of binding,  $B$ , can be expressed as in equation 8.<sup>231</sup> Besides, the degree of binding  $B$  is defined as the ratio of moles of bound ligands per mole of receptor protein, as shown in equation 9.<sup>231</sup> Thus, the degree of binding ( $B$ ) may be described by accurately measuring the free ligand concentration ( $F_{free}$ ); and, from a Scatchard plot displaying  $B/F_{free}$  vs.  $F_{free}$ , the binding constant ( $K$ ) is determined from the slope.<sup>231</sup> Multiple techniques are available in the analytical toolbox for measuring the free concentration of an analyte. Studies on binding between serum albumin and FAs have used equilibrium dialysis, isothermal titration calorimetry,<sup>232</sup> surface plasmon resonance, and fluorescence emission.<sup>233</sup> Yet, these techniques have significant shortcomings in sample preparation, mainly in terms of time and costs, as stated in section 2.2.1. Therefore,

considering the experimental simplicity and its free-concentration extraction mechanism, SPME was proposed to study the ligand-binding study between HSA and  $\alpha$ -LA using a stoichiometric binding approach. The binding association constant for  $\alpha$ -LA was determined via a Scatchard plot, using the experimental data generated by entering experimental data into a COMSOL-based mathematical model to predict the extraction kinetics of  $\alpha$ -LA in the presence of an HSA binding matrix.

### **2.3.2 Experimental**

#### Materials, supplies, and standards

LC/MS-grade methanol (MeOH), isopropyl alcohol (IPA), and phosphate-buffered saline tablets were purchased from Fisher Scientific (Mississauga, ON, Canada). Human serum albumin (HSA, fatty acid-free),  $\alpha$ -Linolenic acid ( $\alpha$ -LA), agarose, and LC-grade chloroform ( $\text{CHCl}_3$ ) were purchased from Sigma–Aldrich (Oakville, ON, Canada). In contrast, linoleic acid (LA) and tridecanoic acid were acquired from Cayman chemicals (Burlington, ON, Canada). Bio-SPME fibers coated with C18 particles were a gift from Millipore–Sigma (Oakville, ON, Canada). Fiber coating dimensions for this study were 15 mm length  $\times$  40  $\mu\text{m}$  thickness. The active surface area for these fibers was estimated by the Brunauer-Emmett-Teller (BET) surface area analysis using  $\text{N}_2$  for the physical adsorption onto the coating pores. The obtained values are in the supplementary information of the published manuscript.<sup>192</sup>

Silanized amber vials (VWR, Mississauga, ON, Canada) were used to minimize non-specific interactions between fatty acids and the glass walls. Lipid standards stock solutions



were prepared daily in MeOH from a stock prepared in CHCl<sub>3</sub>: MeOH (2:1, v/v) and stored at -30 °C in amber silanized vials. Phosphate buffered saline (PBS) was prepared using LC/MS-grade water by simply dissolving one tablet in 200 mL LC-MS-grade water. Using a commercial microwave oven, agarose gel was dissolved in PBS (0.8%, w/v) in 1-minute intervals until complete powder dissolution. The resulting agarose solution started to *solidify* under ~40 °C rapidly; hence, this solution was kept in a water bath at 45 °C until needed.

#### SPME extractions.

All extractions followed the same protocol as described in Section 0. The SPME probes were cleaned and preconditioned as described in Section 0. After each extraction, the fibres were washed using LC-MS grade water (400 µL, 10 s, 2000 rpm) to remove salts and nonspecific attachments. Then, analytes were desorbed (200 µL, 60 min, 1500 rpm) using a mixture of IPA/MeOH/H<sub>2</sub>O (45/45/10, v/v), which contained 20 ng/mL of tridecanoic acid (FA 13:0) as an internal standard. Four independent replicates were utilized in all extractions.

#### Liquid chromatography coupled to Mass Spectrometry conditions

The FAs were characterized using a Vanquish Flex HPLC system coupled to a triple quadrupole mass spectrometer TSQ Vantage (ThermoScientific, San Jose, CA). MS/MS was operated in negative mode, monitoring the pseudo-molecular ion and its dehydration products, the latter being the only fragments obtained from FAs. The instrumental

conditions employed are summarized in Table 2.8. These conditions enabled an instrumental limit of quantification (LOQ) of 5 ng/mL.

Table 2.8. LC-MS/MS conditions used for the analysis of fatty acids.

<b>Liquid Chromatographic conditions – Thermo Vanquish Flex UHPLC</b>			
Column	Waters Acquity CHS® C18 1.7 $\mu$ m, 2.1 $\times$ 100 mm		
Mobile phase A	H <sub>2</sub> O/MeOH (6/4)		
Mobile phase B	MeOH/IPA (2/8)		
Additives in – mode	0.05 % (v/v) acetic acid		
Flow rate	350 $\mu$ L/min		
Column temperature	55 °C		
Samples temperature	5 °C		
Injection volume	10 $\mu$ L		
Gradient [min, %B]	0.0 min, 20%; 1.0 min, 20%; 4.0 min, 80%; 6.0 min, 95%; 8.8 min, 95%; 8.9 min, 20%; 10 min, 20%		
<b>Mass spectrometry conditions – Thermo TSQ Vantage™</b>			
Spray voltage	2.5 kV, negative mode		
Vaporizer temperature	300 °C		
Transfer capillary temp.	350 °C		
Sheath gas, arb	30 arb		
Auxiliary gas, arb	40 arb		
Sweep gas, arb	10 arb		
Dwell time	10 ms/ transition		
<b>MS/MS transitions for fatty acids under study</b>			
Standard	$\alpha$ -Linolenic acid (FA 18:3 – $\omega$ 3)	Linoleic acid (FA 18:2 – $\omega$ 6)	Tridecanoic acid FA 13:0 <sup>§</sup>
Parent mass, <i>m/z</i>	277.3	279.3	213.2
Fragment 1, <i>m/z</i> [CollE.]	277.3 [5]	279.3 [5]	213.2 [5]
Fragment 2, <i>m/z</i> [CollE.]	229.1 [24]	231.1 [24]	169 [24]
S-lens, V	12	12	12

<sup>§</sup> Tridecanoic acid (FA 13:0) was used as internal standard in the desorption solution. CollE. Collision energy.

### Equilibria between $\alpha$ -LA, HSA, and SPME probes

The albumin (fatty acid-free) was dissolved in freshly prepared PBS (pH 7.4). A methanolic solution of the studied FA was used to spike the HSA solution, ensuring the volume of the aliquot was under 1% (v/v). This albumin/fatty acid solution was incubated

overnight at room temperature (18 – 19 °C) with 500 rpm agitation to ensure sufficient analyte-matrix (ligand-receptor) binding.

The protein binding of fatty acids to HSA are generally believed to be >99%,<sup>164,234–237</sup> but as HSA can also bind multiple individual fatty acids in its pockets, hence why we decided to estimate each binding constant. A Scatchard plot was used for its simplicity: an albumin solution was mixed with  $\alpha$ -LA at multiple molar ratios, left to equilibrate overnight (>12 hours, under agitation, at 18 °C), then performed SPME extraction at equilibrium (5 hours, 500 rpm) to determine the free concentration of  $\alpha$ -LA.

### 2.3.3 Results and discussion

The active surface area of the C18-coated bio-SPME fibers was estimated experimentally via N<sub>2</sub> adsorption Brunauer–Emmett–Teller (BET) analysis. Pores over 100 Å were considered significant enough to bind the fatty acid analytes,  $\alpha$ -LA and LA. The active surface area,  $S$ , for the SPME fibre used in all experiments (15 mm long, 40  $\mu$ m coating thickness) was estimated to be 2.0 m<sup>2</sup>/g. The maximum occupancy of  $\alpha$ -LA onto the solid sorptive surface,  $\gamma_S$ , was determined experimentally by performing extractions from various solutions of  $\alpha$ -LA in PBS (0.01 – 20  $\mu$ g/mL range) under agitation. The plateau observed was inferred as the concentration at which  $\alpha$ -LA reached monolayer saturation, based on Langmuir’s isotherm.

The selection of  $\alpha$ -Linolenic acid ( $\alpha$ -LA, FA 18:3) for this study was based on its reported bioactivity;<sup>238–240</sup> its known physicochemical parameters and availability; and binding parameters between  $\alpha$ -LA and albumin are relatively scarce in literature in

comparison to other FAs.<sup>241</sup> The binding parameters of linoleic acid (LA) were used to evaluate our approach in lieu of its structural similarity. Mass transfer in SPME is driven by three main factors: diffusion to the coating, convection (i.e., adequate agitation), and any *reaction* in the system that removes/adds analyte. To investigate each additional factor, we performed three different types of extractions for  $\alpha$ -LA. A first: a static extraction in which the mass transfer of the analyte through the gel sample occurs only via diffusion; an agitated extraction, so the mass transfer happens via diffusion and convection, done in PBS only as a matrix-free environment; an agitated extraction in the presence of HSA as the binding receptor, for which mass transfer includes all three factors.

The experimental extraction time profiles and the in-silico calculations are depicted in Figure 2.19. Without a binding matrix under these extraction conditions, all the  $\alpha$ -LA is in free form. Thus, depletion of the sample occurs. Approximately 65  $\mu$ g of  $\alpha$ -LA is extracted at equilibrium for the receptor-free approaches, static and with convection, shown in Figure 2.19A and Figure 2.19B, respectively. Despite the large extent of depletion (almost 50%), it remained consistent across different experiment iterations driven by the high affinity between analyte and coating and the small sample volume used. Moreover, since all extractions were carried out at equilibrium under the same experimental conditions, it was considered for calculations.

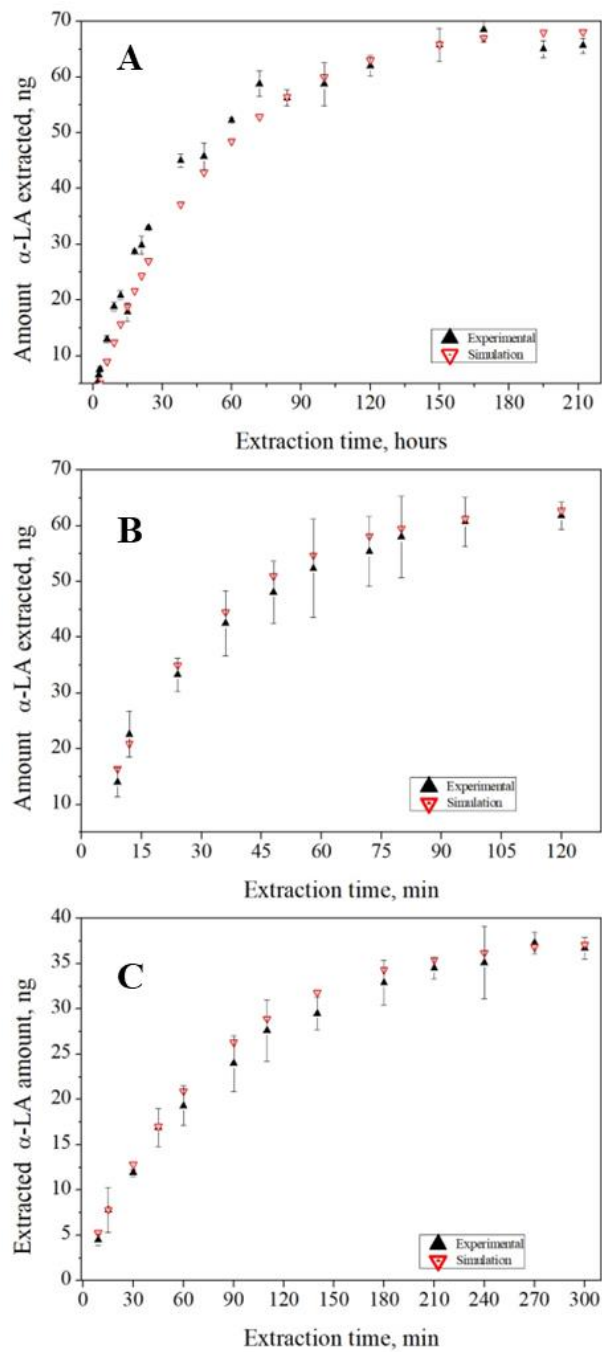


Figure 2.19. Experimental and in silico extraction time profiles for  $\alpha$ -LA under different extraction modes. **(A)** Static extraction from a PSB-agar gel, **(B)** Agitated extraction under convection (500 rpm) in PBS; **(C)** Extraction in the presence of serum albumin at an equimolar ratio (20  $\mu$ M).

The adsorption equilibrium constant,  $K_{ads}$ , for  $\alpha$ -LA was determined experimentally by measuring the amount extracted at equilibrium between the solid-phase sorption phase and the sample matrix. Unlike liquid coatings in which partition occurs, sorption in solid coatings occurs on the “active surface” on the coating’s porous surfaces. The active surface area for the C18-coated probes used was estimated via BET analysis (data presented in the manuscript SI) to be approximately  $2.0 \text{ m}^2/\text{g}$ . Thus,  $K_{ads}$  for  $\alpha$ -LA is approximately  $70 \text{ m}^3/\text{mol}$ , which was used during the in-silico calculations. Conversely, the amount extracted in the presence of the albumin binding receptor was 37.3 ng (a mere 0.4% from the nominal initial concentration), reflecting the non-depletive nature of the SPME device in the presence of a binding matrix.

To obtain the binding isotherms for each fatty acid, a titration-like experiment was carried out, in which the receptor (at  $20 \text{ }\mu\text{M}$ ) was mixed with the ligand at multiple molar ratios and an SPME extraction at equilibrium took place. The degree of binding,  $B$ , was calculated at each ratio, as seen in Figure 2.20. The degree of binding,  $B$ , corresponds to the number of bound ligand molecules per receptor molecule. The number of bound ligands was determined as the difference between the nominal concentration and the amount extracted via SPME.  $B$  can be expressed as a function of the free ligand ( $C_F$ , determined from SPME measurement), the total ligand ( $C_T$ , nominal ligand concentration spiked), and the total concentration of the receptor ( $C_R$ ). The constructed binding isotherms are shown in Figure 2.20.

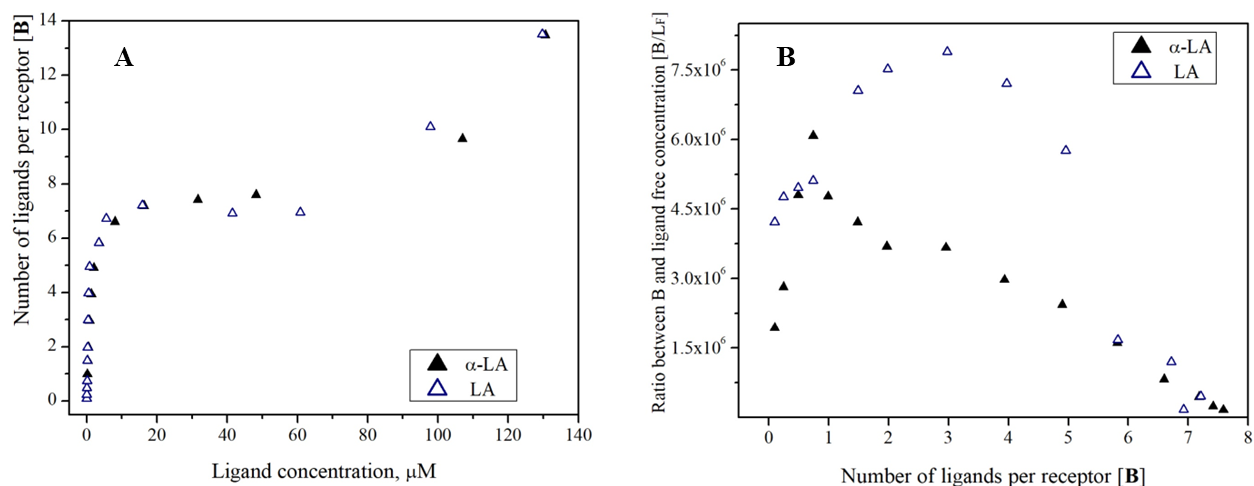


Figure 2.20. Binding isotherm curves constructed for  $\alpha$ -LA and LA in the presence of serum albumin as the binding receptor.

The binding of fatty acids to the albumin occurs readily, even at low ligand concentrations, as noted by the sharp increase in  $B$  for both fatty acids. Both isotherms reach an apparent saturation at  $B \cong 7$ , at a ligand-to-receptor ratio of 7:1, where the free concentrations of  $\alpha$ -LA and LA were calculated to be 8.1 and 5.6  $\mu\text{M}$ , respectively. As the molar ratio of ligands increased, both isotherms depicted a further increase in the degree of binding, presumably due to non-specific interactions with the receptor.<sup>242</sup> This apparent saturation also indicates the presence of at least seven binding sites for fatty acids, as reported previously.<sup>227,237</sup> Despite that, at normal physiological conditions, freely dissolved fatty acids are present at such low concentrations that human serum albumin only interacts with up to two moles of unesterified fatty acids.

Binding dissociation constants were determined from the Scatchard plots, using nonlinear curve fitting using GraphPad Prism 9.0 software.<sup>243</sup> The binding dissociation constants,  $K_d$ , for  $\alpha$ -LA and LA were 1.26 and 0.46  $\mu\text{M}$ , respectively. Their reciprocal was

interpreted as the binding association constant, yielding  $K_{\alpha-LA} = 7.0 \times 10^5$  L/mol and  $K_{LA} = 2.1 \times 10^6$  L/mol for  $\alpha$ -LA and LA, respectively. Comparable results were obtained for the association binding constant of LA,<sup>244</sup> supporting the accuracy of the model. The binding constants determined for  $\alpha$ -LA was used to retroactively calculate the simulated values presented in Figure 2.19C, further endorsing the accuracy of the proposed model. However, the detailed mathematical explanations and the COMSOL conditions are provided elsewhere,<sup>192,245,246</sup> as it falls out of the scope of this dissertation



## 2.4 Summary and conclusions

Using an LC-MS/MS platform, SPME's quantitative capabilities were explored in a few selected applications aiming to explore the parameters that may affect the quantitative aspects of SPME-based determinations. The research in this chapter aimed at exploring the quantitative capabilities of SPME using an LC-MS/MS approach, concluding with a proposed procedure for accurately determining freely dissolved lipids and the total concentration of lipids in plasma. This objective was achieved, albeit in part, for selected lipid subclasses and in sensitive applications.

The desorption kinetics of lipids from matrix components (e.g., lipoproteins) and SPME's own diffusion-based mechanism might impose an unexpected challenge for the quantitation of highly hydrophobic lipids under the selected extraction conditions near equilibrium. Applying a different non-equilibrium quantitation approach for very hydrophobic lipids may be required and revisited for future research. Moreover, detection and quantitative analysis of trace lipid sub-classes (such as PAs and PIs, occurring at infamously low levels in plasma) remained a limitation in this approach.

It was also shown how SPME fibers have minimal absolute matrix effects when extracting from neat plasma samples. The same cannot be said about SPME with blade format (perhaps extending to other TFME geometries), as matrix effects were observed for trace GPLs in neat plasma and wildly exacerbated in ACN-modified plasma. Moreover, some parameters were found to be critical and to influence the mass transfer of lipids in different ways in relation to their relative polarity. Convection parameters (i.e., agitation

speed, presumed desorption rate.) was believed to have a significant effect on the effective mass transfer of hydrophobic lipids, while more polar lipids remained unaffected. This finding highlights mass-transfer to/from the matrix components as a possible rate-limiting step opposite. In essence, the desorption of highly hydrophobic lipids from the matrix components is sluggish, influencing the uptake by the coating and compromising the selectivity and sensitivity attained by the probes. Preliminary strategies should focus on simplifying the system under study and perform more fundamental studies to extract a few selected lipid analytes from an aqueous matrix (e.g., PBS, another buffer) at various nominal concentrations relative to their CMC.

Additionally, by fine-tuning the coating dimensions for an SPME probe (fibre geometry), non-depletive extraction was achieved for a few model compounds. As this extraction took place from a matrix-free sample, the fiber constant for these model compounds was estimated. A perplexing result further highlighted the impending need to study an easily overlooked parameter during SPME method development: the spiking approach.: While fat uptake in plasma seems to occur swiftly by the plasma matrix (led by the fantastic evolutionary machinery behind lipid transport), a possible synergic effect during the uptake of lipids seemingly occurred in a matrix-free environment.

Furthermore, SPME was utilized to determine the ligand-receptor binding parameters successfully and effectively between HSA and two unsaturated long-chained fatty acids,  $\alpha$ -LA and LA. Following the binding association constant for  $\alpha$ -LA was a Scatchard plot created by inserting experimental data into a mathematical model to simulate the extraction

kinetics of  $\alpha$ -LA in the presence of an HSA binding matrix. The satisfying outcomes of the in-silico comparisons highlight the utility of mathematical models in validating SPME experimental data. In addition, the created mathematical models can be applied to in-silico research of analogous interactions between ligands, such as lipids and HSA receptors, saving time, effort, and money. The results presented highlight the principles of non-exhaustive microextraction, notably those of SPME, from a matrix with a high degree of binding. In addition, they enhance our knowledge of how this technique can be applied to receive insights on multiphase equilibria in complex systems, as well as how to optimize microextraction settings and interpret SPME data involving matrix-specific binding sides.

Lastly, this study presented two potential applications of SPME for determining free concentration: first, the free concentration (determined by equilibrium SPME) was the measurable variable used for in-silico calculations on binding extent between  $\alpha$ -linolenic acid ( $\alpha$ -LA, an  $\omega$ -6 polyunsaturated fatty acid) and human serum albumin (HSA). Since the extractions were carried out at equilibrium, depletion of the free concentration was not a concern.<sup>205,247</sup> Second, miniaturized probes were employed to estimate fiber constants of simple lipids under *negligible* depletion. Yet, non-depletive extractions are not always feasible, and said depletion threshold must be set by the authors.<sup>194,247,248</sup> Furthermore, the study also evaluated the feasibility of standard water-generating vials doped with a polar model lipid to construct external calibration curves intended for free concentration determination.

## Chapter 3 Coupling SPME to direct to MS approaches

### 3.1 Introduction

Coupling chromatographic separation systems to mass spectrometry (MS) is considered the “gold standard” approach due to the higher sensitivity and selectivity achieved. However, the samples might require laborious preparation steps to ensure desired chromatographic selectivity, sensitivity, and compatibility with MS. Analytical chromatographic sequences consist of calibration standards, blanks, quality control, and samples; thus, lengthy chromatographic separations rapidly increase the overall analysis time and costs.

Motivated by simplifying analytical methods in the mid-2000s, ambient MS (AMS) techniques pioneered analyte introduction and detection in real-time, in proximity to the studied system, and under ambient pressure.<sup>249–251</sup> Since then, over 40 AMS techniques have been documented, differing in the desorption/ionization processes.<sup>252,253</sup> For instance, analyte desorption may occur using various methods, including interactions with solvents, laser desorption, thermal desorption, or impact by ions or charged droplets. Electrospray Ionization (ESI) and atmospheric pressure chemical ionization (APCI) ionization happen in most AMS techniques; thus, the mass spectra obtained are virtually identical to those of conventional coupling between liquid chromatography and ESI and APCI ionization.<sup>254,255</sup>

For instance, the simplest method for sample introduction, colloquially known as dilute-and-shoot, involves introducing a diluted (compatible) sample to the MS via a flow-injection mechanism.<sup>256–258</sup> This sample introduction approach was used by Han & Gross in their seminal work on lipid analysis in crude lipid extracts, which involved the

application of an MS-based platform without any prior chromatographic separation and coined the term “*shotgun* lipidomics.”<sup>259–261</sup> With the development of AMS sources and MS imaging technologies, the scope of shotgun lipidomics has expanded to cover sample-introduction methods aside from the initial direct infusion with a syringe. In biomedical research, combining direct desorption with imaging has made it possible to obtain information on the spatial distribution of lipids in tissues. For example, DESI uses solvent spray for fast extraction and desorption, achieving a 20–500  $\mu\text{m}$  pixel resolution in various tissues.<sup>262–266</sup> Similarly, higher resolution ( $\sim 350$   $\mu\text{m}$  pixel size) can be accomplished with laser ablation, as in MALDI.<sup>265,267</sup> The use of high-resolution mass spectrometry (HRMS) in shotgun lipidomics can help to resolve isobaric species formed during ionization.<sup>268–270</sup> Moreover, derivatization methods have also been employed in shotgun approaches to enhance the quantitation of trace lipids<sup>271–275</sup> and to aid in the structural characterization of isomeric compounds.<sup>273–277</sup>

Since most direct MS approaches aim to minimize or eliminate sample preparation, some are not comparable to the (gold) standard analytical methods due to a lack of automation, selectivity, sensitivity, and possible instrument contamination.<sup>253,278</sup> Regarding automation, these technologies are typically operated manually, potentially impacting the operator for many samples or variability between operators.<sup>279</sup> Regarding selectivity, direct-to-MS methods cannot separate isomers or isobars, which hinders their broad application for lipid analysis. Ion mobility (IM) can help to bridge this gap by providing sub-second gas-phase separation of ionized species based on their mobility

through a separation cell/flow.<sup>54,280</sup> The other issues mentioned above (i.e., inadequate sensitivity and the propensity for instrument contamination) can occur due to strong matrix effects from the simultaneous ionization of sample components, inadequate sample preparation, or a combination of the two. Thus, modifications to the analytical workflow, such as an enrichment or derivatization step, are considered necessary to improve the method's quantitative capabilities.<sup>281,282</sup>

Given SPME's advantages and the relative *ease* with which it can be coupled with MS, remarkable results have been obtained by directly coupling SPME with ambient MS techniques, particularly in terms of the attained linearity and minimal matrix effects. Various SPME devices have been successfully coupled directly to MS to determine illicit drugs, volatile organic compounds, and pesticides in different biological matrices.<sup>283–288</sup> A simple depiction of some of these approaches is shown in Figure 3.1. Desorption electrospray ionization (DESI) has been coupled to SPME fibers to analyze drugs and metabolites in animal brains.<sup>289</sup> Also, SPME devices have used Direct analysis in real-time (DART) as yet another means of analyte introduction directly to the MS, for example, in the analysis of drugs of abuse,<sup>288,290–292</sup> veterinary drugs,<sup>286</sup> volatile organic compounds,<sup>293</sup> environmental pollutants,<sup>294–296</sup> and metabolites.<sup>297</sup>

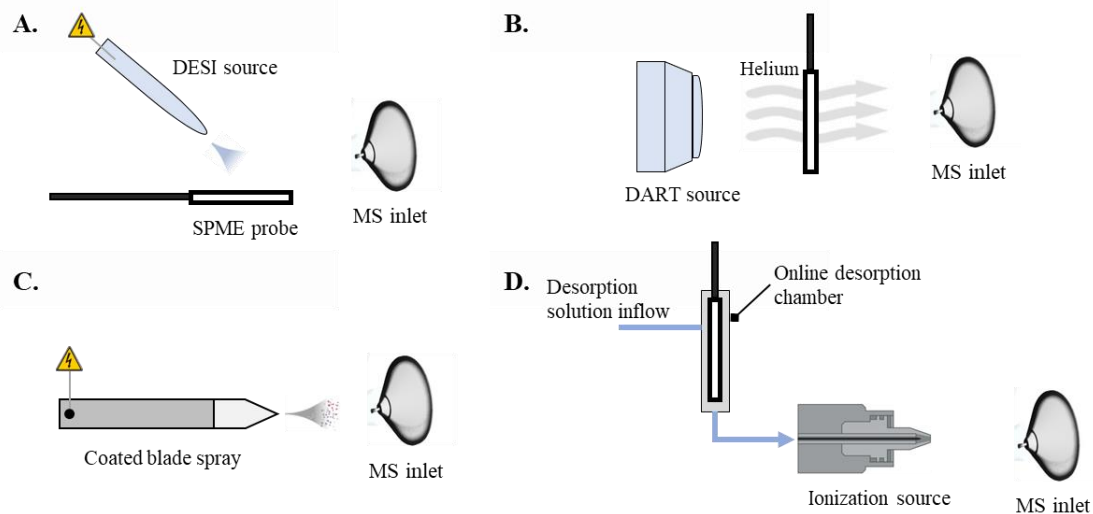


Figure 3.1. Schematic designs of some direct-to-MS techniques coupled to SPME devices: (A) Desorption electrospray ionization, DESI; (B) Direct analysis in real-time, DART; (C) Coated blade spray, CBS; (D) Microfluidic open interface.

From the existing SPME–MS approaches, coated blade spray (CBS) is perhaps one of the most robust ones to date, as it integrates sampling, sample preparation, and sample introduction in a single device. CBS has been used to determine a variety of analytes (e.g., drugs of abuse, pesticides, immunosuppressant drugs) in complex biological and environmental matrices. In essence, the CBS device is a small stainless-steel, sword-like support that enables the enrichment of small molecules onto its thin polymeric coating, from which desorption is attained with a small amount of solvent (i.e., 5–20  $\mu\text{L}$  to desorb the extracted analytes from the coated section within 5–20 seconds). Ionization occurs by application of a high potential (i.e., charged droplets exhibiting the characteristic of a Taylor cone formed on the coated blade’s tip).<sup>298</sup> The resulting ‘square-like’ transient signal lasts until the desorption solvent has been sprayed (or evaporated) or until the high voltage is switched off. Thus, desorption and ionization occur without gas or heating, and

no fluidics are required (i.e., pumps, valves, syringes).<sup>102</sup> In terms of rapid analysis, CBS has provided analysis under 10 s for a large set of analytes using a complex interface,<sup>299</sup> and analysis time per sample as low as 3 min using a high-throughput sample preparation approach.<sup>140</sup>

Similarly, microfluidic open interface (MOI) is an emerging direct-to-MS approach that interfaces SPME devices directly to MS. The MOI approach has been used previously in the analysis of tranexamic acid in plasma,<sup>300</sup> doxorubicin in lung tissue,<sup>301</sup> and immunosuppressants in whole blood.<sup>302</sup> Figure 3.3 depicts the MOI interface inspired by the open port probe design.<sup>301,303,304</sup> Briefly, the MOI interface is composed of four major components: a desorption chamber for the SPME device, a three-way tubing diverting the incoming flow, a pump with a gas-tight syringe to supply the desorption solvent, and the tubing towards the instrument's ESI source, which provides the suction flow. The desorption chamber is a flow-isolated region where the SPME device is placed, and the analytes desorb. This interface offers an alternative for situations in which the desorption time is relatively long (i.e., analyte desorption from the coating is slow) while minimizing excessive dilution in its low volume when compared to LC-based desorptions (for example, 7–10  $\mu\text{L}$  for MOI vs. over 50  $\mu\text{L}$  for LC).



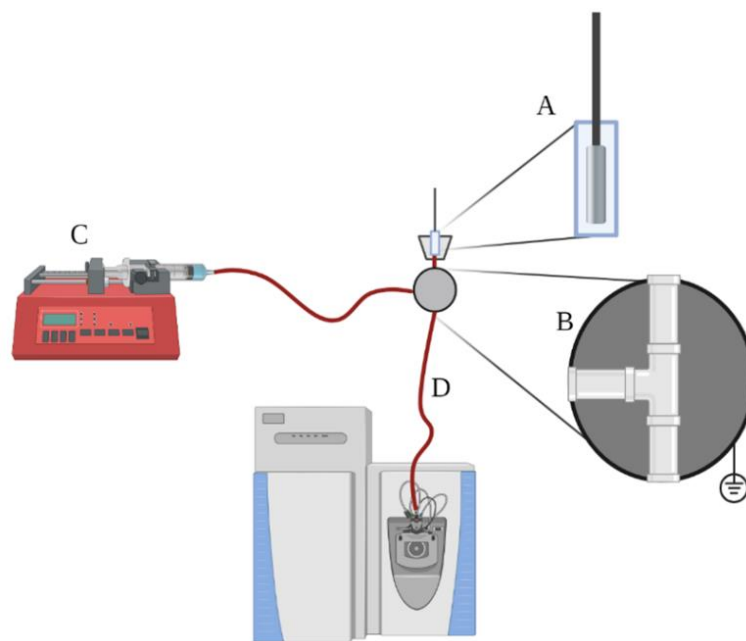


Figure 3.2. Schematics for the MOI interface for SPME–MS. The MOI interface is comprised of (A) the desorption chamber; (B) a tubing ‘tee’ electrically grounded; (C) a syringe which supplies the desorption solvent; and (D) the tubing diverting the solvent inflow towards the instrument’s ESI source. Adapted from Dr. Nazdrajić’s dissertation.<sup>305</sup>

The purpose of this chapter was to apply SPME technology for the shotgun analysis of lipids. Due to its effectiveness with other analytes, the author initially intended to employ the CBS technique. On SPME geometry, the author investigated the effects of variables such as voltage, solvent composition, desorption duration, and coating thickness. The author shifted from the CBS method to the MOI method for the SPME-MS interface due to unforeseen limitations faced during the desorption procedure in CBS. The MOI method for lipid analysis was evaluated, including the selection of desorption solvent and time. The objective intended exploring strategies for fast analysis of lipids by combining SPME devices with mass spectrometry.

## 3.2 Experimental

### 3.2.1 Standards, materials, and probes

All standards, solvents, and materials used in this work are the same as those described in Section 0. All the probes (i.e., stainless-steel blades for CBS, nitinol wire for MOI) employed in this study were etched, coated with a C18/PAN slurry, and cleaned according to the methods described in Section 0. The general workflow for the extractions using the SPME probes was the same as the one described in Section 0; the lone exception was that desorption took place *online*. All solvent mixtures used for desorption contained 0.1% (v/v) of acetic acid and 10 mM of ammonium acetate as additives for ionization.

### 3.2.2 Mass spectrometers

Preliminary experiments for CBS were carried out on a TSQ Vantage™ triple-quadrupole mass spectrometer (Thermo Scientific, CA, USA). These preliminary experiments included voltage evaluation, blade positioning relative to the MS inlet, and an initial desorption optimization. Subsequent experiments were then carried out on a TSQ Quantiva™ triple-quadrupole mass spectrometer (Thermo Scientific, CA, USA) employing a CBS interface enclosed within a clear box. Conversely, all experiments for MOI were carried out on a/the TSQ Vantage™ triple-quadrupole mass spectrometer (Thermo Scientific, CA, USA). The source parameters used for each SPME–MS approach and each instrument are listed in Table 3.1, and the selected MS/MS transitions for the model compounds are listed in Table 3.2. All data analysis was carried out using TraceFinder 4.1 from Thermo Scientific.

Table 3.1. Source parameters for each SPME-MS approach used.

Approach	CBS in Vantage	CBS in Quantiva	MOI in Vantage
Voltage, kV	3.8	5.0	3.0
Ion transfer capillary, °C	325	325	275
Vaporization temp, °C	–	–	40
Sheath gas, arb	–	–	40
Auxiliary gas, arb	–	–	10
Sweep gas, arb	–	–	1

Table 3.2. MS/MS transitions for the model compounds used for the SPME-MS approaches.

Standard	m/z Precursor	m/z Frag. 1 [CE]	m/z Frag. 1 [CE]	S lens (V)
LPC 17:0	510.4	184.1 [16]	104.1 [23]	15
LPC 16:0	496.4	184.1 [16]	104.1 [23]	15
LPE 17:1	465.3	324.1 [19]	–	17
LPS 17:1	510.4	324.1 [19]	–	17
PC 15:0_15:0	706.5	184.1 [25]	464.3 [32]	19
PC 16:0_16:0 (DPPC)	734.5	184.1 [25]	492.3 [32]	20
PE 17:0_17:0	720.6	579.6 [15]	253.2 [25]	17
PS 17:0_17:0	764.5	579.5 [25]	494.2 [34]	16
PG 17:0_17:0	768.6	579.5 [24]	327.3 [27]	16
TG 19:0_19:0_19:0	950.9	635.6 [24]	–	19

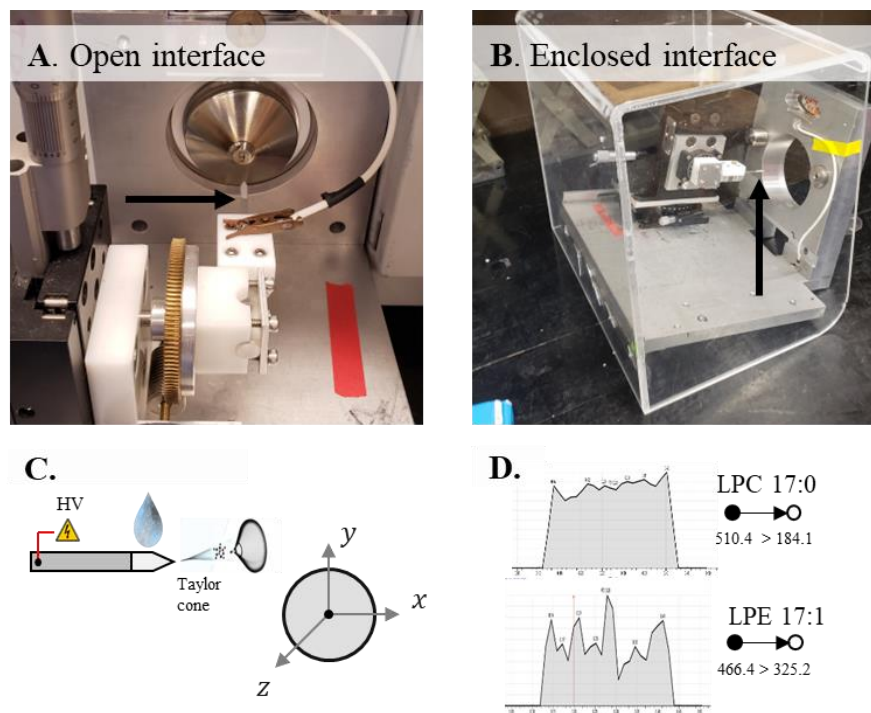


Figure 3.3. Coated blade spray interfaces for the MS instruments (A) TSQ Vantage and (B) TSQ Quantiva. The black arrow points at the position of the SPME CBS device within each interface. (C) Scheme of desorption/ionization process occurring directly on the blade and the  $x,y,z$  alignment of the probe in front of the MS inlet. (D) Example of the resulting transient signal for two model compounds, LPC 17:0 and LPE 17:1.

### 3.2.3 CBS as the SPME–MS approach

Figure 3.3 shows a photograph of the interfaces used for CBS in each MS instrument. Once the high voltage is applied, an ESI mechanism causes ionization on the coated blade's tip, which occurs as charged droplets exhibiting the characteristic Taylor cone.<sup>298</sup> To kickstart desorption, a small amount of solvent (5–20  $\mu\text{L}$ ) is pipetted onto the coated blade, which facilitates the desorption and mass transfer from deeper parts of the coating. After a short desorption period, the analytes are sprayed toward the MS by the high voltage (HV) applied to the blade. The resulting transient signal lasts until the desorption solvent has been sprayed (or evaporated) or until the high voltage is switched off. The optimal voltage,

MS/MS tuning parameters, and blade positioning (relative to the MS inlet) were determined by infusing a mixture of standards (20 ppb, in MeOH/H<sub>2</sub>O, 95/5 + 0.1% acetic acid) onto a blade via a capillary using a Hamilton auto-sample syringe pump (7.5  $\mu$ L/min, Sigma Aldrich, MO, USA). The area under the transient signal was acquired for 30 s and integrated to determine the optimum voltage and positioning.

### 3.2.4 MOI interface as SPME–MS approach

The desorption solution inflow was supplied by a programmable syringe pump with a 20 mL gas-tight syringe (Hamilton, USA) via a green PEEK tube (rigid walls, outer diameter: 0.0625 in, inner diameter: 0.030 in, Millipore Sigma). The metal three-way chromatographic tee (1 mm bore) is connected by a short blue PEEK tube (length: 5.0 cm, outer diameter: 0.0625 in, inner diameter: 0.010 in, Millipore Sigma) to the ESI source

The level of desorption solvent in the chamber was regulated by varying the inflow of desorption solvent (LC pump) while keeping the suction flow rate constant (source parameters). Thus, when the inflow is higher, equal to, or lower than the suction flow rate, the level increases, is stable, or decreases accordingly. The ionization source generates the suction flow via the venturi effect, while the *flow rate* depends on the tubes' dimensions (i.e., their inner diameters and lengths) and the viscosity of the desorption solution. The temperature significantly affects the viscosity of fluids; hence all MOI experiments were conducted at the lowest vaporization temperature possible in the source used, as the reservoir must be filled more frequently at higher suction flows.

The MOI workflow consisted of four main steps. In the first step, the flow rates in the system are equilibrated *empirically* by matching the inflow (supplied by the pump) and aspiration flow rates (provided by the instrument's ESI source). Then, the volume in the desorption chamber remains stagnant and undisturbed at this stage. In the second step, analyte desorption from the SPME probe occurs for a set period. Next, in the third step, the inflow is stopped from the pump, causing the desorbed sample to be aspirated from the desorption chamber by the suction from the ESI source. Thus, the desorbed analytes enter the MS instrument simultaneously as a narrow *plug*, offering great sensitivity. Finally, the solvent influx is resumed and increased in the fourth step to overfill the desorption chamber. This inflow cleans the analyte carryover from the MOI's inner parts and resets the interface for the following sample. These four steps require approximately 2.5 min per sample.

Briefly, the MOI is composed of *three* major components: a three-way chromatographic tee, which acts as a flow-isolated section over the tee, which serves as desorption chamber; a pump with a gas-tight syringe (20 mL, Hamilton) to supply the desorption solvent via a green PEEK tube (rigid walls, outer diameter: 0.0625 in, inner diameter: 0.030 in, Millipore Sigma); and a short blue PEEK tube to transfer the sample to the ESI source (length: 5.0 cm, outer diameter: 0.0625 in, inner diameter: 0.010 in, Millipore Sigma). The level of desorption solvent in the chamber was regulated by varying the inflow of desorption solvent (LC pump) while keeping the suction flow rate constant (source parameters). Thus, when the inflow is higher, equal to, or lower than the suction

flow rate, the level increases, is stable, or decreases accordingly. The ionization source generates the suction flow via the venturi effect, while the *flow rate* depends on the tubes' dimensions (i.e., their inner diameters and lengths) and the viscosity of the desorption solution. The temperature significantly affects the viscosity of fluids; hence all MOI experiments were conducted at the lowest vaporization temperature possible in the source used, as the reservoir must be filled more frequently at higher suction flows.

Additional details relating to the device's operation can be found in Dr. Nazdrajić's doctoral dissertation.<sup>305</sup> The MOI workflow consists of four main steps. In the first step, the flow rates in the system are equilibrated *empirically* by matching the inflow (supplied by the pump) and aspiration flow rates (provided by the instrument's ESI source). Then, the volume in the desorption chamber remains stagnant and undisturbed at this stage.<sup>306</sup> In the second step, analyte desorption from the SPME probe occurs for a set period. Next, in the third step, the inflow is stopped from the pump, causing the desorbed sample to be aspirated from the desorption chamber by the suction from the ESI source. Thus, the desorbed analytes enter the MS instrument simultaneously as a narrow *plug*, offering great sensitivity. Finally, the solvent influx is resumed and increased in the fourth step to overflow the desorption chamber. This inflow cleans the analyte carryover from the MOI's inner parts and resets the interface for the following sample. These four steps require approximately 2.5 min per sample.

### 3.3 Results and Discussion

#### 3.3.1 Coated Blade Spray

The voltage required to produce a stable signal was assessed by continuously infusing a solution of lipid standards (20 ng/mL, in MeOH/H<sub>2</sub>O 95/5, v/v) and integrating the “area under the curve,” as shown in Figure 3.4. The best ionization with the TSQ Vantage was obtained in the 4.3–4.7 kV range, with the lowest variability being observed at 4.5 kV. As such, 4.5 kV was selected as the spray voltage. Voltages higher than 4.7 kV produced an intense response at the cost of spray instability and occasional corona discharge on the blade tip. For the TSQ Quantiva, which was employed in later experiments, 5.5 kV was the best voltage, as reported elsewhere.<sup>142,146,302,307</sup> For both instruments, the most stable spray was obtained by positioning the blade's tip 10 mm from the inlet, with no substantial differences in placement in the *x* and *y* axes. Diminished ionization for some lipid classes is a common challenge in shotgun lipidomics due to inherently low concentrations of these compounds in biological samples such as plasma (e.g., PS, PG, PA) and low ionization efficiencies.<sup>259</sup> Alternative strategies that can be employed to mitigate this issue include using different solvent additives, such as ammonium fluoride,<sup>141,308</sup> and fast polarity switching.<sup>309</sup>



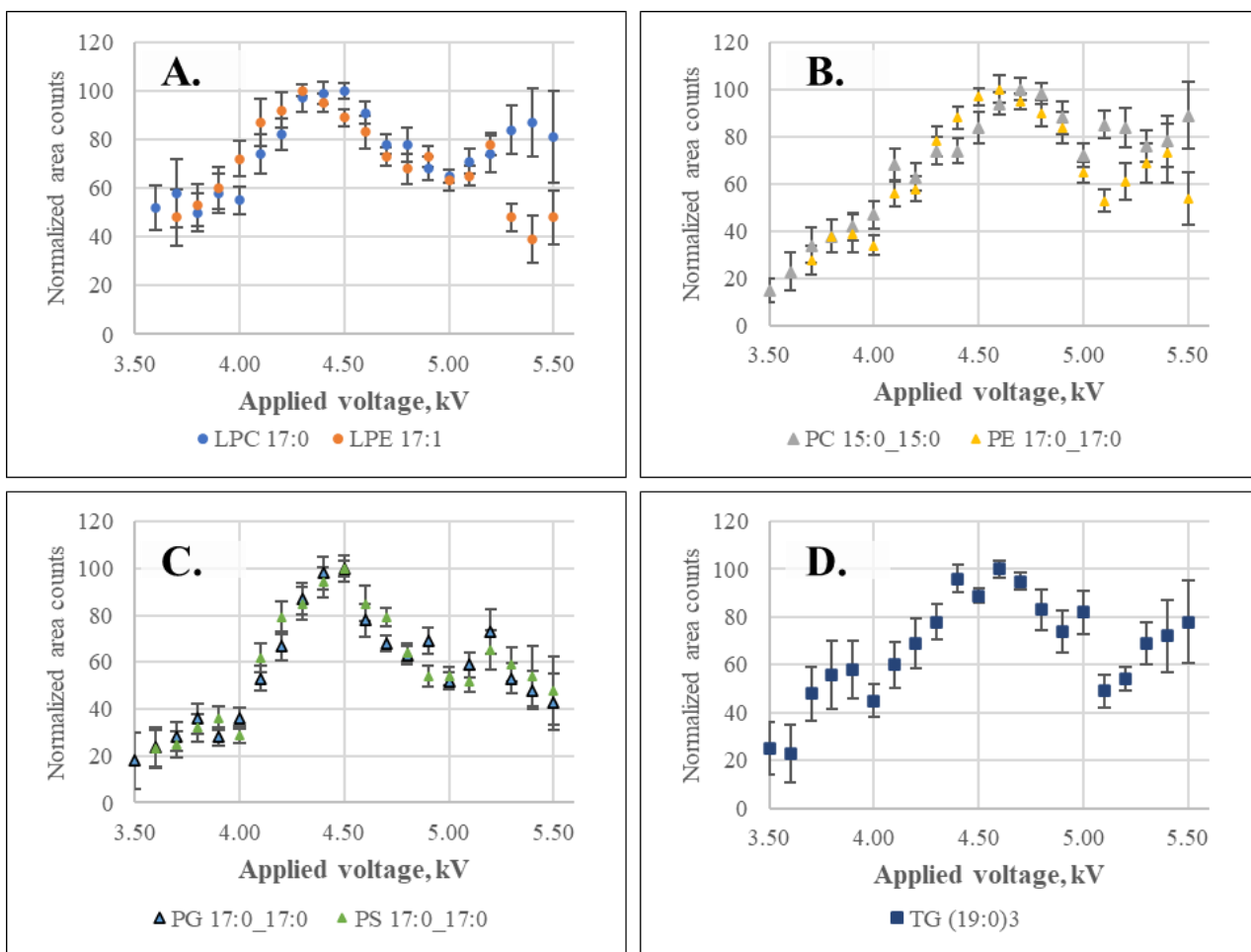


Figure 3.4. Evaluation of the high voltage required for effective ionization in TSQ Vantage. The areas are acquired for 20 s at each voltage value and then normalized to the maximum area. Mixture of lipids injected as a methanolic mixture (50 ng/mL) and continuous flow of 20  $\mu$ L/min. (A) LPC 17:0 and LPE 17:1; (B) PC 15:0\_15:0 and PE 17:0\_17:0; (C) PG 17:0\_17:0 and PS 17:0\_17:0; (D) TG (19:0)<sub>3</sub>

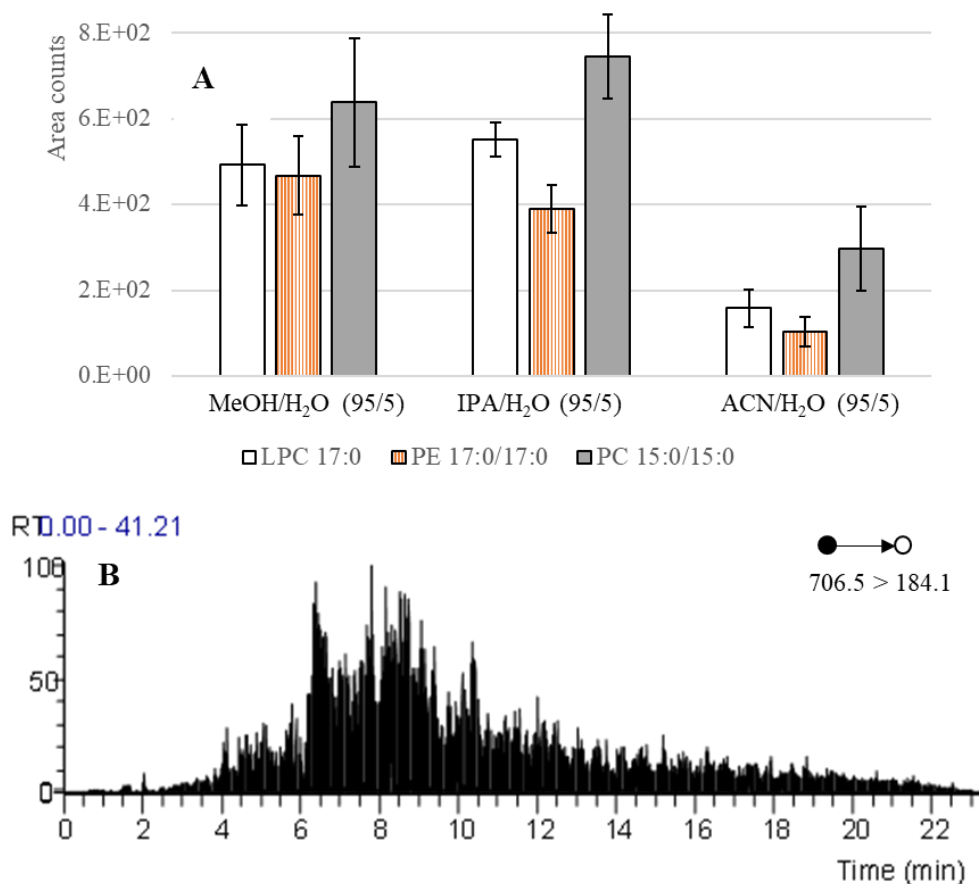


Figure 3.5. (A) Solvent comparison for desorption of selected lipids from CBS blades using TSQ Vantage and its open interface. (B) When a solvent is applied to the blade, the total ion chromatogram/transient signal for PC 15:0\_15:0 ( $m/z$  706.5 > 184.1) is obtained for up to 20 min.

The desorption solvent was optimized by testing the desorption performance of three solvent mixtures (namely, binary combinations between water and MeOH, ACN, or IPA). For these tests, the desorption volume and time (before the application of high voltage) were kept constant at 15  $\mu$ L and 15 s, respectively, 0.1% acetic acid (v/v) was added to the desorption mixtures as a modifier, and the acquisition time was set to 20 s (10 ms dwell time per transition). The area under the transient-signal curve was integrated for each evaluated solvent; these results are shown in Figure 3.5A. The observed desorption

efficiency for the targeted lipids was likely influenced by the solvent's polarity and hydrogen bond-donating abilities. For instance, the most effective detection of lipids was attained with methanol and isopropanol solvents which are already employed for desorption in LC-based applications. In contrast to these solvents, acetonitrile has a slightly higher polarity (polarity index = 5.8) and does not form hydrogen bonds, which may explain its performance.<sup>310,311</sup> While nonpolar solvents may enable the efficient desorption of lipids, one must also consider their ESI-amenability and their effect on the coatings; for instance, chloroform tends to dissolve the PAN binder. Moreover, the low signal intensity obtained in this timescale (< 30 s) and high variability (RSD in the 15–30% range) implied low overall desorption and low spray stability, respectively. To investigate further, the solvent was applied continuously to a blade using a syringe pump, which caused the transient signal to increase past the 2-min mark, continuing for almost 20 min (Figure 3.5B). However, the use of larger volumes for desorption is highly impractical, as small solvent amounts easily spread out past the coated section due to the low surface tension of organic solvents and the (albeit small) presence of surfactant-like analytes.<sup>312</sup> Similarly, the use of longer desorption times (>30 s) is also an impractical approach for use in high-throughput direct-to-MS strategies, which typically aim to reduce sample turnaround times.<sup>299</sup> Furthermore, it is essential to note that solvent evaporation during long desorption times can negatively impact spray stability.

As an alternative, three parameters were reconsidered to increase desorption efficiency: reducing the coating thickness, increasing the water content in the desorption

mixture, and isolating the blade from environmental factors. A thin extraction phase is conducive to faster extraction kinetics and rapid sampling, but this comes at the expense of a possible decline in sensitivity.<sup>313</sup> As noted, the use of thin extraction phases results in faster desorption kinetics, which are noticeable and essential in micro-desorption phenomena.<sup>314,315</sup> A different slurry was prepared using smaller C18 particles (5  $\mu\text{m}$  vs. 40  $\mu\text{m}$ ) and applied in *thinner* coats (10  $\pm$  0.8  $\mu\text{m}$ ). Lowering the organic content in the solvents (from 95% to 90%, v/v) and slightly isolating the source from environmental changes within the lab (e.g., air drafts from air-conditioning ducts, dry air from seasonal temperature control) enabled longer desorption times with lower evaporation. Similarly, the demand for an *isolated* interface prompted the use of a different instrument, the TSQ Quantiva, which features an interface that already included the plastic enclosure depicted in Figure 3.3.

The duration and intensity of the analyte signal are influenced by the amount extracted, the volume and chemical composition of the desorption solvent, the desorption time (wetting time before the application of HV), and the spray voltage. Figure 3.6 presents the results obtained using the enclosed CBS interface to desorb lipids from thinner blades. As can be seen, the amount of analyte desorbed from the coating depends on the strength and, in this approach, the volume of the desorption solvent. Undeniably, the desorption step is the bottleneck in the analytical method considered in this chapter. The desorption time is selected based on the analyte, its affinity towards the coating and the coating thickness. The molecular profiles of lipids during solvent-based ambient mass ionization are dictated

by the solvent used.<sup>316</sup> Nevertheless, while the development of SPME-CBS applications has been pursued vigorously,<sup>140,141,146,299,308</sup> further research is still required to improve the desorption/ionization process from the particles employed in the SPME coated devices, the influence of the binder, and its effect on efficient mass transfer. In addition to the inherent complexity of extraction of hydrophobic analytes in water-rich samples. Thus, an alternative approach for sample introduction was studied: the “microfluidic open interface”, as it provides a better control of the desorption process with minimal evaporation.

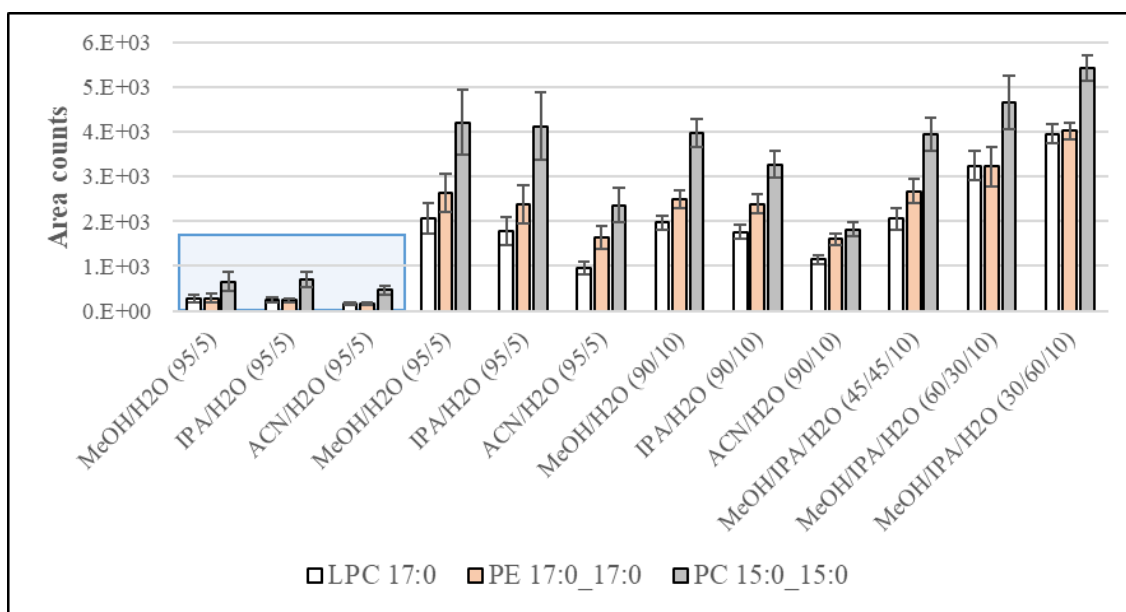


Figure 3.6. Comparison between solvent mixtures regarding desorption performance (18  $\mu$ L solvent, 30 s desorption time,  $n = 5$ ). The highlighted section portrays the obtained area counts for desorption from the *open-air* CBS interface (Vantage TSQ).

### 3.3.2 Microfluidic Open Interface

MOI was investigated because its flow-isolated desorption chamber provides greater control of the desorption process. The signal obtained with the MOI interface has a Gaussian shape, as all the desorbed analytes are introduced (comparatively) simultaneously in a low microliter injection, a narrow analyte plug, thus offering higher signal-to-noise ratios.<sup>301,317</sup> While CBS produces a transient signal that can be extended for as long as the solvent is available (enough collection of samples), MOI delivers a Gaussian peak shape over a limited time, which is determined by the desorption volume and the sample's fluid viscosity, among others variables.<sup>301,317</sup> To determine the aspiration flow caused by the instrument's source, five different solvents were evaluated and the peak width (at the base) was obtained for a 5  $\mu\text{L}$  solvent plug ( $n = 5$  injections), as listed in

Table 3.3. Gaussian peaks were observed for the tested desorption solvent, with different peak widths inversely correlated to the aspiration flow.<sup>302</sup> For instance, Solvent 1 had the highest aspiration flow (135  $\mu\text{L}/\text{min}$ ), thus producing the narrowest peak (10 s at the base); conversely, Solvent 5, which had higher isopropanol-laden viscosity, presented the lowest aspiration flow and the widest peak, at 35  $\mu\text{L}/\text{min}$  and 44 s, respectively. Next, Solvents 1, 2, 4, and 5 were selected to construct the desorption time profiles for the lipids extracted from PBS, as they allowed for coverage of a *wide* range of aspiration flow/viscosity. Certainly, desorption efficiency should be optimized for different lipids.

Table 3.3. Aspiration flow for each solvent and the average peak width using the ESI source for the Vantage and the conditions listed in Table 3.1.

Solvent	Composition (v/v)	Aspiration flow, $\mu\text{L}/\text{min}$	<i>peak width</i> , s
1	MeOH/H <sub>2</sub> O (95/5)	135	10 $\pm$ 0.8
2	IPA/MeOH/H <sub>2</sub> O (20/70/10)	90	15 $\pm$ 1.0
3	IPA/MeOH/H <sub>2</sub> O (45/45/10)	65	20 $\pm$ 1.5
4	IPA/MeOH/H <sub>2</sub> O (70/20/10)	50	24 $\pm$ 1.0
5	IPA/H <sub>2</sub> O (95/5)	35	44 $\pm$ 3.8
6	ACN/H <sub>2</sub> O (95/5)	75	18 $\pm$ 1.2

The obtained desorption time profiles are shown in Figure 3.7. Clearly, the optimum desorption time will strongly depend on the analyte and its affinity towards the desorption solvent. A clear difference among lipids can also be observed based on their hydrophobicity, with polar lipids appearing to be desorbed faster than highly hydrophobic ones. Nevertheless, zwitterionic lipid PC 15:0\_15:0 shows large signals, likely caused by ionization suppression of other lipids present, regardless of the solvent employed. Ultimately, Solvent 2 was selected as the best option, mainly due to its ability to provide higher reproducibility. Thus, this solvent was subsequently employed to construct the calibration curves shown in Figure 3.8 and the matrix-free calibration curves prepared in PBS depicted in Figure 3.9. Similarly, despite the ideal of rapidly desorbing analytes in SPME–MS for increased throughput, all compounds appeared to be in the linear *regime* of desorption. Therefore, seven consecutive desorption steps were attempted from the same SPME probe to assess the extent of carryover on the fiber. The results shown in Figure 3.10 display the amounts desorbed for up to seven sequential desorptions for a single fiber,

showcasing the high affinity between the analytes and the coating. Future research could examine whether desorption throughput can be increased by optimizing coating thickness, binder choice, and perhaps even coating chemistry. Nevertheless, the evaluation of the desorption of SPME probes was considered positive based on the calibration curves obtained in the chamber and the *apparent* linearity for polar lipids. On the other hand, while very hydrophobic lipids were extracted and detected, their mass transfer via SPME must be studied more rigorously for strategies that require fast instrumental analysis (< 1 min per sample). Testing of different solvents could in turn decrease the mass transfer resistance during desorption, though care must be taken so these solvents do not compromise the sorbent coating physical stability (e.g., chloroform can dissolve the PAN binder, thus dislodging sorbent particles).



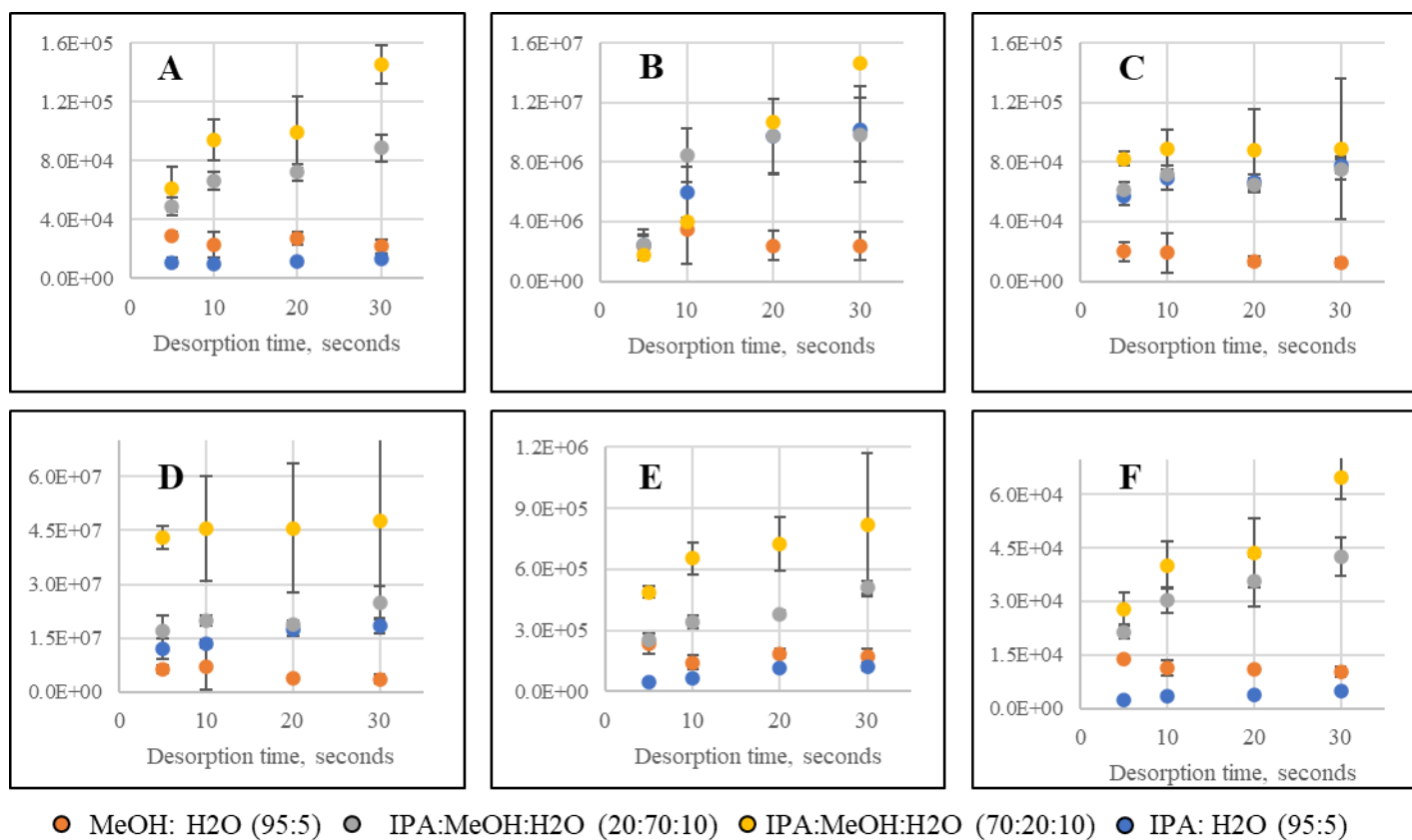


Figure 3.7. Desorption time profiles for studied lipids in the MOI interface with four solvents. Extractions were performed on PBS dispersions (100 ng/mL, 60 min) using C18 fibers (10 mm length×13 μm thickness, n=5). Lipid analytes: (A) LPC 17:0, (B) LPE 17:1, (C) LPS 17:1, (D) PC 15:0\_15:0, (E) PE 17:0\_17:0, (F) TG (19:0)<sub>3</sub>.

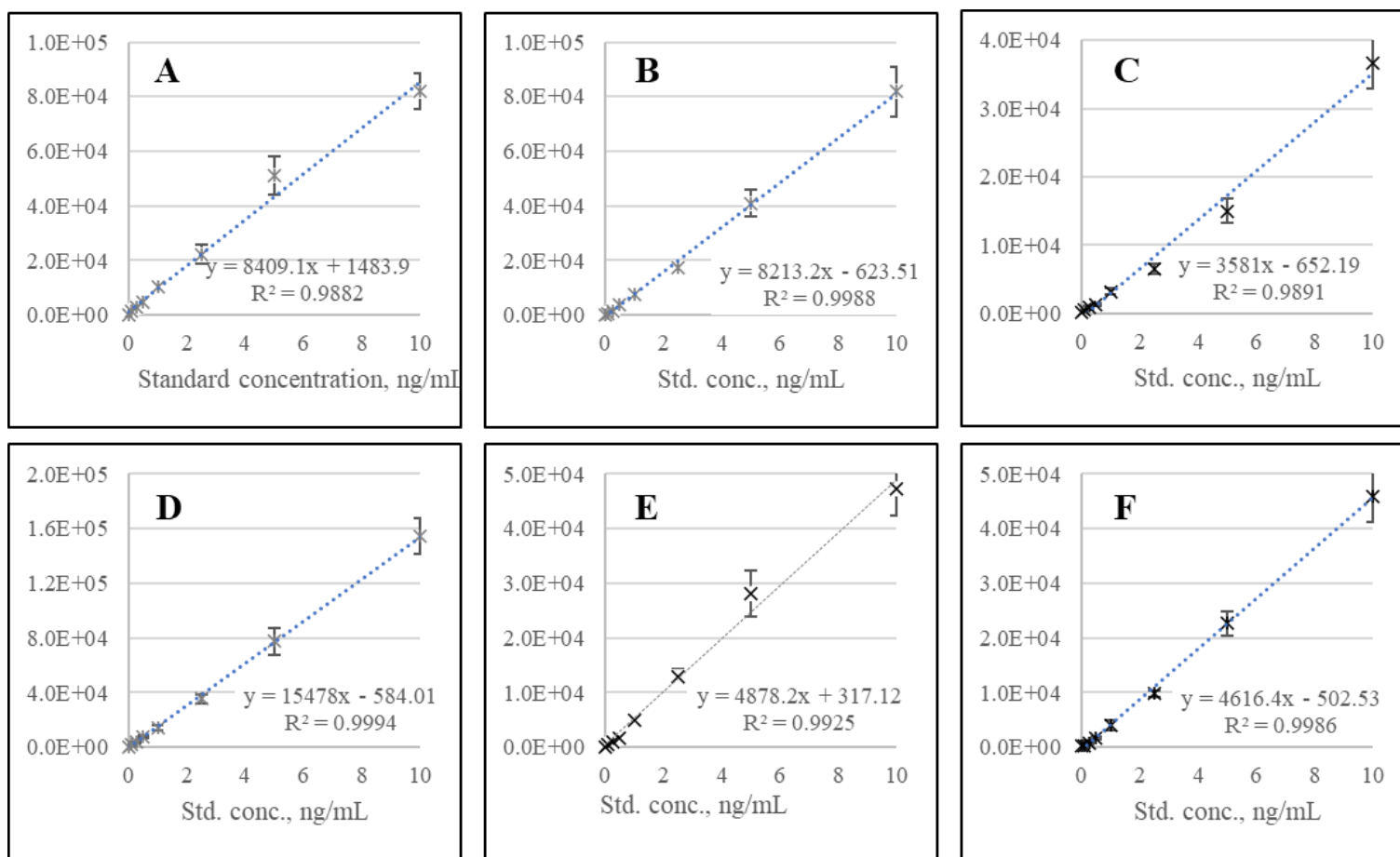


Figure 3.8. Instrumental calibration curves manually prepared in the MOI desorption chamber. Desorption solvent: MeOH/IPA/H<sub>2</sub>O (7/2/1, v/v/v) with 0.1% acetic acid and 10 mM ammonium acetate. Lipid analytes: (A) LPC 17:0, (B) LPE 17:1, (C) LPS 17:1, (D) PC 15:0\_15:0, (E) PE 17:0\_17:0, (F) TG (19:0)<sub>3</sub>.

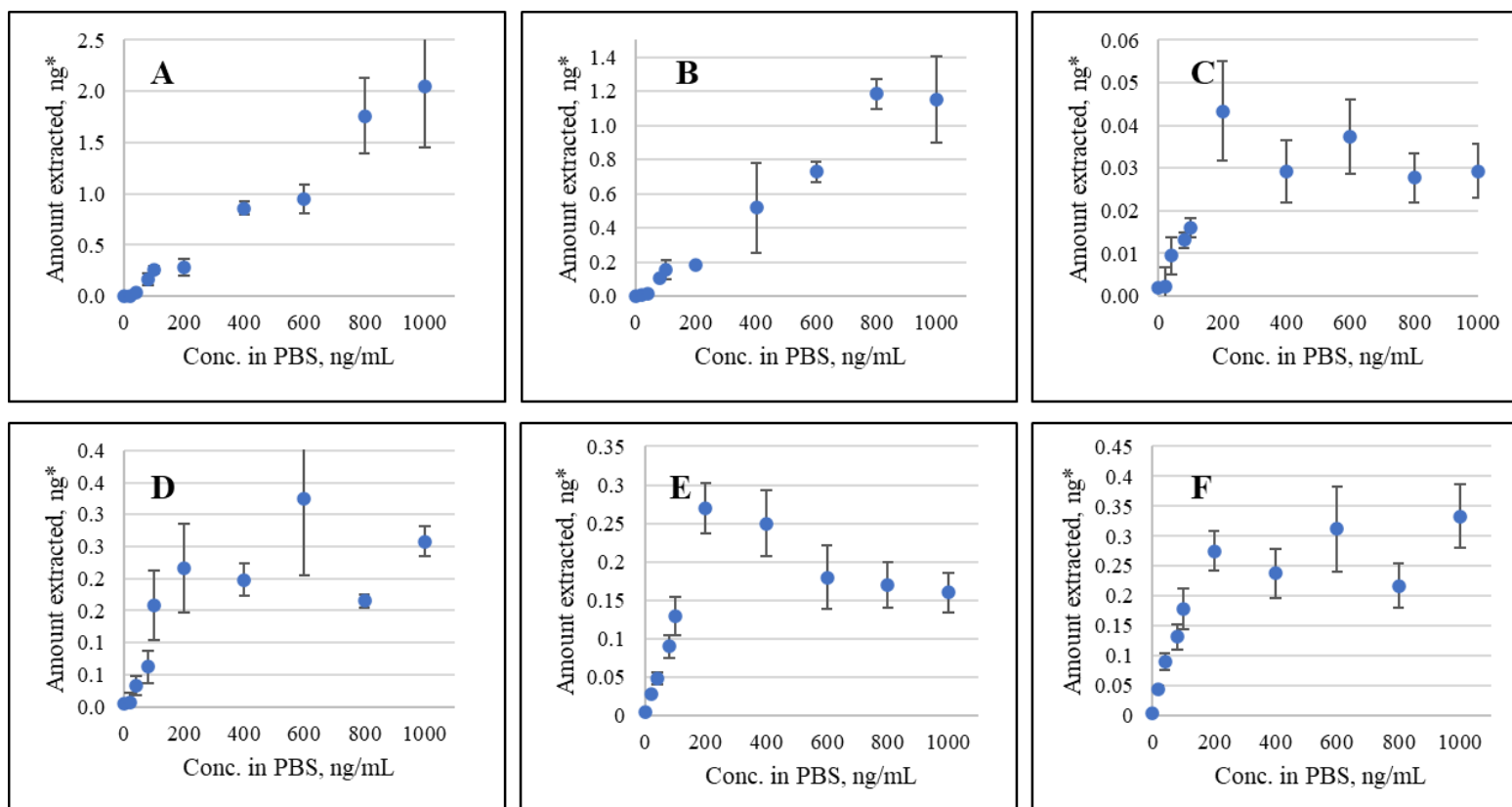


Figure 3.9. Matrix-free calibration curves prepared for lipids in PBS (pH 7.4, 30 min extraction at 1000 rpm). Static desorption was conducted for 30 s using MeOH/IPA/H<sub>2</sub>O (7/2/1, v/v/v) containing 0.1% acetic acid and 10 mM ammonium acetate. Lipid analytes: (A) LPC 17:0, (B) LPE 17:1, (C) LPS 17:1, (D) PC 15:0\_15:0, (E) PE 17:0\_17:0, (F) TG (19:0)<sub>3</sub>. Loss of linearity is likely caused by self-assembly of lipids in PBS.

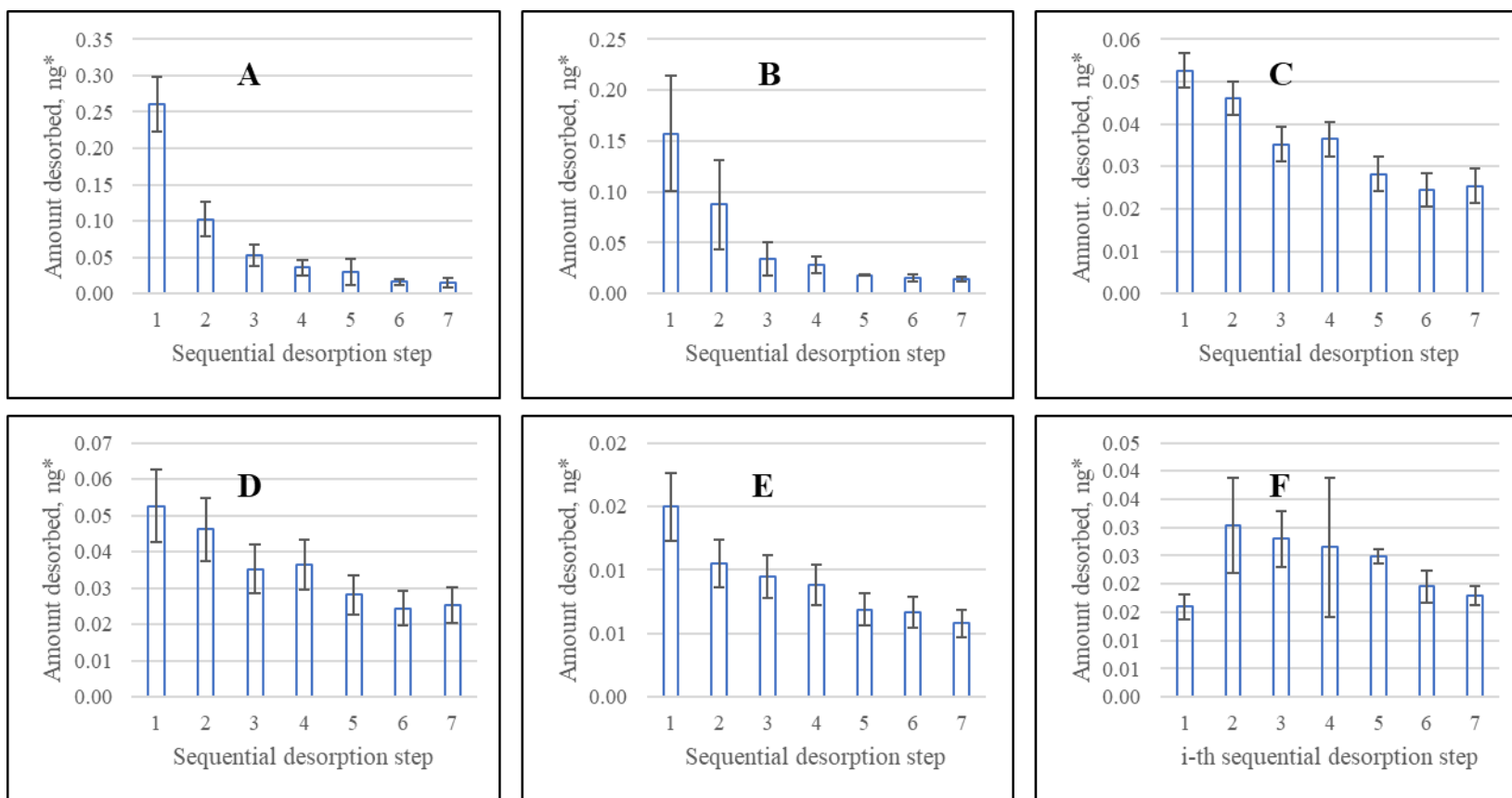


Figure 3.10. Sequential desorption steps from the same SPME probe for lipid standards extracted from PBS (pH 7.4, 100 ng/mL). Desorption time was 30 s for each step using MeOH/IPA/H<sub>2</sub>O (7/2/1, v/v/v) containing 0.1% acetic acid and 10 mM ammonium acetate. Lipid analytes: (A) LPC 17:0, (B) LPE 17:1, (C) LPS 17:1, (D) PC 15:0\_15:0, (E) PE 17:0\_17:0, (F) TG (19:0)<sub>3</sub>.

Furthermore, strict care must be taken when selecting the thickness of the coatings, as it is difficult to achieve complete desorption for lipids, as shown in Figure 3.10. While other authors have noted this phenomenon using SPME–MS,<sup>77,300,305</sup> the extent of carryover must be evaluated more meticulously to propose any quantitation strategies for biological samples. Similarly, considerable ionization suppression was observed for various lipid classes, particularly for the minor phospholipids. The inherent competition occurring during ESI ionization (and ESI-adjacent, as in CBS) is *unavoidable* and is still present in direct SPME-MS couplings, albeit on a reduced scale for some lipid classes. Additionally, the natural disparity in the concentration/abundance of different lipid classes and subclasses in real biological samples may further complicate the detection of trace lipids, as was observed for LPS 17:1. Interactions between the analytes and the C18 coating occur via van der Waals interactions between fatty acyl residues. While these interactions may confer some degree of selectivity towards lipids as a broad group, the accurate detection of specific lipid classes may be enhanced by increasing the coating's selectivity. Moreover, the *naturally* different concentration levels of lipid subclasses (e.g., LPCs being 40 times more abundant by mass compared to other LPLs such as LPEs, LPSs, and other potentially biologically active lipids) could further impact their accurate detection.

As previously noted, SPME devices simultaneously isolate and enrich analytes from the matrix by performing extractions from the unbound pool of analytes in the sample. Moreover, the use of PAN binder makes the coating matrix compatible and allows it to be tuned toward the analytes of interest. In principle, the coating dimensions of SPME devices

enable the simultaneous isolation and enrichment of analytes from the matrix in a *negligible* non-exhaustive fashion, with thin coatings being most conducive to fast desorption.

### 3.4 Conclusions

The work presented in this chapter confirms the viability of directly coupling SPME to MS for the simultaneous analysis of various lipid classes. Two sample introduction methods, namely, CBS and MOI, were tested in conjunction with different triple quadrupole mass spectrometers. For CBS, multiple parameters must work in unison to achieve the best signal-to-noise ratio (e.g., ionization/spray voltage, solvent, solvent additives, desorption time, and distance to MS inlet). While CBS is feasible, further research is required to develop and understanding of it on a more fundamental level and to simplify it, as an alternative, the *micro-desorption* MOI feature was employed, as it provides better control of the desorption volume. This key feature also accentuates MOI's applicability for determining the free concentration of selected bioactive compounds at trace levels. The probes showed minimal absolute matrix effects during extractions from untreated plasma; however, ionization effects were observed in both approaches taken occurring as suppression of some lipid sub-classes with simultaneous ionization enhancement of other lipid sub-classes. Furthermore, typical ionization enhancement was observed for choline-containing glycerophospholipids, which was more pronounced for the PC lipid subclass. In both approaches, the results showed that the mass transfer and desorption amount were more limited over the typical timescale of rapid SPME-MS techniques (15–20 s) compared to standard SPME-LC applications (e.g., > 10 min).

However, an increase in desorption efficiency throughput was obtained by modifying the desorption solvent's composition to minimize its rate of evaporation. It is worth noting that the strict quantitative capabilities of SPME-MS were not reached by the author (within the timeline for completion of the degree) and remain an area needing further study.

#### Future directions and areas of improvement

The immediate extension of this work is a rigorous study focusing on the mass transfer of lipids to and from a thin coating, including their effective mass transfer through the binder used in matrix-compatible probes, which is crucial for the fast desorption of analytes. Special attention must also be given to the device's sorption/desorption kinetics, as the free concentration of analytes in the binder controls their diffusion into the composite with the sorbent particles. When designing an optimum extraction phase, careful consideration must be taken to ensure a good compromise between fast extraction efficiency and mass transfer resistance. Furthermore, future research should examine how increasing the temperature in the desorption chamber could enhance desorption within a timescale amenable for rapid analysis.

Coupling these strategies for fast profiling can take almost full advantage of their respective rapid analysis abilities, mainly when used in a simplified system. For instance, MOI and its small desorption chamber have great promise for further research on using a standard water vial system to analyze compounds with very low solubility. The small volume of the desorption chamber and the MOI system's flexibility (it can be made smaller if needed) can significantly increase sensitivity and decrease LOD/LOQs.

Simplifying the SPME extraction process and the samples used is paramount to developing a more robust understanding of this challenging group of compounds. For instance, future work should target fewer compounds with known physicochemical parameters (e.g., water solubility, critical micelle concentration, acidity/basicity as pKa). Additionally, future work could examine if and how other parameters (i.e., other lipids, ionic strengths, pHs, glucose concentration.) influence the free concentration of analytes, as these factors govern all manner of mass transfer. Such research would be integral to identifying optimum matrix-free environments that better reflect the sample.

Finally, increasing the method's selectivity is crucial to achieving better quantitative results. Numerous strategies could be implemented (and studied further) to this end, including rationally designed coatings for the selective/targeted extraction of a smaller pool of analytes (e.g., silver for unsaturated lipids, zirconia for phospholipids, and SCX for fatty acids and eicosanoids); modifying the matrix pH to enable the extraction of trace pH-sensitive lipids (e.g., fatty acids, PAs, and some sphingolipids); derivatization at whichever stage is more conducive to more selectivity in MS (e.g., derivatize fatty acids, derivatization of unsaturated fatty acids to pin-point location of double bonds; derivatization for non-ESI-amenable analytes like sterols).



## **Chapter 4 Profiling of unsaturated lipids by Raman spectroscopy directly on SPME probes**

### **Preamble**

Chapter 6 has been published as a short technical note under the title “Profiling of Unsaturated Lipids by Raman Spectroscopy Directly on Solid-Phase Microextraction Probes” (*Analytical Chemistry*, **2022**, *94*(2), 606–611). This manuscript was coauthored with Victor Galievsky and Khaled Murtada and supervised by Janusz Pawliszyn and Pavle Radovanovic. Experimental design, data analysis, and manuscript writing were done by the author of this thesis in collaboration with Khaled Murtada and Victor Galievsky. Probe manufacturing, SPME sample preparation, and LC-MS/MS instrumental determinations were done entirely by the author of this thesis. Victor Galievsky performed all Raman measurements and their corresponding data acquisition. Janusz Pawliszyn and Pavle Radovanovic supervised the collaboration and contributed to the manuscript revision.

### **4.1 Introduction**

Lipids are an important class of biomolecules that play a fundamental role in the composition of membranes and as energy storage vehicles in lipid droplets.<sup>318, 319</sup> Lipids can act as signalling molecules in intra-cellular and inter-cellular processes.<sup>320,321</sup> The functions performed by lipids are as broad and diverse as their structural characteristics. Structure plays a crucial role in defining lipid classes and subclasses and, to some degree, their biochemical functions and biophysical properties.<sup>319,322</sup> The detection and monitoring of lipids are critical for maintaining human health, with cholesterol being the most prominent lipid linked to cardiovascular disease.<sup>323</sup>

Over the past few decades, innovations in separation technologies and mass spectrometry (MS) have sparked a renaissance in lipid research, which has come to be known as lipidomics. The primary aim of lipidomics is to integrate the roles of these biomolecules in cellular functions, as well as to track changes and quantify lipids in diverse samples. Furthermore, introducing soft ionization techniques to MS – electro-spray ionization (ESI) and matrix-assisted laser desorption/ionization MALDI<sup>324–327</sup> has made it even easier to analyze lipids—including low-abundance lipids, such as endocannabinoids—in their natural state.<sup>15,328</sup>

However, chromatographic and MS-based technologies can be complicated and require expensive instruments and consumables. In addition, these state-of-the-art techniques must also be implemented by highly qualified personnel. In contrast, optical spectroscopy is a fast and inexpensive option for analyzing biological materials, with absorption and fluorescence spectroscopy being the simplest and most widely used variants.<sup>329</sup> However, the application of these approaches in lipidomics is somewhat limited, as they usually require using derivatization protocols to introduce chromophore/fluorophore moieties into lipid structures. For example, diacylglycerols in multiple matrices were determined using visible spectroscopy after derivatization with iodine and phosphomolybdic acid.<sup>330</sup> Thus, when analyzing the composition of analytes, it is preferable to use methods that do not require a labelling procedure, for example, Raman spectroscopy. Raman spectroscopy identifies molecules based on their characteristic vibrations. It can be employed to analyze chemical components and detect structural and

conformational changes in applications such as assessing meat quality,<sup>331</sup> qualitative differentiation between waste oil and vegetable oil,<sup>332</sup> and detecting and diagnosing cancer in tissues.<sup>65,70</sup>

However, Raman spectroscopy is hampered by low sensitivity, which often requires sample-preparation protocols, including the isolation and enrichment of analytes. Thus, the availability of simple and effective sample-preparation protocols with minimal steps is highly desirable. The coupling of Raman spectroscopy with solid-phase microextraction (SPME)—which combines extraction and preconcentration into one stage—is an exemplary configuration for rapidly analyzing diverse classes of analytes in complex matrices. SPME relies on using a thin sorbent film immobilized onto support, which preconcentrates desired analytes from a sample via equilibration between the extraction and sample phases. The extraction phase's affinity towards different analytes can be modulated by carefully selecting the coating sorbent that provides maximum sensitivity. Additionally, SPME is a platform technology that can be used in a wide range of food, environmental, and bioanalytical applications<sup>70</sup> Indeed, coupling miniature SPME to Raman spectroscopy is an intriguing option for fast screening applications and ones that require the non-destructive bedside analysis of metabolites and drugs in their natural state.<sup>333,334</sup>

In the current work, SPME probes coated with C18 particles embedded in PAN extracted unsaturated lipids, which were then identified via Raman spectroscopy. Further proof-of-concept test was conducted wherein the developed method was employed to

extract and identify unsaturated lipids in different complex matrices, such as cod liver oil and vegetable oils (coconut, canola, sunflower, and grapeseed), followed by Raman spectroscopy analyses. The results of this proof-of-concept test revealed that the proposed SPME method offers adequate performance not only for extracting unsaturated lipids but also for screening their degree of saturation, in addition to being the first time Raman spectroscopy is used for lipid detection directly on SPME probes, to the best of our knowledge.

## **4.2 Experimental**

### **4.2.1 Materials, supplies, and chemicals**

Fatty acid standards were acquired as follows: stearic acid, oleic acid (OA), linoleic acid (LA), and  $\alpha$ -Linolenic ( $\alpha$ -LA) acid were purchased from Sigma-Aldrich (Hamilton, ON, Canada); while arachidonic acid (AA), eicosapentaenoic acid (EPA), and docosahexaenoic acid (DHA) were purchased from Cayman Chemicals (Ann Harbor, MI, USA). The triglycerides (1,2,3-tri-eicosapentaenoyl glycerol and 1,2,3-docosahexaenoyl glycerol) were also acquired from Cayman Chemicals. MS-grade methanol (MeOH) and isopropanol (IPA), HPLC-grade chloroform ( $\text{CHCl}_3$ ) and hexane were obtained from Fischer Scientific (Hampton, USA). Lipid standard stock solutions were prepared in  $\text{CHCl}_3$ : MeOH (1:1, v/v) at  $5 \text{ mg mL}^{-1}$  and stored in amber vials at  $-30 \text{ }^\circ\text{C}$ . Working standard solutions were prepared as needed by diluting the stock solution to the required concentration with methanol.

SPME fibers coated (40  $\mu\text{m}$  thickness) with octadecyl particles (C18) and octyl mixed with strong cation exchange particles (C8-SCX, also known as mixed-mode) were kindly provided by Millipore Sigma (Bellefonte, PA, USA). The HLB fibers were prepared following the procedure outlined elsewhere/in Section 0. Finally, vegetable oils and cod liver oil supplements (CLO) were acquired from a local market in Waterloo, Ontario.

#### **4.2.2 Raman measurements**

All Raman measurements were acquired on a Raman Microscope Systems 1000 (Renishaw, Chicago, USA) equipped with an Olympus MD Plan 50x/0.75 objective lens and a spectrograph with a 1200 l/mm grating and an entrance slit of 100  $\mu\text{m}$ . The Raman signal was collected in back-scattering geometry. Excitation was achieved using a 785 nm SLM laser (Integrated Optics, Vilnius, Lithuania) with a power of 35 mW, and spectra were recorded using an extended data-capture mode with an acquisition time of 30 s. The spectral calibration was checked daily against the 520.7  $\text{cm}^{-1}$  Raman line of silicon. For each probe measurement, several spectra were obtained from across the fiber's surface with good uniformity; therefore, three points were chosen arbitrarily, and the obtained spectra were averaged. It should be noted that, in this case, no Raman signal loss was observed. The obtained spectra were treated using SpectraGryph 1.2 (Dr. Friedrich Menges, Germany) spectroscopy software. Following advanced baseline correction, all spectra were normalized to the peak intensity of the PAN line at 2242  $\text{cm}^{-1}$ , which had been used as the particle binder in the SPME solid coatings. This approach minimized signal variations due

to different laser beam focusing and backscattering on the convex fiber surface when changing the detection spot.

#### **4.2.3 Sample preparation and SPME procedure.**

Prior to extractions, the SPME probes were cleaned via vortex agitation in a mixture of MeOH: IPA (1:1, v/v) for 30 min, followed by preconditioning in MeOH: H<sub>2</sub>O (1:1, v/v) under the same conditions. Extractions were performed in amber glass vials with vortex agitation at 1500 rpm. Following extraction, the probes were cleaned with a lint-free wipe and quickly rinsed in solvent to remove any loosely attached matrix components/sample residue, which can cause high levels of interference in the Raman measurements – namely water: methanol (9:1, v/v), water: acetone (9:1, v/v), and hexane. Next, an extraction time profile was constructed using the SPME probes to perform extractions from 1 mL oil samples at extraction times ranging between 5 and 90 min. Once again, the probes were cleaned with a lint-free wipe and rinsed for 10 sec in water: acetone (9:1, v/v) after each extraction and then promptly analyzed. Finally, we evaluated the effect of temperature to determine whether decreasing the oil samples' viscosity would result in enhanced extraction or reduced equilibration times. To this end, SPME extractions were performed for 20 min from 1 mL of cod liver oil at temperatures between 25 and 65 °C. For all tests related to SPME method development, the area of the 1655 cm<sup>-1</sup> Raman shift, which corresponds to C=C stretching, was used as a response variable. Furthermore, all extractions used, at least, three independent measurements. Fatty acid aqueous samples were prepared in silanized vials in PBS (pH 7.4) and from the standard solutions made in

methanol. It should be emphasized that polyunsaturated fatty acids are *poorly* soluble in water, thus all samples prepared in aqueous system (such as PBS) likely resulted in self-association of fatty acids into colloidal particles. However, these samples will be described as ‘solutions’ instead of the more accurate term ‘dispersions’ to avoid confusion with the term ‘optic dispersion’ term, prevalent in spectroscopy. No effort was adopted for characterization of these colloidal particles as SPME *extracts* via free concentration,<sup>66,68</sup> thus analyte extraction occurred from the pool of freely dissolved monomers. To spike the oil samples, a large amount of standard solution (>5% v/v) would be required, thus the spiking approach involved evaporation of the solvent with a gentle flow of high-purity nitrogen, followed by addition of the oil to the layer of the standard, and vigorous agitation (30 min, 1800 rpm).

### 4.3 Results and discussion:

#### 4.3.1 Evaluation of SPME coating chemistry.

Table 4.1 Major peaks of different SPME fiber coatings and their assignment.

HLB/PAN		Mixed mode/PAN		C18/PAN	
R. shift, $cm^{-1}$	Assignment	R. shift, $cm^{-1}$	Assignment	R. shift, $cm^{-1}$	Assignment
2910	$\nu$ C–H in $CH_2$	2910	$\nu$ C–H in $CH_2$	2910	$\nu$ C–H in $CH_2$
2242	$\nu$ $C\equiv N$	2242	$\nu$ $C\equiv N$	2242	$\nu$ $C\equiv N$
1630	$\nu$ C=C	1630	$\nu$ C=C	-	-
-	-	1608	$\nu$ S–OH	-	-
1300-1317	$\delta$ $CH_2$ and $CH_3$	1300-1317	$\delta$ $CH_2$ and $CH_3$	1300-1317	$\delta$ $CH_2$ and $CH_3$
1080	$\nu$ C=C	1080	$\nu$ C=C	1080	$\nu$ C=C

$\nu$ : stretching;  $\delta$ : bending.

Three different (and readily available) coating chemistries (namely, C18, C8-SCX “mixed mode,” and HLB) were tested to assess their fit for the present study. All Raman spectra for the different SPME coating chemistries, which were tested in the region

between  $200\text{ cm}^{-1}$  and  $3200\text{ cm}^{-1}$ , are presented in Figure 4.1. As can be seen, the HLB/PAN, C18/PAN, and C8-SCX/PAN fibers all have a strong band at  $2242\text{ cm}^{-1}$  (from the PAN binder and identified independently) that is absent in plain C18 particles. The PAN that was used as a binder in the three probes provides bands at  $2242$  and  $2910\text{ cm}^{-1}$  because of  $\text{C}\equiv\text{N}$  stretching and  $\text{C-H}$  stretching, respectively. In addition, it creates peaks at  $1080$  and  $1116\text{ cm}^{-1}$  from  $\text{C-C}$  skeletal stretching, and a shift at  $1452\text{ cm}^{-1}$  from  $\text{CH}_2$  bending. Some notable Raman shifts for the HLB coating appear at  $999\text{ cm}^{-1}$ , which corresponds to aromatic ring breath, while the bands at  $1630\text{ cm}^{-1}$  correspond to  $\text{C=C}$  stretching, and the band clusters at  $1181$ ,  $1206$ , and  $1228\text{ cm}^{-1}$  are related to aromatic moiety. Significantly, the HLB/PAN and C8-SCX/PAN coatings have characteristic peaks at  $1608/1630$  and  $1600/1610\text{ cm}^{-1}$ , respectively, which can interfere with the characteristic peaks of the unsaturated fatty acids. For this reason, we selected the C18/PAN-coated SPME device for this study. Table 4.1 provides an assignment of three SPME coatings' vibrational peaks. Among the three evaluated coatings, C18/PAN has fewer bands, mainly corresponding to the stretching and bending of the  $\text{C-C}$  and  $\text{C-H}$  bonds in its simple hydrocarbon structure.<sup>335</sup> On the other hand, the Raman spectra of the HLB coating was significantly more *noisy* (Raman bands likely stemming from polar moieties within the sorbent polymer), thus discouraging its use in further experiments despite its potential for superior/similar extraction capacities.



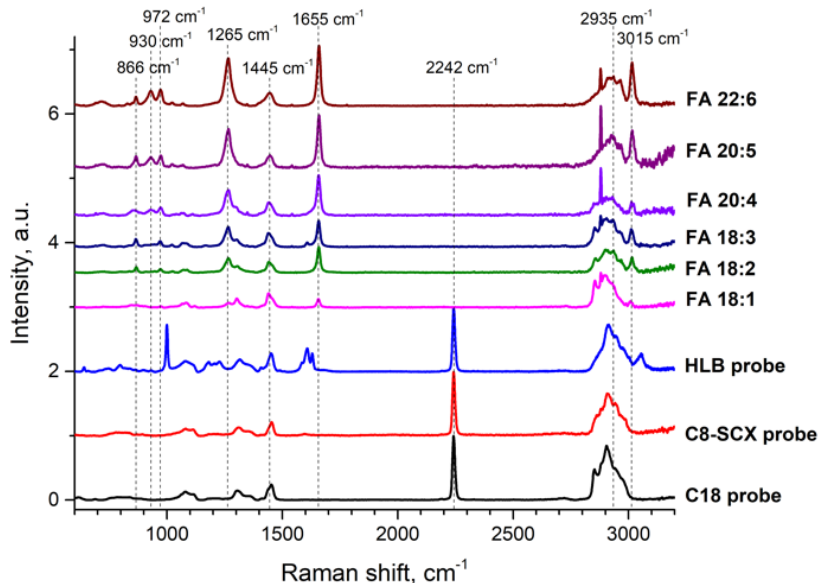


Figure 4.1. Raman spectra of blank SPME fiber probes bearing different coating chemistries and liquid solutions of fatty acids with an increasing number of double bonds. The Raman spectra of probes normalized at line  $2242\text{ cm}^{-1}$  and the spectra of FAs normalized at the line of  $1445\text{ cm}^{-1}$

#### 4.3.2 SPME optimization procedure.

It is critical to study appropriate rinsing procedures for the SPME probes after extraction, especially for complex samples, as rinsing helps to remove loosely attached matrix components that can affect the analysis (e.g., by causing higher background fluorescence). In addition, introducing a washing step can also help extend the life of the SPME fiber. A Kim Wipe tissue was used to clean the fiber further when the washing solvent could not sufficiently remove matrix constituents. In the case of cod liver oil, the effect of the washing solvent was evaluated on the C=C stretching band at  $1650\text{ cm}^{-1}$  (Figure 4.2A), with results revealing that the water-based rinsing solutions provided better performance than hexane. This result can be explained by the fact that hexane is a much

stronger non-polar solvent, which removes most of the extracted analytes. Furthermore, there is no significant difference between the water/methanol and water/acetone washings.

The bio-compatible PAN binder used in the probe coating provides good mechanical strength and chemical stability required for handling and multiple extraction/desorption steps. Extraction time is necessary for the adsorption process to reach equilibrium, and it is closely related to the rate-limiting factor of SPME. It is essential to determine the optimal extraction time, as maximum analyte adsorption and method sensitivity are achieved in an equilibrium state. Extraction time profiles for DHA and EPA in the cod-liver oil were carried out in the 5 – 90 min range. The results indicated that an extraction time of 15 min was sufficient for achieving equilibrium (Figure 4.2B). As such, this time interval was used throughout this study for all samples.

Extraction temperature is another essential parameter in SPME, as it can significantly influence extraction efficiency due to its ability to modulate the diffusion coefficient, alter the viscosity of the matrix, and diminish the distribution coefficient between analytes and the extracting phase.<sup>70</sup> Thus, increasing the extraction temperature was examined as a possible way of speeding the mass transfer of analytes while limiting potential reductions in sensitivity. To this end, extractions from cod liver oil were performed at temperatures ranging from 25 – 65 °C for 20 min at 1500 rpm. As shown in Figure 4.2C, no significant changes in the intensity/area of the C=C stretching band were observed across the tested temperatures. Nevertheless, the relative standard deviation in intensity increased with the temperature, under 10% and over 50% at 25 °C and 65 °C, respectively. Thus, subsequent

extractions were performed at 25 °C. Said increase in deviation could be attributed to a decreased affinity between the analytes and the coating at higher temperatures, thus modifying the analyte partition/mass transfer.<sup>68</sup>

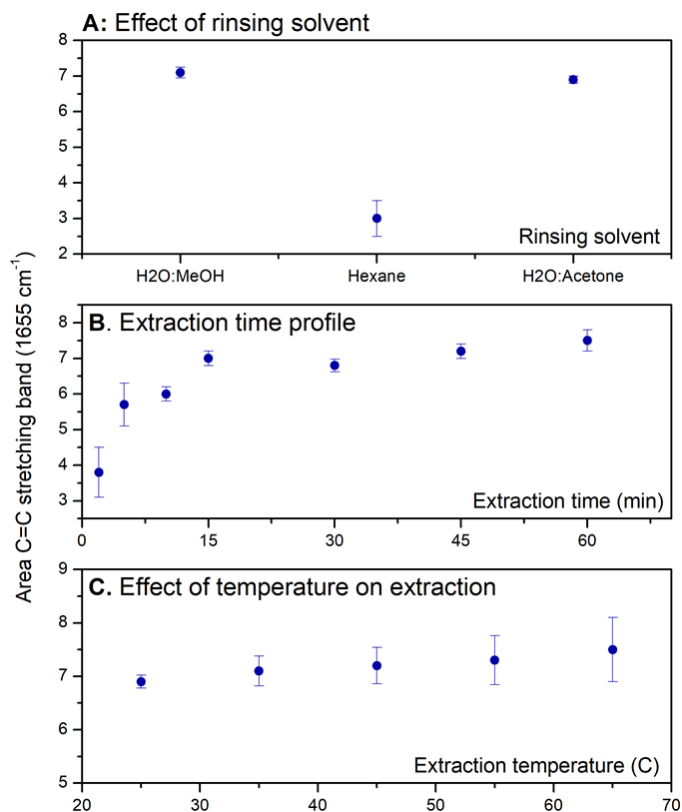


Figure 4.2 SPME extraction method development using cod liver oil and 1655  $cm^{-1}$  Raman shift as the response variable (due to unsaturated lipids, C=C stretching). **A:** Comparison of washing solvent composition. **B:** Extraction time profile; and **C:** Effect of temperature on the extraction of unsaturated lipids. All extractions were performed from 1.0 mL of oil under vortex agitation at 1500 rpm.

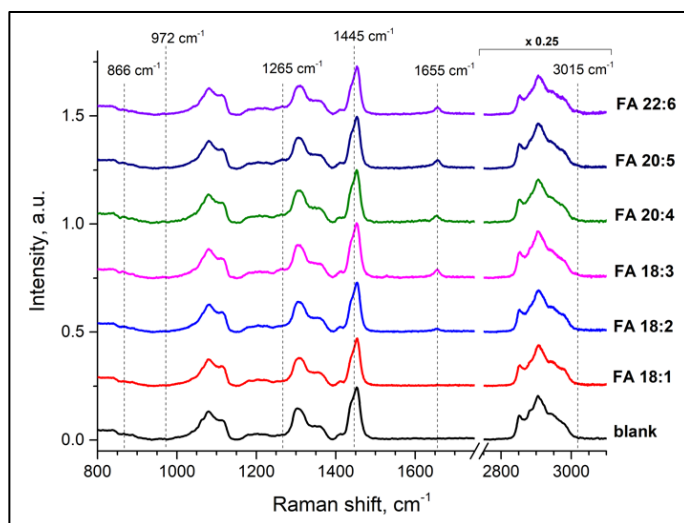


Figure 4.3 On-fiber Raman spectra of fatty acids with increasing double bonds. The spectra normalized at the PAN line of  $2242\text{ cm}^{-1}$ . Extractions performed using C18 coated probes from aqueous *solutions* of fatty acids (0.5 mM, PBS at  $25\text{ }^{\circ}\text{C}$ ).

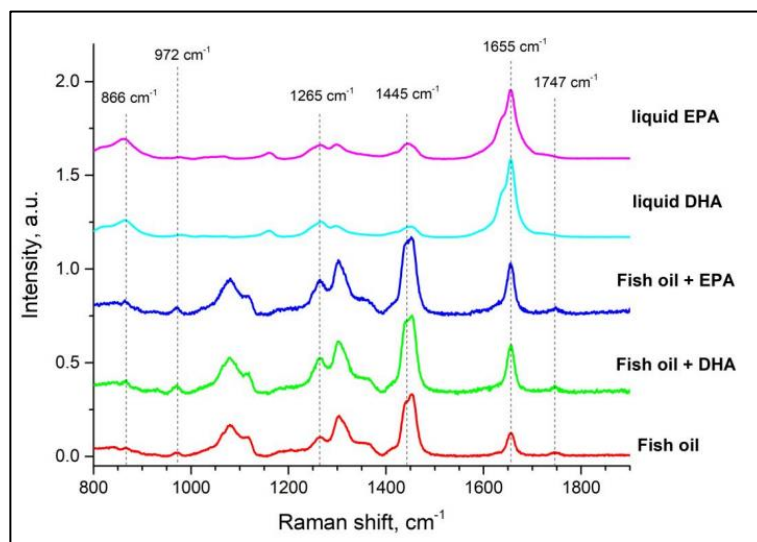


Figure 4.4. On-fiber Raman spectra of pure eicosapentaenoic (TG 20:5\_20:5\_20:5, TG EPA) and docosahexaenoic (TG 22:6\_22:6\_22:6, TG-DHA) triglycerides, locally acquired fish oil, fish oil enriched/doped with 50 mM of each PUFA triglyceride

### 4.3.3 Spectra analysis of lipids.

Table 4.2 Assignment for Raman band for the fatty acids used as analytes, using the small library presented in Figure 4.1.<sup>64</sup>

Raman shift, $cm^{-1}$	Assignment
866	skeletal C–O–O
972	$\beta$ C–H
1265	$\delta$ =C–H
1445	$\alpha$ CH <sub>2</sub> / CH <sub>3</sub>
1655	$\nu$ C=C
2935	$\nu$ =CH <sub>3</sub>
3015	$\nu$ =C–H

The Raman spectra of fatty acids usually present in biological samples are shown in Figure 4.3. Fatty acids were selected for analysis because they constitute the most common building block for more complex lipids. The Raman bands from fatty acids detected on the SPME fiber were attributed to CH<sub>2</sub> stretching at 1445  $cm^{-1}$ , C-H in-plane stretching at 1265  $cm^{-1}$ , and a strong band at 1655  $cm^{-1}$  from C=C stretching.<sup>64,336</sup> It is known that the intensity and location of bands in the Raman spectra of a given lipid are influenced by its degree of unsaturation and, to some degree, by the cis/trans configuration of its double bonds.<sup>337</sup> Raman spectra for triglycerides with polyunsaturated fatty acyl residues triglycerides, particularly EPA and DHA, were also acquired and are depicted in Figure 4.4. The Raman spectra between PUFAs and TG-PUFAs are identical, except for the presence of bands from the ester motifs in 1720–1750  $cm^{-1}$  region. Table 4.2 shows a detailed assignment of the vibrational peaks of the extracted fatty acids. The Raman line at 1655  $cm^{-1}$  seems very suitable for quantitative analysis of fatty acids because it does not overlap with other bands.

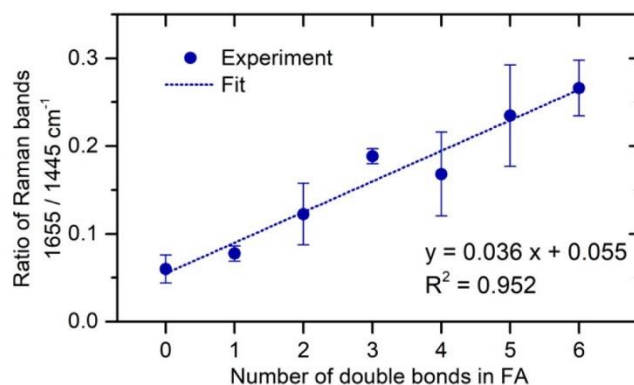


Figure 4.5. Degree of unsaturation obtained from PUFAs solutions with increasing double bonds (0.5 mM in PBS, at 25 °C). The degree of unsaturation is determined as the ratio of Raman band areas at 1655 and 1445  $\text{cm}^{-1}$ , obtained by integrating the spectral ranges of 1601–1700  $\text{cm}^{-1}$  and 1425–1475  $\text{cm}^{-1}$ , respectively.

As shown in Figure 4.5, the integrated area of this band, related to the C=C stretching, increased alongside the number of double bonds in the fatty acid molecule when extractions were performed from equimolar solutions of these lipids. The degree of lipid unsaturation, calculated as the ratio of  $n(\text{C}=\text{C})/n(\text{CH}_2)$  using the ratio of intensities of the Raman bands at 1655 and 1445  $\text{cm}^{-1}$ , linearly depends on the number of double bonds with a coefficient of determination,  $R^2 = 0.952$ . Other spectral markers, such as bands corresponding to the =C–H deformation ( $\sim 1265 \text{ cm}^{-1}$ ) and stretching ( $\sim 3015 \text{ cm}^{-1}$ ) vibrations, can also be used for analyzing lipid unsaturation. However, the low intensity of these lines and the overlap with the Raman bands of the SPME probe reduce the accuracy of determining the degree of lipid unsaturation. Raman spectroscopic markers have already been used for discrimination among red meat tissues and the average composition of fatty acids.<sup>338,339</sup> As a proof-of-concept, we demonstrated the method's ability to detect unsaturated lipids in different vegetable oil samples and dietary supplement samples enriched with omega-3 and omega-6 fatty acids, whose Raman spectra are depicted in Figure 4.6. However, being able

to differentiate the contributions of either omega-3 or omega-6 fatty acids in vegetable oils falls outside the scope (and limitations) of this proof of principle study. The SPME probes coated with C18/PAN were used for this test due to their suitability for unsaturated lipid analysis and ability to provide adequate rapid sample preparation for Raman detection. The obtained spectra reflect the complex composition of these samples, which stems from diverse fatty acid profiles (present as triglycerides), as denoted by the Raman shift at  $1747\text{ cm}^{-1}$  produced by the C=O stretching in the ester bonds and the peak at  $1655\text{ cm}^{-1}$  corresponding to the cis (C=C) group of unsaturated fatty acids. Though SPME has been used extensively for quantitative analysis with MS-based analysis, the capabilities for quantitation of more complex mixtures of lipids using SPME probes and Raman spectroscopy are yet to be explored.

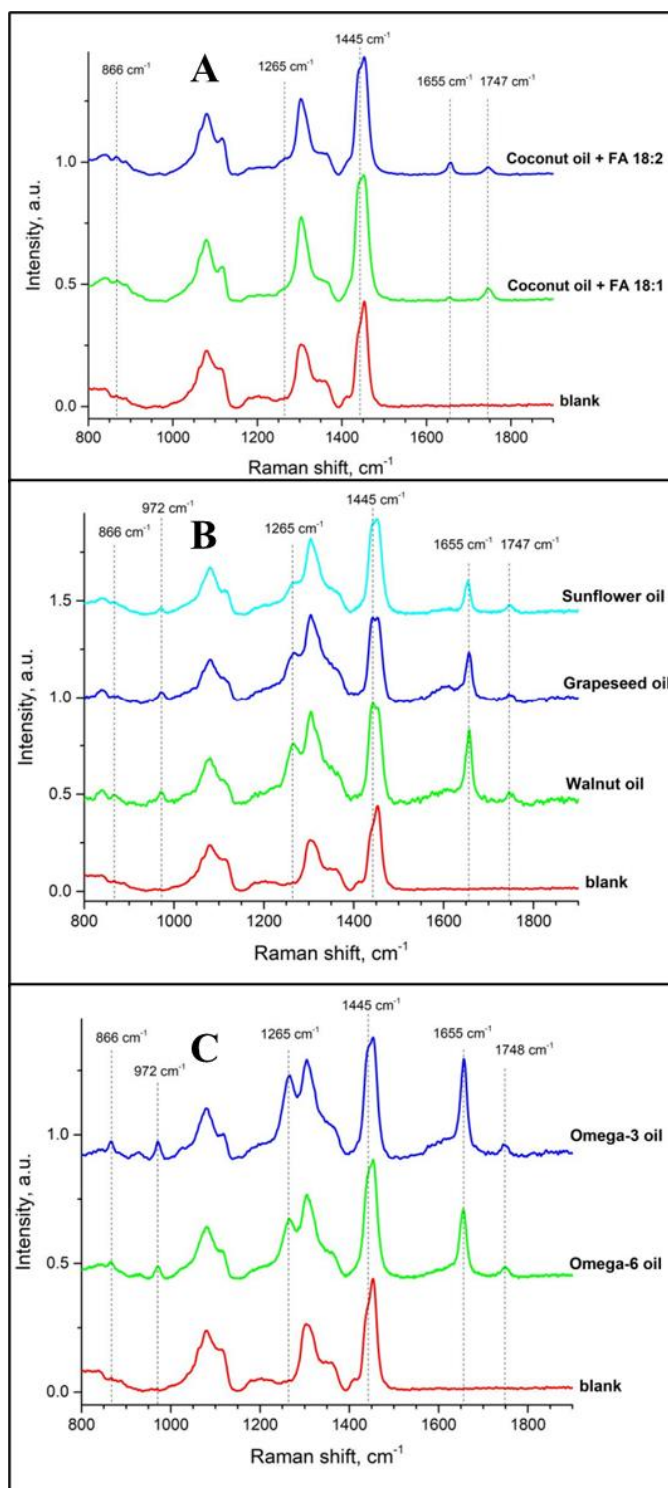


Figure 4.6. (A) Spectra of coconut oil enriched with 50 mM of two unsaturated fatty acids: oleic acid (FA 18:1) and linoleic acid (FA 18:3). (B) Spectra of vegetable cooking oils measured on fiber. (C) Spectra of dietary supplements enriched with PUFA triglycerides.

#### 4.4 Chapter conclusions



In summary, this work details the development of an analytical methodology that couples SPME probes and Raman spectroscopy to achieve sensitive optical detection for the determination of unsaturated lipids in simple matrices. The detection of unsaturated lipids using SPME probes coupled to Raman spectroscopy served as a proof-of-concept for detecting extracted compounds/lipids directly on the probe surface. The coupling of SPME probes and Raman spectrometry is a viable alternative for determining lipids due to its low investment costs, low solvent consumption, short processing time, and ability to provide rapid analysis. Although other instrumental platforms may provide more sensitive determinations, the proposed SPME–Raman approach could detect lipids extracted from more complex matrices, such as cod liver oil and vegetable oils. Finally, this approach may be used for fast, minimally invasive food quality screening.

Indeed, as a simple proof-of-concept study, this technology could improve in many aspects. First (and foremost), increasing the scope of quantitation from simple solutions/dispersions of fatty acids in PBS to progressively more complex samples (e.g., multiple unsaturated fatty acids in solution at various concentrations, unsaturated lipids from different lipid classes, *actual* models with increasing complexity). Second, the sensitivity attained by this method ought to be boosted by employing a more selective coating. For example, a layer based on silver structures may provide surface-enhanced Raman scattering while simultaneously providing selectivity towards unsaturations via silver complexation ( $\text{Ag} - \pi$ ). Third, a major unforeseen drawback was the high background produced by the PAN binder in the tested SPME probes. Using PAN as a

binder presents various advantages to MS-based platforms, such as matrix compatibility with/to different samples and reduced concomitant extraction of matrix components/*contaminants*; however, the choice of binder must be re-evaluated (or excluded) for spectroscopic platforms.

## Conclusions and future directions

### Conclusions

The chemical analysis of lipids in complex biological matrices using modern MS-based analytical technologies has grown in depth and breadth in recent decades. Indeed, the literature contains many studies that provide evidence of SPME's effectiveness in quantifying different compounds in various matrices of bioanalytical interest.<sup>70</sup> While many studies have explored the application of SPME for the extraction of lipids from biological samples,<sup>43,80,85,202</sup> its use for the quantitation of lipids remains relatively unexplored. In addition, this thesis contributes to the development of research aimed at the (*in vitro*) quantitation of lipids by examining three approaches based on the coupling of SPME and MS-based approaches (Chapter 2 and Chapter 3) and Raman spectroscopy (Chapter 4, as a non-destructive approach).

In Chapter 2, a targeted RPLC-MS/MS method was applied to study the underlying aspects of the SPME sampling devices using exogenous lipids as probes to understand the behaviour of lipid metabolites. SPME's quantitative capabilities were demonstrated for the quantitative extraction of these exogenous lipids using the matrix-matched calibration approach. Likewise, SPME's quantitative capacities were also demonstrated for the quantitation of selected endogenous lipid metabolites in the standard reference sample NIST SRM® 1950 using the standard addition approach, which provided a good quantitative agreement to similar studies on this sample.<sup>99,158,159</sup> Following the study of the SRM® 1950 plasma sample, SPME was effectively employed for the lipidome profiling

using an untargeted approach, which resulted in acceptable qualitative agreement with similar studies on this sample for the major lipid classes and species.<sup>99,159</sup> Chapter 2 also described simple, yet effective, strategies to estimate the distribution coefficient and to construct external calibration curves intended for the quantitative determination of the free concentration of lipid metabolites. Chapter 2, in addition, studied the binding equilibrium existing between fatty acids and serum albumin from a fundamental perspective, taking advantage of SPME's feature: extraction via free concentration.

Chapter 3 explored the direct coupling of SPME and MS for rapid analysis without chromatographic separation. To this end, two recently developed approaches were employed: coated-blade spray (CBS) and microfluidic open interface (MOI). First, the sword-like blade geometry of CBS was examined, with a primary focus on tactics for rapidly desorbing the extracted lipids from plasma. Nevertheless, CBS posed challenges relating to desorption, as relatively long desorption times (>30 s) were required, and the evaporation of desorption solvent resulted in irreproducible spray and unreliable instrumental signals. Consequently, MOI was employed instead, as desorption takes place inside a flow-isolated microfluidic (~5  $\mu$ L) chamber, which provides a more reproducible and reliable instrumental signal, even at >30 s of desorption time. The efficiencies of various desorption solutions were tested for the MOI application, with multiple desorptions being carried out from the same SPME probe. The results revealed that lipids have a very high affinity for C18 coatings, which meant that the tested desorption solvents were unable to desorb most of the extracted analytes from the coating, even after several desorption

steps. In some cases, several lipid analytes were detectable for up to seven consecutive desorptions.

Chapter 4 presented a series of proof-of-concept experiments investigating the extraction and non-destructive optical detection of unsaturated lipids. To this end, Raman spectroscopy was employed to enable the contactless detection of lipids adsorbed onto the surface of the SPME probes. Although MS-based methodologies are known to provide lower limits of detection and quantitation, the coupling of Raman spectroscopy and SPME is a viable alternative method for rapid on-site screening that also offers low solvent consumption and short probe-processing times. The relative lack of selectivity in spectroscopic methods (compared to MS-based methodologies) and the aliphatic (lipid-like) structure in the C18/PAN coating resulted in considerable chemical/structural background, which is an area that will need to be improved upon in future work.

Moreover, SPME is highly amenable to automation and high-throughput analysis, which significantly reduces analysis time and increases sample throughput, while also improving precision through the reduction of human intervention, higher reproducibility in extraction times, and excellent reproducibility in probe positioning within the wells.

### **Future Perspectives**

While this work showed that the proposed SPME-LC-MS/MS method could be applied to determine the free and total concentrations for specific lipids classes, the obtained results could certainly be improved upon either by increasing the method's sensitivity or directing its scope for a smaller pool of biologically relevant analytes. Further expanding the

application of this technology to biochemical/clinical investigations will rely directly on efforts to improve various aspects and investigate its extraction fundamentals.

Another major aspect to explore in future research is the fundamentals that must be considered in selecting a coating and the potential application of newer materials. The kinetics of mass transfer to/from the coating could also be investigated in more depth, particularly for approaches to *shotgun* lipid analysis. Such research could examine whether the mass transfer kinetics for desorption increase for SPME devices with thinner coatings (i.e., the requirement for smaller polymeric particles) and larger surface areas (e.g., larger coatings in thin-film/coated-blade or dispersive format), as well as the effects of the corresponding customization of the desorption chambers (longer chamber for MOI, or controlled atmosphere for CBS). Furthermore, customizing the coating chemistry to enable higher selectivity would result in improved sensitivity, which would be helpful in targeted studies. For instance, silver-doped coatings could enhance the extraction of unsaturated lipids (as has been done for decades in silver chromatography), or HLB particles could be modified to enhance interaction with the polar heads of highly coveted trace lipids (such as PIs, PSs, and PGs).


Samples of biological origin and their inherent complexity continue to pose challenges for emerging analytical technologies, as they often provide unexpected reality checks as they often highlight the limitations of such technologies and areas where improvement is necessary. Focusing on simpler systems can provide a deeper understanding of a method's extraction fundamentals while simultaneously confirming the lipid proxies that mimic

endogenous lipids. Conversely, reducing the complexity of the sample may minimize the relative matrix effects due to lot-to-lot variability (e.g., lipoprotein content, diet influence, health, gender, etc.). While matrix-modification approaches are common in SPME method development, such modifications must ensure analyte stability, enhance relative recovery, and minimize negative impacts. Examples of matrix modifications that could be used to increase selectivity in lipid analysis could include adjusting the pH (e.g., fatty acids, acid trace phospholipids, sphingolipids), controlling the ionic strength (i.e., phosphoserines in cell-containing tissues), altering the volume (e.g., dilution of undesired concomitant polar co-extractants), or adding organic solvents. While a matrix-modification step is not possible for *in vivo* studies, the promising untargeted results obtained via *chemical biopsies* can provide a wealth of information for qualitative and semi-quantitative (as most untargeted studies currently are) exploratory purposes.

It is imperative to develop more sensitive methodologies and instrumentation if the interest in using microextraction techniques to assess free concentrations of lipids persists. While MS has been a cornerstone in this research, multi-disciplinary analysis would enrich the quality of information and provide more sensitive instrumentation (i.e., radiolabelled lipids, labelled lipids, the dreaded derivatization) or shorter timescales (i.e., fluorescence-based fundamental studies on mass transfer kinetics). Ultimately, SPME has proven to be a critical addition to the analytical toolbox for the analysis of small molecules.

## Letters of copyright permission

### For Chapter 2: Towards determination of total and free lipid concentration



**Standard Water Generating Vials for Lipophilic Compounds**  
**Author:** Demet Dincel, Hernando Rosales-Solano, Shakiba Zeinali, et al  
**Publication:** Analytical Chemistry  
**Publisher:** American Chemical Society  
**Date:** Dec 1, 2022  
*Copyright © 2022, American Chemical Society*


**PERMISSION/LICENSE IS GRANTED FOR YOUR ORDER AT NO CHARGE**

This type of permission/license, instead of the standard Terms and Conditions, is sent to you because no fee is being charged for your order. Please note the following:

- Permission is granted for your request in both print and electronic formats, and translations.
- If figures and/or tables were requested, they may be adapted or used in part.
- Please print this page for your records and send a copy of it to your publisher/graduate school.
- Appropriate credit for the requested material should be given as follows: "Reprinted (adapted) with permission from {COMPLETE REFERENCE CITATION}. Copyright {YEAR} American Chemical Society." Insert appropriate information in place of the capitalized words.
- One-time permission is granted only for the use specified in your RightsLink request. No additional uses are granted (such as derivative works or other editions). For any uses, please submit a new request.

If credit is given to another source for the material you requested from RightsLink, permission must be obtained from that source.

[BACK](#) [CLOSE WINDOW](#)



**Investigation of binding of fatty acids to serum albumin to determine free concentrations: Experimental and in-silico approaches**  
**Author:** Mohammad Huq, Hernando Rosales-Solano, Janusz Pawliszyn  
**Publication:** Analytica Chimica Acta  
**Publisher:** Elsevier  
**Date:** 1 February 2022  
*© 2021 Elsevier B.V. All rights reserved.*

**Journal Author Rights**

Please note that, as the author of this Elsevier article, you retain the right to include it in a thesis or dissertation, provided it is not published commercially. Permission is not required, but please ensure that you reference the journal as the original source. For more information on this and on your other retained rights, please visit: <https://www.elsevier.com/about/our-business/policies/copyright#Author-rights>

[BACK](#) [CLOSE WINDOW](#)



## For Chapter 4: Raman as a screening tool for unsaturation for SPME in lipid analysis.



### Profiling of Unsaturated Lipids by Raman Spectroscopy Directly on Solid-Phase Microextraction Probes

**Author:** Hernando Rosales-Solano, Victor Galievsky, Khaled Murtada, et al

**Publication:** Analytical Chemistry

**Publisher:** American Chemical Society

**Date:** Jan 1, 2022

*Copyright © 2022, American Chemical Society*

#### PERMISSION/LICENSE IS GRANTED FOR YOUR ORDER AT NO CHARGE

This type of permission/license, instead of the standard Terms and Conditions, is sent to you because no fee is being charged for your order. Please note the following:

- Permission is granted for your request in both print and electronic formats, and translations.
- If figures and/or tables were requested, they may be adapted or used in part.
- Please print this page for your records and send a copy of it to your publisher/graduate school.
- Appropriate credit for the requested material should be given as follows: "Reprinted (adapted) with permission from {COMPLETE REFERENCE CITATION}. Copyright {YEAR} American Chemical Society." Insert appropriate information in place of the capitalized words.
- One-time permission is granted only for the use specified in your RightsLink request. No additional uses are granted (such as derivative works or other editions). For any uses, please submit a new request.

If credit is given to another source for the material you requested from RightsLink, permission must be obtained from that source.

BACK

CLOSE WINDOW

## References

1. Han, X. Lipids and Lipidomics. in *Lipidomics* 1–20 (John Wiley & Sons, Inc, 2016). doi:10.1002/9781119085263.ch1.
2. The LIPID MAPS Lipidomics Gateway. <http://www.lipidmaps.org/>.
3. Fahy, E. *et al.* A comprehensive classification system for lipids. *J Lipid Res* **46**, 839–862 (2005).
4. Ibarguren, M., López, D. J. & Escribá, P. v. The effect of natural and synthetic fatty acids on membrane structure, microdomain organization, cellular functions and human health. *Biochimica et Biophysica Acta - Biomembranes* vol. 1838 1518–1528 Preprint at <https://doi.org/10.1016/j.bbamem.2013.12.021> (2014).
5. Kerner, J. & Hoppel, C. Fatty acid import into mitochondria. *Biochimica et Biophysica Acta (BBA) - Molecular and Cell Biology of Lipids* **1486**, 1–17 (2000).
6. Schmelzer, K., Fahy, E., Subramaniam, S. & Dennis, E. A. The Lipid Maps Initiative in Lipidomics. *Methods Enzymol* **432**, 171–183 (2007).
7. Fahy, E. *et al.* Update of the LIPID MAPS comprehensive classification system for lipids. *J Lipid Res* **50**, S9–S14 (2009).
8. Dowhan, W. Molecular genetic approaches to defining lipid function. *J Lipid Res* **50 Suppl**, S305–S310 (2009).
9. Ernst, R., Ejsing, C. S. & Antonny, B. Homeoviscous Adaptation and the Regulation of Membrane Lipids. *J Mol Biol* **428**, 4776–4791 (2016).

10. Pike, L. J. Lipid rafts: bringing order to chaos. *J Lipid Res* **44**, 655–67 (2003).
11. Brown, D. A. & London, E. Structure and function of sphingolipid- and cholesterol-rich membrane rafts. *J Biol Chem* **275**, 17221–4 (2000).
12. Hannun, Y. A. & Obeid, L. M. Principles of bioactive lipid signalling: lessons from sphingolipids. *Nat Rev Mol Cell Biol* **9**, 139–150 (2008).
13. Serhan, C. N. & Savill, J. Resolution of inflammation: the beginning programs the end. *Nat Immunol* **6**, 1191–1197 (2005).
14. Chen, C. & Bazan, N. G. Lipid signaling: Sleep, synaptic plasticity, and neuroprotection. *Prostaglandins Other Lipid Mediat* **77**, 65–76 (2005).
15. Aizpurua-Olaizola, O. *et al.* Targeting the endocannabinoid system: future therapeutic strategies. *Drug Discov Today* **22**, 105–110 (2017).
16. Tumanov, S. & Kamphorst, J. J. Recent advances in expanding the coverage of the lipidome. *Curr Opin Biotechnol* **43**, 127–133 (2017).
17. Kraegen, E. W., Cooney, G. J., Ye, J. M., Thompson, A. L. & Furler, S. M. The role of lipids in the pathogenesis of muscle insulin resistance and beta cell failure in type II diabetes and obesity. *Experimental and Clinical Endocrinology & Diabetes* **109**, 189–201 (2001).
18. Kompauer, I. *et al.* Association of fatty acids in serum phospholipids with lung function and bronchial hyperresponsiveness in adults. *Eur J Epidemiol* **23**, 175–190 (2008).

19. Ekroos, K., Jänis, M., Tarasov, K., Hurme, R. & Laaksonen, R. Lipidomics: A tool for studies of atherosclerosis. *Curr Atheroscler Rep* **12**, 273–281 (2010).
20. Ma, Q.-L. *et al.* Omega-3 Fatty Acid Docosahexaenoic Acid Increases SorLA/LR11, a Sorting Protein with Reduced Expression in Sporadic Alzheimer's Disease (AD): Relevance to AD Prevention. *Journal of Neuroscience* **27**, 14299–14307 (2007).
21. Spener, F., Lagarde, M., Geloën, a & Record, M. Editorial: What is lipidomics? *Eur. J. Lipid Sci. Technol* 481–482 (2003) doi:10.1002/ejlt.200390101.
22. Rustam, Y. H. & Reid, G. E. Analytical Challenges and Recent Advances in Mass Spectrometry Based Lipidomics. *Anal Chem* **90**, 374–397 (2018).
23. Hu, C. *et al.* Analytical strategies in lipidomics and applications in disease biomarker discovery. *Journal of Chromatography B* **877**, 2836–2846 (2009).
24. Sethi, S. & Brietzke, E. Recent advances in lipidomics: Analytical and clinical perspectives. *Prostaglandins Other Lipid Mediat* **128–129**, 8–16 (2017).
25. Li, M., Yang, L., Bai, Y. & Liu, H. Analytical Methods in Lipidomics and Their Applications. *Anal Chem* **86**, 161–175 (2014).
26. Fernando, H., Bhopale, K. K., Kondraganti, S., Kaphalia, B. S. & Shakeel Ansari, G. A. Lipidomic changes in rat liver after long-term exposure to ethanol. *Toxicol Appl Pharmacol* **255**, 127–137 (2011).
27. Yang, K. & Han, X. Lipidomics: Techniques, applications, and outcomes related to biomedical sciences. *Trends Biochem Sci* **41**, 954 (2016).

28. Shevchenko, A. & Simons, K. Lipidomics: coming to grips with lipid diversity. *Nature Reviews* **11**, 53–598 (2010).
29. Zhao, Y. Y., Vaziri, N. D. & Lin, R. C. Lipidomics: New Insight Into Kidney Disease. *Adv Clin Chem* **68**, 153–175 (2015).
30. Sandra, K. & Sandra, P. Lipidomics from an analytical perspective. *Curr Opin Chem Biol* **17**, 847–853 (2013).
31. Jurowski, K. *et al.* Comprehensive review of trends and analytical strategies applied for biological samples preparation and storage in modern medical lipidomics: State of the art. *TrAC Trends in Analytical Chemistry* **86**, 276–289 (2017).
32. Teo, C. C. *et al.* Advances in sample preparation and analytical techniques for lipidomics study of clinical samples. *TrAC Trends in Analytical Chemistry* **66**, 1–18 (2015).
33. Bowden, J. A. *et al.* Harmonizing lipidomics: NIST interlaboratory comparison exercise for lipidomics using SRM 1950–Metabolites in Frozen Human Plasma [S]. *J Lipid Res* **58**, 2275–2288 (2017).
34. Matyash, V., Liebisch, G., Kurzchalia, T. v, Shevchenko, A. & Schwudke, D. Lipid extraction by methyl-tert-butyl ether for high-throughput lipidomics. *J Lipid Res* **49**, 1137–46 (2008).
35. Ismaiel, O. A., Zhang, T., Jenkins, R. G. & Karnes, H. T. Investigation of endogenous blood plasma phospholipids, cholesterol and glycerides that contribute

- to matrix effects in bioanalysis by liquid chromatography/mass spectrometry. *Journal of Chromatography B* **878**, 3303–3316 (2010).
36. Trufelli, H., Palma, P., Famiglini, G. & Cappiello, A. An overview of matrix effects in liquid chromatography-mass spectrometry. *Mass Spectrom Rev* **30**, 491–509 (2011).
  37. Orozco-Solano, M., Ruiz-Jiménez, J. & Luque de Castro, M. D. Ultrasound-assisted extraction and derivatization of sterols and fatty alcohols from olive leaves and drupes prior to determination by gas chromatography–tandem mass spectrometry. *J Chromatogr A* **1217**, 1227–1235 (2010).
  38. Herrero, M., Vicente, M. J., Cifuentes, A. & Ibáñez, E. Characterization by high-performance liquid chromatography/electrospray ionization quadrupole time-of-flight mass spectrometry of the lipid fraction of *Spirulina platensis* pressurized ethanol extract. *Rapid Communications in Mass Spectrometry* **21**, 1729–1738 (2007).
  39. Puvaskiene, E., Januskevicius, B., Prichodko, A. & Vickackaite, V. Simultaneous Derivatization and Dispersive Liquid–Liquid Microextraction for Fatty Acid GC Determination in Water. *Chromatographia* **69**, 271–276 (2009).
  40. Horák, T., Čulík, J., Jurková, M., Čejka, P. & Kellner, V. Determination of free medium-chain fatty acids in beer by stir bar sorptive extraction. *J Chromatogr A* **1196–1197**, 96–99 (2008).

41. Meng, Y., Pino, V. & Anderson, J. L. Exploiting the Versatility of Ionic Liquids in Separation Science: Determination of Low-Volatility Aliphatic Hydrocarbons and Fatty Acid Methyl Esters Using Headspace Solid-Phase Microextraction Coupled to Gas Chromatography. *Anal Chem* **81**, 7107–7112 (2009).
42. Bogusz, S. *et al.* Solid-phase microextraction combined with comprehensive two-dimensional gas chromatography for fatty acid profiling of cell wall phospholipids. *J Sep Sci* **35**, 2438–2444 (2012).
43. Birjandi, A. P., Mirnaghi, F. S., Bojko, B., Wasowicz, M. & Pawliszyn, J. Application of solid phase microextraction for quantitation of polyunsaturated fatty acids in biological fluids. *Anal Chem* **86**, 12022–12029 (2014).
44. Myher, J. J. & Kuksis, A. General strategies in chromatographic analysis of lipids. *J Chromatogr B Biomed Sci Appl* **671**, 3–33 (1995).
45. Cajka, T. & Fiehn, O. Comprehensive analysis of lipids in biological systems by liquid chromatography-mass spectrometry. *TrAC Trends in Analytical Chemistry* **61**, 192–206 (2014).
46. Li, M., Yang, L., Bai, Y. & Liu, H. Analytical methods in lipidomics and their applications. *Anal Chem* **86**, 161–175 (2014).
47. Wang, M., Wang, C. & Han, X. Selection of internal standards for accurate quantification of complex lipid species in biological extracts by electrospray

- ionization mass spectrometry—What, how and why? *Mass Spectrom Rev* **36**, 693–714 (2017).
48. Fuchs, B., Süß, R., Teuber, K., Eibisch, M. & Schiller, J. Lipid analysis by thin-layer chromatography—A review of the current state. *J Chromatogr A* **1218**, 2754–2774 (2011).
  49. Donato, P., Inferrera, V., Sciarrone, D. & Mondello, L. Supercritical fluid chromatography for lipid analysis in foodstuffs. *J Sep Sci* **40**, 361–382 (2017).
  50. Mondello, L. *et al.* Silver-ion reversed-phase comprehensive two-dimensional liquid chromatography combined with mass spectrometric detection in lipidic food analysis. *J Chromatogr A* **1086**, 91–98 (2005).
  51. Sandra, P., Medvedovici, A., Zhao, Y. & David, F. Characterization of triglycerides in vegetable oils by silver-ion packed-column supercritical fluid chromatography coupled to mass spectroscopy with atmospheric pressure chemical ionization and coordination ion spray. *J Chromatogr A* **974**, 231–241 (2002).
  52. Dobson, Gary; Christie, William W.; Nikolova-Damyanova, B. Silver ion chromatography of lipids and fatty acids. *J Chromatogr B Biomed Sci Appl* **671**, 197–222 (1995).
  53. Lintonen, T. P. I. *et al.* Differential mobility spectrometry-driven shotgun lipidomics. *Anal Chem* **86**, 9662–9669 (2014).



54. Paglia, G., Kliman, M., Claude, E., Geromanos, S. & Astarita, G. Applications of ion-mobility mass spectrometry for lipid analysis. *Anal Bioanal Chem* **407**, 4995–5007 (2015).
55. Wang, M. & Han, X. Multidimensional mass spectrometry-based shotgun lipidomics. *Methods in Molecular Biology* **1198**, 203–220 (2014).
56. Li, M., Yang, L., Bai, Y. & Liu, H. Analytical Methods in Lipidomics and Their Applications. *Anal Chem* **86**, 161–175 (2013).
57. Jung, H. R. *et al.* High throughput quantitative molecular lipidomics. *Biochimica et Biophysica Acta (BBA) - Molecular and Cell Biology of Lipids* **1811**, 925–934 (2011).
58. Wang, M., Wang, C. & Han, X. Selection of internal standards for accurate quantification of complex lipid species in biological extracts by electrospray ionization mass spectrometry—What, how and why? *Mass Spectrom Rev* **36**, 693–714 (2017).
59. Li, M., Yang, L., Bai, Y. & Liu, H. Analytical methods in lipidomics and their applications. *Anal Chem* **86**, 161–175 (2014).
60. Paglia, G., Kliman, M., Claude, E., Geromanos, S. & Astarita, G. Applications of ion-mobility mass spectrometry for lipid analysis. *Anal Bioanal Chem* **407**, 4995–5007 (2015).

61. Hinz, C., Liggi, S. & Griffin, J. L. The potential of Ion Mobility Mass Spectrometry for high-throughput and high-resolution lipidomics. *Curr Opin Chem Biol* **42**, 42–50 (2018).
62. Kliman, M., May, J. C. & McLean, J. A. Lipid analysis and lipidomics by structurally selective ion mobility-mass spectrometry. *Biochimica et Biophysica Acta (BBA) - Molecular and Cell Biology of Lipids* **1811**, 935–945 (2011).
63. Bisht, B. *et al.* The potential of nuclear magnetic resonance (NMR) in metabolomics and lipidomics of microalgae- a review. *Arch Biochem Biophys* **710**, 108987 (2021).
64. Czamara, K. *et al.* Raman spectroscopy of lipids: A review. *Journal of Raman Spectroscopy* vol. 46 4–20 Preprint at <https://doi.org/10.1002/jrs.4607> (2015).
65. Mahadevan-Jansen, A. & Richards-Kortum, R. Raman spectroscopy for cancer detection: a review. *Annual International Conference of the IEEE Engineering in Medicine and Biology - Proceedings* **6**, 2722–2728 (1997).
66. Pawliszyn, J. Solid-Phase Microextraction in Perspective. in *Handbook of Solid Phase Microextraction* 1–12 (Elsevier, 2012). doi:10.1016/B978-0-12-416017-0.00001-2.
67. Ouyang, G. Calibration. in *Handbook of Solid Phase Microextraction* 167–199 (Elsevier, 2012). doi:10.1016/B978-0-12-416017-0.00006-1.

68. Pawliszyn, J. Theory of Solid-Phase Microextraction. in *Handbook of Solid Phase Microextraction* 13–59 (Elsevier, 2012). doi:10.1016/B978-0-12-416017-0.00002-4.
69. Vuckovic, D., Cudjoe, E., Musteata, F. M. & Pawliszyn, J. Automated solid-phase microextraction and thin-film microextraction for high-throughput analysis of biological fluids and ligand–receptor binding studies. *Nat Protoc* **5**, 140–161 (2010).
70. Reyes-Garcés, N. *et al.* Advances in Solid Phase Microextraction and Perspective on Future Directions. *Anal Chem* **90**, 302–360 (2018).
71. Chen, Y. & Pawliszyn, J. Kinetics and the on-site application of standards in a solid-phase microextraction fiber. *Anal Chem* **76**, 5807–5815 (2004).
72. Ai, J. Solid Phase Microextraction for Quantitative Analysis in Nonequilibrium Situations. *Anal Chem* **69**, 1230–1236 (1997).
73. Lord, H. & Pawliszyn, J. Evolution of solid-phase microextraction technology. *J Chromatogr A* **885**, 153–193 (2000).
74. Musteata, M. L., Musteata, F. M. & Pawliszyn, J. Biocompatible solid-phase microextraction coatings based on polyacrylonitrile and solid-phase extraction phases. *Anal Chem* **79**, 6903–6911 (2007).
75. Mousavi, F., Gionfriddo, E., Carasek, E., Souza-Silva, E. A. & Pawliszyn, J. Coupling solid phase microextraction to complementary separation platforms for

- metabotyping of *E. coli* metabolome in response to natural antibacterial agents. *Metabolomics* **12**, 169 (2016).
76. Gionfriddo, E., Boyacı, E. & Pawliszyn, J. New Generation of Solid-Phase Microextraction Coatings for Complementary Separation Approaches: A Step toward Comprehensive Metabolomics and Multiresidue Analyses in Complex Matrices. *Anal Chem* **89**, 4046–4054 (2017).
77. Gómez-Ríos, G. A., Reyes-Garcés, N., Bojko, B. & Pawliszyn, J. Biocompatible Solid-Phase Microextraction Nanoelectrospray Ionization: An Unexploited Tool in Bioanalysis. *Anal Chem* **88**, 1259–1265 (2016).
78. Vuckovic, D. *et al.* In Vivo Solid-Phase Microextraction: Capturing the Elusive Portion of Metabolome. *Angewandte Chemie International Edition* **50**, 5344–5348 (2011).
79. Alam, Md. N. & Pawliszyn, J. Effect of Binding Components in Complex Sample Matrices on Recovery in Direct Immersion Solid-Phase Microextraction: Friends or Foe? *Anal Chem* **90**, 2430–2433 (2018).
80. Birjandi, A. P., Bojko, B., Ning, Z., Figeys, D. & Pawliszyn, J. High throughput solid phase microextraction: A new alternative for analysis of cellular lipidome? *Journal of Chromatography B* **1043**, 12–19 (2017).

81. Garwolińska, D. *et al.* Rapid Characterization of the Human Breast Milk Lipidome Using a Solid-Phase Microextraction and Liquid Chromatography – Mass Spectrometry-Based Approach. *J Proteome Res* **16**, 3200–3208 (2017).
82. Alnajim, I. *et al.* New Method of Analysis of Lipids in *Tribolium castaneum* (Herbst) and *Rhyzopertha dominica* (Fabricius) Insects by Direct Immersion Solid-Phase Microextraction (DI-SPME) Coupled with GC–MS. *Insects 2019, Vol. 10, Page 363* **10**, 363 (2019).
83. Lendor, S. *et al.* Investigation of Early Death-Induced Changes in Rat Brain by Solid Phase Microextraction via Untargeted High Resolution Mass Spectrometry: In Vivo versus Postmortem Comparative Study. *ACS Chem Neurosci* **11**, 1827–1840 (2020).
84. Reyes-Garcés, N. *et al.* In vivo brain sampling using a microextraction probe reveals metabolic changes in rodents after deep brain stimulation. *Anal Chem* **91**, 9875–9884 (2019).
85. Napylov, A. *et al.* In Vivo Solid-Phase Microextraction for Sampling of Oxylipins in Brain of Awake, Moving Rats. *Angewandte Chemie International Edition* **59**, 2392–2398 (2020).
86. Boyaci, E. *et al.* Comprehensive Investigation of Metabolic Changes Occurring in the Rat Brain Hippocampus after Fluoxetine Administration Using Two Complementary in Vivo Techniques: Solid Phase Microextraction and Microdialysis. *ACS Chem Neurosci* **11**, 3749–3760 (2020).

87. Roszkowska, A. *et al.* Tissue storage affects lipidome profiling in comparison to in vivo microsampling approach. *Scientific Reports 2018 8:1* **8**, 1–10 (2018).
88. Deng, J. *et al.* Surface-Coated Probe Nanoelectrospray Ionization Mass Spectrometry for Analysis of Target Compounds in Individual Small Organisms. *Anal Chem* **87**, 9923–9930 (2015).
89. Deng, J. *et al.* Biocompatible Surface-Coated Probe for in Vivo, in Situ, and Microscale Lipidomics of Small Biological Organisms and Cells Using Mass Spectrometry. *Anal Chem* **90**, 6936–6944 (2018).
90. Olkowicz, M., Rosales-Solano, H., Kulasingam, V. & Pawliszyn, J. SPME-LC/MS-based serum metabolomic phenotyping for distinguishing ovarian cancer histologic subtypes: a pilot study. *Scientific Reports 2021 11:1* **11**, 1–14 (2021).
91. Olkowicz, M. *et al.* The metabolic fate of oxaliplatin in the biological milieu investigated during in vivo lung perfusion using a unique miniaturized sampling approach based on solid-phase microextraction coupled with liquid chromatography-mass spectrometry. *Front Cell Dev Biol* **10**, (2022).
92. Bojko, B. *et al.* Solid phase microextraction chemical biopsy tool for monitoring of doxorubicin residue during in vivo lung chemo-perfusion. *J Pharm Anal* **11**, 37–47 (2021).
93. Silva, C. L., Perestrelo, R., Silva, P., Tomás, H. & Câmara, J. S. Implementing a central composite design for the optimization of solid phase microextraction to

- establish the urinary volatome expression: a first approach for breast cancer. *Metabolomics* **15**, 1–13 (2019).
94. Ma, M. Y., Yu, L. Q., Wang, S. W., Meng, Y. & Lv, Y. K. Hybrid ZIF-8-90 for Selective Solid-Phase Microextraction of Exhaled Breath from Gastric Cancer Patients. *ACS Appl Bio Mater* **4**, 3608–3613 (2021).
  95. Bogusiewicz, J. *et al.* Profiling of Carnitine Shuttle System Intermediates in Gliomas Using Solid-Phase Microextraction (SPME). *Molecules* 2021, Vol. 26, Page 6112 **26**, 6112 (2021).
  96. Proitsi, P. *et al.* Association of blood lipids with Alzheimer's disease: A comprehensive lipidomics analysis. *Alzheimer's and Dementia* **13**, 140–151 (2017).
  97. Rodenburg, K. W. & van der Horst, D. J. Lipoprotein-mediated lipid transport in insects: Analogy to the mammalian lipid carrier system and novel concepts for the functioning of LDL receptor family members. *Biochimica et Biophysica Acta (BBA) - Molecular and Cell Biology of Lipids* **1736**, 10–29 (2005).
  98. Jonas, A. & Phillips, M. C. Lipoprotein structure. in *Biochemistry of Lipids, Lipoproteins and Membranes*. (eds. Vance, D. E. & Vance, J. E.) vol. 36 485–506 (Elsevier, 2008).
  99. Quehenberger, O. *et al.* Lipidomics reveals a remarkable diversity of lipids in human plasma. *J Lipid Res* **51**, 3299–3305 (2010).

100. Pajand Birjandi, A. Application of Solid Phase Microextraction for Lipid Analysis and Lipidomics. (University of Waterloo, 2016).
101. Grandy, J. J., Singh, V., Lashgari, M., Gauthier, M. & Pawliszyn, J. Development of a Hydrophilic Lipophilic Balanced Thin Film Solid Phase Microextraction Device for Balanced Determination of Volatile Organic Compounds. *Anal Chem* **90**, 14072–14080 (2018).
102. Gómez-Ríos, G. A. *et al.* Quantitative analysis of biofluid spots by coated blade spray mass spectrometry, a new approach to rapid screening. *Sci Rep* **7**, 16104 (2017).
103. Khaled, A. Automated High-throughput Analysis of Multi-class Multi-residue Pharmaceutical Drugs in Animal Tissue Using Solid Phase Microextraction. (2020).
104. Brinker, C. J., Frye, G. C., Hurd, A. J. & Ashley, C. S. Fundamentals of sol-gel dip coating. *Thin Solid Films* **201**, 97–108 (1991).
105. Jurowski, K. *et al.* Comprehensive review of trends and analytical strategies applied for biological samples preparation and storage in modern medical lipidomics: State of the art. *TrAC Trends in Analytical Chemistry* **86**, 276–289 (2017).
106. Monnin, C., Ramrup, P., Daigle-Young, C. & Vuckovic, D. Improving negative liquid chromatography/electrospray ionization mass spectrometry lipidomic analysis of human plasma using acetic acid as a mobile-phase additive. *Rapid Communications in Mass Spectrometry* **32**, 201–211 (2018).



107. Matuszewski, B. K., Constanzer, M. L. & Chavez-Eng, C. M. Strategies for the assessment of matrix effect in quantitative bioanalytical methods based on HPLC-MS/MS. *Anal Chem* **75**, 3019–3030 (2003).
108. Chambers, M. C. *et al.* A cross-platform toolkit for mass spectrometry and proteomics. *Nature Biotechnology* *2012 30:10* **30**, 918–920 (2012).
109. Libiseller, G. *et al.* IPO: A tool for automated optimization of XCMS parameters. *BMC Bioinformatics* **16**, 1–10 (2015).
110. Smith, C. A., Want, E. J., O’Maille, G., Abagyan, R. & Siuzdak, G. XCMS: Processing mass spectrometry data for metabolite profiling using nonlinear peak alignment, matching, and identification. *Anal Chem* **78**, 779–787 (2006).
111. R: The R Project for Statistical Computing. <https://www.r-project.org/>.
112. Uppal, K., Walker, D. I. & Jones, D. P. xMSannotator: An R package for network-based annotation of high-resolution metabolomics data. *Anal Chem* **89**, 1063–1067 (2017).
113. Smith, C. A. *et al.* METLIN: A metabolite mass spectral database. *Ther Drug Monit* **27**, 747–751 (2005).
114. Liebisch, G. *et al.* Shorthand notation for lipid structures derived from mass spectrometry. *J Lipid Res* **54**, 1523–1530 (2013).
115. Holčápek, M. Lipidomics. *Anal Bioanal Chem* **407**, 4971–4972 (2015).

116. Reyes-Garcés, N. *et al.* Assessment of solid phase microextraction as a sample preparation tool for untargeted analysis of brain tissue using liquid chromatography-mass spectrometry. *J Chromatogr A* **1638**, 461862 (2021).
117. Yang, W. C., Adamec, J. & Regnier, F. E. Enhancement of the LC/MS analysis of fatty acids through derivatization and stable isotope coding. *Anal Chem* **79**, 5150–5157 (2007).
118. Dei Cas, M. *et al.* A straightforward LC-MS/MS analysis to study serum profile of short and medium chain fatty acids. *Journal of Chromatography B* **1154**, 121982 (2020).
119. Dimitrios Tsikas, Alexandre A. Zoerner, Anja Mitschke, F.-M. G. Nitro-fatty Acids Occur in Human Plasma in the Picomolar Range: a Targeted Nitro-lipidomics GC – MS / MS Study. *Lipids* **44**, 855–865 (2009).
120. Risticvic, S., Lord, H., Górecki, T., Arthur, C. L. & Pawliszyn, J. Protocol for solid-phase microextraction method development. *Nat Protoc* **5**, 122–139 (2010).
121. Antonietti, M. & Förster, S. Vesicles and Liposomes: A Self-Assembly Principle Beyond Lipids. *Advanced Materials* **15**, 1323–1333 (2003).
122. Kudlejova, L., Risticvic, S. & Vuckovic, D. Solid-Phase Microextraction Method Development. in *Handbook of Solid Phase Microextraction* 174–211 (2012).
123. Birjandi, A. P. Application of Solid Phase Microextraction for Lipid Analysis and Lipidomics. (University of Waterloo, 2015).

124. Reyes-Garcés, N., Bojko, B. & Pawliszyn, J. High throughput quantification of prohibited substances in plasma using thin film solid phase microextraction. *J Chromatogr A* **1374**, 40–49 (2014).
125. Wylie Nichols, J. Phospholipid Transfer between Phosphatidylcholine-Taurocholate Mixed Micelles"1". *Proc. Natl. Acad. Sci. U.S.A* **27**, 93–101 (1988).
126. Nakagawa, T. Critical examination of published data concerning the rate of micelle dissociation and proposal of a new interpretation. *Colloid and Polymer Science Kolloid Zeitschrift & Zeitschrift für Polymere* **252**, 56–64 (1974).
127. Illingworth, D. R. & Portman, O. W. Exchange of phospholipids between low and high density lipoproteins of squirrel monkeys. *Journal Lipid Research* **13**, 220–227 (1972).
128. Wirtz, K. W. A. Transfer of phospholipids between membrane. *Biochimica et Biophysica Acta (BBA) - Reviews on Biomembranes* **344**, 95–117 (1974).
129. Smith, R. & Tanford, C. The critical micelle concentration of 1- $\alpha$ -dipalmitoylphosphatidylcholine in water and water/methanol solutions. *J Mol Biol* **67**, 75–83 (1972).
130. Li, Z., Mintzer, E. & Bittman, R. The critical micelle concentrations of lysophosphatidic acid and sphingosylphosphorylcholine. *Chem Phys Lipids* **130**, 197–201 (2004).

131. Kol, M. A., De Kruijff, B. & De Kroon, A. I. P. M. Phospholipid flip-flop in biogenic membranes: what is needed to connect opposite sides. *Semin Cell Dev Biol* **13**, 163–170 (2002).
132. Chan, D. C. *et al.* Apolipoprotein B-100 and ApoA-II Kinetics as Determinants of Cellular Cholesterol Efflux. *J Clin Endocrinol Metab* **97**, E1658–E1666 (2012).
133. Gonzalez, C. A. & Choquette, S. J. Certificate of Analysis Standard Reference Material □ 1950 Metabolites in Frozen Human Plasma.
134. Lange, M. & Fedorova, M. Evaluation of lipid quantification accuracy using HILIC and RPLC MS on the example of NIST® SRM® 1950 metabolites in human plasma. *Anal Bioanal Chem* **412**, 3573–3584 (2020).
135. Ulmer, C. Z. *et al.* LipidQC: Method Validation Tool for Visual Comparison to SRM 1950 Using NIST Interlaboratory Comparison Exercise Lipid Consensus Mean Estimate Values. *Anal Chem* **89**, 13069–13073 (2017).
136. Lange, M. & Fedorova, M. Evaluation of lipid quantification accuracy using HILIC and RPLC MS on the example of NIST® SRM® 1950 metabolites in human plasma. *Anal Bioanal Chem* **412**, 3573–3584 (2020).
137. Reyes-Garcés, N., Alam, M. N. & Pawliszyn, J. The effect of hematocrit on solid-phase microextraction. *Anal Chim Acta* **1001**, 40–50 (2018).

138. Boyacı, E. *et al.* High-throughput analysis using non-depletive SPME: challenges and applications to the determination of free and total concentrations in small sample volumes. *Sci Rep* **8**, 1167 (2018).
139. Zhang, X. *et al.* Pre-equilibrium solid-phase microextraction of free analyte in complex samples: Correction for mass transfer variation from protein binding and matrix tortuosity. *Anal Chem* **83**, 3365–3370 (2011).
140. Gómez-Ríos, G. A. *et al.* Rapid determination of immunosuppressive drug concentrations in whole blood by coated blade spray-tandem mass spectrometry (CBS-MS/MS). *Anal Chim Acta* **999**, 69–75 (2018).
141. Khaled, A., Gómez-Ríos, G. A. & Pawliszyn, J. Optimization of Coated Blade Spray for Rapid Screening and Quantitation of 105 Veterinary Drugs in Biological Tissue Samples. *Anal Chem* **92**, 5937–5943 (2020).
142. Gómez-Ríos, G. A. *et al.* Quantitative analysis of biofluid spots by coated blade spray mass spectrometry, a new approach to rapid screening. *Scientific Reports* **2017** *7:1* **7**, 1–7 (2017).
143. Boyacı, E. & Pawliszyn, J. Micelle assisted thin-film solid phase microextraction: A new approach for determination of quaternary ammonium compounds in environmental samples. *Anal Chem* **86**, 8916–8921 (2014).

144. Trufelli, H., Palma, P., Famiglioni, G. & Cappiello, A. An overview of matrix effects in liquid chromatography–mass spectrometry. *Mass Spectrom Rev* **30**, 491–509 (2011).
145. Taylor, P. J. Matrix effects: the Achilles heel of quantitative high-performance liquid chromatography–electrospray–tandem mass spectrometry. *Clin Biochem* **38**, 328–334 (2005).
146. Rickert, D. A. *et al.* Evaluation of a coated blade spray-tandem mass spectrometry assay as a new tool for the determination of immunosuppressive drugs in whole blood. *Anal Bioanal Chem* **412**, 5067–5076 (2020).
147. Alam, M. N., Ricardez-Sandoval, L. & Pawliszyn, J. Calibrant Free Sampling and Enrichment with Solid-Phase Microextraction: Computational Simulation and Experimental Verification. *Ind Eng Chem Res* **56**, 3679–3686 (2017).
148. Adalsteinsson, T. & Yu, H. Lipid lateral diffusion in multi-bilayers, and in monolayers at the air/water and heptane/water interfaces. *Langmuir* **16**, 9410–9413 (2000).
149. Walder, R. B., Honciuc, A. & Schwartz, D. K. Phospholipid diffusion at the oil-water interface. *Journal of Physical Chemistry B* **114**, 11484–11488 (2010).
150. Negishi, M., Seto, H., Hase, M. & Yoshikawa, K. How does the mobility of phospholipid molecules at a water/oil interface reflect the viscosity of the surrounding oil? *Langmuir* **24**, 8431–8434 (2008).

151. O Quehenberger, E. D. The human plasma lipidome. *N Engl J Med* **365**, 1812–1823 (2011).
152. Ouyang, G. & Pawliszyn, J. A critical review in calibration methods for solid-phase microextraction. *Anal Chim Acta* **627**, 184–197 (2008).
153. Contrepois, K. *et al.* Cross-Platform Comparison of Untargeted and Targeted Lipidomics Approaches on Aging Mouse Plasma. *Sci Rep* **8**, (2018).
154. Cajka, T. & Fiehn, O. Toward Merging Untargeted and Targeted Methods in Mass Spectrometry-Based Metabolomics and Lipidomics. *Anal Chem* **88**, 524–545 (2016).
155. Lam, S. M., Tian, H. & Shui, G. Lipidomics, en route to accurate quantitation. *Biochimica et Biophysica Acta (BBA) - Molecular and Cell Biology of Lipids* **1862**, 752–761 (2017).
156. Navas-Iglesias, N., Carrasco-Pancorbo, A. & Cuadros-Rodríguez, L. From lipids analysis towards lipidomics, a new challenge for the analytical chemistry of the 21st century. Part II: Analytical lipidomics. **28**, 393–403 (2009).
157. Aristizabal Henao, J. J., Bradley, R. M., Duncan, R. E. & Stark, K. D. Categorizing and qualifying nutritional lipidomic data: Defining brutto, medio, genio, and infinio lipid species within macrolipidomics and microlipidomics. *Curr Opin Clin Nutr Metab Care* **21**, 352–359 (2018).

158. Steckel, K. E. Characterization of the Human Plasma Macrolipidome using Standard Reference Material 1950-Metabolites in frozen human plasma. (University of Waterloo, 2021).
159. Bowden, J. A., Jones, C. & Koelmel, J. Harmonizing Lipidomics: NIST Interlaboratory Comparison Exercise for Lipidomics using Standard Reference Material 1950 Metabolites in Frozen Human Plasma Lipidomics View project Proteometabolomics of Melphalan Resistance in Multiple Myeloma View project. *Article in Journal of Lipid Research* (2017) doi:10.1194/jlr.M079012.
160. Booij, K. *et al.* Passive Sampling in Regulatory Chemical Monitoring of Nonpolar Organic Compounds in the Aquatic Environment. *Environ Sci Technol* **50**, 3–17 (2016).
161. Musteata, F. M. Monitoring free drug concentrations: Challenges. *Bioanalysis* **3**, 1753–1768 (2011).
162. Chianese, S., Fenti, A., Iovino, P., Musmarra, D. & Salvestrini, S. Sorption of Organic Pollutants by Humic Acids: A Review. *Molecules* 2020, Vol. 25, Page 918 **25**, 918 (2020).
163. Chan, W. L., Carrell, R. W., Zhou, A. & Read, R. J. How Changes in Affinity of Corticosteroid-binding Globulin Modulate Free Cortisol Concentration. *J Clin Endocrinol Metab* **98**, 3315–3322 (2013).



164. Fujiwara, S. I. & Amisaki, T. Fatty acid binding to serum albumin: Molecular simulation approaches. *Biochimica et Biophysica Acta (BBA) - General Subjects* **1830**, 5427–5434 (2013).
165. Drisaldi, A. *et al.* Accuracy of Valproic Acid Concentration Correction Based on Serum Albumin. *Neurocrit Care* **30**, 301–306 (2019).
166. Bouillon, R., van Assche, F. A., van Baelen, H., Heyns, W. & de Moor, P. Influence of the Vitamin D-binding Protein on the Serum Concentration of 1,25-Dihydroxyvitamin D<sub>3</sub>: SIGNIFICANCE OF THE FREE 1,25-DIHYDROXYVITAMIN D<sub>3</sub> CONCENTRATION. *J Clin Invest* **67**, 589–596 (1981).
167. Avery, L. B., Sacktor, N., McArthur, J. C. & Hendrix, C. W. Protein-free efavirenz concentrations in cerebrospinal fluid and blood plasma are equivalent: Applying the law of mass action to predict protein-free drug concentration. *Antimicrob Agents Chemother* **57**, 1409–1414 (2013).
168. Nagel, S. C., vom Saal, F. S. & Welshons, W. v. The Effective Free Fraction of Estradiol and Xenoestrogens in Human Serum Measured by Whole Cell Uptake Assays: Physiology of Delivery Modifies Estrogenic Activity. <https://doi.org/10.3181/00379727-217-44236> **217**, 300–309 (2017).

169. Kurz, H., Trunk, H. & Weitz, B. Evaluation of methods to determine protein-binding of drugs. Equilibrium dialysis, ultrafiltration, ultracentrifugation, gel filtration. *Arzneimittelforschung* **27**, 1373–1380 (1977).
170. Svensson, C. K., Woodruff, M. N., Baxter, J. G. & Lalka, D. Free Drug Concentration Monitoring in Clinical Practice. *Clinical Pharmacokinetics* 1986 **11**:6 **11**, 450–469 (2012).
171. Vuignier, K., Schappler, J., Veuthey, J. L., Carrupt, P. A. & Martel, S. Drug-protein binding: A critical review of analytical tools. *Anal Bioanal Chem* **398**, 53–66 (2010).
172. Haes, A. J., Zou, S., Schatz, G. C. & van Duyne, R. P. A nanoscale optical biosensor: The long range distance dependence of the localized surface plasmon resonance of noble metal nanoparticles. *Journal of Physical Chemistry B* **108**, 109–116 (2004).
173. Bjelić, S. & Jelesarov, I. A survey of the year 2007 literature on applications of isothermal titration calorimetry. *Journal of Molecular Recognition* **21**, 289–312 (2008).
174. Holdgate, G. A. & Ward, W. H. J. Measurements of binding thermodynamics in drug discovery. *Drug Discov Today* **10**, 1543–1550 (2005).
175. Meza-Sánchez, D. E., Maravillas-Montero, J. L. & Luis Maravillas-Montero, J. Clinical and Biomedical Applications of Surface Plasmon Resonance Systems. doi:10.24875/RIC.18002754.

176. Heringa, M. B. & Hermens, J. L. M. Measurement of free concentrations using negligible depletion-solid phase microextraction (nd-SPME). *TrAC Trends in Analytical Chemistry* **22**, 575–587 (2003).
177. Vaes, W. H. J., Urrestarazu Ramos, E., Verhaar, H. J. M., Seinen, W. & Hermens, J. L. M. Measurement of the free concentration using solid-phase microextraction: Binding to protein. *Anal Chem* **68**, 4463–4467 (1996).
178. Musteata, F. M. Monitoring free drug concentrations: challenges. <http://dx.doi.org/10.4155/bio.11.187> **3**, 1753–1768 (2011).
179. Seyfinejad, B., Ozkan, S. A. & Jouyban, A. Recent advances in the determination of unbound concentration and plasma protein binding of drugs: Analytical methods. *Talanta* **225**, 122052 (2021).
180. Patzer, J. Principles of Bound Solute Dialysis. *Therapeutic Apheresis and Dialysis* **10**, 118–124 (2006).
181. Banker, M. J., Clark, T. H. & Williams, J. A. Development and validation of a 96-well equilibrium dialysis apparatus for measuring plasma protein binding. *J Pharm Sci* **92**, 967–974 (2003).
182. Barre, J., Chamouard, J. M., Houin, G. & Tillement, J. P. Equilibrium dialysis, ultrafiltration, and ultracentrifugation compared for determining the plasma-protein-binding characteristics of valproic acid. *Clin Chem* **31**, 60–64 (1985).

183. Landrum, P. F., Nihart, S. R., Eadle, B. J. & Gardner, W. S. Reverse-Phase Separation Method for Determining Pollutant Binding to Aldrich Humic Acid and Dissolved Organic Carbon of Natural Waters. *Environ Sci Technol* **18**, 187–192 (1984).
184. Lagercrantz, C., Larsson, T. & Karlsson, H. Binding of some fatty acids and drugs to immobilized bovine serum albumin studied by column affinity chromatography. *Anal Biochem* **99**, 352–364 (1979).
185. Rawel, H. M., Meidtner, K. & Kroll, J. Binding of selected phenolic compounds to proteins. *J Agric Food Chem* **53**, 4228–4235 (2005).
186. Khodarahmi, R. *et al.* Comparative spectroscopic studies on drug binding characteristics and protein surface hydrophobicity of native and modified forms of bovine serum albumin: Possible relevance to change in protein structure/function upon non-enzymatic glycation. *Spectrochim Acta A Mol Biomol Spectrosc* **89**, 177–186 (2012).
187. Perozzo, R., Folkers, G. & Scapozza, L. Thermodynamics of Protein–Ligand Interactions: History, Presence, and Future Aspects. <http://dx.doi.org/10.1081/RRS-120037896> **24**, 1–52 (2009).
188. Holdgate, G. A. & Ward, W. H. J. Measurements of binding thermodynamics in drug discovery. *Drug Discov Today* **10**, 1543–1550 (2005).

189. Kraak, J. C., Busch, S. & Poppe, H. Study of protein-drug binding using capillary zone electrophoresis. *J Chromatogr A* **608**, 257–264 (1992).
190. Chu, Y. H., Avila, L. Z., Biebuyck, H. A. & Whitesides, G. M. Use of Affinity Capillary Electrophoresis To Measure Binding Constants of Ligands to Proteins. *J Med Chem* **35**, 2915–2917 (1992).
191. Ahmad, S., Baker, D., Murnane, D., Spooner, N. & Gerhard, U. Solid-phase microextraction for assessment of plasma protein binding, a complement to rapid equilibrium dialysis. *Bioanalysis* **13**, 1101–1111 (2021).
192. Huq, M., Rosales-Solano, H. & Pawliszyn, J. Investigation of binding of fatty acids to serum albumin to determine free concentrations: Experimental and in-silico approaches. *Anal Chim Acta* **1192**, 339370 (2022).
193. Musteata, F. M. & Pawliszyn, J. Study of ligand-receptor binding using SPME: Investigation of receptor, free, and total ligand concentrations. *J Proteome Res* **4**, 789–800 (2005).
194. Górecki, T. & Pawliszyn, J. Effect of sample volume on quantitative analysis by solid-phase microextraction: Part 1. Theoretical considerations. *Analyst* **122**, 1079–1086 (1997).
195. Parkerton, T. F., Stone, M. A. & Letinski, D. J. Assessing the aquatic toxicity of complex hydrocarbon mixtures using solid phase microextraction. *Toxicol Lett* **112–113**, 273–282 (2000).

196. Grandy, J. J., Boyaci, E. & Pawliszyn, J. Development of a Carbon Mesh Supported Thin Film Microextraction Membrane As a Means to Lower the Detection Limits of Benchtop and Portable GC/MS Instrumentation. *Anal Chem* **88**, 1760–1767 (2016).
197. Zeinali, S., Natalia Wieczorek, M. & Pawliszyn, J. Free versus droplet-bound aroma compounds in sparkling beverages. *Food Chem* **378**, 131985 (2022).
198. Wieczorek, M. N., Zhou, W. & Pawliszyn, J. Sequential thin film-solid phase microextraction as a new strategy for addressing displacement and saturation effects in food analysis. *Food Chem* **389**, 133038 (2022).
199. de Jager, L. & Andrews, A. R. J. Development of a screening method for cocaine and cocaine metabolites in saliva using hollow fiber membrane solvent microextraction. *Anal Chim Acta* **458**, 311–320 (2002).
200. Jeannot, M. A. & Cantwell, F. F. Solvent Microextraction as a Speciation Tool: Determination of Free Progesterone in a Protein Solution. *Anal Chem* **69**, 2935–2940 (1997).
201. Cárdenas-Soracá, D. M., Tucca, F. I., Mardones-Peña, C. A. & Barra-Ríos, R. O. Development of an analytical methodology for the determination of organochlorine pesticides by ethylene-vinyl acetate passive samplers in marine surface waters based on ultrasound-assisted solvent extraction followed with headspace solid-phase microextraction and gas chromatography-tandem mass spectrometry. *J Chromatogr A* **1605**, 360341 (2019).

202. Hassani, S. A., Lendor, S., Boyaci, E., Pawliszyn, J. & Womelsdorf, T. Multineuromodulator measurements across fronto-striatal network areas of the behaving macaque using solid-phase microextraction. *J Neurophysiol* **122**, 1649–1660 (2019).
203. Hassani, S. A. *et al.* Dose-Dependent Dissociation of Pro-cognitive Effects of Donepezil on Attention and Cognitive Flexibility in Rhesus Monkeys. *Biological Psychiatry Global Open Science* (2021) doi:10.1016/J.BPSGOS.2021.11.012.
204. Gouliarmou, V. & Mayer, P. Sorptive bioaccessibility extraction (SBE) of soils: Combining a mobilization medium with an absorption sink. *Environ Sci Technol* **46**, 10682–10689 (2012).
205. Oomen, A. G., Mayer, P. & Tolls, J. Nonequilibrium solid-phase microextraction for determination of the freely dissolved concentration of hydrophobic organic compounds: Matrix effects and limitations. *Anal Chem* **72**, 2802–2808 (2000).
206. Holland, P. M. Nonideal mixed micellar solutions. *Adv Colloid Interface Sci* **26**, 111–129 (1986).
207. Pal, A., Punia, R. & Dubey, G. P. Formation of mixed micelles in an aqueous mixture of a biamphiphilic surface active ionic liquid and an anionic surfactant: Experimental and theoretical study. *J Mol Liq* **337**, 116355 (2021).

208. Del Regno, A., Warren, P. B., Bray, D. J. & Anderson, R. L. Critical Micelle Concentrations in Surfactant Mixtures and Blends by Simulation. *Journal of Physical Chemistry B* **125**, 5983–5990 (2021).
209. Schulz, H. Beta oxidation of fatty acids. *Biochimica et Biophysica Acta (BBA) - Lipids and Lipid Metabolism* **1081**, 109–120 (1991).
210. Pavoncello, V., Barras, F. & Bouveret, E. Degradation of Exogenous Fatty Acids in *Escherichia coli*. (2022) doi:10.3390/biom12081019.
211. Smith, W. L. & Murphy, R. C. The Eicosanoids: Cyclooxygenase, Lipoxygenase and Epoxygenase Pathways. *Biochemistry of Lipids, Lipoproteins and Membranes: Sixth Edition* 259–296 (2015) doi:10.1016/B978-0-444-63438-2.00009-2.
212. Weber, H. Fatty acid-derived signals in plants. *Trends Plant Sci* **7**, 217–224 (2002).
213. Farmer, E. E. Fatty acid signalling in plants and their associated microorganisms. *Signals and Signal Transduction Pathways in Plants* **26**, 187–201 (1994).
214. Spector, A. A. & Yorek, M. A. Membrane lipid composition and cellular function. *J Lipid Res* **26**, 1015–1035 (1985).
215. Harayama, T. & Riezman, H. Understanding the diversity of membrane lipid composition. *Nature Reviews Molecular Cell Biology* *2018 19:5* **19**, 281–296 (2018).
216. Downes, C. P., Gray, A. & Lucocq, J. M. Probing phosphoinositide functions in signaling and membrane trafficking. *Trends Cell Biol* **15**, 259–268 (2005).



217. Leonard, A. E., Pereira, S. L., Sprecher, H. & Huang, Y. S. Elongation of long-chain fatty acids. *Prog Lipid Res* **43**, 36–54 (2004).
218. Stark, K. D., van Elswyk, M. E., Higgins, M. R., Weatherford, C. A. & Salem, N. Global survey of the omega-3 fatty acids, docosahexaenoic acid and eicosapentaenoic acid in the blood stream of healthy adults. *Prog Lipid Res* **63**, 132–152 (2016).
219. Heird, W. C. The Role of Polyunsaturated Fatty Acids in Term and Preterm Infants and Breastfeeding Mothers. *Pediatr Clin North Am* **48**, 173–188 (2001).
220. Hibbeln, J. R. & Salem, N. Dietary polyunsaturated fatty acids and depression: When cholesterol does not satisfy. *American Journal of Clinical Nutrition* **62**, 1–9 (1995).
221. Maskrey, B. H. & Donnell, V. B. O. Analysis of eicosanoids and related lipid mediators using mass spectrometry. **1**, 1055–1059 (2008).
222. Ramsden, C. E. *et al.* Effects of diets enriched in linoleic acid and its peroxidation products on brain fatty acids, oxylipins, and aldehydes in mice. *Biochimica et Biophysica Acta (BBA) - Molecular and Cell Biology of Lipids* **1863**, 1206–1213 (2018).
223. Simard, J. R. *et al.* Locating high-affinity fatty acid-binding sites on albumin by x-ray crystallography and NMR spectroscopy. *Proc Natl Acad Sci U S A* **102**, 17958–17963 (2005).

224. Krenzel, E. S., Chen, Z. & Hamilton, J. A. Correspondence of fatty acid and drug binding sites on human serum albumin: A two-dimensional nuclear magnetic resonance study. *Biochemistry* **52**, 1559–1567 (2013).
225. Petitpas, I., Grüne, T., Bhattacharya, A. A. & Curry, S. Crystal structures of human serum albumin complexed with monounsaturated and polyunsaturated fatty acids. *J Mol Biol* **314**, 955–960 (2001).
226. Fujiwara, S. I. & Amisaki, T. Identification of High Affinity Fatty Acid Binding Sites on Human Serum Albumin by MM-PBSA Method. *Biophys J* **94**, 95–103 (2008).
227. Lee, P. & Wu, X. Review: Modifications of Human Serum Albumin and Their Binding Effect. *Curr Pharm Des* **21**, 1862 (2015).
228. Paál, K., Müller, J. & Hegedûs, L. High affinity binding of paclitaxel to human serum albumin. *Eur J Biochem* **268**, 2187–2191 (2001).
229. Kitamura, K., Takegami, S., Tanaka, R., Omran, A. A. & Kitade, T. Effect of Long-Chain Fatty Acids on the Binding of Triflupromazine to Human Serum Albumin: A Spectrophotometric Study. *Scientia Pharmaceutica 2014, Vol. 82, Pages 233-246* **82**, 233–246 (2013).
230. Goodman, D. W. S. The Interaction of Human Serum Albumin with Long-chain Fatty Acid Anions. *J Am Chem Soc* **80**, 3892–3898 (1958).

231. Hamacek, J. & Piguet, C. How to Adapt Scatchard Plot for Graphically Addressing Cooperativity in Multicomponent Self-Assemblies. *Journal of Physical Chemistry B* **110**, 7783–7792 (2006).
232. Zhu, T. T. *et al.* Difference in Binding of Long- and Medium-Chain Fatty Acids with Serum Albumin: The Role of Macromolecular Crowding Effect. *J Agric Food Chem* **66**, 1242–1250 (2018).
233. Richieri, G. v., Ogata, R. T. & Kleinfeld, A. M. A fluorescently labeled intestinal fatty acid binding protein. Interactions with fatty acids and its use in monitoring free fatty acids. *Journal of Biological Chemistry* **267**, 23495–23501 (1992).
234. Bojesen, I. N. & Bojesen, E. Water-phase palmitate concentrations in equilibrium with albumin-bound palmitate in a biological system. *J Lipid Res* **33**, 1327–1334 (1992).
235. van der Vusse, G. J. Albumin as Fatty Acid Transporter. *Drug Metab Pharmacokinet* **24**, 300–307 (2009).
236. PEDERSEN, A. O., HUST, B., ANDERSEN, S., NIELSEN, F. & BRODERSEN, R. Laurate binding to human serum albumin. *Eur J Biochem* **154**, 545–552 (1986).
237. Spector, A. A. Fatty acid binding to plasma albumin. *J Lipid Res* **16**, 165–179 (1975).
238. Galano, J. M. *et al.* Non-enzymatic cyclic oxygenated metabolites of adrenic, docosahexaenoic, eicosapentaenoic and  $\alpha$ -linolenic acids; bioactivities and potential

- use as biomarkers. *Biochimica et Biophysica Acta (BBA) - Molecular and Cell Biology of Lipids* **1851**, 446–455 (2015).
239. Yuan, G. F., Chen, X. E. & Li, D. Conjugated linolenic acids and their bioactivities: a review. *Food Funct* **5**, 1360–1368 (2014).
240. Stark, A. H., Crawford, M. A. & Reifen, R. Update on alpha-linolenic acid. *Nutr Rev* **66**, 326–332 (2008).
241. Serth, J., Lautwein, A., Frech, M., Wittinghofer, A. & Pingoud, A. The inhibition of the GTPase activating protein-Ha-ras interaction by acidic lipids is due to physical association of the C-terminal domain of the GTPase activating protein with micellar structures. *EMBO J* **10**, 1325–1330 (1991).
242. Zenei, T. & Hiroshi, T. Specific and non-specific ligand binding to serum albumin. *Biochem Pharmacol* **34**, 1999–2005 (1985).
243. Prism - GraphPad. <https://www.graphpad.com/scientific-software/prism/>.
244. Richieri, G. v., Ogata, R. T. & Kleinfeld, A. M. A fluorescently labeled intestinal fatty acid binding protein. Interactions with fatty acids and its use in monitoring free fatty acids. *Journal of Biological Chemistry* **267**, 23495–23501 (1992).
245. Huq, M. M. Fundamentals of SPME extraction of tissue and plasma: experimental and in-silico approaches. (2021).

246. Huq, M., Tascon, M., Nazdrajic, E., Roszkowska, A. & Pawliszyn, J. Measurement of Free Drug Concentration from Biological Tissue by Solid-Phase Microextraction: In Silico and Experimental Study. *Anal Chem* **91**, 7719–7728 (2019).
247. Vaes, W. H. J., Urrestarazu Ramos, E., Verhaar, H. J. M., Seinen, W. & Hermens, J. L. M. Measurement of the free concentration using solid-phase microextraction: Binding to protein. *Anal Chem* **68**, 4463–4467 (1996).
248. Artola-Garicano, E., Vaes, W. H. J. & Hermens, J. L. M. Validation of negligible depletion solid-phase microextraction as a tool to determine tissue/blood partition coefficients for semivolatile and nonvolatile organic chemicals. *Toxicol Appl Pharmacol* **166**, 138–144 (2000).
249. Cody, R. B., Laramée, J. A. & Durst, H. D. Versatile new ion source for the analysis of materials in open air under ambient conditions. *Anal Chem* **77**, 2297–2302 (2005).
250. Takáts, Z., Wiseman, J. M., Gologan, B. & Cooks, R. G. Mass spectrometry sampling under ambient conditions with desorption electrospray ionization. *Science (1979)* **306**, 471–473 (2004).
251. Cooks, R. G., Ouyang, Z., Takats, Z. & Wiseman, J. M. Ambient Mass Spectrometry. *Science (1979)* **311**, 1566–1570 (2006).
252. Javanshad, R. & Venter, A. R. Ambient ionization mass spectrometry: real-time, proximal sample processing and ionization. *Analytical Methods* **9**, 4896–4907 (2017).

253. Peacock, P. M., Zhang, W. J. & Trimpin, S. Advances in Ionization for Mass Spectrometry. *Anal Chem* **89**, 372–388 (2017).
254. Venter, A., Nefliu, M. & Graham Cooks, R. Ambient desorption ionization mass spectrometry. *TrAC Trends in Analytical Chemistry* **27**, 284–290 (2008).
255. Chen, H., Gamez, G. & Zenobi, R. What can we learn from ambient ionization techniques? *J Am Soc Mass Spectrom* **20**, 1947–1963 (2011).
256. Reiter, A., Herbst, L., Wiechert, W. & Oldiges, M. Need for speed: evaluation of dilute and shoot-mass spectrometry for accelerated metabolic phenotyping in bioprocess development. *Anal Bioanal Chem* **413**, 3253–3268 (2021).
257. Bukowski, M. R., Voeller, K. & Jahns, L. Simple and sensitive dilute-and-shoot analysis of carotenoids in human plasma. *Journal of Chromatography B* **1095**, 32–38 (2018).
258. Gross, R. W. & Han, X. Shotgun lipidomics of neutral lipids as an enabling technology for elucidation of lipid-related diseases. *Am J Physiol Endocrinol Metab* **297**, 297–303 (2009).
259. Han, X. & Gross, R. W. Shotgun lipidomics: Electrospray ionization mass spectrometric analysis and quantitation of cellular lipidomes directly from crude extracts of biological samples. *Mass Spectrom Rev* **24**, 367–412 (2005).

260. Han, X. & Gross, R. W. Electrospray ionization mass spectroscopic analysis of human erythrocyte plasma membrane phospholipids. *Proc. Natl. Acad. Sci. USA* **91**, 10635–10639 (1994).
261. Han, X. & Gross, R. W. Structural determination of picomole amounts of phospholipids via electrospray ionization tandem mass spectrometry. *J Am Soc Mass Spectrom* **6**, 1202–1210 (1995).
262. Jackson, S. N. *et al.* MALDI-ion mobility-TOFMS imaging of lipids in rat brain tissue. *Journal of Mass Spectrometry* **42**, 1093–1098 (2007).
263. Girod, M., Shi, Y., Cheng, J. X. & Cooks, R. G. Mapping lipid alterations in traumatically injured rat spinal cord by desorption electrospray ionization imaging mass spectrometry. *Anal Chem* **83**, 207–215 (2011).
264. Sparvero, L. J. *et al.* Mapping of phospholipids by MALDI imaging (MALDI-MSI): Realities and expectations. *Chem Phys Lipids* **165**, 545–562 (2012).
265. Ellis, S. R., Brown, S. H., in het Panhuis, M., Blanksby, S. J. & Mitchell, T. W. Surface analysis of lipids by mass spectrometry: More than just imaging. *Prog Lipid Res* **52**, 329–353 (2013).
266. Ford, D. A. & Gross, R. W. Plasménylethanolamine is the major storage depot for arachidonic acid in rabbit vascular smooth muscle and is rapidly hydrolyzed after angiotensin II stimulation. *Proceedings of the National Academy of Sciences* **86**, 3479–3483 (1989).

267. Hall, Z., Chu, Y. & Griffin, J. L. Liquid Extraction Surface Analysis Mass Spectrometry Method for Identifying the Presence and Severity of Nonalcoholic Fatty Liver Disease. *Anal Chem* **89**, 5161–5170 (2017).
268. Ryan, E. & Reid, G. E. Chemical Derivatization and Ultrahigh Resolution and Accurate Mass Spectrometry Strategies for ‘shotgun’ Lipidome Analysis. *Acc Chem Res* **49**, 1596–1604 (2016).
269. Mitchell, T. W., Pham, H., Thomas, M. C. & Blanksby, S. J. Identification of double bond position in lipids: From GC to OzID. *Journal of Chromatography B* **877**, 2722–2735 (2009).
270. Ma, X. & Xia, Y. Pinpointing Double Bonds in Lipids by Paternò-Büchi Reactions and Mass Spectrometry. *Angewandte Chemie International Edition* **53**, 2592–2596 (2014).
271. Brügger, B., Erben, G., Sandhoff, R., Wieland, F. T. & Lehmann, W. D. Quantitative analysis of biological membrane lipids at the low picomole level by nano-electrospray ionization tandem mass spectrometry. *Proc Natl Acad Sci U S A* **94**, 2339–2344 (1997).
272. Pan, M., Qin, C. & Han, X. Quantitative Analysis of Polyphosphoinositide, Bis(monoacylglycerol)phosphate, and Phosphatidylglycerol Species by Shotgun Lipidomics After Methylation. *Methods in Molecular Biology* **2306**, 77–91 (2021).



273. Wang, C. *et al.* Comprehensive and quantitative analysis of polyphosphoinositide species by shotgun lipidomics revealed their alterations in db/db mouse brain. *Anal Chem* **88**, 12137–12144 (2016).
274. Li, Y. L., Su, X., Stahl, P. D. & Gross, M. L. Quantification of diacylglycerol molecular species in biological samples by electrospray ionization mass spectrometry after one-step derivatization. *Anal Chem* **79**, 1569–1574 (2007).
275. Wang, M., Hayakawa, J., Yang, K. & Han, X. Characterization and quantification of diacylglycerol species in biological extracts after one-step derivatization: A shotgun lipidomics approach. *Anal Chem* **86**, 2146–2155 (2014).
276. Thomas, M. C. *et al.* Ozone-induced dissociation: Elucidation of double bond position within mass-selected lipid ions. *Anal Chem* **80**, 303–311 (2008).
277. Wang, M., Han, R. H. & Han, X. Fatty acidomics: Global analysis of lipid species containing a carboxyl group with a charge-remote fragmentation-assisted approach. *Anal Chem* **85**, 9312–9320 (2013).
278. Takyi-Williams, J., Liu, C. F. & Tang, K. Ambient ionization MS for bioanalysis: recent developments and challenges. <http://dx.doi.org/10.4155/bio.15.116> **7**, 1901–1923 (2015).
279. Christians, U. *et al.* Impact of laboratory practices on interlaboratory variability in therapeutic drug monitoring of immunosuppressive drugs. *Ther Drug Monit* **37**, 718–724 (2015).

280. Jackson, S. N. *et al.* Direct tissue analysis of phospholipids in rat brain using MALDI-TOFMS and MALDI-ion mobility-TOFMS. *J Am Soc Mass Spectrom* **16**, 133–138 (2005).
281. Xia, F. & Wan, J. B. Chemical derivatization strategy for mass spectrometry-based lipidomics. *Mass Spectrom Rev* e21729 (2021) doi:10.1002/MAS.21729.
282. Deng, J., Yang, Y., Wang, X. & Luan, T. Strategies for coupling solid-phase microextraction with mass spectrometry. *TrAC Trends in Analytical Chemistry* **55**, 55–67 (2014).
283. Watt, L. & Sisco, E. Detection of trace drugs of abuse in baby formula using solid-phase microextraction direct analysis in real-time mass spectrometry (SPME-DART-MS). *J Forensic Sci* **66**, 172–178 (2021).
284. Arora, M. *et al.* Machine Learning Approaches to Identify Discriminative Signatures of Volatile Organic Compounds (VOCs) from Bacteria and Fungi Using SPME-DART-MS. *Metabolites 2022, Vol. 12, Page 232* **12**, 232 (2022).
285. Vasiljevic, T. & Pawliszyn, J. Direct analysis in real time (DART) and solid-phase microextraction (SPME) transmission mode (TM): a suitable platform for analysis of prohibited substances in small volumes. *Analytical Methods* **11**, 3882–3889 (2019).
286. Khaled, A., Belinato, J. R. & Pawliszyn, J. Rapid and high-throughput screening of multi-residue pharmaceutical drugs in bovine tissue using solid phase

- microextraction and direct analysis in real time-tandem mass spectrometry (SPME-DART-MS/MS). *Talanta* **217**, 121095 (2020).
287. Gómez-Ríos, G. A., Gionfriddo, E., Poole, J. & Pawliszyn, J. Ultrafast Screening and Quantitation of Pesticides in Food and Environmental Matrices by Solid-Phase Microextraction-Transmission Mode (SPME-TM) and Direct Analysis in Real Time (DART). *Anal Chem* **89**, 7240–7248 (2017).
288. Gómez-Ríos, G. A. & Pawliszyn, J. Solid phase microextraction (SPME)-transmission mode (TM) pushes down detection limits in direct analysis in real time (DART). *Chemical Communications* **50**, 12937–12940 (2014).
289. Lendor, S. Chemical biopsy via solid phase microextraction: strategies and applications for in vivo brain studies. (University of Waterloo, 2020).
290. Vasiljevic, T., Gómez-Ríos, G. A., Li, F., Liang, P. & Pawliszyn, J. High-throughput quantification of drugs of abuse in biofluids via 96-solid-phase microextraction–transmission mode and direct analysis in real time mass spectrometry. *Rapid Communications in Mass Spectrometry* **33**, 1423–1433 (2019).
291. Vasiljevic, T. & Pawliszyn, J. Direct analysis in real time (DART) and solid-phase microextraction (SPME) transmission mode (TM): a suitable platform for analysis of prohibited substances in small volumes. *Analytical Methods* **11**, 3882–3889 (2019).

292. Watt, L. & Sisco, E. Detection of trace drugs of abuse in baby formula using solid-phase microextraction direct analysis in real-time mass spectrometry (SPME-DART-MS). *J Forensic Sci* **66**, 172–178 (2021).
293. Arora, M. *et al.* Machine Learning Approaches to Identify Discriminative Signatures of Volatile Organic Compounds (VOCs) from Bacteria and Fungi Using SPME-DART-MS. *Metabolites* **2022**, Vol. 12, Page 232 **12**, 232 (2022).
294. Wang, X. *et al.* Online coupling of in-tube solid-phase microextraction with direct analysis in real time mass spectrometry for rapid determination of triazine herbicides in water using carbon-nanotubes-incorporated polymer monolith. *Anal Chem* **86**, 4739–4747 (2014).
295. Cody, R. & Maleknia, S. D. Coated glass capillaries as SPME devices for DART mass spectrometry. *Rapid Communications in Mass Spectrometry* **34**, e8946 (2020).
296. Haunschmidt, M., Klampfl, C. W., Buchberger, W. & Hertsens, R. Determination of organic UV filters in water by stir bar sorptive extraction and direct analysis in real-time mass spectrometry. *Anal Bioanal Chem* **397**, 269–275 (2010).
297. Cajka, T., Riddellova, K., Tomaniova, M. & Hajslova, J. Ambient mass spectrometry employing a DART ion source for metabolomic fingerprinting/profiling: A powerful tool for beer origin recognition. *Metabolomics* **7**, 500–508 (2011).

298. Gómez-Ríos, G. A. & Pawliszyn, J. Development of Coated Blade Spray Ionization Mass Spectrometry for the Quantitation of Target Analytes Present in Complex Matrices. *Angewandte Chemie International Edition* **53**, 14503–14507 (2014).
299. Kasperkiewicz, A., Gómez-Ríos, G. A., Hein, D. & Pawliszyn, J. Breaching the 10 Second Barrier of Total Analysis Time for Complex Matrices via Automated Coated Blade Spray. *Anal Chem* **91**, 13039–13046 (2019).
300. Looby, N. T. *et al.* Solid phase microextraction coupled to mass spectrometry via a microfluidic open interface for rapid therapeutic drug monitoring. *Analyst* **144**, 3721–3728 (2019).
301. Tascon, M., Alam, M. N., Gómez-Ríos, G. A. & Pawliszyn, J. Development of a Microfluidic Open Interface with Flow Isolated Desorption Volume for the Direct Coupling of SPME Devices to Mass Spectrometry. *Anal Chem* **90**, 2631–2638 (2018).
302. Nazdrajić, E. *et al.* Rapid determination of tacrolimus and sirolimus in whole human blood by direct coupling of solid-phase microextraction to mass spectrometry via microfluidic open interface. *Anal Chim Acta* **1144**, 53–60 (2021).
303. Gómez-Ríos, G. A. *et al.* Open Port Probe Sampling Interface for the Direct Coupling of Biocompatible Solid-Phase Microextraction to Atmospheric Pressure Ionization Mass Spectrometry. *Anal Chem* **89**, 3805–3809 (2017).

304. van Berkel, G. J. & Kertesz, V. An open port sampling interface for liquid introduction atmospheric pressure ionization mass spectrometry. *Rapid Communications in Mass Spectrometry* **29**, 1749–1756 (2015).
305. Nazdrajić, E. Development and Study of the Microfluidic Open Interface Coupled with Solid-phase Microextraction for Rapid Analysis. (University of Waterloo).
306. Tascon, M., Alam, M. N., Gómez-Ríos, G. A. & Pawliszyn, J. Development of a Microfluidic Open Interface with Flow Isolated Desorption Volume for the Direct Coupling of SPME Devices to Mass Spectrometry. *Anal Chem* **90**, 2631–2638 (2018).
307. Tascon, M. *et al.* Ultra-fast quantitation of voriconazole in human plasma by coated blade spray mass spectrometry. *J Pharm Biomed Anal* **144**, 106–111 (2017).
308. Zhou, W., Nazdrajić, E. & Pawliszyn, J. Rapid Screening and Quantitation of Drugs of Abuse by Both Positive and Negative Modes via Coated Blade Spray-Mass Spectrometry. *J Am Soc Mass Spectrom* **33**, 1187–1193 (2022).
309. Schuhmann, K. *et al.* Shotgun lipidomics on a LTQ Orbitrap mass spectrometer by successive switching between acquisition polarity modes. *Journal of Mass Spectrometry* **47**, 96–104 (2012).
310. Boggs, J. M. Lipid intermolecular hydrogen bonding: influence on structural organization and membrane function. *Biochimica et Biophysica Acta (BBA) - Reviews on Biomembranes* **906**, 353–404 (1987).

311. Cole, R. B. & Harrata, A. K. Solvent effect on analyte charge state, signal intensity, and stability in negative ion electrospray mass spectrometry; implications for the mechanism of negative ion formation. *Journal of the American Society for Mass Spectrometry* 1993 4:7 **4**, 546–556 (1993).
312. Niraula, T. P., Shah, S. K., Chatterjee, S. K. & Bhattarai, A. Effect of methanol on the surface tension and viscosity of sodiumdodecyl sulfate (SDS) in aqueous medium at 298.15–323.15 K. *Karbala International Journal of Modern Science* **4**, 26–34 (2018).
313. Piri-Moghadam, H. *et al.* Fast Quantitation of Target Analytes in Small Volumes of Complex Samples by Matrix-Compatible Solid-Phase Microextraction Devices. *Angewandte Chemie - International Edition* **55**, 7510–7514 (2016).
314. Thirukumaran, M. *et al.* Solid-phase microextraction- probe electrospray ionization devices for screening and quantitating drugs of abuse in small amounts of biofluids. *Talanta* **231**, 122317 (2021).
315. Lendor, S., Gómez-Ríos, G. A., Boyaci, E., vander Heide, H. & Pawliszyn, J. Space-resolved tissue analysis by solid-phase microextraction coupled to high-resolution mass spectrometry via desorption electrospray ionization. *Anal Chem* **91**, 10141–10148 (2019).
316. Lin, M., Blevins, M. S., Sans, M., Brodbelt, J. S. & Eberlin, L. S. Deeper Understanding of Solvent-Based Ambient Ionization Mass Spectrometry: Are

- Molecular Profiles Primarily Dictated by Extraction Mechanisms? *Anal Chem* **94**, 14734–14744 (2022).
317. van Berkel, G. J. & Kertesz, V. An open port sampling interface for liquid introduction atmospheric pressure ionization mass spectrometry. *Rapid Communications in Mass Spectrometry* **29**, 1749–1756 (2015).
318. Welte, M. A. & Gould, A. P. Lipid droplet functions beyond energy storage. *Biochimica et Biophysica Acta - Molecular and Cell Biology of Lipids* vol. 1862 1260–1272 Preprint at <https://doi.org/10.1016/j.bbalip.2017.07.006> (2017).
319. Harayama, T. & Riezman, H. Understanding the diversity of membrane lipid composition. *Nature Publishing Group* **19**, (2018).
320. Bairstow, S. F., Bunce, M. W. & Anderson, R. A. Phosphoinositide 4- and 5-Kinases and Phosphatases. in *Encyclopedia of Biological Chemistry: Second Edition* 459–462 (Elsevier Inc., 2013). doi:10.1016/B978-0-12-378630-2.00492-8.
321. Gozzelino, L., de Santis, M. C., Gulluni, F., Hirsch, E. & Martini, M. PI(3,4)P2 Signaling in Cancer and Metabolism. *Frontiers in Oncology* vol. 10 360 Preprint at <https://doi.org/10.3389/fonc.2020.00360> (2020).
322. Fahy, E. *et al.* A comprehensive classification system for lipids. *European Journal of Lipid Science and Technology* **107**, 337–364 (2005).
323. Visioli, F. & Poli, A. Fatty Acids and Cardiovascular Risk. Evidence, Lack of Evidence, and Diligence. *Nutrients* 2020, Vol. 12, Page 3782 **12**, 3782 (2020).



324. Han, X. & Gross, R. W. Electrospray ionization mass spectroscopic analysis of human erythrocyte plasma membrane phospholipids. *Proc Natl Acad Sci U S A* **91**, 10635–10639 (1994).
325. Han, X. & Gross, R. W. Global analyses of cellular lipidomes directly from crude extracts of biological samples by ESI mass spectrometry: A bridge to lipidomics. *Journal of Lipid Research* vol. 44 1071–1079 Preprint at <https://doi.org/10.1194/jlr.R300004-JLR200> (2003).
326. Fuchs, B. & Schiller, J. Application of MALDI-TOF mass spectrometry in lipidomics. *European Journal of Lipid Science and Technology* vol. 111 83–98 Preprint at <https://doi.org/10.1002/ejlt.200800223> (2009).
327. Schiller, J. *et al.* Matrix-assisted laser desorption and ionization time-of-flight (MALDI-TOF) mass spectrometry in lipid and phospholipid research. *Progress in Lipid Research* vol. 43 449–488 Preprint at <https://doi.org/10.1016/j.plipres.2004.08.001> (2004).
328. Astarita, G. & Piomelli, D. Lipidomic analysis of endocannabinoid metabolism in biological samples. *Journal of Chromatography B: Analytical Technologies in the Biomedical and Life Sciences* vol. 877 2755–2767 Preprint at <https://doi.org/10.1016/j.jchromb.2009.01.008> (2009).
329. Sezgin, E. & Schwille, P. Fluorescence Techniques to Study Lipid Dynamics. *Cold Spring Harb Perspect Biol* **3**, a009803 (2011).

330. Li, Q., Yu, X., Yang, Y. & Liu, X. Simple Determination of Diacylglycerols Using Thin Layer Chromatography and Visible Spectrophotometry. *Food Anal Methods* **11**, 236–242 (2018).
331. Herrero, A. M. Raman spectroscopy a promising technique for quality assessment of meat and fish: A review. *Food Chemistry* vol. 107 1642–1651 Preprint at <https://doi.org/10.1016/j.foodchem.2007.10.014> (2008).
332. Huang, F. *et al.* Identification of waste cooking oil and vegetable oil via Raman spectroscopy. *Journal of Raman Spectroscopy* **47**, 860–864 (2016).
333. Galievsky, V. & Pawliszyn, J. Fluorometer for Screening of Doxorubicin in Perfusate Solution and Tissue with Solid-Phase Microextraction Chemical Biopsy Sampling. *Anal Chem* **92**, 13025–13033 (2020).
334. Nwaneshiudu, I. C., Nwaneshiudu, C. A. & Schwartz, D. T. Separation and enhanced detection of anesthetic compounds using Solid Phase Micro-Extraction (SPME) - Raman spectroscopy. *Appl Spectrosc* **68**, 1254–1259 (2014).
335. Doyle, C. A., Vickers, T. J., Mann, C. K. & Dorsey, J. G. Characterization of C18-bonded liquid chromatographic stationary phases by Raman spectroscopy: The effect of temperature. *J Chromatogr A* **877**, 41–59 (2000).
336. de Gelder, J., de Gussem, K., Vandenabeele, P. & Moens, L. Reference database of Raman spectra of biological molecules. *Journal of Raman Spectroscopy* **38**, 1133–1147 (2007).

337. Baeten, V., Meurens, M., Morales, M. T. & Aparicio, R. Detection of Virgin Olive Oil Adulteration by Fourier Transform Raman Spectroscopy. *J Agric Food Chem* **44**, 2225–2230 (1996).
338. Robert, C. *et al.* Rapid discrimination of intact beef, venison and lamb meat using Raman spectroscopy. *Food Chem* **343**, 128441 (2021).
339. Beattie, J. R., Bell, S. E. J., Borggaard, C., Fearon, A. & Moss, B. W. Prediction of adipose tissue composition using raman spectroscopy: Average properties and individual fatty acids. *Lipids* 2006 41:3 **41**, 287–294 (2006).